UNIVERSITÀ DEGLI STUDI FIRENZE

**FACOLTA DI SCIENZE**
**********
**RICERCA POST-LAUREA**
*********

**REPUBLIC OF CAMEROON**
**********
**THE UNIVERSITY OF YAOUNDE I**
**********
**FACULTY OF SCIENCE**
**********
**POST GRADUATE RESEARCH AND TRAINING PROGRAMME OF SCIENCES, TECHNOLOGY AND GEOSCIENCES**
**********
**DOCTORATE RESEARCH UNIT FOR GEOSCIENCES AND APPLICATIONS**
**********

**DIPARTIMENTO DI SCIENZE DELLA TERRE**
***DEPARTMENT OF EARTH SCIENCES***

**JOINT DOCTORAL PROGRAM**

# CHEMICAL AND ISOTOPIC CHARACTERIZATION OF WATER RESOURCES IN THE FRACTURED CRYSTALLINE AQUIFERS OF THE BAFIA AREA, CENTRE REGION-CAMEROON: IMPLICATIONS FOR WATER MANAGEMENT

**THESIS**
Submitted in partial fulfillment of the requirements for the award of a Doctorate/PhD degree in Earth Sciences

Academic Discipline (SSD). Geo-08/Geochemistry and Volcanology (UNIFI)
Speciality: Geosciences of Superficial Formations (UYI)
Option: Soils-Water-Geotechnical Sciences (UYI)

By

**TARKANG Carine ENOW-AYOR**
Master of Science in Applied Geology
Matricule : 19T2036

**Supervisor**
Prof. *Jules Rémy Ndam Ngoupayou*
*Professor University of Yaounde I*

**Co-supervisors**
Prof. Franco Tassi
Professor University of Florence
Dr. Ako Andrew Ako
Senior Research Officer, MINRESI

**Coordinators**
Prof. *Sandro Conticelli*
Prof. Bisso Dieudonné

***Year:*** *2025-2026*

# DEDICATION

To my family:

My beloved husband, Mr. Taboko Armstrong,

My children, Oben, Praise, Jedidiah, Annabel, Kesiah and Emmanuel,

My mother, Mama Ebangha Anna Ebot,

My siblings, Joanita, Nixon, Maureen, Margaret, Derrick and Cynthia

and to my late father, Pa Tarkang Timothy Enowkpa

# ACKNOWLEDGEMENTS

Firstly, I wish to thank God Almighty for the grace, love, favor, strength, health, protection, provision and guidance he gave to me throughout these years, without which it would have been impossible for me.

I am sincerely thankful to my supervisors; Prof. Ndam Ngoupayou Jules Rémy, Prof. Franco Tassi and Dr. Ako Andrew Ako, not leaving out Dr. Dmitri Rouwet of the Istituto Nazionale di Geofisica e vulcanologia of Bologna, Italy, for their steadfast follow-up and insightful feedback which shaped this piece of work.

I gratefully acknowledge the financial support offered by the International Atomic Energy Agency (IAEA) through a fellowship grant (EVT2106130-0001-CMR) within the RAF 7021 TC project which covered my entire Ph.D studies. I am deeply grateful to Dr. Ele Abiama Dr. Njama Joséphine, Dr. Fouepé Takounjou and Dr. Fantong Wilson, for believing in me and giving me the opportunity to be a beneficiary of this wonderful fellowship grant.

I thank the administrations of the University of Yaounde I (Cameroon) and the University of Florence (Italy), for the Joint Supervision Ph.D opportunity given to me. I am grateful to the Ministry of Scientific Research and Innovation (MINRESI) and the Institute of Geological and Mining Research (IRGM) for putting me on study leave uring my Ph.D studies.

I also thank my course mates of UNIFI, especially Rebecca Biagi, Alesio Monani, Francesca Amico, Francesa Giannetti and Frederica and those of UYI, especially Zobe Mbele Henri and Ngah Mohamed, not forgetting Mme Eyenga, for their kind assistance during this research.

I wish to thank all my colleagues, under the leadership of Dr. Ntonga Jean Claude, and more especially Mme Ateba Henriette, Dr. Mengjo Jude Wirmverm, Dr. Gloria Eneke Takem Eyong, Mme Ghislaine Madjiki, Dr. Nka Benadette, Dr. Mero Yannah, and Ms Kankeu Gisèle Auroe.

I Finally, I wish to thank my dear friends, Dr. Akenji Victorine Neh, Dr. Gwendoline Egbe Arikai and Dr. Ojong Agbor Ntane who, by virtue of going through this same phase of life, encouraged me to look up to the finish crown.

# TABLE OF CONTENTS

# LIST OF ABBREVIATIONS AND ACRONYMS

ADD: Average Daily Dose

AT: Average Time

BDL: Below Detection Limit

BW: Body Weight

CAMWATER: Cameroon Water Utilities

$C_d$: Degree of Contamination

CRDS: Cavity ring-down spectroscopy

CSF: Cancer Slope Factor

ED: Exposure Duration

EF: Exposure Frequency

HEI: Heavy Metal Evaluation Index

HI: Hazard Index

HPI: Heavy metal Pollution Index

HQ: Hazard Quotient

IAEA: International Atomic Energy Agency

IC system: Ion Chromatography system

ICP-MS: Inductively coupled plasma-mass spectrometry

ILCR: Incremental Lifetime Cancer Risk

IR: Ingestion Rate

MI: Metal Index

OLR: Over the Limit Ratio

SF: Slope Factor

WQI: Water Quality Index

## LIST OF TABLES

# LIST OF FIGURES

# ABSTRACT

The sustainable management of groundwater resources in the Bafia crystalline aquifers is challenging owing to their complex hydrogeological characteristics, limited understanding of the aquifer system, increasing demand for potable water and vulnerability to nitrate contamination. This study focuses on the chemical and isotopic characterization of water resources in the crystalline aquifers of Bafia**,** aiming to understand the hydrogeochemical processes controlling water composition. A total of 117 water samples from boreholes, shallow hand-dug wells, rivers, and springs (57 for wet and 60 for dry season) were analyzed for major ions by IC system; trace elements by ICP-MS; stable isotopes ($\delta^{18}O$, $\delta^{2}H$) by CRDS; tritium by liquid scintillation and dual nitrogen isotopes ($\delta^{15}N\text{-}NO_3$ and $\delta^{18}O\text{-}NO_3$) by Laser isotope spectrometry using $TiCl_3$ extraction. Hydrochemical data were processed using multivariate statistical methods and graphical tools such as Piper and Gibbs diagrams, stable isotopic results were compared with the Global Meteoric Water Line (GMWL) and the Yaounde Local Meteoric Water Line (YLMWL), while nitrate contamination was assessed using the Kendall diagram. Results reveal mainly Ca-Mg-$HCO_3$ water type, generally acidic to neutral ($3.2 < pH < 7.4$) and moderately mineralized ($30 < EC < 2220$ µS/cm), indicating active and rapid recharge, with minimal changes prior to infiltration. Two main factors influence water quality, namely: natural factors (rock/mineral weathering and dissolution, ion exchange, soil leaching, topography) and anthropogenic activities (manure/fertilizer, untreated wastes disposal, leaky/poorly constructed pit latrines, well chlorination). Groundwater and especially surface water, is excellent for drinking (WQI < 25 and HPI < 100) and irrigation. Isotopic signatures reveal recharge from recent meteoric water, with minor evidence of evaporation and localized mixing processes. More than 70% samples demonstrate a mixture of sub-modern and recently recharged water, with some protected areas identified. High $NO_3/Cl$ ratios and $\delta^{15}N\text{-}NO_3$ (>10%) insinuate a mixture of urban and agricultural nitrate contamination sources. These findings provide critical insights into the dynamics of the crystalline aquifer system and emphasize the need for integrated water management strategies that account for both natural hydrogeological conditions and increasing anthropogenic pressures in the Bafia area.

**Key words:** Environmental isotopes, hydrogeochemistry, dual nitrogen, trace elements, apparent age, recharge processes.

# ASTRATTA

La gestione sostenibile delle risorse idriche sotterranee nelle falde acquifere cristalline di Bafia è difficile a causa delle loro complesse caratteristiche idrogeologiche, della comprensione limitata del sistema acquifero, della crescente domanda di acqua potabile e della vulnerabilità alla contaminazione. Questo studio si concentra sulla caratterizzazione chimica e isotopica delle risorse idriche nelle falde acquifere cristalline di Bafia, con l'obiettivo di comprendere i processi idrogeochimici che controllano la composizione dell'acqua. Sono stati analizzati un totale di 117 campioni d'acqua provenienti da pozzi trivellati, pozzi poco profondi scavati a mano, fiumi e sorgenti (57 per la stagione umida e 60 per la stagione secca) per determinare gli ioni principali mediante sistema IC; gli oligoelementi mediante ICP-MS; gli isotopi stabili ($\delta^{18}O$, $\delta^{2}H$) mediante CRDS; il trizio mediante scintillazione liquida e i doppi isotopi dell'azoto ($\delta^{15}N\text{-}NO_3$ e $\delta^{18}O\text{-}NO_3$) mediante spettrometria isotopica laser con estrazione $TiCl_3$. I dati idrochimici sono stati elaborati utilizzando metodi statistici multivariati e strumenti grafici come i diagrammi di Piper e Gibbs, i risultati degli isotopi stabili sono stati confrontati con la Global Meteoric Water Line (GMWL) e la Linea Meteorica Locale di Yaoundé (LMLY), mentre la contaminazione da nitrati è stata valutata utilizzando il diagramma di Kendall. I risultati rivelano principalmente un tipo di acqua Ca-Mg-HCO3, generalmente da acida a neutra (3,2 < pH < 7,4) e moderatamente mineralizzata (30 < EC < 2220 µS/cm), indicando una ricarica attiva e rapida, con variazioni minime prima dell'infiltrazione. Due fattori principali influenzano la qualità dell'acqua, ovvero: fattori naturali (alterazione e dissoluzione di rocce/minerali, scambio ionico, lisciviazione del suolo, topografia) e attività antropiche (letame/fertilizzanti, smaltimento di rifiuti non trattati, latrine a fossa mal costruite e con perdite, clorazione dei pozzi). Le acque sotterranee e soprattutto quelle superficiali sono eccellenti per il consumo (WQI < 25 e HPI < 100) e l'irrigazione. Le firme isotopiche rivelano una ricarica da acqua meteorica recente, con lievi segni di evaporazione e processi di miscelazione localizzati. Oltre il 70% dei campioni mostra una miscela di acqua submoderna e ricaricata di recente, con alcune aree protette identificate. Gli elevati rapporti NO3/Cl e δ15N-NO3 (>10%) suggeriscono una miscela di fonti di contaminazione da nitrati urbani e agricoli. Questi risultati forniscono informazioni fondamentali sulle dinamiche del sistema acquifero cristallino e sottolineano la necessità di strategie integrate di gestione delle risorse idriche che tengano conto sia delle condizioni idrogeologiche naturali sia delle crescenti pressioni antropiche nell'area di Bafia.

**Parole chiave:** Isotopi ambientali, idrogeochimica, azoto doppio, oligoelementi, età apparente, processi di ricarica.

# RESUMÉ

La gestion durable des ressources en eau souterraine dans les aquifères cristallins de Bafia est difficile en raison de leurs caractéristiques hydrogéologiques complexes, la connaissance limitée du système aquifère, la demande croissante en eau potable et la vulnérabilité à la contamination. Cette étude se concentre sur la caractérisation chimique et isotopique des ressources en eau dans les aquifères cristallins de Bafia, dans le but de comprendre les processus hydrogéochimiques qui contrôlent la composition de l'eau. Au total, 117 échantillons d'eau provenant de forages, de puits, de rivières et de sources (57 pour la saison humide et 60 pour la saison sèche) ont été analysés pour déterminer les ions majeurs par un système IC ; les oligo-éléments par ICP-MS ; les isotopes stables ($\delta^{18}O$, $\delta^{2}H$) par CRDS ; le tritium par scintillation liquide et les deux isotopes d'azote ($\delta^{15}N\text{-}NO_3$ et $\delta^{18}O\text{-}NO_3$) par spectrométrie isotopique laser utilisant l'extraction au $TiCl_3$. Les données hydrochimiques ont été traitées à l'aide de méthodes statistiques multivariées et d'outils graphiques tels que les diagrammes de Piper et de Gibbs, les résultats isotopiques stables ont été comparés à la ligne mondiale de l'eau météorique (GMWL) et la Ligne Météorique Locale de Yaoundé (LMLY), tandis que la contamination par les nitrates a été évaluée à l'aide du diagramme de Kendall. Les résultats révèlent principalement un type d'eau Ca-Mg-$HCO_3$, généralement acide à neutre ($3,2 < pH < 7,4$) et modérément minéralisée ($30 < EC < 2220$ µS/cm), indiquant une recharge active et rapide, avec des changements minimes avant l'infiltration. Deux facteurs principaux influencent la qualité de l'eau, à savoir : les facteurs naturels (altération et dissolution des roches/minéraux, échange d'ions, lessivage des sols, topographie) et les activités anthropiques (fumier/engrais, élimination des déchets non traités, latrines à fosse mal construites ou qui fuient, chloration des puits). Les eaux souterraines, et en particulier les eaux de surface, sont excellentes pour la consommation (WQI < 25 et HPI < 100) et l'irrigation. Les signatures isotopiques révèlent une recharge provenant d'eau météorique récente, avec des signes mineurs d'évaporation et de processus de mélange localisés. Plus de 70 % des échantillons montrent un mélange d'eau submoderne et d'eau récemment rechargée, avec quelques zones protégées identifiées. Des rapports $NO_3^-/Cl^-$ élevés et des valeurs $\delta^{15}N\text{-}NO_3^-$ (>10 %) suggèrent un mélange de sources de contamination par les nitrates urbains et agricoles. Ces résultats fournissent des informations essentielles sur la dynamique du système aquifère cristallin et soulignent la nécessité de stratégies intégrées de gestion de l'eau qui tiennent compte à la fois des conditions hydrogéologiques naturelles et des pressions anthropiques croissantes dans la région de Bafia.

**Mots clés :** Isotopes environnementaux, hydrogéochimie, azote double, éléments traces, âge apparent, processus de recharge.

# GENERAL INTRODUCTION

## 1. Research context and problem statement

Water is an economic, social and environmental asset, often considered to be part of a "natural heritage" (Mutin, 2000). Despite its degradation by human activities, it is increasingly a source of conflict, particularly in regions where water scarcity is on the increase. In recent times, access to clean water has become one of the main challenges facing humanity. For example, over a billion people do not have access to safe drinking water and sanitation (Action Contre la Faim, 2008; WHO and UNICEF, 2013), leading to the deaths of nearly 10,000 people a day, the vast majority of which are children. During the World Water Council in Mexico City in March 2006, it was re-iterated that "the lack or poor quality of water kills ten times more people every year than all wars combined" (Action Contre la Faim, 2008). Inadequate and poor-quality water is not only a major public health issue; it also affects the socio-economic development of the people. Agriculture, livestock breeding, industry, commerce and daily household life all depend on access to water in sustainable quantity and quality.

Of all available water, groundwater constitutes only about 30% of the total freshwater accessible to man. In most developing nations, especially in rural areas, groundwater is the most valuable potable water source with relatively good quality, easy to find, affordable and easily consumed with little or no treatment required (Tabué et al. 2021). However, many water bodies worldwide continuously face a reduction in quality and quantity, thus limiting the United Nations' objective of high-quality potable water supply (SDG 6) by 2030 (United Nations, 2016). Despite its natural buffering capacity, groundwater is neither a universal panacea to water problems nor invulnerable to degradation. Present-day estimations show that between two and three billion people worldwide experience water shortages for at least one month per year, posing severe risks to livelihoods, notably through food security, health and access to electricity. (United Nations Development Programme (UNDP), 2023). With the massive extraction of groundwater for drinking (50 % of available freshwater) and irrigation (40 %) from aquifers in the world, there is need for careful characterization to guide water supply investments and sustainably manage the resource to minimize degradation it is essential to implement strategies and take action to slow down the degradation of these resources (Foster and Chilton, 2003; Abascal et al. 2022).

Although access to potable water supply and sanitation has improved in Sub-Saharan Africa over the past two decades (from 49 % to 60 % - West Africa and from 28 % to 31 % - Central Africa), the region still lags behind all other developing regions (Pare and Bonzi-Coulibaly, 2013). According to the 2023 Africa Sustainable Development Report, about 411 million Africans still lack access to safe water, and almost three-fourths do not enjoy good sanitation services (UNDP, 2023). Besides the many other factors behind poor water quality in Africa, the most prominent are related to aspects like (i) intensive use of pesticides and fertilizers, (ii) uncontrolled dumping of solid wastes, (iii) improper pit toilet constructions, (iv) discharge of untreated wastewaters from households and industries, and (v) some natural pollutants of geological origin (Pare and Bonzi-Coulibaly, 2013). Hence, it is important to derive strategies to ensure sustainable development and management of groundwater resources.

Crystalline aquifers are often complex to understand due to their heterogeneous character, which changes even within short local extents. However, different approaches have been used in diverse research activities to enable effective evaluation of these aquifers, identifying the influence of natural and anthropogenic interactions that occur within, as well their effect on the overall groundwater character. A combination of these approaches provides an excellent view of the aquifer, delineating zones to be protected.

The Bafia area is a good region to understand the complexity of crystalline aquifer properties. The rich soils in Bafia favor the growth of different crops and cash crops, especially cocoa, thus encouraging many indigenes and migrants to engage in farming activities. This has led to greater groundwater exploitation from shallow aquifers to meet agricultural, domestic and even industrial needs. Due to the unreliable and erratic nature of piped-borne water in Bafia, more than 80% of the dwellers depend on groundwater (boreholes and hand dug well) and untreated, raw surface water for drinking and other domestic activities. However, the changing hydro-climatic conditions in the area makes groundwater quantity and quality very unreliable especially during the dry season, when many boreholes fail due to limited recharge in the fractures, while some hand-dug wells dry-up or even collapse, leaving the population in a perplexed state. Additionally, the lack of relevant information concerning the behavior and potentials of crystalline aquifers, coupled with the aggressive exploitation of water from these fast-drying aquifers also intensify the water issues in the area (Enyegue et al. 2014; Boretti and Rosa 2019).

Recent studies in Yaounde (120 km away from Bafia) have revealed an increasing trend of $NO_3^-$ contamination in groundwater and surface water due to improper solid/liquid waste disposal and urban agricultural wastes, hence, placing an urgent need for regular monitoring to ensure future sustainability (Takounjou et al. 2013; Fongoh et al. 2023). Just like in Yaounde, there is also a high rate of open defecation, poor sanitation, and the use of farm yard manure in the peripheries of Bafia, which leach into the shallow aquifers thereby degrading the water quality. Chemical fertilizers (NPK, Urea and ammonium sulfate) and pesticides are also increasingly being used in the farming areas. The relief in this area gradually changes from steeply sloping to gently sloping terrains, with a forest-savannah transition, hence favoring groundwater infiltration, which in most cases is influenced by contamination. Given that shallow groundwater is the main source of water in the Bafia area, it is crucial to systematically evaluate the available resources for sustainability, minimizing environmental degradation, guide water policy makers and above all, protect human and aquatic life. Furthermore, surface water systems are mostly and constantly in close interactions with groundwater. Although very erratic in supply, surface water (the Mbam River) is main source of water which is treated and distributed in the whole of Bafia, hence deserve attention.

Many studies have been carried out in the world with regards to the hydrogeochemical and isotopic characterization of water resources, characterizing groundwater evolution, recharge source/mechanisms, trace element composition and apparent age (Vengosh et al. 2002; Srinivasamoorthy et al. 2008; Khan et al. 2020). Some studies have equally been carried out in parts of Africa, especially in aquifers found within bigger, more populated and urbanized cities, with less attention paid to less developed parts. (Aggarwal et al. 2011; Aghazadeh et al. 2016; Tay 2021; Dieng et al. 2016, Akosua et al. 2022; Mapoma et al. 2017; Bayou et al. 2024; Loehnert, 1998 ; Lapworth et al. 2017). In Cameroon, most of these works have been carried out in the southern part of the country, more specifically in the interlocking Mfoundi-Mefou sub-basins (Takounjou et al. 2013, Ewodo et al. 2012 ; Tabué et al. 2009, 2013 ; Bon et al. 2016; Anaba et al. 2017; Fongoh et al. 2023, 2024), in the Litoral Region especially within the Douala Basin (Kamtchueng et al. 2016, 2022; Boum-Nkot et al. 2023; Wirmvem et al. 2016) the Mount Cameroon area (Ako et al. 2012, Akenji et al. 2023) and the East Region (Menti et al. 2023).

The different scientific studies carried out in the Sanaga Basin, including the Bafia area, have focused on the petrography, petrology and geochemistry of the various rock formations (Bessoles and Trompette, 1980; Noizet 1982; Tchakounté et al. 2017, 2021; Gentry et al. 2021; Ganwa 2022). Some groundwater studies carried out in Bafia (Enyegue et al. 2014, 2020; Ngouokouo et al. 2025) have focused mostly on the geoelectrical investigation of aquifers, groundwater quality and groundwater potential using hydrochemical and statistical methods. Very little or no information exists concerning the isotope composition (stable and radiogenic), the trace element content and the nitrate levels, hence the relevance of the present thesis entitled "Chemical and isotopic characterization of ground and surface water in the fractured crystalline aquifers of the Bafia area, Centre Region-Cameroon: Implications for water management". This study is part of a vast program initiated by the Geoscience Laboratory of Superficial formations and Applications, specialty: Water-Soils and Geotechnical Sciences of the and the Geochemistry and Volcanology Laboratory of the University of University of Yaoundé I, Cameroon and the University of Florence, Italy. This program by the University ensures the assessment, management and protection of groundwater and surface water resources in most of Cameroon's cities.

## 2. Objectives

The main goal of this Ph.D research project (conceived as part of a fully-funded RAF7021 TC project) (funded by the IAEA) is to characterize groundwater and surface water resources in the Bafia area in order to fully understand the origin, recharge, hydrogeochemical processes/evolution and contamination sources. The specific objectives of this Ph.D. research are:

- To assess the natural and anthropogenic factors influencing groundwater chemistry and its usability
- To determine recharge areas/origin, mechanisms and apparent age of groundwater
- To assess nitrate contamination and possible nitrate sources
- Implications for water management

## 3. Thesis outline

This work will be divided into two parts:

**Part I** is divided into three chapters, including the environmental settings of the study area, Literature Review and the methodology used to attain the objectives of the study.

**Chapter I** is the environmental settings of the study area, including the physical milieu (geographic location, climate, hydrography, geomorphology, geology, soils, hydrogeology etc.) and the human and socio-economic aspects.

**Chapter II** is the literature based on the specific objectives

**Chapter III** is the methodology, including reasons for the choice of site, the materials used, field activities, laboratory analyses and data treatment.

**Part II** focuses on the results, interpretations and discussion, divided into three chapters:

**Chapter IV** is the Water chemistry and usability

**Chapter V** focuses on the recharge sources, mechanisms and apparent groundwater age

**Chapter VI** emphasizes on nitrate contamination, source identification and overall implications for water management

# PART I

# ENVIRONMENTAL SETTINGS, LITERATURE REVIEW AND METHODOLOGY

# CHAPTER I: ENVIRONMENTAL SETTINGS OF THE STUDY AREA

## INTRODUCTION

This chapter gives a general outlook of the geographical location, physical, human and socio-economic activities, the climate, vegetation, geology and main geomorphological features of Bafia. It also gives a brief literature review and different techniques used in the evaluation of crystalline aquifers in Africa and Cameroon, with emphasis on the gaps and limitations of each method.

## I.1. Physical settings of the study area

### I.1.1. Geographical location of the study site

Bafia is located in Cameroon West Africa and is bordered by Nigeria to the west; Chad to the northeast; the Central African Republic to the east; and Equatorial Guinea, Gabon, and the Republic of the Congo to the south (Fig. I.1). The administrative capital is Yaoundé, found in the Centre Region.

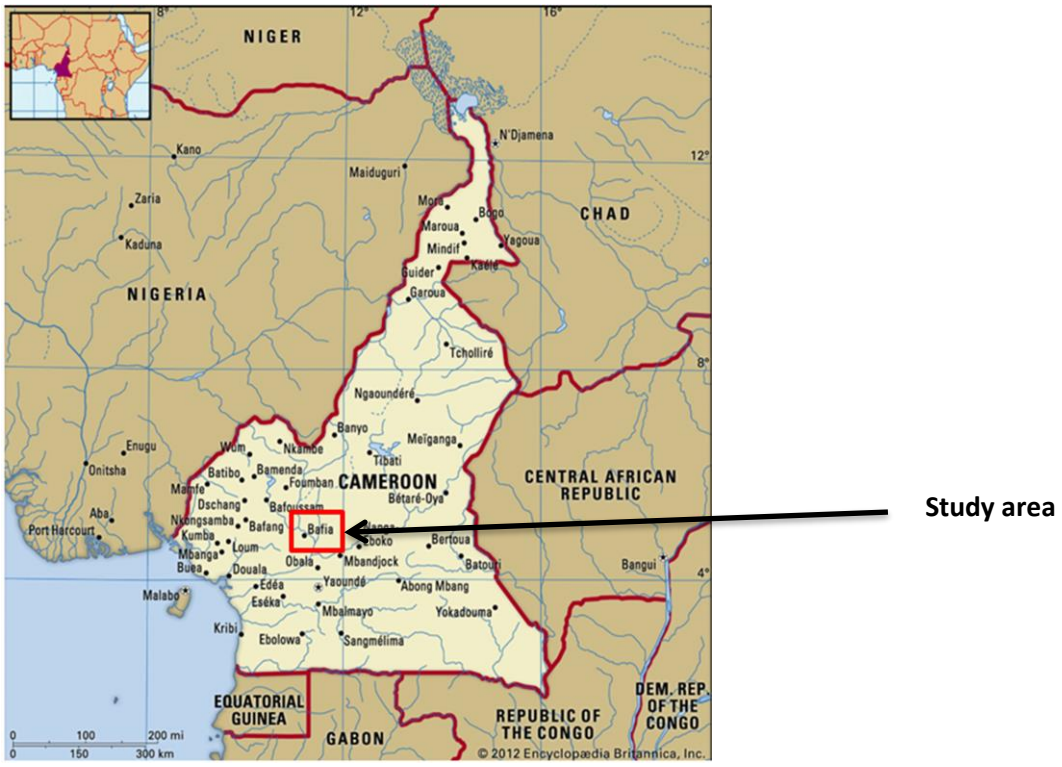


**Figure I.1: Location of study area within Cameroon**

The Centre Region is made up of various divisions, one of which is the Mbam and Inoubou Division, which covers a total area of about 7,125 $km^2$. Bafia is the head quarter of the Mbam and Inoubou Division (extending between latitude 04°20’ and 5°0’N and longitude 10°40’ and 11°20’E). Bafia is located about 120km north of Yaoundé, linked through very accessible roads. The study area (including Bafia and some neighboring villages) lies between latitude 04°30’ and 04°50’N and longitude 11°0’ and 11°20’E, covering an estimated 1200 $km^2$ surface area.

### I.1.2. Climate

The varied relief and coastal settings of Cameroon introduce some climate variability. Cameroon, located in the Gulf of Guinea, basically comprises of eight (8) climatic zones (Fig.I.2), one of the reasons it bears the name Africa in miniature (Olivry, 1986).

Bafia has an equatorial and tropical transitional climate type, with four alternating seasons. Precipitations are frequent in Bafia even in the driest months, ranging from 155 mm to 2000 mm/year (Ngouokouo et al. 2025). The bimodal climate is made up a succession of a long rainy (August–November) and long dry (December–February) followed by a short rainy (March–June) season and short dry (July) Seasons (Enyegue A Nyam et al. 2014; Ngoupayou et al. 2019; Djoufounna et al. 2022; Ngouokouo et al. 2025). Rainfall and temperature data from 2002 to 2022 ploted on the Ombrothermic diagram (Fig. 1.3) shows three dry months (in red), with the rest of the months being humid. The least rainfall is observed in January and the highest in September (Fig. I.3); the lowest temperatures are recorded in August (22.7°C) and the highest in February (25.5°C). During the night, temperatures drop to the coldest point of 20°C in August.

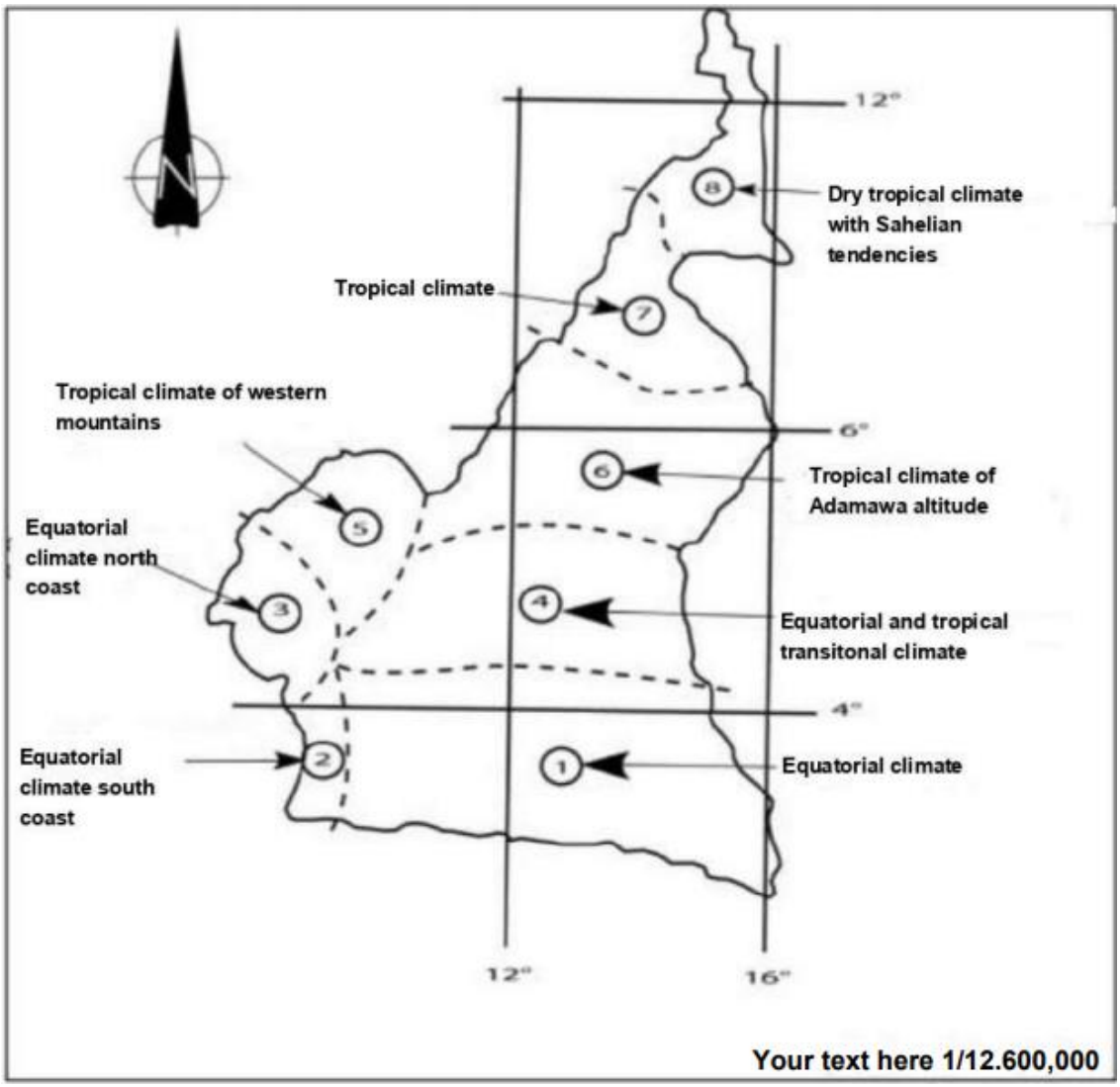


**Figure I.2: Principal climatic units of Cameroon**

**(Olivry, 1986; Sighommou, 2004)**

Humidity levels in Bafia increase progressively from the start of the year, from 62% in January to about 98% between July and September, after which it decreases again to about 67% in December. The maximum relative humidity throughout the year varies between 85 and 95%, with the minimum between 60 and 74% (Jiofack et al. 2013). Visibility generally fluctuates throughout the year, from the lowest of 5km between July and September, to the highest at 9km during the months of January, February, March, and from November to December.

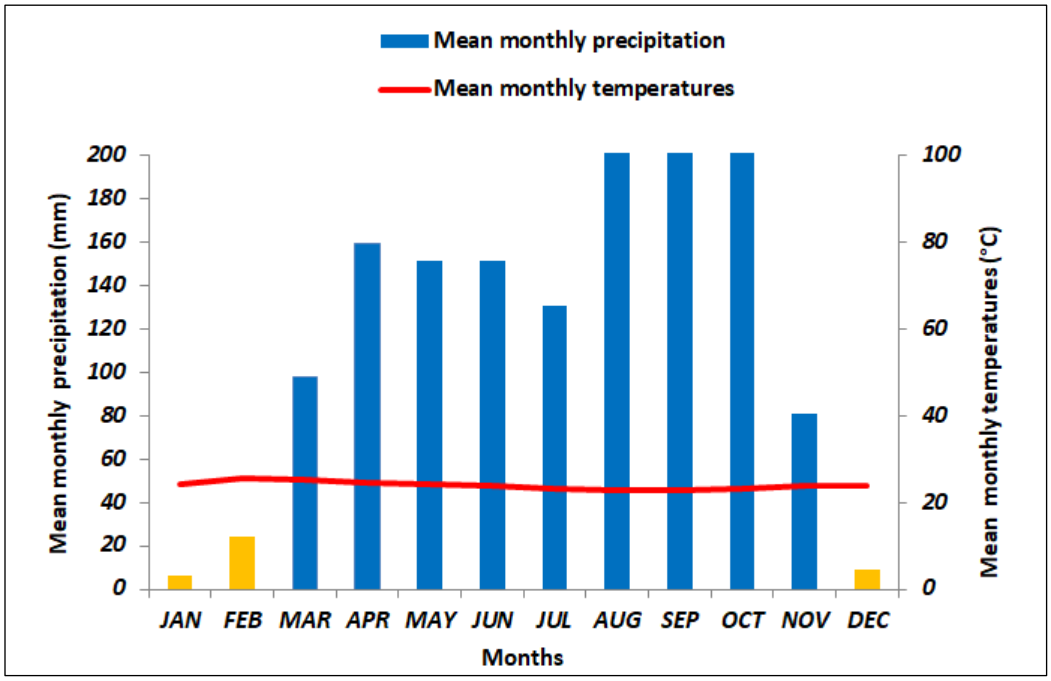


**Figure I.3: Ombrothermic diagram showing three months of no rain (NASA Power Data Access Viewer, Bafia 2002 to 2022)**

### I.1.3. Vegetation

The vegetation in the most part of the country is made up of dense forest. Climatic formations and human activities have modified this vegetation to the savannah type in some areas (Segalen, 1967). The vegetation varies from the savannah-type in the Sudano-Sahelian zone in northern Cameroon to the forest type in the southern part (Fig. I.4). The Mbam and Inoubou Division is located between the forest-savanna transition zone, otherwise known as the Sudano-Guinean post forest domain which generally favors agriculture and, because of its latitudinal location, the forest in this area is easily converted to savanna (Embom et al. 2024). It is a transition zone between the dense, evergreen rainforests in the south and the more open, tree-dotted savannas in the north. This transition creates a unique mix of plant and animal species adapted to varying ecological conditions. Like many ecosystems worldwide, the Guinean forest-savanna mosaic of the Bafia area is susceptible to climate change impacts like altered rainfall patterns and increased temperatures.

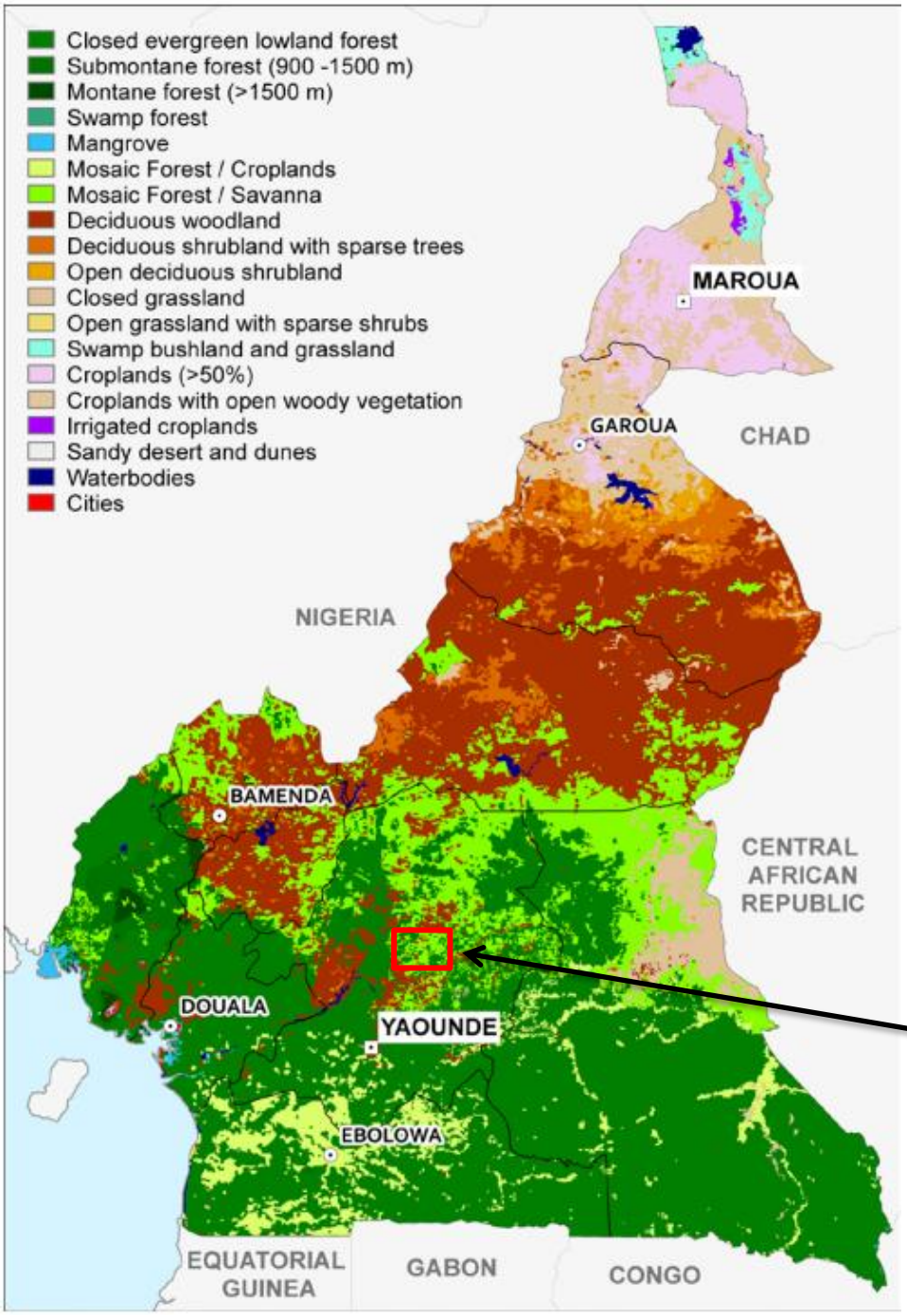


**Figure I.4: Vegetation cover in Cameroon**

**(Source: Interactive Atlas of forestry resources of Cameroon, version 2.0. Cameroon Ministry of Forestry and Fauna/ World Resources Institute 2007)**

### I.1.4. Hydrographic system in the study area

Cameroon has several major rivers, including the Sanaga, Wouri, Benue, and Logone. One of the most important hydrographic networks in Cameroon is the Sanaga River. It is about 920 km long; it covers a surface area of about 133,000 $km^2$ running through six regions in Cameroon which are the Adamawa, East, Centre, North West, West and Littoral Regions. It takes its source from the Adamawa plateau (between altitudes between 1000 m and 1200), with main tributaries being the Lom in the south and the Djerem in the north. Three main divisions are distinguished in the Sanaga River namely: the upper Sanaga dominated by the Djerem and Lom Rivers in Adamawa; the middle Sanaga with the Mbam River being the major tributary; and the lower Sanaga after the Edea hydroelectric dam right to the Atlantic Ocean (Embom et al. 2024).

Different minor water bodies like the Gamba, Nguen, Bohboro and Ronfi flow throw the town of Bafia, but the Mbam River forms the biggest hydrographic network (Fig. I.5). The Mbam River has a total length of 548 km and covers a total drainage basin of 42, 300 $km^2$, with an average annual flow of 750$m3/s^2$. It represents almost one third of the entire area covered by the Sanaga watershed – about 133,000 $km^2$ (Ngoupayou et al. 2016). The Mbam originates in the northern savannah region of the Adamawa Plateau and flows through the transitional forest–savannah mosaic surrounding Bafia before joining the Sanaga River. It drains the entire western part of the basin, with the Noun as its main tributary. It flows through the Tikar Plain for about 120 km and then receives the Mapè, the Vi, the Noun tributaries on the right bank, and the Kim on the left bank. The right bank tributaries originate from the western high volcanic peaks, specifically the slopes of Mount Oku and they in turn drain the Tikar Plain, the Bamoun Plateau, and the Ndop Plain.

### I.1.5. Geomorphology

Cameroon has a much-diversified geomorphology, presenting different landscape forms, from coastal plains to high volcanic mountains and plateaus resulting from different tectonic events (Segalen, 1967; Viennois et al. 2022). The geomorphology of Cameroon, as partially described by Segalen (1967), is made up of seven units, with marked differences from one region to another. Bafia is found within the interior surface and has a relief that gradually changes from steeply sloping to gently sloping terrains, between 300 and 1100m, with an average altitude of 497m.

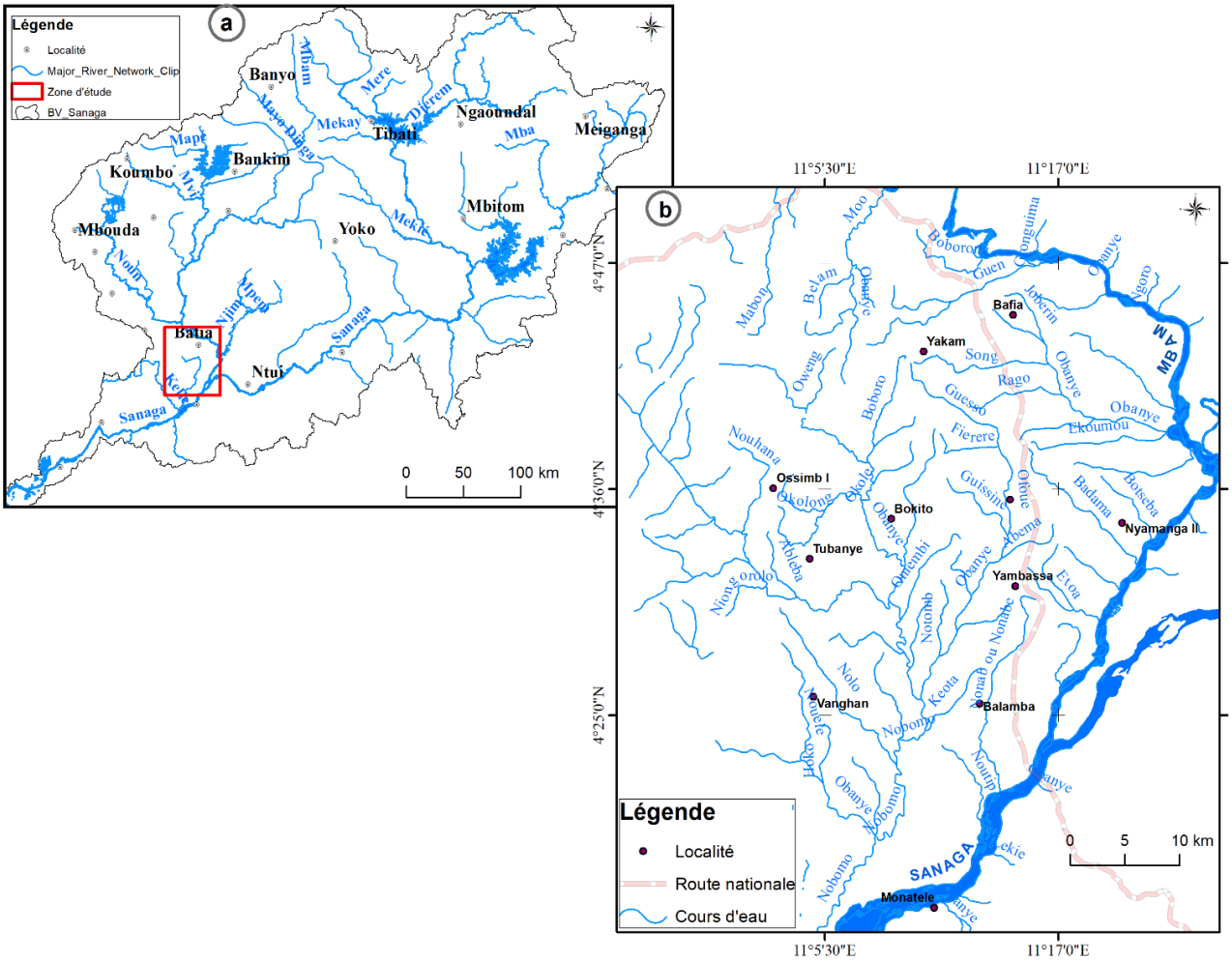


**Figure I.5: Hydrographic section of the Sanaga Basin and the Mbam River (Olivry, 1986 modified by MINEE/GWP Cameroon, 2009)**

The morphology distinguishes three main reliefs depending on their altitude:

- High rectilinear reliefs, roughly parallel, with a NNE-SSW orientation like the Konne-Madon and Bapé massifs, with altitudes ranging between 900 and 1100m;
- Medium hills of altitudes between 600 and 700m. They are inselbergs located in variable directions: N-S to NE-SW at the edge of the massifs and WSW-ENE to W-E north of the Mbam.
- Plains (plateaus) like the Bafia-Ombessa plain East of Bapé, the Mo'O plain between Bapé and Kon-KidouméKon-Madang, the Mabonne plain West of the Kon-Kidoum/Kon-Madang chain and the Etoundou plain located West of the Mbamokoute

plain ( Vallerie, 1973). The low plain corresponds to the lower Mbam valley and the Sanaga valley between the Nachtigal and Kikot waterfalls (Fig. I.6).

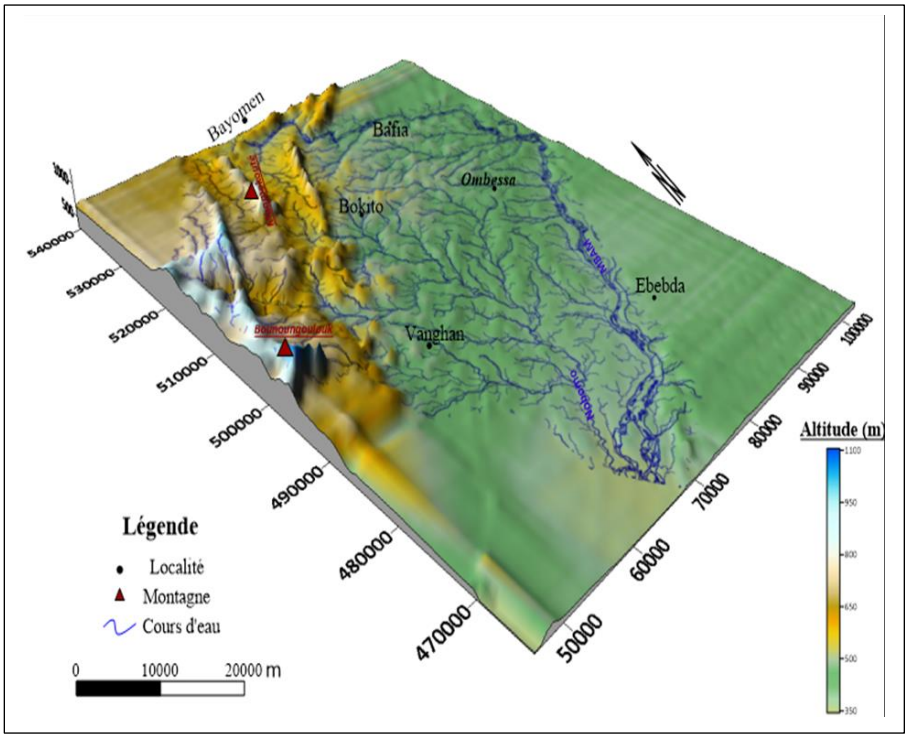


**Figure I.6: 3D Geomorphological map of the Bafia area with elevations ranging from lowlands (Bokito) to high hills (Bapé granitoids)**

## I.1.6. Geology

### I.1.6.1. Lithology

The Pan-African Belt of Central Africa (PBCA) includes three lithotectonic domains (Fig. I.7) in the Cameroonian territory namely: (1) the Poli group (North domain), (2) the Adamawa-Yadé domain (Center Domain) and (3) the Yaoundé group (South Domain) (Tchakounté et al. 2017; Toteu et al. 2004). The Yaoundé and the Adamawa-Yadé domains are made up of high-grade metamorphic rocks with a wide range mineral assemblage (Tchakounté et al. 2007).

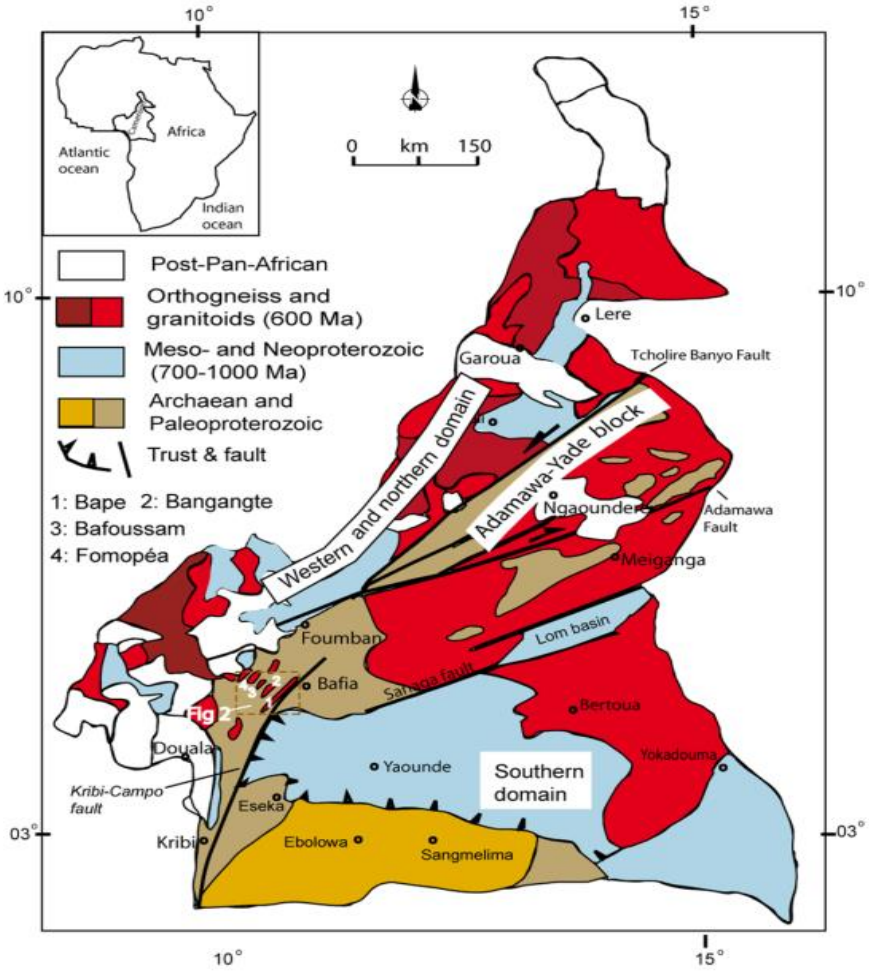


**Figure I.7: Geologic map of Cameroon showing the different rock types (Tchakounté et al. 2021)**

Previous studies (Bessoles and Trompette, 1980; Noizet 1982) assumed Bafia to be part of the bigger Yaoundé group, but after several studies (Tchakounté et al. 2017; Gentry et al. 2021; Ganwa 2022), it was established that it is a separate litho-structural group, forming the southernmost termination of the Adamawa- Yadé Domain of the Central African Fold belt in Cameroon. It is considered as a piece of the Archaean/Palaeoproterozoic crust detached from the Congo craton in the early Neoproterozoic times (Ganwa et al. 2008; Tchakounté et al. 2017).

The Bafia group, as defined by Noizet (1982), contains older basement rocks overthrusted towards the south above the Yaoundé group. It is composed of granitoids, trapped in a meta-

sedimentary complex (Dumort 1968; Tchakounté et al. 2007). These formations underwent metamorphism, followed by sedimentation, magmatism, and finally Neoproterozoic metamorphism, which led to the formation of the Bapé massif (Tchakounté et al. 2017). The low to high-grade meta-sediments (shales, volcanogenic greywackes, associated with minor dolomitic rocks, evaporitic and iron-rich sediments, quartzite and gneisses) were thrusted onto the Congo craton (Toteu et al. 2004; Tchakounté et al. 2017; Gentry et al. 2021).

The Bafia area is mostly made up of metamorphic rocks, mainly orthogneisses, amphibolites, micaschists, granitoids, and quartzites, with some NNE-SSW stretching structures underlain by quartzites (Fig. I.8). The gneisses are amphibole-biotite gneiss, garnet-biotite gneiss, biotite gneiss and the two-mica gneisses. The schist present was formed from clay or limestone sediments, while the mica-schist is assumed to have been formed on top of the chlorite-schist. The primary minerals of the schist include muscovite, biotite, quartz and garnet; disthene, rutile and ilmenite are secondary minerals (Tchakounté et al. 2021).

### I.1.6.2. Soils

Climatic, geological, and topographic variability in Cameroon has resulted in the formation of different soil types, from one region to another (Kamga et al. 2016) (Fig. I.9). They generally include lateritic soils, volcanic soils, Ferralitic soils, Alluvial soils, Vertisols, Arenosols, sandy soils and cambisoils, to name a few.

Bafia is dominated by ferralitic soils, which are advanced soils developed on crystalline and crystallophyllous bedrock. Mineralogically, they are composed of kaolinite, iron and alumina hydroxides. (Segalen, 1967). These soils have low thicknesses due to the erosion that perpetually scours their upper parts. They are moderately de-saturated, with low exchangeable bases, mainly the sandy loam and the sandy-clay-loam groups, with an increasing clay content with depth (71% sand within the first 30 cm) (Vallérie, 1973; Jiofack et al. 2013; Leumbe et al. 2022; Ketchiemo et al. 2024).

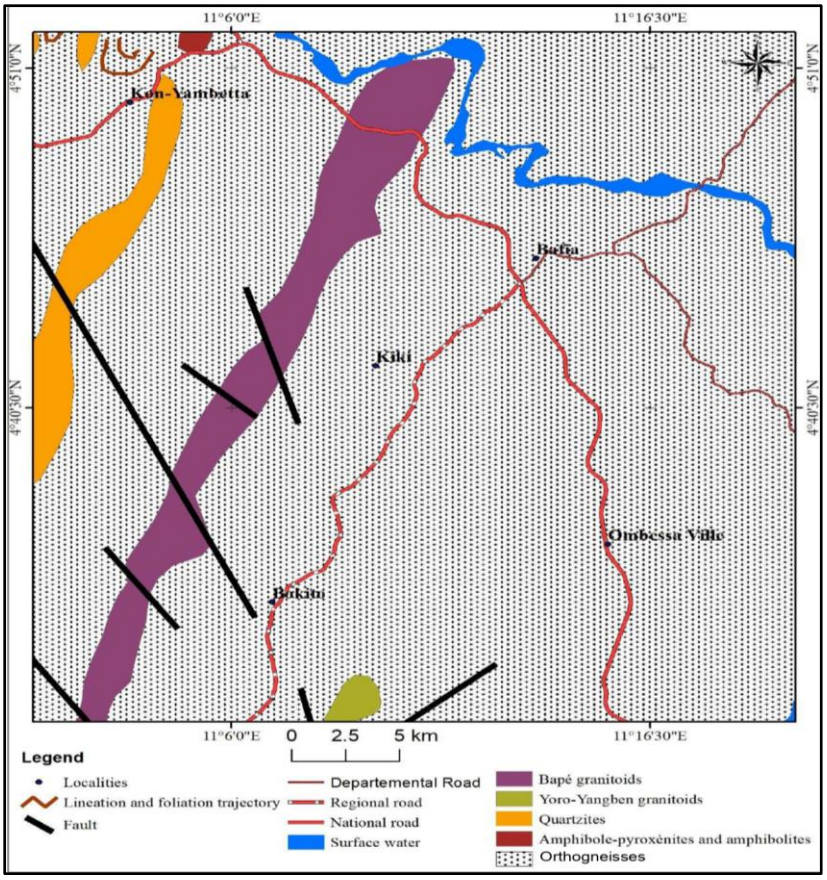


**Figure I.8 - Geologic sketch map of the Bafia area showing some lineaments, the Bape granitoids along with main lithological units**
**(Modified after Tchakounté et al. 2017)**

The sandy fraction of the soil allows for easier root penetration and good aeration, while the clay and silt content contribute to nutrient retention. The crystalline bedrock detected at depths between 17 and 50 m is overlain by an irregular alterite interval up to 50 m thick, showing a variable amount of clay contents (Tamehe et al. 2019). The pH is slightly acidic (between 5.5 and 6) while the soil organic matter is relatively high (6.14%) reducing with increasing depth (Ketchiemo et al. 2024).

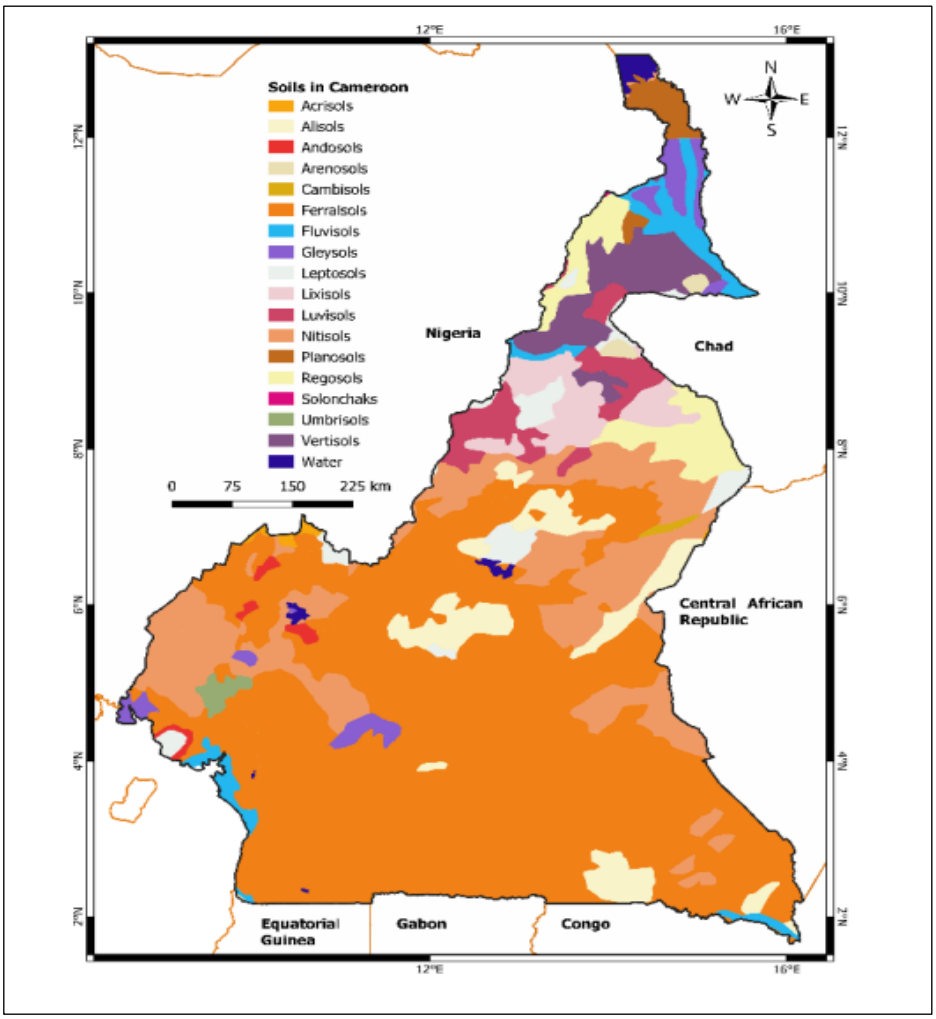


**Figure I.9 - Majors soil types in Cameroon**

**(Modified from Jones et al. (2013)**

### I.1.6.3. Hydrogeology

Hard rocks make up the basement of the continents and, as such, outcrop over large areas throughout the world (namely a large part of Africa, South and North America, India, Australia, etc.) mostly in tectonically stable regions such as ancient cratons. Crystalline rocks are generally characterized by negligible porosity and permeability in terms of groundwater exploitability (Ngoupayou et al. 2019). However, alteration processes (i.e, weathering, which is said to have more positive impacts on the fractured rock permeability than tectonic activities) happening within the first 10–100m depth introduce fractures which can be very permeable, depending on the depth and other factors (Lachassagne, 2011; Tabué et al. 2021). About 90% of the Cameroonian territory is made up of crystalline basement rocks and the rest is covered by

sedimentary and volcanic terrains (Ondoa, 2009). They typically form small, local and poorly productive aquifers, limited to areas where the rock has been fractured and/or weathered to increase its permeability (Fig. 1.10).

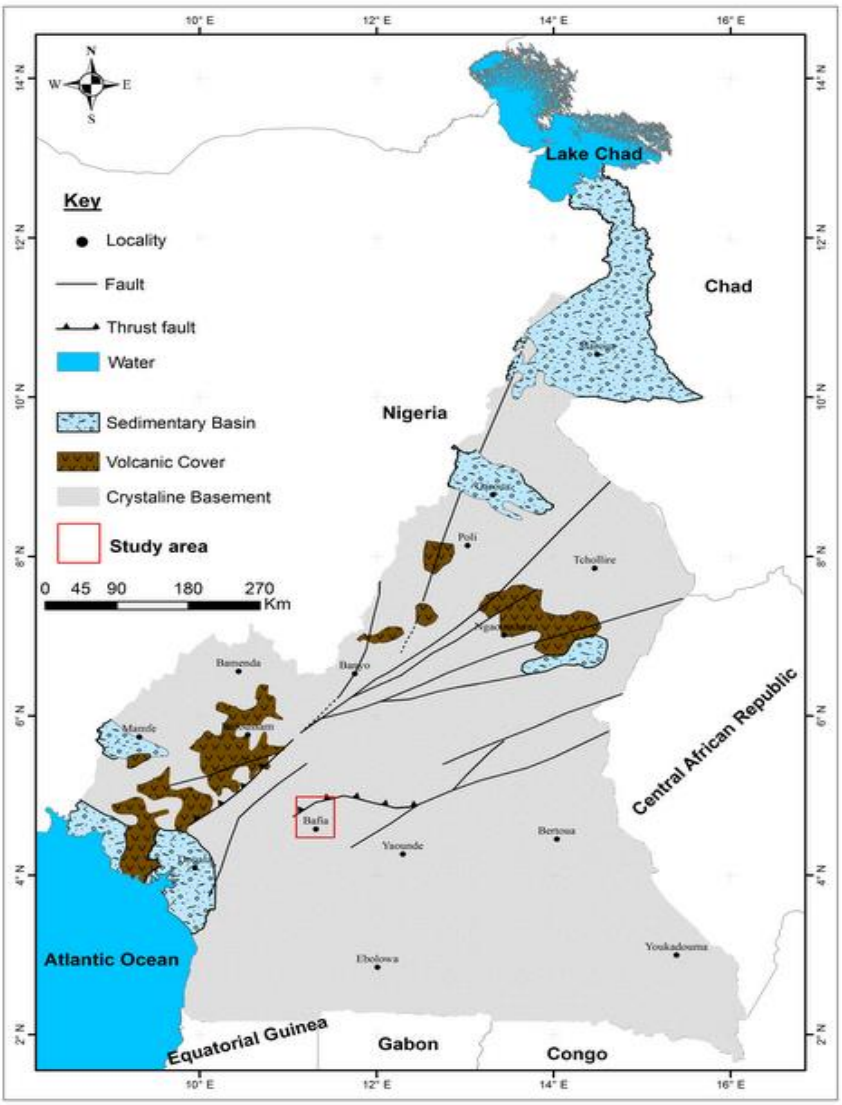


**Figure 1.10 Groundwater didstribution in Cameroon**

Modified after Defo et al. (2016)

In a composite aquifer like would be the case of Bafia, most of the groundwater flow occurs in the water-bearing fracture zones at the base of the regolith (lower saprolite) and in the saprock layer, while the upper saprolite provides significant groundwater storage due to the high

porosity, allowing water to drain towards the underlying productive zone (Lachassagne et al. 2021). The saprock transitions into a layer of relatively unaltered rock with significant fracturing, whose density reduce with depth (Lachassagne et al. 2021). A typical weathering profile of crystalline rocks is show in Fugure I.11a (lachassagne P. and R. Wyns, 2005).

Some borehole pump tests in the Centre Region of Cameroon, including Bafia, revealed five water strikes which represent the hydraulically active fractures, but the most important being the first strike ranging between 5 and 74m and these ties with results of studies carried out in other parts of Africa (Davis and Turk, 1964; Enyegue et al. 2014; Anaba et al. 2017;). The borehole depth in most parts of Bafia is between 39 and 80m, while shallow hand-dug wells are located in the weathering depth between 4 and 20m. Productivity of these wells decreases with depth (above 60m, there is a marked decrease) due to the closure of fractures and hence lower permeability. Amongst the schist, gneisses and quartzites found in the Bafia area, the schist are the most productive, their productivity is closely linked to their proximity to and density of lineaments, orientation of the fractures, nature and thickness of alterites, drilling depth, rainfall, topography and lithology (Anaba et al 2017; Tabué et al. 2021).

The hydrogeology of the Centre Region of Cameroon is marked by the presence of two types of aquifers: one of them in the weathered saprolite zone and another in the fractured crystalline bedrock (Enyegue et al. 2014; Anaba et al. 2017). Geoelectric sounding in the Bafia area reveals 4 main geoelectrical layers, namely: the top soil (between thickness of 0.1 and 6.6m, consisting of soil water, vadose zone, capillary fringe), the sandy clay (thickness between 0.9 and 48m, mostly the saprolite), the shale layer (the saprock) and the fresh bedrock (Enyegue et al. 2014), with a few borehole points demonstrated in Fig I.11b. The electrical resistivity of the area showed high resistivity at 4.4m, correlating with depths of about 3m which correspond to the topsoil layer. This is followed by a much lower resistivity at about 58m that correlate with depths of about 40m, corresponding to the water-bearing layer.

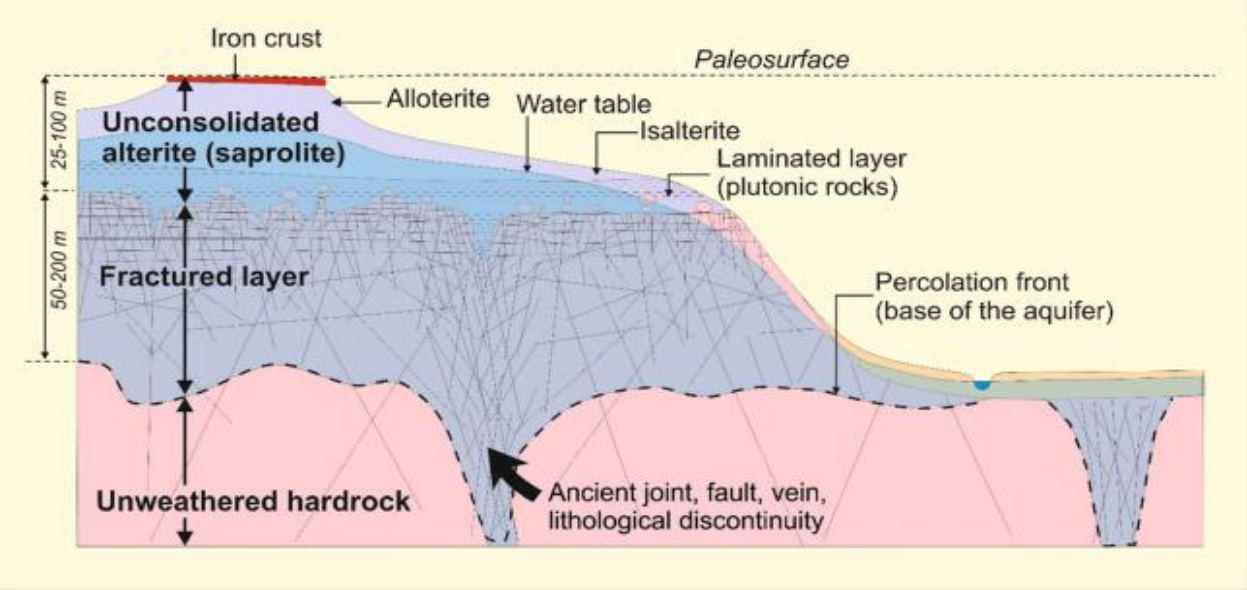


**Figure I.11a: Typical weathering profile developed on basement rocks (LACHASSAGNE and WYNS, 2005)**

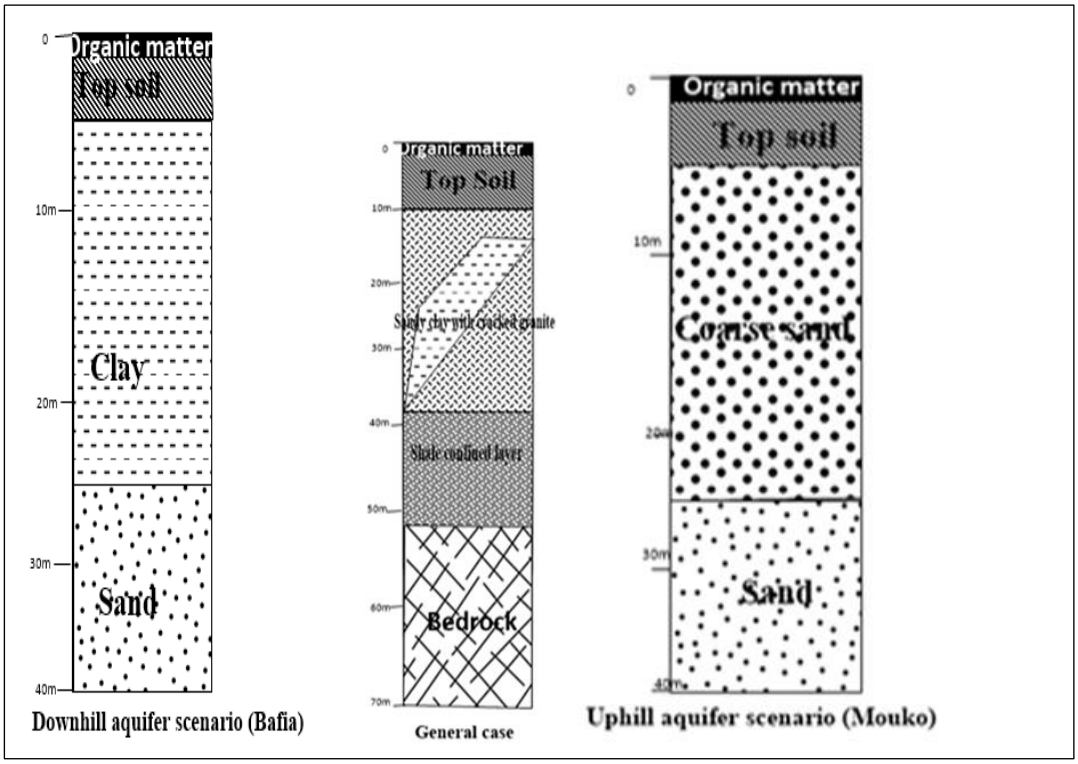


**Figure I.11b: Lithostratigraphic sections of some boreholes in the Bafia area showing the different lithological layers (Modified after Enyegue et al., 2014)**

Unlike other localities, the hydraulic conductivity of Bafia aquifers generally ranges between 4.5 and $6*10^{-6}$ m/s, with low transmissivity and discharge rates (Enyegue et al. 2014). Most of the wells in this area (hand dug or boreholes) easily dry up during the hottest part of the dry season. This could be partly because of the thin saprolite unit (< 7 m thick in most cases), which is presumed to be the water reservoir to supply the aquifers (Embom et al. 2024).

## I.2. Human and Socio-economic aspect

### I.2.1. Population and urbanization

In 1976, Cameroon had a population of 7,663,246. In 1987, the population was 10,493,655 inhabitants. In 2005, the final results of the 3rd Census of Population and Housing (RGPH) showed a population of 17,463,836 and the population is estimated today at 29.3 million people. This demographic trend confirms the country's continued high human potential, with an average annual population growth rate of 2.8% over the period 1987-2005 and 2.6% between 2005- and 2010 (BUCREP, 2010). According to the census conducted in 2005, Bafia had approximately 55,505 inhabitants. Based on the Community-directed census in 2014 (CDD), this number significantly increased to about 226,073 inhabitants (Kamga et al. 2016), thus ranking Bafia as the third largest city in the Centre Region after Yaoundé and Mbalmayo.

In the Sanaga watershed, rapid urbanization is noticeable in major towns like Bafoussam, Bafia, Yaoundé, Edéa and Douala due to different livelihood activities tied to the Sanaga River. Owing to rural exodus, these areas can reach densities up to 6,340 inhabitants per $km^2$. Hence, deforestation, uncontrolled constructions and development plans are on an increase in the Bafia area. This constant urbanization can be at the root of the phenomenon of waterproofing of the soil, thus limiting the infiltration process.

### I.2.2. Agriculture

Cameroon in general, is considered to fall within the low to middle income class, with agriculture being the main source of livelihood for over 60% of the population, accounting for about 23% of the Gross Domestic Product and two thirds of the labor force (Goufo, 2008). Bafia is one of the many different agricultural hubs in Cameroon. Being one of the main food suppliers in the Centre Region, many farmers are increasingly adopting the habits of fertilizers and pesticide application on constantly leached ferralitic soils in order to enhance crop yield Rapid

urbanization extending outwardly, has drawn many farmlands closer to human habitations thus increasing the risk of groundwater contamination by agrochemicals used on farmland. Some households in Bafia also engage in livestock farming, including raising goats, poultry, and pigs. This complements their agricultural activities and provides additional income. Between the months of November and May each year, some nomadic pastoralists migrate to the Bafia area with their cattle, where they end up selling and repeat the cycle in the upcoming year (Kamga, 2016).

### I.2.3 Land use and land cover

According to the Food and Agriculture Organization (FAO), Land cover refers to the observed physical and biological cover of the earth's land. Land can be covered by various forms of vegetation, grasslands, scrubs, water bodies, bare soil, built-up-areas etc. On the other hand, Land use is as "the total of arrangements, activities, and inputs that people undertake in a certain land cover type" (FAO/UNEP, 1999). The increasing practice of the slash and burn agriculture, cutting of fuel woods, burning of woods for charcoal, mining, infrastructure and urbanization are the main drivers of land use land cover changes in Cameroon.

Land use/land cover data obtained for the Bafia area from 2013 to 2023 (20 years) show the following five main land uses, with gradual yearly changes (Table 1.1): Surface water, Forest, built-up area, Agriculture (growing area) and others (Bare soils and rocks). The data show a major decline in forest land, while Agriculture, Bare soil/rock, Settlement and Surface water areas greatly increased (Fig. 1.12).

***Table 1.1: Land use/Land cover changes in the Bafia area from 2013 to 2023***

| | | **Lulc_2023** | | | | | |
|---|---|---|---|---|---|---|---|
| **Lulc_2013** | | Others | Surface water | Forest | Built-up | Agriculture | **Grand Total** |
| | Others | 2158.179 | 321.320 | 12855.187 | 394.976 | 2202.259 | 17931.921 |
| | Surface water | 378.870 | 2805.364 | 4333.704 | 356.914 | 505.500 | 8380.352 |
| | Forest | 456.146 | 1013.881 | 35908.032 | 1152.693 | 4740.450 | 43271.202 |
| | Built-up | 410.525 | 152.035 | 3386.969 | 2736.517 | 2692.232 | 9378.278 |
| | Agriculture | 4876.530 | 1149.639 | 16206.445 | 5911.155 | 12959.187 | 41102.957 |
| | **Grand Total** | **8280.250** | **5442.239** | **72690.337** | **10552.255** | **23099.628** | **120064.709** |

**Source: Landsat 8 and 9 (2013 and 2023)**

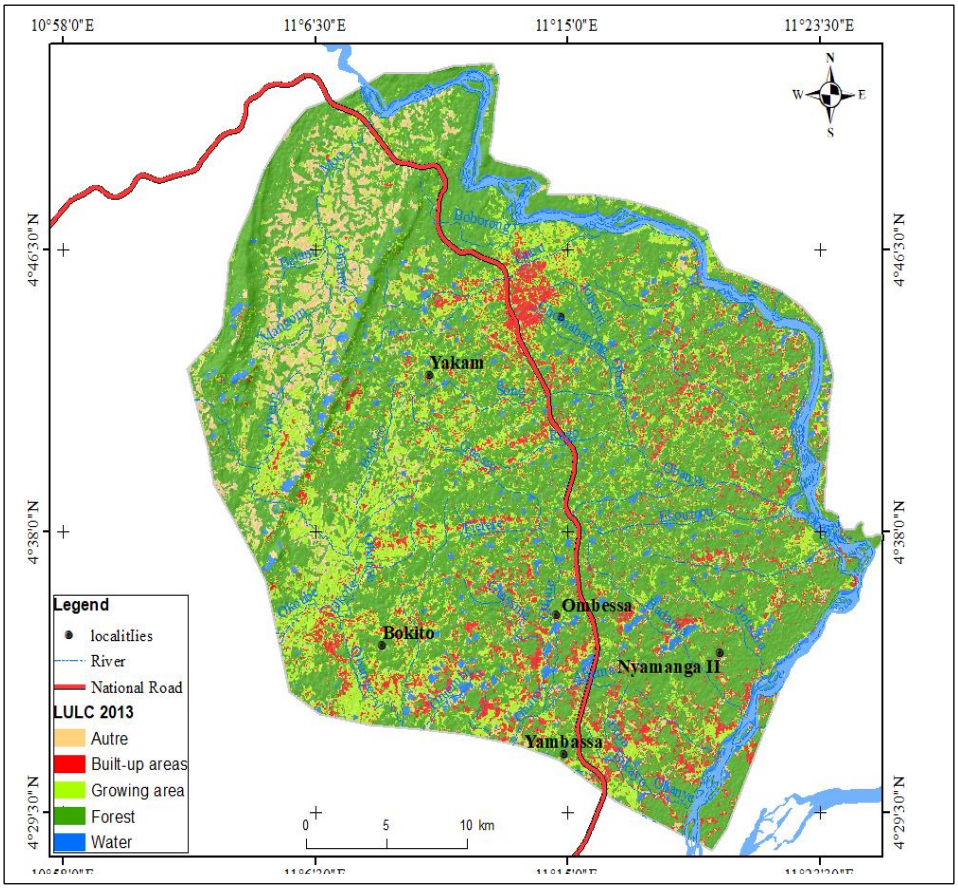


**Figure I.12a: Land cover/land use map of the Bafia area in 2013**

**Source: Landsat 8 and 9, 2013 and 2023**

The forest area greatly increased from 43,271 hectares in 2013 to 72,690 hectares in 2023, about 40% increase. This is possible through indirect reforestation of cocoa plants and other fruit trees for extra income. The major promoters of forest decline are human activities like felling of trees for firewood, construction, and charcoal production. However, unconscious and conscious reforestation occurs when farmers plant trees to shade their cocoa plants. There has been an increase in settlements area from 9,378.3 hectares in 2013 to 10,552.2 hectares (11% increase) in 2023. Pressure from the growing population and urban expansion are the main factors promoting the increase in settlement areas over the past years. Interestingly, agricultural land decreased from 41,102.9 hectares in 2013 to 23,099.6 hectares in 2023 (78% decrease).

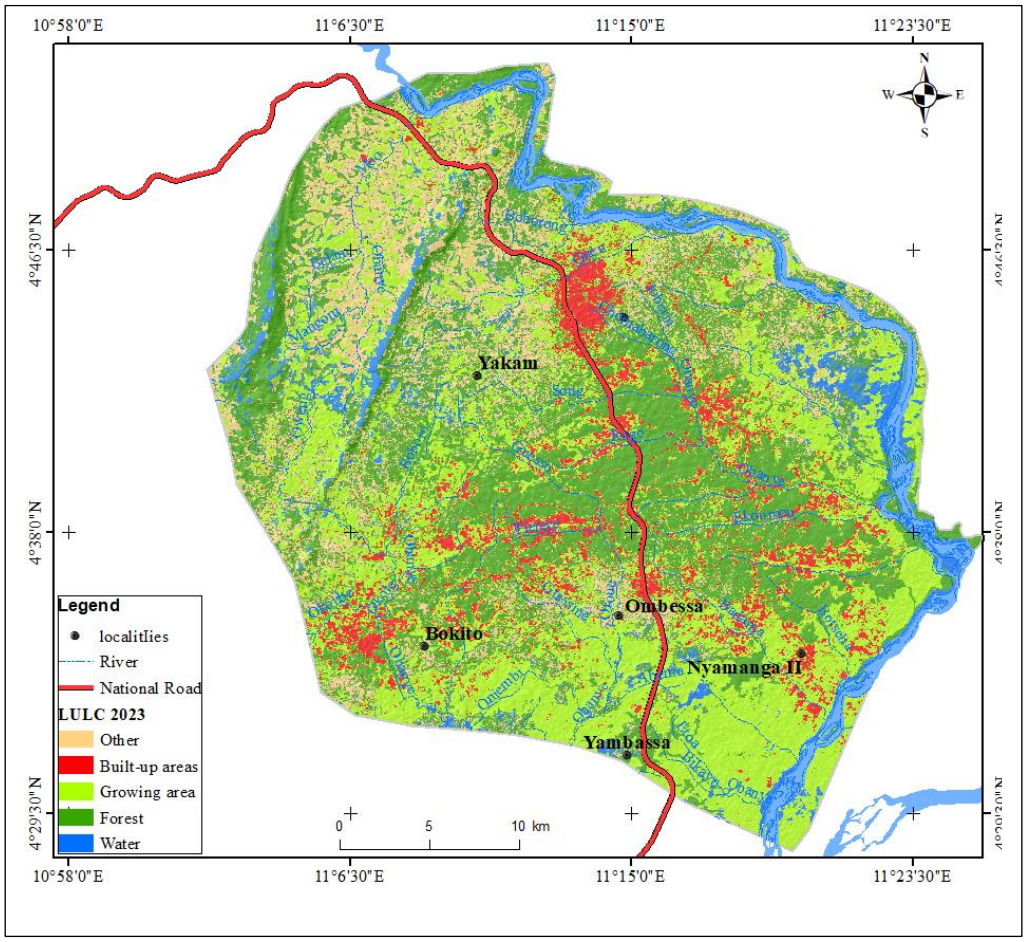


**Figure I.12b: Land cover/land use map of the Bafia area in 2023**

**Source: Landsat 8 and 9, 2013 and 2023**

In as much as more land is required to for sustainable agriculture, local population explosion and inter-regional migration come with increased housing demand, thus the decrease agricultural land to build more habitations. There has been a decrease in Surface water total area from 8,380.4 hectares in 2013 to 5,442.2 hectares in 2023, a total 54% decrease. Many rivers and stream have been obstructed through land reclamation and urban construction, thereby narrowing their courses. Other land which is either bare soil or rocky areas decreased from 17,931 hectares in 2013 to 8,280 hectares in 2023, demonstrating pressure on the land to meet other human needs.

## CONCLUSION

Bafia is located in the Centre Region of Cameroon. It is the capital of the Mbam and Inoubou Division. It has an equatorial and tropical transitional climate with four alternating seasons and located within the forest-savannah transition zone. It is well watered by several streams, with the Mbam River (a major tributary of the Sanaga River) constituting the main drainage system in the area. The relief is gently sloping, with some low hills, high hills and plateaus. The geology is mainly made up of metamorphic and meta-sedimentary rocks upon which the moderately de-saturated ferallitic soils have developed. Two main aquifers are identified in the Bafia area, namely; the shallow unconfined aquifer located in the weathered lateritic layers and the deep fractured aquifers which develop within the metamorphic basement rocks. Agriculture (Cocoa, corn, cassava, groundnut, plantain, banana, cocoyams etc) is the main source of income for the inhabitants of Bafia, besides other activities like small scale businesses, fishing, and animal farms.

# CHAPTER II: LITERATURE REVIEW

## INTRODUCTION

Groundwater resources hosted in fractured crystalline basement aquifers constitute a major source of water supply in many parts of the world, especially in sub-Saharan Africa (Lapworth et al. 2017). In such geological environments, the occurrence, movement, and quality of groundwater are mainly controlled by the degree of weathering and the existence/development of fracture networks. Understanding the hydrochemical and isotopic characteristics of these aquifers is therefore priority in assessing groundwater origin, evolution, and usability.

Previous studies around the world have illustrated that groundwater chemistry in fractured crystalline aquifers is primarily influenced by water–rock interaction processes, including silicate weathering and ion exchange (Hem, 1985: Appelo and Postma, 2005). Additionally, isotopic techniques-especially the use of stable isotopes of oxygen and hydrogen-have been very effective in identifying groundwater recharge sources, infiltration mechanisms, and the role of evaporation (Craig, 1961; Clark and Fritz, 1997). Other tools like the tritium content (Adomako et al. 2011; Ako et al. 2012) and the dual nitrogen isotope techniques (Mayer et al. 2001; Bourke et al. 2019) have been used in diverse studies to attempt groundwater age and to trace the source of nitrates in groundwater. These tools provide complementary information that enhances the understanding and interpretation of hydrogeological processes in complex basement terrains.

Despite the increasing application of chemical and isotopic toold in groundwater studies, their integrated use remains limited in many parts of Cameroon, especially in the Bafia area. Existing studies in the Centre Region of Cameroon have focused largely on the hydrochemical characterization of the shallow groundwater resources (Kuitcha et al. 2012; Takounjou et al. 2020), the estimation of groundwater recharge within te Anga'a watershed (Takounjou el al. 2010), the isotopic content of water resources and the sustainable management of these resources (Wirmvem et al. 2016; Fongoh et al. 2023). s area have largely focused on the geology, groundwater availability, quality and borehole productivity, with comparatively less emphasis on recharge sources/processes, and vulnerability (Ganwa et al. 2008; Tchakounté et al. 2017; Enyegue et al. 2014, 2020; Ngouokouo et al. 2025). This chapter therefore reviews relevant literature on fractured crystalline aquifers, hydrochemical processes, isotopic applications in

groundwater studies, and groundwater management practices. The aim is to establish the scientific context of the study and to identify gaps in knowledge that justify the objectives and methodology adopted in this research.

## II.1. Natural and anthropogenic factors influencing groundwater chemistry and its usability

Despite being a crucial water resource for domestic and agricultural purposes, groundwater chemistry and quality within the Bafia crystalline aquifers are strongly influenced by both natural geochemical processes (mineral weathering, ion exchange, redox reactions, residence time, evaporation, mixing) and anthropogenic pressures (fertilizer leaching, on-site sanitation, urban runoff, mining, over-abstraction). Understanding these factors is essential for evaluating groundwater usability and facilitates the implementation of management strategies (Appelo & Postma, 2005; Edmunds et al., 2003).

### II.1.1. Natural factors influencing groundwater chemistry and its usability

#### II.1.1.1. Geological and hydrogeological controls

Crystalline aquifers are mostly buried under thick weathered/fractured bedrock and saprock that typically extends up to 50 m deep. Saprock is a fractured and fissured rock issued from extensive fracturing and slight in-situ weathering of bedrock. It is usually characterized by vertical, sub-vertical, and sub-horizontal fractures. Aquifers found in the saprock are different from those in sedimentary terrains; they display low porosity due to the nature of the basement lithology, but the permeability can increase if there is good connectivity and high density of fractures (Drew et al. 2001). Hydro-geophysical studies and pumping/tracer tests carried out in crystalline aquifers around the world (Clément et al. 2014; Enyegue et al. 2014; Anaba et al. 2017) demonstrate that groundwater flow at depth depends on rock porosity, fracture aperture distribution, connectivity of the fracture network, drilling depths, weathering depth, rock type, topographic settings and proximity to the lineaments. These studies also show that connected fractures produce rapid flow with less-evolved chemistry while isolated and deep fractures have less-rapid flow with more evolved groundwater signatures.

This structural complexity of crystalline aquifers implies that the nature of flow behavior is highly complicated and often challenging to constrain. Consequently, the origin and chemical composition of groundwater in these aquifers often vary greatly, depending not only on permeability properties of the aquifer matrix, but also on rock mineralogy, residence-time, as well as the proximity to the surface, composition of precipitation, climate, topography and anthropogenic source influences (Gibbs, 1970; Hem, 1989). More than 90% of Cameroon's groundwater is hosted in crystalline aquifers, some of which have been studied like in the Centre Region (Ondoa, 2009; Enyegue et al. 2014; Anaba et al. 2017; Wirmvem et al. 2016; Bon et al. 2021; Fongoh et al. 2023), the North West Region (Wirmvem et al. 2017), the East Region (Menti et al. 2023), the West Region (Zakari et al. 2021), the Mount Cameroon area (Ako et al. 2012; Akenji et al, 2023) and the North Region (Jokam et al. 2022).

The crystalline basement complex of Bafia is composed primarily of orthogneisses, amphibolites, micaschists, granitoids, and quartzites (Tchakounté et al. 2017; Gentry et al. 2021; Ganwa 2022). These lithologies are relatively impermeable, and groundwater occurs mainly in secondary structures such as fractures and weathered zones (Lachassagne et al. 2021). The interaction of infiltrating water with these mineral assemblages largely alters the chemical composition of groundwater (Appelo & Postma, 2005). In the Bafia area, major ionic constituents such as $Ca^{2+}$, $Na^{+}$, $Mg^{2+}$, and $HCO_3^{-}$ originate from silicate weathering reactions involving feldspars, micas, and amphiboles. Moshood et al. (2014) and Akpataku et al. (2019) in Nigeria and Togo reported similar geological influences over water chemistry in crystalline terrains. Ako et al. (2012) and Fongoh et al. (2023) reported that the dominant hydrochemical facies in similar basement terrains of the Banana Plain and Yaounde are Ca–$HCO_3$ and Na–$HCO_3$ types, indicating the predominance of natural interactions between rock and water.

Previous studies carried out in Bafia focus mainly on the geology, with a few more on groundwater (Noizet, 1982; Toteu et al. 2004; Ganwa et al. 2008; Tchakounté et al. 2017; Enyegue et al. 2014, 2020). Enyegue et al. (2014) used electrical resistivity methods to delineate the different aquifer structures and they obtained different aquifer properties for 50 boreholes. The variability in aquifer properties in short local extents equally suggests changes in chemical contents, hence the need for a detailed chemical evaluation.

### II.1.1.2. Water-rock interactions

Water-rock interactions include natural processes such as the dissolution of atmospheric gases in groundwater, dissolution of primary minerals of the hosting rock, secondary mineral precipitation, ion exchange, and mixing with connate water (Cristofi et al. 2020). In crystalline groundwater aquifer settings, these processes depend on the rock type, residence time and the geo-environmental conditions (Yidana et al. 2012). The degree of fracturing and weathering controls groundwater flow, storage, and chemistry: Highly weathered zones exhibit low ionic strength due to rapid recharge, whereas deeper fractured zones often contain more mineralized water with longer residence time. Changes in chemical content, hydrochemical facies and total dissolved solids (TDS) provide insight into aquifer connectivity and the main processes controlling the mineralization. Longer residence times imply longer interaction time between water and the aquifer material, and this increases TDS. This pattern is widely reported in fractured basement aquifers where deep fractured flow paths generate more mineralized waters than shallow weathered zones. The variations in TDS and ionic composition observed in Bafia differentiate between shallow, rapidly recharged weathered laterite zone aquifers and deeper, more mineralized fractured aquifers (Enyegue et al. 2014; Anaba et al. 2017). The longer contact time in deeper aquifers equally enhances ion exchange, notably the replacement of $Ca^{2+}$ and $Mg^{2+}$ by $Na^{+}$ on clay minerals and the development of more evolved species like $NaHCO_3$ or mixed Na-Cl and Ca-Mg-$NO_3$-Cl types (Boum-Nkot et al., 2019; Kamtchueng et al. 2016).

Bayou et al. (2024) reported the presence of low-to moderately mineralized Ca-Mg-$HCO_3$ water type in the Sor and Gebba watershed of Ethiopia mainly influenced by water-rock interactions. Studies carried out in the Centre Region of Cameroon (precisely in Yaounde), Bon et al. (2021) and Fongoh et al. (2023) reported moderate mineralization, with an evolution from a Ca-$HCO_3$ to a NaK-$NO_3$Cl type. Similar observations were made by Menti el al. (2023) in the East Region (Bertoua), and Kamtchueng et al. (2016) in the West Region (Lake Monoun), where groundwater mineralization was mainly influenced by the chemical weathering of rock-forming minerals, ion exchange and anthropogenic activities.

### II.1.1.3. Climatic control and isotopic footprints

Climate, whether humid or dry, greatly influences groundwater composition. High rainfall enhances dilution and somehow reduces ionic concentrations. Conversely, in the dry season, reduced recharge leads to solute concentration due to localized evaporation and decreased dilution in shallow wells (Enyegue et al. 2014; Wirmvem et al. 2016; Anaba et al. 2017; Fongoh et al. 2023). The Bafia area has an equatorial and tropical transitional climate type with a bimodal rainfall pattern, yielding an annual precipitation of about 155mm to 2000 mm (Ngouokouo et al. 2025). Recharge in this area occurs mainly during the rainy seasons through direct rainwater infiltration, with minimal evaporation. Hence, dilution by rainwater greatly reduces ionic concentrations, even for some toxic elements and contaminants (Enyegue et al. 2014).

Additionally, climatic conditions influence isotopic composition of groundwater ($\delta^{18}O$, $\delta^{2}H$), distinguishing groundwater recently recharged by meteoric water from groundwater under evaporative effects as discussed in section II.2. Studies across Africa show that many basement aquifers are recharged locally by recent rainfall (isotope values close to the Global Meteoric Water Line - GMWL) with some localized evaporative enrichment in some exposed shallow systems (Adomako et al. 2011; Akpataku et al. 2019; Bayou et al. 2024). Comparably, aquifers in similar crystalline terrains in central Cameroon have isotopic signatures very close to the GMWL, insinuating recharge by modern rainfall with insignificant evaporation (Wirmverm et al. 2016; Fongoh et al. 2023).

### II.1.1.4. pH, temperature and Redox control

The release and mobility of ionic components during weathering and dissolution processes, including trace elements, is often enhanced by natural factors like temperature, pH, and the redox potential of the medium. As earlier mentioned high temperatures favor evaporation and increase the concentration of ions in water. Low pH in groundwater is a signal of silicate weathering, dissolution of $CO_2$ from the atmosphere, and the subsurface geologic formations that lead to the formation of $HCO_3$. The water type is related to natural processes like rock-water interaction and anthropogenic pollution like waste disposal (Bayou et al. 2024). Both pH and Redox potential critically influence solubility and mobility of ionic species in solution. For example, during high

pH, metals like iron, manganese and aluminum form insoluble hydroxide precipitates, thus reducing their dissolved concentration and mobility (Mapoma et al. 2017; Marszałek, 2022). The toxicity and mobility of certain elements like chromium is more intense in its oxidized hexavalent chromium ($Cr^{6+}$) state than in the reduced trivalent state ($Cr^{3+}$).

Studies show that at shallow levels, groundwater is generally oxidizing and gradually changes to a reducing environment as surface oxygen reduces with depth. This in turn affects the presence of certain ionic species at greater depth. For instance, nitrate concentrations reduce with depth due to denitrification enhanced by a reducing environment (Ako et al. 2013). The pH of groundwater in and around Bafia is slightly acidic to neutral, with oxidizing water conditions near surface (Enyegue et al. 2014; Fongoh et al. 2023). This implies the solubility and mobility of certain species at shallow levels.

### II.1.2. Anthropogenic factors influencing groundwater chemistry

#### II.1.2.1. Agricultural Practices

Groundwater resources are important for agricultural purposes and the quality is a key issue for the management of these resources. Population growth, increased food demand and changes in agricultural practices have introduced the use of fertilizers and agrochemicals, which in some areas, is applied in an uncontrolled manner (Bijay-Singh and Craswell, 2021). Studies carried out around cocoa farms in Ghana confirmed the presence of pesticides in soils and water samples, increasing the risk of environmental contamination (Fosu-Mensa et al. 2016). Increased accumulation of pesticide residues in the food chain and drinking water have been reported to pose serious human health hazards (Agbeve et al. 2014). Increased nitrate concentrations in groundwater aquifers are often a result of the excessive use of nitrogenous fertilizers in agricultural areas, animal breeding operations, and waste disposal from centralized and individual sewage systems in urban areas (Andersen et al., 2014; Böhlke, 2002).

Agriculture is the main economic activity in the Bafia area, involving the cultivation of groundnut, cassava, maize, plantain, banana and cash crops like cocoa. In addition to the yearly population increase, Bafia is equally one of the main food suppliers to neighboring towns like Yaounde. Hence, to increase and improve yields, most farmers engage the use of agrochemicals and manure, which greatly contributes to elevated concentrations of nitrate ($NO_3^-$), phosphate

($PO_4^{3-}$), and potassium ($K^+$) especially in shallow groundwater (Ako et al., 2012; Enyegue et al. 2014). Fonge et al. (2012) identified relatively high concentrations of $NO_3^-$ and $PO_4^{3-}$ in soil water (<5 cm deep) from rice farms in the Ndop area. High nitrate concentrations have also been reported in the crystalline aquifers of Yaounde (Takounjou et al. 2013; Fongoh et al. 2023), the Banana Plain (Ako et al. 2013) and Bertoua (Menti et al. 2023) and have been closely associated to shallow wells especially around farmlands, indicating leaching from fertilizers and manure.

In addition to crop farming, the population of Bafia is involved in animal farming activities, an activity which equally generates farm wastes which infiltrate and contaminate groundwater resources. Groundwater studies carried out in Bafia reported low nitrate concentrations in deep boreholes attributed to denitrification processes at depth (Enyegue et al. 2020). However, given the similar local geology and soil types of the entire Centre Region, it is anticipated to have similar influences of agricultural waste products in shallow water resources in Bafia.

**II.1.2.2. Urbanization, domestic waste and sanitation**

Urbanization in Africa and most parts of the world leads to significant groundwater contamination from inadequate sanitation, industrial waste, and poor waste management, which poses a major health risk, especially in rapidly growing informal settlements (Morales, 2017), including groundwater pollution via seepage (Lapworth et al. 2017). Key contaminants include microbial pathogens and nutrients like nitrate, originating from sources like pit latrines, which seep into vulnerable shallow aquifers. The natural drainage, flow paths and recharge patterns in most of Cameroon, including Bafia, have been obstructed by rapid population growth and land use changes. As discussed in section 1.2.3 above, land use patterns have greatly changed between 2013 and 2023 (sampling time), mostly involving the construction of infrastructures, which encroach on stream/river banks. This has altered flow and recharge in some areas, increasing surface runoff and the infiltration of chloride, nitrate and sulfate-rich wastewater in permeable soils (Lapworth et al. 2017).

Pit latrines in Africa can contribute to groundwater nitrate contamination, particularly in areas with shallow water tables, due to human waste seeping through the soil. In Malawi for example, about 85% of the population depends on groundwater with another 90% proportion that use pit latrines, increasing the risk of drinking water contamination (Hinton et al., 2023). Statistics show that in Cameroon, more than 90% households use pit latrines, including in Bafia. These toilets

are often poorly constructed and even very close to water points. In addition, uncontrolled waste dumping increases chances for leachate infiltration. The absence of well-constructed drainage paths, centralized sewage treatment plants and the presence of leaky septic tanks increase groundwater contamination risks in Bafia shallow groundwater. Furthermore, most shallow hand-dug wells in Bafia are poorly constructed and uncovered, facilitating the entry of surface contaminants from runoff. Studies in similar crystalline settings in Cameroon attributed high groundwater faecal content, nitrate and chloride to irregular placement of pit latrines upstream and/or at close proximity (Takounjou et al. 2013; Fongoh et al. 2023).

#### II.1.2.3. Overexploitation and aquifer depletion

Overexploitation of groundwater modifies natural hydraulic gradients, induces mixing between aquifers, can lead to salt water intrusion in coastal areas and contamination from pollutants such as nitrates and bacteria from agriculture and sanitation. This results in depleted water tables**,** making water less accessible, and can cause ground subsidence **(**Custodio, 2002).

Worldwide increase demand for potable water for domestic, agricultural and industrial purposes has led to ever-abstraction in most aquifers. Additionally, groundwater recharge in crystalline rock aquifers is relatively slower, especially in poorly connected fractures. Hence, there is overexploitation of certain aquifers which alters the water chemistry due to drawdown mechanisms.

### II.1.3. Trace element geochemistry

Trace element contamination of water sources is also a significant issue in most sub-Saharan African countries. These elements are generally present at low trace levels (less than 0.1 %) in soils, sediments, surface waters and living organisms. Some, like Mn, Fe, Cu, and Zn, are essential for the human body in low concentrations but become toxic after bioaccumulation in the system. Other trace elements such as Cd, As, Pb, Hg and Pb are very harmful in excess (Verma and Dwivedi, 2013).

They are amongst the most common environmental pollutants, and could have diverse sources including atmospheric precipitation, agricultural wastes, industrial wastewater discharge, agro-pesticides, urban sewage, mineral mining, infiltration of surface runoff, bush burning, fossil fuel combustion, paints, and natural sources (Bon et al. 2021; Kana, 2022). Given that water is a

chemical reaction medium, some elements are more mobile than others (due to changes in pH and/or temperature). Thus, the chemical species, concentration, bioaccumulation capacity (natural) and anthropogenic activities are the principal factors controlling the distribution of heavy metals in groundwater (Mapoma et al. 2017). Their occurrence is usually in small amounts, thus anomalies are easily detected. Although some trace elements are important to maintain the normal operation of human functions, excess doses in groundwater have adverse effects. For instance, drinking As-rich water for a long time causes cardiovascular, neurological and renal diseases while Cr-rich drinking water leads to skin, respiratory and digestive diseases (Mink et al. 2008).

Amongst these trace elements are heavy metals, a group of metals and metalloids with atomic density greater than 5 $g/m^{-3}$, or five times more than water with an atomic weight between 63.54 and 200.59. Some of them like Pb, As, Cd and Sb are very toxic to health when accumulated in the human body. Given the diversity of sources (natural and anthropogenic), it is important to regularly monitor and quantify them in water (Appiah-Opong et al. 2021). Pollution indices have been used in many studies to evaluate the health effects of heavy metals (Edet and Offiong, 2003; Boum-Nkot et al. 2023).

According to Lapworth et al. (2017), few studies have been conducted in Sub-Saharan Africa related to trace element contamination in groundwater. Despite the high cost of analyses and lack of analytical equipment, few studies have been carried out in Sub-Saharan Africa. For example, studies on heavy metal health risks for bottled water in South Africa (Ogana et al. 2024) showed low trace element concentrations in most of the studied waters. In Ghana, Boateng et al. (2019) reported high levels of Fe, Pb, Cd and Cr in groundwater around landfills. Studies carried out in the central part of Nigeria (Kana, 2022) revealed high levels of Fe, Pb and As. In Cameroon, studies revealed high concentrations of certain elements in some parts of Douala (Fe, Ni, Cr) and Yaounde (Fe, Mn and Al) (Bon et al. 2021; Ndjama et al. 2021; Kamtchueng et al. 2022; Boum-Nkot et al. 2023). The difference in trace element concentrations from one place to another depends on the variability in sources, which in Africa, ranges from rock weathering, to mining; fertilizer and pesticide use (Zhou et al. 2020).

Presently, there are no studies carried in Bafia with regards to trace element content in water; hence there is an uncertainty in this aspect of groundwater. Trace element studies in Bafia will

check the vulnerability of the population to some heavy metals, (both carcinogenic and non-carcinogenic), which are already elevated in some parts on the Centre Region with similar geological settings.

## II.2. Recharge mechanisms and groundwater age

### II.2.1. Recharge mechanisms and source of groundwater

Groundwater recharge is the process by which water moves from the surface into the groundwater system, replenishing aquifers, ensuring the sustainability of water resources essential for agriculture, drinking, and ecosystem health (Khan et al. 2024a). This occurs when precipitation, surface water, or other forms of water infiltrate the soil and percolate down through various soil layers until they reach the saturated zone, where the soil or rock is fully saturated with water. Groundwater recharge can occur naturally through rainfall and snowmelt or artificially through methods such as recharge basins, infiltration wells, and rainwater harvesting systems. Effective recharge mechanisms help maintain aquifer levels, ensuring a reliable water supply, especially in arid and semi-arid regions where surface water may be scarce. Identifying the source and mechanisms of groundwater recharge is an essential component for modeling and protecting groundwater systems from overexploitation and contamination (Galliari et al., 2021).

#### II.2.1.1.Factors influencing recharge

Groundwater recharge is influenced by a variety of natural and anthropogenic factors. An understanding of these factors is essential to effectively manage these water resources. Some main factors include:

- **Climate:** Consistent rainfall favors infiltration and percolation unlike intense or sporadic events which enhance rapid runoff rather than infiltration. In like manner, high temperatures promote evapotranspiration, reducing surface water and soil moisture. Most of Centre Region, including Bafia, has a transitional equatorial - tropical climate type, with two rainy seasons which increase the chances for recharge at least twice a year (Enyegue et al. 2020; Djoufounna et al. 2022). Similar mean annual rainfall amounts and temperatures have been reported in other equatorial climate zones in Africa, accounting for the constant replenishment of their resources (Adomako et al. 2011).

- **Soil Characteristics:** Soil texture and structure influences water permeability and hydraulic conductivity and they either hinder or facilitate recharge: Coarse-textured soils (sands and gravels) generally have higher infiltration rates compared to fine-textured soils (clays), which can hinder water movement. Most of Bafia is made up of Bafia is made up of ferralitic soils which of the sandy-loam and sandy-clay loam groups, with about 71% sand content that promotes infiltration and percolation. However, the clay fraction in some parts increases the soil moisture content, thereby slowing down recharge rates (Vallérie, 1973; Jiofack et al. 2013; Leumbe et al. 2022; Ketchiemo et al. 2024).
- **Geological and hydrogeological aspects:** Geological and tectonic settings play a significant role in the process of groundwater discharge and recharge mechanism. The presence of impermeable layers (e.g., clay or bedrock) can limit recharge by preventing water from percolating deeper into the aquifer. The Centre Region (Bafia inclusive) is generally made of metamorphic rocks, mainly orthogneisses, amphibolites, micaschists, granitoids, and quartzites which are almost impermeable but depend on cracks for groundwater recharge. Researchers have also reported the presence of some lineaments which serve as easy passages for groundwater (Anaba et al. 2017; Tabué et al. 2021). Studies carried out in Bafia by Enyegue et al. (2014, 2020) showed that shallow groundwater in the weathered zone is principally recharged by rainfall while deeper boreholes are fed by cracks and fractures. Similar scenarios have been reported in Yaounde and other basement terrains in Cameroon (Kamtchueng et al. 2016; Fongoh et al. 2023).
- **Land Use and human activities:** Hydrological processes, including precipitation, infiltration, evapotranspiration, and runoff, are all influenced by land use and land cover changes. Practices such as crop rotation, cover cropping, and reduced tillage promote soil health and improve infiltration, while excessive tillage can lead to soil compaction. This change affects the soil's ability to absorb and retain water, impacting the recharge of aquifers (Chinye-Ikejiunor et al., 2021). Intensive irrigation often relies heavily on groundwater extraction, reducing the levels of aquifers and threatening the sustainability of the water supply.

  Deforestation practices can lead to soil erosion and reduced soil structure, negatively impacting the land's ability to absorb water and hence, poor groundwater recharge.

Additionally, urban development often involves the exposure of impervious surfaces (e.g., roads, buildings), which greatly reduce infiltration and increase erosion, flooding and runoff, thereby decreasing groundwater recharge. Studies carried out by Ngouokouo et al. (2025) in the Bafia area listed forests areas as high potential groundwater areas, indicating that land use/land cover is an important factor in groundwater circulation and infiltration. Rcently, land use in the Bafia area has shifted, with more areas being developed for urban and agricultural purposes as the population has grown, leading to increased groundwater usage with possible increase in runoff (See section 1.2.3 above).

### II.2.1.2. Stable isotopes and recharge source

Isotopes are widely used in many disciplines of earth and environmental sciences as tracers of several natural and anthropogenic processes. Among several isotopes, the stable isotopic composition of oxygen and hydrogen in precipitation ($\delta^{18}O$ and $\delta^{2}H$) is considered a powerful tool to trace the hydrological cycle (Clark and Fritz, 1997; Adomako et al. 2011), characterize the regional atmospheric patterns (Baldini et al., 2008; Comas-Bru et al., 2016), understand the aquifer recharge mechanisms and groundwater dynamics, and carry out hydrological balances (Gat et al., 1996; Jasechko, 2019).

Stable isotopes have been used to investigate groundwater flow paths, velocity, inter-relation between surface and ground waters, contaminant transport processes, geochemical evolution, residence time (groundwater age) and recharge origin (Fontes, 1980; Adomako et al. 2011; Ako et al. 2012; Kamtchueng et al. 2022). Stable isotopes of oxygen and hydrogen in groundwater of an active hydrological cycle reflect the initial composition of the recharging water, unless when diluted or mixed with water of different isotopic compositions (Gat, 1981). With the challenges that come with hydrological/hydrogeological studies in difficult terrains like in crystalline aquifers, these isotopes have proven to be so useful because they cover greater depths and larger regional investigation extents (Akpataku et al. 2019; Kamtchueng et al. 2016).

Variation in stable isotopes of hydrogen (D) and oxygen ($^{18}O$) in precipitation forms primary background data for groundwater recharge investigations (Gat 2010). Regrettably, stable isotopes data of precipitation are absent in the Bafia area, but available in Yaounde – the closest observation station (IAEA/WMO, 2024). Additionally, the meteoric water line, which is

important in groundwater recharge evaluation, has not been established in the town of Bafia. Hence, for a comprehensive groundwater recharge assessment in Bafia, there will be a combination of rainfall data (Yaounde) including the Yaounde Meteoric Water line (Wirmvem et al. 2016), groundwater and surface water data in Bafia.

Given that groundwater and surface water are basically being recharged by rainfall, their isotopic compositions depend on the hydrogen and oxygen fractionation processes that take place from precipitation to infiltration (Dansgaard, 1964). These fractionation processes can be influenced by different factors, including temperature, altitude, latitude, humidity, distance from the ocean and even rainfall amount (Dansgaard, 1964; Araguás-Araguás et al. 2000; Gonfiantini et al. 2001). The temperature-dependence of $\delta^{18}O$ and $\delta$ D has been used to demonstrate seasonal effects on groundwater recharge, paleo-recharge and mountainous recharge. During high temperatures, evaporation enhances isotopic kinetic fractionation; the heavier isotopes ($^{2}H$ and $^{18}O$) have a greater tendency to enter the liquid/solid phase than the lighter ones ($^{1}H$ and $^{16}O$), which preferably remain in the vapor phase. As a result, heavy isotopes are more depleted in precipitation produced at lower temperatures (Gat and Gonfiantini, 1981). These fractionation processes define a global $\delta^{18}O$ - $\delta D$ relationship, which is summarized by the Global Meteoric Water Line (GMWL) (Craig, 1961). This relationship is defined as

$$\delta D = 8 * \delta^{18}O + 10 \quad (1)$$

where the slope value (8) corresponds to the ratio between the enrichment factors between liquid and vapor of oxygen and hydrogen under relative humidity and sea surface temperature theoretical conditions of 85% and 25°C, whereas the intercept (10) provides an estimate of non-equilibrium fractionation processes (Dansgaard, 1964). Changes in fractionation factors might lead to a deviation from the GMWL, as observed by Wirmvem et al. (2016) in Yaounde, 120 km away from Bafia (equation 2).

$$\delta D = 8.35 * \delta^{18}O + 15.29 \quad (2)$$

The combination of decreasing temperatures with higher altitude and gradual rain-out of heavier isotopes results in a noticeable altitude effect in the isotopic composition of precipitation (Clark and Fritz, 1997; Gat, 2010). Hence, groundwater recharged by rain from higher altitude will retain the depleted signatures of higher altitudes.

Apart from $\delta^{18}O$ and $\delta D$, the deuterium excess (d-excess) is another parameter which is commonly used to trace the moisture sources of precipitation (Wirmvem et al. 2016). It is a second-order isotope parameter that is a function of the isotopic composition of oxygen and hydrogen in water (Dansgaard, 1964), defined by the following equation:

$$\text{d-excess} = \delta^{2}H - 8 * \delta^{18}O \quad (3)$$

The d-excess value is useful to identify secondary processes that influence the atmospheric vapor content in the evaporation-condensation cycle and in vapor source regions. It expresses the excess of deuterium compared to the heavier oxygen isotope in vapor, which is encountered when water molecules formed by different hydrogen and oxygen isotopes diffuse across a density gradient during evaporation processes. Several factors control the d-excess of rainfall, especially temperature, relative humidity (RH) and changes in seasons; it is higher in the rainy seasons and lower in dry periods (Masiol et al. 2021).

Several groundwater studies carried out in some crystalline aquifers in the world using stable isotope revealed that groundwater in a particular area aligns with a given Local Meteoric Water Line (LMWL), which often times deviates slightly from the GMWL (Adomako et al. 2011; Akpataku et al. 2019; Silva et al. 2021; Bayou et al. 2024). In tropical Africa, stable isotopes have been useful in groundwater recharge studies (e.g Wirmvem et al. 2015; Adomako et al. 2015) as well as in climatological studies (Risi et al. 2008). Despite their wide application, the use of stable isotopes in recharge evaluation studies is scarce, and even absent in the Bafia area. However, few studies in the Centre Region reported the significance of continental recycled moisture and evidence of the amount effect (Kuitcha et al. 2012; Wirmvem et al. 2016; Fongoh et al. 2023). These studies also suggest that groundwater in the Centre Region, including the Bafia area, has a meteoric origin, usually infiltrating rapidly with minimal evaporation.

### II.2.1.3. Groundwater age

Besides the stable isotopes, radiogenic isotopes like tritium ($^{3}H$) have been useful in estimating the groundwater age. Tritium occurs naturally in low amounts but higher levels were released into the atmosphere in the early 1950s during the bomb test. Bomb tritium traces in water have been effectively used to date young groundwater based on the presence or absence of tritium and analyzing the decay rate of naturally existing tritium (Clark and Fritz, 1997). Knowledge of

present-day rainfall tritium concentrations is required to assess groundwater tritium levels in a particular area. According to Clark and Fritz (1997), the decline in precipitation tritium is not only due to its decay, which decreases tritium only by 5.5%. Groundwater and oceans are the major factors behind the decrease, since they act as big reservoirs for thermonuclear tritium. Tritium contents vary depending on the proximity to the equator and oceans; regions at low latitudes have lower contents than in higher latitudes. Estimating groundwater age in crystalline aquifers is often complex due to different flow paths and groundwater mixing.

Despite the high cost of analysis and the lack of analytical equipment in most of Africa, many more groundwater studies focus on the need to determine the approximate age of groundwater using tritium (Loehnert, 1988; Adomako et al. 2011; Rooyen et al. 2021). Studies carried out by Rooyen et al. (2021) in South Africa showed seasonal variations in tritium content; higher contents in summer rains than in winter rains. Others revealed progressive decay of tritium content; Adomako et al. (2011) in Ghana observed that between 1978 (Akiti, 1980) and 2007 during their sampling, tritium levels decayed by half the amounts. Similar observations have been made in Cameroon in the Littoral Region (Ako et al. 2012; Emvoutou et al. 2023), the North West Region (Wirmvem et al. 2017), and the South West Region (Ako et al. 2012). However, tritium levels recorded in Cameroon are relatively lower than those in Ghana and South Africa. Many factors account for this, including higher nuclear bomb input (at higher latitudes) and high evaporation effects experienced in South Africa. Additionally, studies carried out in similar crystalline terrains show that groundwater in deep fractures are not frequently recharged, hence reflecting old groundwater with less tritium activities (Akpataku et al. 2019; Rooyen et al. 2021).

Previous research works carried out in Bafia focused on the geology, hydrogeological layers and suitability (Enyegue et al. 2014; 2020). However, no research has been carried out to characterize recharge using isotopes. A combination of hydrogeochemistry and isotopes (stable and radiogenic) gives a better understanding of groundwater systems, highlighting the origin, recharge processes, tracing contamination sources and isolating protected areas based on the estimated groundwater age. Thus, to effectively plan and manage water resources in Bafia, incorporating tritium studies in the regular monitoring scheme is priority.

## II.3. Nitrate contamination and possible nitrate sources

Nitrate is a particular contaminant of concern worldwide, arising in groundwater from the oxidation of ammonia, a principal component of human excreta. The United States Environmental Protection Agency (USEPA) has set the maximum contamination level (MCL) of nitrogen present in nitrate form at 10 mg/L, with adverse effects at high concentrations (Temkin et al. 2019). High nitrate in water is both an environmental and public health hazard. Nitrate in itself is relatively non-toxic; however, it can be microbially reduced to nitrite, a form which poses several health threats to humans including methemoglobinemia in infants by oxidizing the heme $Fe^{2+}$ of hemoglobin and this oxidized ($Fe^{3+}$) hemoglobin, called methemoglobin, does not bind with oxygen (Powlson et al. 2008). Nitrite also causes thyroid diseases, stomach cancer and liver damage in adults, and irreparable damage in the aquatic system (Abascal et al. 2022).

The increase in human population associated with increasing human activities has caused a significant increase of reactive nitrogen (N) loadings to hydro-systems. Nitrate is one of the reactive forms of molecular nitrogen ($N_2$) which has both natural and anthropogenic sources. The natural sources of nitrogen in soils and groundwater include weathering, atmospheric deposition, microbial transformation of ammonia in soil and cyanobacteria-plant symbioses. However, due to anthropogenic activities such as increasing use of nitrogen fertilizer, improper disposal of leachate from landfills and livestock manure, and wastewater leakage from sewage and septic systems, the nitrate contamination in groundwater has increased significantly in recent years (Pare and Bonzi-Coulibaly, 2013; Ako et al. 2014; Abascal et al. 2022). Inorganic fertilizers enrich soils with potash, nitrogen and phosphorous, soluble components, which may easily leach into the groundwater system. Hence, the inappropriate use of fertilizers and pesticides in agriculture introduces high levels of pollutants into water, leading to its degradation. Thus, monitoring pollution levels and subsequent actions, including nitrogen source control, are essential to prevent nitrate pollution, given that once aquifers get contaminated, mitigation becomes difficult and remediation even more expensive (Re et al. 2017).

Given that nitrate is very mobile and primarily originates from non-point sources, it can spread in different groundwater flow paths, making it difficult to trace the actual source. Therefore, for control and management purposes, besides the identification of the presence of nitrates, it is very important to trace the source (Boumaiza et al. 2024). Researchers have focused on identification

of nitrogen sources leading to $NO_3^-$ contamination in groundwater through various processes including hydro chemical, statistics, and stable isotopic approach (Elumalai et al. 2020). Recent studies reveal the utility of measuring nitrogen isotopes in saturated and unsaturated zones helps in identifying the major sources of nitrate in groundwater (Jung et al. 2020). The stable isotopes of nitrogen and oxygen ($\delta^{15}N$ and $\delta^{18}O$), generally called the dual isotope technique, are very useful in the identification of nitrate sources (Mayer et al. 2001). Since different $NO_3^-$ sources exhibit different isotopic signatures in watersheds, several studies have been successfully undertaken to identify the $NO_3^-$ sources using stable isotopic techniques involving dual nitrogen isotopes ($\delta^{15}N$ and $\delta^{18}O$) and boron (B) (Kendall et al., 2007; Fongoh et al., 2023). Furthermore, denitrifcation and nitrification can largely alter the $NO_3^-$ isotopic fractionation and signatures, and should be taken into account when tracing $NO_3^-$ sources in complex watersheds (Adebowale et al., 2019).

In a global survey on groundwater nitrate pollution (Abascal et al. 2022), Africa's results were of big concern, with more than one third of sampled areas recording nitrate values above the WHO threshold values. Amongst the sampled nations, the Democratic Republic of Congo reported mean values between 189 mg/L and 775 mg/L, while Cameroon reported an average of 50 mg/L and a maximum of 646 mg/L in the Grand Yaéré of the Far North Region. Bello et al. (2019) observed that these nitrates increased independently of $K^+$, thus suggesting that fertilizers are not the main sources of nitrates but rather associated them with the oxidation-reduction processes of organic matter in septic tank effluents, sewage and animal wastes. These concentrations generally increase in areas with high population density, and some streams and rivers which serve as waste dumpsites for these poorly developed neighborhoods (Pare and Bonzi-Coulibaly, 2013; Branchet et al. 2018).

Through the use of dual nitrogen isotopes, Gibrilla et al (2020) observed that sewage/manure contribute the highest levels of nitrate in some water resources in Ghana while other water resources showed a complex mixture of sewage/manure, chemical fertilizer and soil nitrogen. In Kenya, Nyility et al (2021) identified manure as the main nitrate source in the farming areas. Other studies carried out on manure obtained from livestock bomas in Kenya (Xiantao et al. 2024) reported that besides $N_2O$ reduction to $N_2$, denitrification was the main mechanism behind high $N_2O$ emissions from livestock enclosures in Kenya.

Over the past decades, many studies have been carried out in Cameroon to assess the quality of groundwater and surface water (Takem et al. 2010; Ako et al. 2011; Takounjou et al. 2013; Kamtchueng et al. 2022). Most of these studies reported high $NO_3^-$ levels in drinking water (surface water and groundwater) across the country. However, given that nitrate in water originates from different sources, it is very important to track and quantify the exact $NO_3^-$ sources causing contamination in water (Gibrilla et al. 2020). This information is important to control $NO_3^-$ contamination, improving management of water resources, and targeted remediation techniques for contaminated waters to effectively improve. Despite the number of groundwater quality studies done in Cameroon (including Bafia), information on nitrate apportionment using dual isotopes is still scarce. Fongoh et al. (2023) used the dual nitrogen isotope to study groundwater resources in Yaounde, and they identified sewage and human waste, soil organic matter and, to a limited extent, natural fertilizers as the main nitrate sources. Therefore, the isolation of nitrate sources using the dual nitrogen isotope will maximize and facilitate groundwater management in Bafia, especially given its agricultural background.

### II.4. Water resources management

Literature shows that Bafia has good exploitable groundwater resources typical found in crystalline basement terrains but faces water-management problems which are typical in small towns (Enyegue et al. 2020). Just like in many other communities in Cameroon, Water management in the Bafia area is ensured through semi-urban water supply projects and local initiatives, which keep these resources in an “up-to-standard” state. However, as identified by Boutin and Tally (2012), these resources face recurring problems like the uneven distribution of water points across the town with more than 35% failed boreholes, operation and maintenance issues, poor sanitation standards, source to home contamination risks, and lack of continuous and adequate groundwater monitoring and aquifer protection.

#### II.4.1. Geology and aquifer spatial heterogeneity

Bafia is located within the crystalline terrains of Cameroon, with mainly gneisses, quartzites and granite-gneisses. Studies show that there two aquifer types: the shallow aquifer located in the weathered mantle and the fractured bedrock aquifer which is tapped by deeper boreholes where fractures are available (Enyegue et al. 2014). Anaba et al. (2017) identified large spatial

variability in weathering thickness, fracture density and depth and hence influencing borehole productivity. However, these findings have not been established on a regional extent, thus complicating uniform water-supply planning.

### II.4.2. Data gaps

Most studies carried out in Bafia are related to the geological setting of the area (Noiset, 1988; Tchakounté et al. 2017; Ganwa et al. 2022). Presently, Bafia relies on very groundwater data limited to the evaluation of chemical and bacteriological properties for drinking purposes (Enyegue et al. 2020); and the absence of relevant data makes it challenging to establish present situations, especially with the changing land use and land cover scenarios. To effectively manage these resources and secure protected areas, there is need for continuous, long-term monitoring, not only for the hydrochemical properties but equally for isotopic signatures, nitrate and trace element contamination potential sources.

### II.4.3. Source-to-home contamination risk

Water contamination risks are very high in semi-rural settings. This could be contamination at water point, along the road to the house or at home. One of the main sources of high nitrate and microbial contamination especially in shallow wells in peri-urban areas like Bafia is the uncontrolled use of pit latrines. According to Enyegue et al. (2020), the occurrence of bacteriological contamination in certain shallow wells suggests that most of these sources are exposed to contamination sources; hence require treatment (chlorination/boiling) and proper sanitation. Additionally, the gradual increase in agricultural activities, poorly constructed septic tanks; uncontrolled waste dumping and poor domestic waste sorting habits increase the risks of water contamination in Bafia. Similar scenarios have been reported in other peri-urban settings of Cameroon (Ako et al. 2014; Fongoh et al. 2023).

### II.4.4. Maintenance and governance

Many boreholes, developed wells and springs in Bafia are under community maintenance schemes. However, studies and observations show that more than 35% of these water points are non-functional (Boutin and Tally, 2012). As observed in other parts of Cameroon, this could be due to lack of technicians with good maintenance knowledge, poor operating systems and lack of maintenance funds (Mvongo et al. 2024). This might also be due to poor local governance

initiatives which are weak in organizing capacity building programs, delegate roles and ensure implementation to ease management.

## CONCLUSION

The review of literature underlines that fractured crystalline basement aquifers are heterogeneous in nature, with complex groundwater flow paths and manifesting spatial variability in water quality. Hydrochemical studies in basement terrains indicate that groundwater chemistry is predominnatly controlled by water–rock interaction processes, especially silicate weathering, with limited evaporation prior to infiltration in humid tropical environments.

Stable isotopes of oxygen and hydrogen have been widely recognized and applied in different groundwater studies to understand recharge sources, infiltration/recharge conditions, identify mixing scenarios and the influence of evaporation. The determination of groundwater age has also been a great tool in differentiating young water from old water, especially in areas vulnerable to surface contaminations like nitrate. A combination of these techniques provides a more exhaustive interpretation of groundwater systems especially in such complex basement terrains. Nevertheless, the literature reveals that such intergrated studies remain scanty in the Centre Region of Cameroon, particularly in Bafia. Aditionally, studies carried out in the Bafia area weakly establish the link between the scientific findings of the groundwater systems and the practical groundwater management phase, thus leaving the population unimformed.

This gap underlines the need for studies that translate scientific knowledge into management-intended guidelines. In this context, this study seeks to contribute to knowledge that shall boost the understanding of fractured crystalline aquifers in the Bafia area, providing science-based recommendations for sustainable groundwater management.

# CHAPTER III: METHODOLOGY

## INTRODUCTION

This chapter focuses on the research materials and methods used, including the choice of sampling points, water sampling procedures, in-situ measurements, rock sampling and laboratory works. The methods are divided into two: the field and laboratory methods.

### III.1. Research bibliography/choice of site

A reconnaissance study was carried out in the study area prior to the first sampling campaign during which sample points were identified. This study was executed using hydraulic structures like hand dug wells, boreholes, rivers/streams and springs located in Bafia and the peripheries. There were several reasons for choosing Bafia, including socio-economic and environmental issues. On the socio-economic part, Bafia has inadequate and insufficient drinking water supply network by Camwater, which often times is irregular. Additionally, the poor waste collection and management and the population growth linked to rural exodus greatly deteriorates water quality, especially in shallow wells. On the environmental point of view, Bafia is located in the forest-savannah contact zone, where the savannah is currently encroaching on the forest, and climate variability and/or change are having more or less direct effects on natural resources, including water resources (Ngoupayou et al. 2016).

The choice of sampling sites in Bafia was based on the prevailing anthropogenic activity (farmlands, toilets, wastes dumpsites) around sampling sites, the usability of water points, the accessibility of the points, especially for surface water, and off course, owners' consent. To demonstrate the influence of the geographical, geomorphological and anthropogenic settings on the water quality, about 70% of the sampling sites were taken within the more populated Bafia town and 30% in the less populated peripheries. Based on the information obtained from some informal interviews, most of the inhabitants in the study area have little or no knowledge regarding water quality and management techniques but due to diverse water-related illnesses encountered, many wells were chlorinated by the owners just around the time of sampling. The geographical coordinates of sampling sites were obtained using a Garmin GPS and these co-ordinates were later treated on an SRTM image to obtain the actual sample area and topographic maps of the area.

## III.2. Field work

### III.2.1. Water sample collection and preservation

Two field campaigns were organized-one in September 2022 (rainy season) and another one in March 2023 (dry season), during which samples were collected from previously identified points. During the first campaign (rainy season), a total of 57 water samples were collected (4 rivers, 19 open wells, 12 developed wells, 20 boreholes and 2 springs) for major ions, stable isotopes, trace elements and tritium analyses while 60 water samples (5 rivers, 18 boreholes, 2 springs, 8 developed wells and 27 open dug wells) were collected during the second campaign (dry season) for major ions, stable isotopes, tritium analyses. Based on the nitrate results obtained during the rainy season, 18 sample points ($NO_3$>10 mg/L) were sampled and used for the dual nitrogen isotope analysis ($\delta^{15}N\text{-}NO_3$ and $\delta^{18}O\text{-}NO_3$). Prior to sample collection, all sample bottles were washed, rinsed with deionized water and oven-dried at 150 °C (Fig. III.1a). Static water levels of hand-dug wells were measured using a water level indicator. Field measurements and sampling followed methods described by Karklins (1996).

- River samples were collected differently, depending on the accessibility and depth of the river course. For the Mbam River, samples were collected with the help of local canoes (Fig. III.1b). Samples were collected in the middle of the watercourse at depths generally less than 1m, preferably where water velocities are high enough to homogenize solid and dissolved particles.

- Open well samples were collected using a ten-liter bucket tied to a rope (Fig. III.1c). After purging the well for about 5 minutes, the sampling bottle was rinsed three times with the sample and then filtered into the bottle using the 0.45 µm cellulose filters (Fig. III.1d). Samples for cation and trace elements analyses were acidified using pure $HNO_3$ to prevent further chemical reactions while those for anions remained un-acidified. Borehole samples were collected after the pumping for about 15 minutes and similar steps followed for sampling and preservation. Spring samples were collected directly into the sampling bottles following similar procedures for the open wells and boreholes (Figs. III.1 e, f).

- Stable isotope samples were collected in 50ml polyethylene bottles which had been pre-washed in the laboratory. These samples were rapidly collected below the surface of the water in the bucket or flowing borehole to avoid atmospheric interaction; they were neither filtered nor acidified.

- Samples for dual nitrogen isotopes were filtered (using a 0.45 µm filter), not acidified and immediately stored in an ice box. Tritium samples (neither filtered nor acidified) were collected in 1L polyethylene bottles from some randomly selected boreholes (Fig. III.1g). Nitrate samples were frozen; samples for cation, anion and stable isotope were stored at 4 °C while for tritium samples were preserved at room temperature for a maximum of 14 days before analyses. Duplicate samples were collected for each set of analysis to ensure repeatability and data reliability. All bottles were properly sealed and preserved in ice block coolers to stop any further reaction following standard sampling procedures (Rodier, 2009; Ngoupayou et al. 2016).




**) Mb**

**Noun River), (c) hand-dug wells, and (d) Sample filtration using the 0.45µm cellulose filter**



**Figure II.1 (e): Borehole purging, (f) Spring water collection and (g) Sample set per site**

### III.*2.2*. Measurement of in-situ parameters

Sensitive physico-chemical parameters like electrical conductivity (EC), water temperature, dissolved oxygen (DO), pH and redox potential (Eh) were measured in-situ using the Hanna Multi-parameter Probe (*HI98194* HANNA) (Fig. III.2a), whose electrode was constantly preserved in a 3 mol/l potassium chloride (KCl) solution. After every sampling point, the instruments were carefully rinsed with de-ionized water to avoid cross contamination (Rodier, 2009; Ngoupayou et al. 2016) and at the end of each day's field work, the pH meter was re-calibrated with calibration solutions beginning with the pH 7.00 solution and then the pH 4.00 solution. The geographical coordinates of each sampling point was recorded using a Garmin GPS (Fig. III.2b), the static water levels, well depth and collar height were measured using a water level indicator (Fig. III.2c) and the alkalinity was measured using the mobile alkalinity kit (Fig. III.2d)


**Figure III.2: Materials for in-situ parameters (a) Hanna Multi-parameter Probe, (b) Gamin GPS, (c) Water level indicator and (d) Alkalinity kit**

To carry out the alkalinity measurement, concentrated sulphuric acid and Bromocresol Green-methyl red indicator powder were used. A clean delivery tube was inserted into the 1.600N sulphuric acid titration cartridge and then to the to the titrator body. Holding the titrator pointing upward, the delivery knob was turned gradually to remove air and a few drops of the titrant before resetting the counter to zero and also cleaning the tip. At each sampling site, 100ml of water sample was collected using a graduated cylinder and then poured into a 250ml beaker. The pH electrode was rinsed with distilled water and inserted into the beaker to measure the pH while the delivery tube was equally inverted into the beaker containing the sample. The delivery knob was turned continuously to release the acid while swirling until the appearance of a light pink coloration corresponding to pH 4.5. At this point, the number of turns (digits) recorded by the counter was noted and multiplied by the digit multiplier (1.0 in this case) to have the bicarbonate

alkalinity. Since the pH range was less than the phenolphthalein alkalinity pH (8.3), the bicarbonate alkalinity is this case is considered the total alkalinity.

### III.2.3. Rock sampling

The rainy season sampling included both water and rock sampling. Rock outcrops are generally scarce in Bafia, especially with urbanization, with a few exceptions like the Bapé granitoid and the river banks. Different outcrops were identified, observed and described. Four rock samples were collected and considered as a representative of the whole study area. These rock samples were collected to analyze their trace element content in order to understand the sources of trace elements in the water samples.

At each outcrop, the GPS coordinates were taken, the rock was briefly described based on the deposition orientation and visible mineralogy, pictures were taken, and samples were collected and properly labeled. The weathered parts of the outcrops were carefully removed to obtain the fresh rock, with relatively less weathered or deformed structures and mineral phases (Fig. III.3). Figure III.4 is a sample location map, indicating the water and rock collection points. The rock descriptions are as follows:

1) **Sample 1- Gamba stream**

- N4.73169°; E11.25216°; Altitude-469m
- In situ rock that outcrops on a stream bed
- Dark and deformed, showing banding and foliations
- Contain ≤50 % dark mineral phase
- It contains quartz, k-feldspars, plagioclase, biotite and muscovite
- Foliations : N65E, 24NW

  N60E, 20nw

  N51E, 25nw

- Suggested Rock is a 2-mica gneiss

2) **Sample 2-Biamo**

- N4.80406°; E11.20861°; Altitude-526m
- Rock outcropped on a hill as large boulders and blocks ranging in size from 1-5 m large, 1.5-2 m high

- The rocks are deformed, weathered, and show thin bands that generally trend NE-SW
- locally bearing quartzo-feldspathic veins
- Contain <50 % dark mineral phase
- High in quartz and k-feldspars contains plagioclase, muscovite, and biotite.
- Magnetite occurs as the main accessory mineral in the rock
- Suggested Rock is a 2-mica granite gneiss

**3) Sample 3-Mbam River**

- N4.8087°; E11.2101°;
- This outcrop occurs along the river bank and on the river bed as in situ rock.
- The outcrop also displays 2- 6 m long and 1-2 m wide loose blocks
- Rock is deformed and foliated but not in place
- The foliations generally trend N-S
- Have >50 dark phase minerals
- Bearing pegmatite veins rich in k-feldspars, quartz and some plagioclase
- The mineral content of the rock includes quartz, k-feldspars, some plagioclase, muscovite and biotite
- Epidote occurs as the main alteration mineral phase
- Proposed Rock is a 2-mica granite gneiss

**4) Sample 4-Nyamsong**

- N4.73019°; E11.25191°
- In situ rock that outcrops on a stream bed
- Dark and deformed, showing banding and foliations
- Contain ≤50 % dark mineral phase
- It contains quartz, k-feldspars, plagioclase, biotite and muscovite


**Figure III.3: Field geology for the identification and collection of rock samples in the Bafia area**

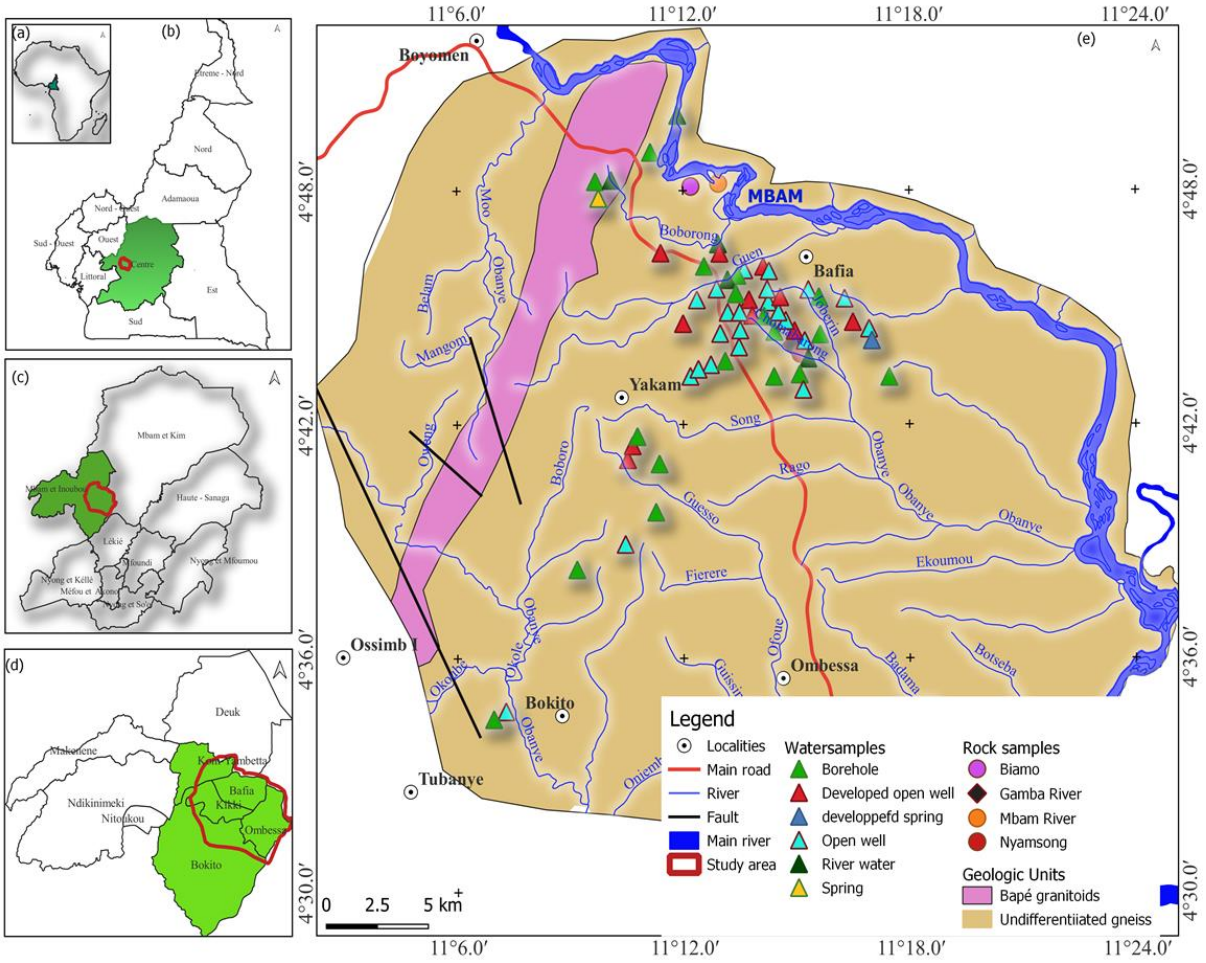


**Figure III.4: Sample location map showing water and rock samples**

## III.3. Laboratory works

All analyses for the rainy season samples were carried out in the « Centre Nationale de l'Energie, des Sciences et des Techniques Nucléaires, Laboratoire d'Analyses Structurales et Isotopique" (CNESTEN), Rabat Morocco. During the dry season, tritium analysis was done in the CNESTEN, dual nitrogen and oxygen isotope analysis was done in the Isotope hydrology laboratory, Vienna, while the major ions and stable isotopes analyses were done in Cellule de Gestion des Heures d'Enseignement" of Lome University, Togo.

For control and validation purposes, physico-chemical parameters were once again measured in the laboratory. Generally, the values obtained from the lab were very close to field values.

### III.3.1. Major Ion analyses- Ion Chromatoography

Major ions ($Ca^{2+}$, $Ma^{2+,}$ $Na^{+}$, $K^{+,}$ $NH_4^{+}$, $HCO_3^{-}$, $NO_3^{-}$, $SO_4^{-}$, $F^{-}$ and $Cl^{-}$) were analyzed by Ion chromatography. Ion chromatography system (ICS) (Fig. III.5) is a technique that separates and quantifies anions and cations in an ionic solution using the ion exchange method of liquid chromatography (LC) (Fritz, 1987). This method is based on the column retention time; each parameter is characterized by the time retained with the column, with a measurement precision of 5%. Samples with EC values greater than 200µS/cm were diluted 20 times using distilled water before analyzing for major ions to avoid the formation of precipitates along the ICS columns and to be able to identify ions like $NO_3^{-}$ and $F^{-}$, which are often low in concentration. The concentrations of $Li^{+}$ and $Br^{-}$ were below detection limit (0.01 mg/l) in both seasons. Blank samples were run after every set of five samples to prevent contamination and ensure the accuracy and reliability of the results. The reliability of chemical measurements was verified by using the ionic balance error (IBE) equation (Appelo and Postma, 2005). About 96% of the analysis was within ±6 %; hence, suitable for geochemical interpretations.


**Figure III.5: Typical Ion Chomatography System**

### III.3.2. Trace element analysis for water and rock samples

#### a) Rock sample preparation (thin sections and crushing) and analysis

The rock samples (04) collected were analyzed in the Geology Laboratory of the University of Florence, Italy. First, thin sections were prepared to determine the petrographic characteristics of the rocks. Depending on the orientation of minerals, samples were cut using a rock saw (≈1cm). The rock chips were polished and bound on glass using an adhesive. After a couple of hours, the sections were further polished, washed thoroughly to remove excess particles and preserved for microscopic examination.

The remaining rock fragments were pulverized in a step-by-step manner, beginning with a crusher and then pulverized using the "Agatha" to < 75µm in a Ball Mill (Fig III.6).

#### b) Rock leaching process

The powder obtained was sieved and used to determine the trace element content by using the Leaching procedure, during which natural interactions between acid rain and rocks are simulated. During this process, 10g of each rock powder was placed in different 100ml plastic sealable containers. Acidified water (pH approximately 4.01) was produced by connecting a gas bubbler to a $CO_2$ cylinder at a pressure of 7.5 kPa, and then 125ml milliQ water was allowed to bubble through the cylinder for 15 minutes, ensuring a constant flow of $CO_2$ using a flow-meter (Fig. III.7a).


**Figure III.6: Simplified Laboratory steps involved in rock sample preparations, from crushing to powder state**

At the end of the bubbling process, the pH of the water was measured again. 20ml of the $CO_2$ water produced was added into the rock powder, ensuring that the samples were completely saturated (covered with water) and in direct contact with the water. The containers were sealed and kept for 72 hours (to maximize the interaction between water and the rock powder), with manual swirling from time to time (Fig. III.7b). At the end of the 72 hours, 10ml of the solution was withdrawn using a syringe, filtered through 0.45 µm cellulose filters and placed in previously weighed tubes acidified with 2% HNO3 for ICP-MS analysis.

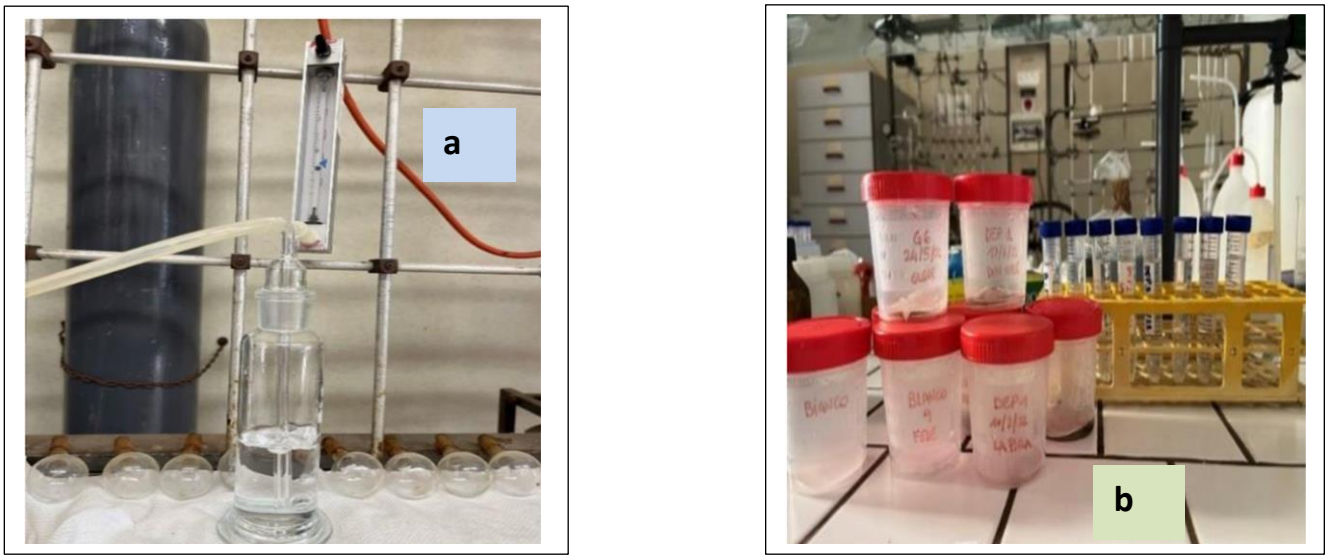


**Figure III.7 (a): $CO_2$ bubbler and flow-meter and (b) Leaching of powdered rock samples**

### c) Inductively Coupled Plasma-Mass Spectrometry (ICP-MS analysis)

The concentration of trace elements (Fe, Co, Se, Ti, Sr, Sn, Sb, Al, B, Cr, Cu, Pb, Ni, As, Cd, Zn and Mn) in water and rocks was determined using the ICP-MS technique, which is an extremely sensible analytic technique that is able to measure the concentrations of inorganic substances, metals and non-metals, even when occurring in ppb (parts per billion), without any additional treatment of the sample. The instrument uses gaseous argon as a plasma source (ICP) to generate the ionization state for elements and subsequently, a quadrupole mass filter (the mass spectrometer - MS) for separating the produced ions. The determination of the analytes is carried out on the basis of the different mass/charge ratios.

## II.3.3. Stable isotope analysis

The stable isotopic compositions of oxygen and hydrogen ($\delta^{18}O$ and $\delta^{2}H$) of water resources were measured by laser spectrometry (Picarro L2130i) (Fig. III.8). The Picarro Cavity ring down spectroscopy technique for stable isotope analysis is preferred over the traditional methods like the Isotope-ratio mass spectrometry (IRMS), because of the high sensitivity and precision, less sample preparation, fast analysis and less cost. The Cavity ring-down spectroscopy (CRDS) measures the isotopic composition by analyzing how a laser beam interacts with a sample gas in a reflective optical cavity. It measures the rate at which the light decays (known as the ring-down time). Based on the different absorption intensities of wavelengths by the oxygen and hydrogen isotope, the laser then measures and calculates the amount of $\delta^{18}O$ and $\delta$ D present. $\delta^{18}O$ and $\delta$ D contents are reported in parts per thousand (‰) using the usual $\delta$ notation relative to the Vienna Standard Mean Ocean Water (V-SMOW). Analytical uncertainty of the reported values is ± 0.10 ‰ for $\delta^{18}O$ and ± 0.8 ‰ for $\delta^{2}H$.


**Figure III.8: Picarro L2130-i for stable isotope ananlysis**

### III.3.4. Tritium analysis

To determine the groundwater ages, 13 and 11 borehole samples were collected for the rainy and dry seasons respectively. Tritium analysis was done using the electrolytic enrichment and low-level liquid scintillation counting (Thatcher et al. 1977) technique, and the values were reported in Tritium units (TU). The analytical procedure involves four stages, namely:

- Distillation: All samples are distilled before electrolysis because the presence of salts during electrolysis can corrode or poison the cathode layer, reducing the efficacy of isotope separation.

- Enrichment: The water analyzed often contains low concentrations of tritium. Hence electrolyte enrichment is necessary for each analysis in order to increase the concentration of the heavy atom ($^{3}H$) and eliminate the light atoms ($^{1}H$, $^{2}H$) by pyrolysis of the chemical bonds via redox reactions. To carry out these reactions, 2g of sodium peroxide ($Na_2O_2$) is added to each cell containing 500 ml of sample, and the reaction is as follows:

$$2Na_2O_2 + 2\ H_2O \longrightarrow 4\ Na^+ + 4\ OH^- + O_2 \qquad (4)$$

- Neutralization: This is done to remove the sodium hydroxide remaining in the sample, and to reduce the pH (between 5 and 7) so that the liquid scintillation counting can be acceptable. Neutralization is done by adding 6g of lead chloride ($PbCl_2$) to the sample through the following reactions:

$$PbCl_2 + 2NaOH \longrightarrow Pb(OH)_2 + 2NaCl \quad (5)$$

$$Pb(OH)_2 \longrightarrow PbO + H_2O \quad (6)$$

- Liquid scintillation counting: In this case, the decay of tritium emits beta particles that interact with the scintillation, producing light pulses, which were counted to determine tritium concentration. The detection limit for the equipment was 0.2 TU and the analytical uncertainty for all samples was below ± 0.4 TU.

### III.3.5. Dual nitrogen isotope analysis ($\delta^{15}N\text{-}N_{NO3}$ and $\delta^{18}O\text{-}NO_3$)

Water samples for this analysis are filtered through GF/F filters (0.2 or 0.45 μm) into HDPE bottles, and acidified to pH 2–3 by adding 1 ml of 2.5 M sulfanilic acid in 10% (degassed) HCl to remove $NO_2^-$ to each 100 mL. Samples are then frozen (-20°C) until analysis time. The analysis was done at the International Atomic Energy Agency (IAEA) Isotope Hydrology laboratory (Vienna) using Titanium (III) Chloride extraction, with Trace Gas purge and trap system (TG-IRMS) coupled with Laser isotope spectrometry (Altabet et al. 2019). The chemical reduction of aqueous nitrate to $N_2O$ utilized Ti (III) chloride reagent in 30% hydrochloric acid. The Ti (III) chloride was pre-conditioned by reacting 1g of Zn powder with 10 ml of Ti (III) chloride in a 250ml beaker to remove potential Ti (IV) impurities from the reagent and ensure consistent reaction results and this was done through the following equation:

$$2Zn_{(s)} + Ti^{+4}Cl_4 + 2H^+ \longrightarrow 2ZnCl_{2(s)} + Ti^{+3} + H_2 \quad (7)$$

The detection limit was 0.1 mg/L $NO_3$-N. All results were reported with respect to VSMOW-SLAP for $\delta^{18}O$ and AIR for $\delta^{15}N$, normalized to USGS/IAEA standards.

### III.4. Data treatment

Different methods were used to validate and process the results of various parameters, some of which include the calculation of the ionic balance (IB), determination of hydrochemical facies

and factors governing them using Piper and Stiff diagrams, Gibbs diagram, mixing plots, chloro-alkaline indices, saturation indices (SI) using PHREEQC, water quality index (WQI) and heavy metal pollution indices (HPI). Besides the hydrochemical analyses, several approaches were used to process the isotopic data, including the Craig plot, mixing plots and graphs. The Kendall, (1998) diagram was used to determine the sources of nitrates in water. Multivariate statistical analyses (Factor analysis, correlation matrix) were used to infer the relationship between different analyzed parameters.

### III.4.1. Ionic Balance (IB)

To verify the quality and reliability of analyses and reduce analytical errors, the ions are balanced as follows:

$$[Ca^{2+}] + [Na^{+}] + [Mg^{2+}] + [K^{+}] + [NH_4^{+}] = [HCO_3^{-}] + [NO_3^{-}] + [SO_4^{2-}] + [Cl^{-}] + [F^{-}] \quad (8)$$

The IB is then calculated using the following equation:

$$IB = [(TZ^{+} - TZ^{-})]/[(TZ^{+} + TZ^{-})] \times 100 \quad (9)$$

where $TZ^{+}$ is the total cations and $TZ^{-}$ is the total anions. For the validation of results in this research, the IB should be $< \pm 10\%$ (Scheoller, 1962).

### III.4.2. Determination of hydrochemical facies and processes

To verify the dominant water types, the Piper (Piper,1944) and Stiff diagrams were derived using the Diagrammes 6.77. The Piper diagram is made up of two triangles representing cationic and anionic facies and a rhombus synthesizing the overall facies. The concentration of points in one pole represents the combination of cationic and anionic elements for the different samples. Just like the Pipers diagram, the Stiff diagram is used to illustrate the ionic composition of water samples, visualizing and comparing the chemical characteristics of different water sources. It has a cation axis to the left and an anion axis to the right, with the x-axis representing the ion concentrations in milli equivalents per liter (Meq/L) while the y-axis represents the ions. The Gibbs (1970) diagram, along with several mixing plots, was used to determine the major processes that control the water chemistry and evolution along their flow paths.

### III.4.3. Determination of Natural Background Levels (NBL) and Threshold Values (TV)

According to Edmunds et al. (2003), the background level of a substance in groundwater is defined as the concentration of a given element, species or chemical present in solution which is derived from natural geological, biological or atmospheric sources. Several methods are used to determine NBLs, including pre-selection (Coetsiers et al. 2009), hydrochemical simulation of solution in aquifers (Sellerino, 2014), component separation, probability plot and other statistical methods (e.g., Sellerino, 2014; Zhang et al. 2017). Despite the method used, a good NBL assessment eliminates samples heavily influenced by human activities. Amongst the existing methods, the pre-selection method is the simplest, although it is often biased due to the elimination of samples collected from unknown well depths (Nlend et al. 2023). In this study, the NBL of major ions and trace elements was determined using cumulative probability plot, which refers to the probability that a random variable is less than or equal to a specified value. This method naturally separates samples with high human influences from those influenced by the natural system by means of inflection points, without pre-selection of hydrochemical data (Panno et al. 2006). The first inflection point is assumed as the lower natural background level. Given the local setting of the Bafia area, we considered the second inflection point (maximum value) to be the NBL.

The NBLs were used to estimate the threshold value TV), representing the maximum concentration of a parameter that is safe for human consumption taking into account the local geological/hydrogeological functioning of an area. The TV is calculated based on the relationship between the NBL and standard relevant reference (REF) value (Muller et al. 2006) as follows:

$$NBL < REF: TV = (NBL + REF)/2 \quad (10)$$

$$NBL > REF: TV = NBL \quad (11)$$

### III.4.4. Chloro-alkaline indices (CAI)

The reaction between water and aquifer materials often releases ions which can be interchanged between water and the clays, thereby influencing groundwater chemistry. Clays generally have sticky surfaces on to which ions can adhere, depending on their sizes and affinity for clays. The

ionic interaction between aquifer material and water was demonstrated using the Chloro-alkaline indices (CAI) proposed by Schoeller (1967) using the following equations

$$\textbf{CAI – I} = Cl - \frac{Na+K}{Cl} \quad (12)$$

$$\textbf{CAI – II} = Cl - (Na + K/(SO4 + HCO3 + CO3 + NO3) \quad (13)$$

When there is normal exchange (ion exchange) between $Ca^{2+}$or $Mg^{2+}$ in water with $Na^{+}$ and $K^{+}$ in the aquifer material, both of the above indices are positive. Conversely during reverse ion exchange, $Na^{+}$ or $K^{+}$ in groundwater is exchanged with $Ca^{2+}$or $Mg^{2+}$ in the host rock and both indices are negative. These indices give insight into the factors controlling groundwater mineralization

### III.4.5. Reverse geochemical analysis

A reverse hydrogeochemical simulation can be carried out to determine the actual contribution of each major mineral phase in the groundwater evolution process. It simulates the natural processes that present in the water environment that lead to the release of ions (Lloyd and Heathcoat 1985). This is done by calculating the saturation index of each mineral phase, assessing its contribution to the overall chemistry. PREEQC was used to calculate the saturation indices (SI) of calcite, dolomite, gypsum, halite, anhydrite for major ions and celestite, goethite, hematite, magnetite and strontianite for trace elements in groundwater and surface water. The SI was calculated using PREEQC in Diagrammes version 6.77, based on the formula

$$SI = \log (IAP/K_{sp}) \quad (14)$$

Where IAP is the ion activity product of the solution, and Ksp is the solubility product of the mineral in the water. When SI <0, it implies under-saturation with no precipitation of mineral phases; while SI >0 indicates super-saturation, with possibility of precipitation. For this study, the SI of some carbonate minerals (aragonite, calcite and dolomite) and sulfate minerals (gypsum and anhydrite) were calculated using PHREEQC and the samples were under-saturated (SI<0) in sulfate and carbonate.

### III.4.6. Water quality index (WQI)

WQI is a numerical rating that summarizes the general quality of water based on several parameters, facilitating the communication of the water's suitability for various uses (such as drinking, recreation, irrigation, and aquatic life support). WQI is obtained by assigning to each parameter a weight ranging from 1 to 5, depending on its importance in drinking water quality. The highest weight (5) is assigned to parameters which have critical effects on the quality of water intended for human consumption compared with the limits recommended by the WHO. It was calculated using the Weighted Arithmetic Index method as described by Brown et al. (1972) using ten parameters, namely: pH, EC, TDS, total hardness, $Ca^{2+}$, $Mg^{2+}$, $NO_3^-$, $SO_4^{2-}$, $Cl^-$ and $F^-$. The WQI calculation includes four stages:

1. Calculation of the sub-index of quality rating (Qi)
2. Calculation of the quality rating for pH
3. Calculation of unit weight (Wi) and
4. Calculation of the WQI using the following equation

$$WQI = \sum QiWi \; / \; \sum Wi \quad (15)$$

$$Qi = 100\,(V_i - V_0) / S_i - V_0 \quad (16)$$

Where $V_i$ is the actual amount of the $i^{th}$ parameter, $V_0$ represents the ideal value of the parameter ($V_0 = 0$), except for the pH ($V_0 = 7$), Si is the standard allowable value for the $i^{th}$ parameter. The unit weight (Wi) is calculated as

$$Wi = \frac{K}{Si},\ K = \frac{1}{\sum \frac{1}{Si}} \quad (17)$$

The final WQI score categorizes water (Tiwari et al. 2014) into different water quality classes as shown in Table 3.1below:

*Table 3.1: Classification of WQI range and category of water and their suitability*

| WQI range | Water quality | Description |
|---|---|---|
| < 50 | Excellent | Suitable for all uses |
| 50 – 10 | Good | Suitable for most uses |
| 101 – 200 | poor | Requires treatment for some uses |
| 201 – 300 | Very poor | Limited usability, treatment needed |
| >300 | Unfit | Unfit for most uses |

### III.4.7. Heavy metal pollution indices and health risks

#### III.4.7.1. Heavy Metal Pollution Index (HPI)

It is an excellent tool used to assess the overall quality of water with regards to its heavy metal content. HPI gives an easy way to evaluate and communicate the level of pollution by heavy metals. This method involves assigning a weight or index ($W_i$) to each metal, according to its contribution to the water quality degradation process (Singh and Rakesh, 2016). The metal pollution index is calculated in three steps:

- The determination of the relative weight or index ($W_i$) assigned to each mineral using the following formula:

$$W_i = {K}/{Si} \quad (18)$$

Where k is the proportionality constant (1), Si is the permitted standard value of parameter i according to the WHO standard (2017)

- The calculation of sub-index values (Qi) for each parameter using the following formula:

$$Qi = {Vi}/{Si} \quad (19)$$

Where Vi is the monitored concentration of the $i^{th}$ parameter (µg/L) and Si is the standard or permissible limit of the $i^{th}$ metal.

- Calculation of the HPI

$$HPI = \frac{\sum_{i=1}^{n} WiQi}{\sum_{i=1}^{n} Wi} \quad (20)$$

### III.4.7.2. Heavy Metal Evaluation Index (HEI)

**HEI** involves the evaluation of the role of each metal in relation to the overall pollution levels in water (Edet and Ofiong, 2003). It was calculated as follows:

$$\text{HEI} = \frac{\sum Hc}{\sum Hmac} \quad (21)$$

Where Hc is the monitored concentration of the heavy metal and Hmac is the maximum allowable limit of the metal.

### *III.4.7.3. Degree of Contamination ($C_d$)*

**Cd** is used to assess the cumulative contamination level in water by adding up the concentrations of various contaminants vis-a-vis their permissible levels (Backman et al. 1998). It gives an overall image of pollution levels by evaluating the combined effect of multiple heavy metals. It is calculated as follows:

$$\text{Cd} = \sum Cf = \sum {}^{Ci}/_{Si} - 1 \quad (22)$$

Where Ci is the measured concentration of heavy metal in sample, Si is the standard or permissible limit of the metal and Cf is the contamination factor for each cmetal, representing its concentration relative to the standard. A summary of the classification of the water quality based on the HPI, HEI and Cd is shown in Table 3.2.

***Table 3.2a: Water classification based on the HPI, HEI and Cd***

| **HPI** | **Reference ranges** | **Characteristics** |
|---|---|---|
| | <25 | Excellent |
| | 26 to 50 | Good |
| | 51 to 75 | Poor |
| | 76 to 100 | Very poor |
| | >100 | Unsuitatble |
| **HEI** | | **Characteristics** |
| | <10 | Low |
| | 10 to 20 | Medium |
| | >20 | High |
| **Cd** | | **Characteristics** |
| | <1 Low | Low |
| | 1-3 Medium | Medium |
| | >3 High | High |

### III.4.8. Assessment of human health Risk

Some heavy metals are known to be toxic to both humans and the environment; hence it is paramount to assess the toxicity levels in water. The assessment of human health risks involves weighing the harmful health effects of a particular toxic metal due to prolonged exposure/consumption and classifying them in terms of carcinogenic or non-carcinogenic health risks (Ogana et al. 2024). Health risk evaluation is assessed using threat isolation, dosage assessment, evaluation of exposure, and Hazard characterization, as suggested by the United States environmental protection agency (USEPA 1989).

Ingestion of drinking water is one of the most important pathways through which humans are exposed to harmful and toxic contaminants with diverse health impacts. In this research, the determination of the carcinogenic or non-carcinogenic health hazards mainly due to ingestion of groundwater and surface water in Bafia was done using the general exposure pathway equations (Eqs. 23 to 25) adopted from (USEPA 1989). Risk assessment parameters and methods by Wongsasuluk et al. (2014) were utilized in this study. Health risk assessment comprises dose–response, exposure assessment, hazard identification, and risk characterization. To evaluate the health risk, the first step was to calculate the average daily dose (ADD) of each heavy metal using the following:

$$ADD = (C_i \times IR \times EF \times ED)/(BW \times AT) \quad (23)$$

All the parameters used in Eq. (23) are defined in Table 3.4a for adults and children, with the assumption that the people in the Bafia community drink water from the boreholes, open wells, springs, developed wells and even river sources. The non-carcinogenic risk was obtained using the ADD calculation as follows:

$$HQ \text{ for non-carcinogenic effects, } = ADD/RfD \quad (24)$$

$$H\,I_i = \sum HQ_i \quad (25)$$

Where HQ is the hazard quotient, HI is the hazard index and RfD is the reference dose of each metal. Usually, HI values <1 signify an acceptable level of risk, while HI values >1 represent an unacceptable risk of non-carcinogenic effect (USEPA, 1995).

***Table 3.4a: Input parameters to calculate the average daily dose value***

| Exposure parameters | Symbols | Units | Value (Adult) | Value (Child) |
|---|---|---|---|---|
| Ingestion rate | IR | L/day | 2.2 | 1 |
| Average time | AT | year | 70 | 6 |
| Exposure duration | ED | Years | 70 | 6 |
| Exposure frequency | EF | days/year | 365 days | 365 days |
| Body weight | BW | Kg | 70 | 15 |

The cumulative effect of certain toxic trace elements in water and the prolonged human exposure to such water sources, that is, the incremental lifetime cancer risk (ILCR), might lead to the breakout of most cancers in the body (Ogana et al. 2024). The carcinogenic risk is the possibility of an individual to develop any type of cancer during the lifetime exposure to certain metals. According to USEPA (1989), the cancer slope factor (CSF) directly transforms the ADD to the continual risk of becoming a cancer patient: The values for the oral RfD and SF in mg/kg-day of some selected metals used for this study are presented in Table 3.4b and the incremental lifetime cancer risk (ILCR) was calculated as follows:

$$ILCR = ADD \times CSF \quad (26)$$

Usually, risk values < $10^{-6}$ represent no carcinogenic risk to health, while a risk values > $1 \times 10^{-4}$ suggest a high risk of developing cancer. A risk value ranging from $1 \times 10^{-6}$ to $1 \times 10^{-4}$ signifies an acceptable risk to human health.

***Table 3.4b: Heavy metal Oral Reference Dose and Slope Factor***

| | Oral RfD | Slope factor |
|---|---|---|
| **Fe** | 0.7 | NA |
| **Ti** | 3 | NA |
| **Sr** | 0.6 | NA |
| **Al** | 7 | NA |
| **Cr** | 0.003 | 0.5 |
| **Cu** | 0.04 | NA |
| **Pb** | 0.0014 | 0.0085 |
| **Ni** | 0.02 | 0.84 |
| **As** | 0.0003 | 1.5 |
| **Zn** | 0.3 | NA |
| **Mn** | 0.14 | NA |

### III.4.9. Local Meteoric Water Line (LMWL)

The LMWL is a simplified representation of the mean site-specific covariation of hydrogen and oxygen stable isotope ratios, which results from water isotope fractionation during phase changes (e.g. evaporation and condensation), across regions with different humidity gradients (e.g. vapor diffusion from a saturated water surface into dry air at the water-air interface) (Craig and Gordon, 1965). LMWLs are often developed based on the long-term distribution of $\delta^{18}O$ and $\delta$ D in a particular location, and these lines can provide a baseline for the interpretation of isotope variability over given a region (Bowen et al. 2018). The LMWL has diverse applications, including defining the relationship between surface and/or groundwater to a potential precipitation source, the estimation of seasonal changes in groundwater recharge and the concentration enrichment factor of lake (Bowen et al. 2018).

Given that there is no established LMWL in the study area (Bafia), the Yaoundé LMWL (nearest locality, 120 km away from Bafia) was used to evaluate the isotopic behavior of water resources in that area.

### II.4.10. Determination of Nitrate sources using the Kendall diagram

Generally, nitrate and oxygen isotopes vary depending on the environment and activities therein (Fig. III.9). For example, nitrogen found in commercial fertilizers (urea and anhydrous ammonia) has an isotope composition very similar to atmospheric nitrogen, and varies between -6 and +6 ‰ (Kendall et al. 2007).

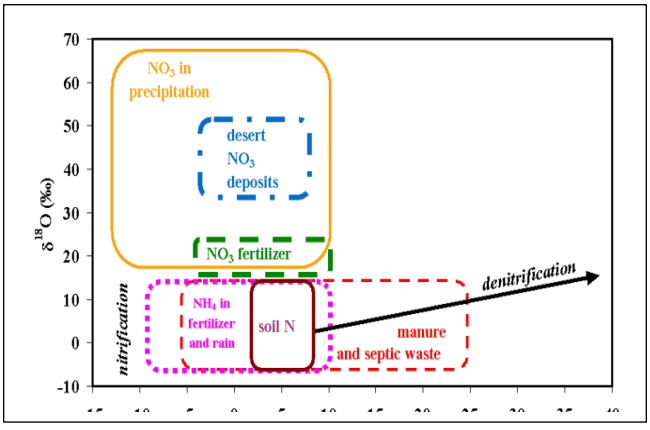


**Figure III.9: Isotopic signatures for different nitrate sources**

(Kendall et al. 2007)

Nitrogen from animal manure, sewage or biosolids is more enriched in the heavier $^{15}N$ isotope, especially after deposition and conversion to the highly volatile ammonia, and its range tends to be significantly higher, typically between +10 and +25‰; Synthetic nitrogen fertilizers have $\delta^{15}N$ values in the range of -4 to +4‰ and the $\delta^{15}N$ value of nitrogen in the soil ranges from +2‰ to +8‰ (Böhlke et al. 1997).

The analysis of $\delta^{18}O$ in $NO_3^-$ differentiates atmospheric nitrate deposition from synthetic fertilizer nitrate and microbial nitrate; $\delta^{18}O$-$NO_3$ values ≤ 10 ‰ indicate nitrates derived from the nitrification of ammonium in soil (Böhlke et al. 1997); $NO_3^-$ derived from atmospheric deposition has $\delta^{18}O$ values varying between +18 to 75.0‰; while $NO_3^-$ from fertilizers has $\delta^{18}O$ values in the range of +18 to 25.0‰ (Kendall, 1998).

### III.4.11. Statistical analysis

In order to quantitatively describe features of the chemical and isotopic datasets obtained in this Ph.D. study, descriptive statistics such as the mean, standard deviations, minimum and maximum value were calculated. A Spearman's rank correlation analysis (Spearman, 1904) was applied to summarize the data, bringing out the relationships between the investigated parameters, either positive or negative. Multivariate statistical analyses like Factor Analysis (FA), cluster analysis (CA), and hierarchical cluster analysis (HCA) have been used to decrease the complexity of multiple parameters, isolate the primary component from a vast amount of data and also group variables that have similar characteristics (Loganathan & Ahamed, 2017).

Prior to the Factor analysis, the raw datasets were transformed using the Centered log-ratio (CLR) based on the following equation:

$$CLR\ (x) = \log(x_1/g(x)),\ldots\ldots\ldots,\log(x_n/g(x))) \quad (27)$$

Where x is the hydrochemical paramater, $g(x)$ is the geometric mean of the hydrochemical parameter x, and x1 …. $X_n$ are the concentrations of the individual hydrochemical parameters. This transformation ensures that the data are normally distributed and reliable (Aitchison and Greenacre, 2002). After the CLR transformation, R-mode factor analysis with principal component analysis as the extraction method was done using SPSS version 20 to recognize patterns and explain the variance of inter-correlated variables (Ravikumar and Somashekar,

2017). The Kaiser criterion (Kaiser, 1960) was used to extract factors with Eigenvalues and Eigenvectors > 1, after which Varimax rotation was applied on the extracted factors.

Factor analysis is a statistical method aimed at reducing a large number of variables into a smaller set of factors. This technique is useful for extracting the maximum common variance from all variables, transforming them into a single score for further analysis. It is particularly resourceful for understanding hidden relationships that may not be immediately apparent from the observed variables. The first factor obtained explains the greatest part of the variance, while the subsequent factors explain a smaller part of the variance. The factor loadings give an idea of how much the particular factor contributes to the total variance. For example, high factor loadings (close +1 or -1) signify strong relationship between the variables-either positive or negative relationship (Vijay and Tripathi, 1979).

Although there are different types of hierarchical clustering techniques, all of which are often used in earth sciences, the most widely used measure of ordering is Ward's criterion. It uses an analysis of variance approach that minimizes the sum of squares within the clusters and maximizes the variance between separate clusters (Ward 1963). A classification scheme using Euclidean distance (straight line distance between two points in X-dimensional space defined by x-variables) for similarity measurement, together with Ward's method for linkage produces the most distinctive groups where each member of the group is more similar to its fellow members than to any member outside the group. The second step involves building a dendrogram connecting the above groups (Rencher 2002). The dendrogram shows the linkage points and clusters that are connected at increasing levels of dissimilarity (Chérif and Gargouri-Ellouze, 2023). The height of the branch indicates how similar or different they are from each other; the greater the height, the greater the difference. Many authors, including Fongoh et al. (2023) and Adomako et al. (2011) have demonstrated the usefulness and practicability of HCA in groundwater studies.

Q GIS 3.28.2 and Golden software was used to generate spatial distribution maps of some hydrochemical parameters for easy interpretation.

## CONCLUSION

Generally, the choice of Bafia as study area was based on socio-economic and environmental issues. Each sampling point within the study area was selected based on the prevailing surrounding anthropogenic activities, especially farming, and hygiene habits around water points. A total of 117 sampling points located in Bafia town and the peripheries were considered for both seasons, 57 in the rainy season and 60 in the dry season. Samples collected were analyzed for major ions, trace elements, stable isotopes, tritium and dual nitrogen isotopes. Results obtained were treated using different techniques, including descriptive and multivariate statistical methods (Factor analyses, Correlation analysis) using SPSS and Excel, and map treatment using Q-GIS and Golden software.

# PART II

# RESULTS, INTERPRETATION AND DISCUSSION

# CHAPTER IV: WATER CHEMISTRY AND USABILITY

## INTRODUCTION

Every groundwater system has a unique water chemistry which is acquired during the chemical alteration of meteoric water from the recharge to the discharge point (Drever, 1982). This chemical alteration water depends on several factors including soil-water interaction, dissolution of mineral species, climate, anthropogenic activities, and the duration of water-rock interaction (Subba Rao, 2002). The results of the hydrochemical characteristics, spatio-temporal variability and interaction processes influencing water chemistry will be presented in this section.

## IV.1. General water chemistry and spatio-temporal variabilities

### IV.1.1. Physical parameters

Appendix 1 shows the physical parameters of water resources in the Bafia area during the (a) rainy season and (b) dry season while Table 4.1 (a,b) presents a summary of these parameters. The physical composition of groundwater and surface water varies slightly over time and space, indicating uniformity in most parts of Bafia. However, groundwater composition is slightly different from surface water in most aspects (see Table 4.c).

***Table 4.1 a: Rainy season physical parameters of water resources in the Bafia area***

| Parameters | Min | Max | Mean | Median | Std. Dev | WHO (2017) |
|---|---|---|---|---|---|---|
| WD | 3.38 | 90 | 19.12 | 8.22 | 22.76 | |
| WL | 1 | 15.86 | 5.45 | 3.75 | 4.05 | |
| pH | 3.2 | 7 | 5.72 | 6 | 0.65 | 6.5<pH<8.5 |
| Temp | 24 | 30 | 26.95 | 27 | 1.16 | |
| ECµScm | 40 | 2220 | 355.35 | 210 | 371.53 | 1500 |
| TDS | 20 | 1110 | 176.05 | 110 | 185.97 | 600 |
| Eh | -590 | 261 | -86.54 | -52.5 | 152.81 | |
| TH | 82.51 | 56.29 | 81.08 | 7.78 | 405.07 | 500 |
| DO | 2 | 8 | 4.07 | 4 | 1.32 | |
| Alkalinity (mg/L) | 4 | 331 | 66.18 | 50 | 60.47 | |
| Salinity | 0.1 | 3 | 0.53214286 | 0.3 | 0.51702194 | |

***Table 4.1 b: Dry season physical parameters of water resources in the Bafia area***

| Parameters | Min | Max | Mean | Median | Std. dev | WHO (2017) |
|---|---|---|---|---|---|---|
| WL | 2 | 90 | 16.89 | 6 | 22.47 | |
| WD | 0 | 17 | 5.33 | 5 | 3.52 | |
| DO | 1.3 | 3.35 | 2.44 | 2.49 | 0.43 | |
| pH | 3.5 | 7.4 | 5.97 | 6 | 0.63 | 6.5<pH<8.5 |
| Temp | 24 | 31 | 27.53 | 27 | 1.7 | |
| ECµScm | 30 | 1240 | 258.67 | 170 | 244.36 | 1500 |
| TDS | 10 | 620 | 127.83 | 80 | 122.68 | 600 |
| Eh | -354.6 | 167 | -93.56 | -70.45 | 129.16 | |
| TH | 9.94 | 708.1 | 110.35 | 64.66 | 118.4 | 500 |
| Salinity | 0.01 | 0.8 | 0.13 | 0.08 | 0.14 | |
| Alkalinity (mg/L) | 2 | 1606 | 225.4 | 98 | 337.9 | |

Generally, water resources in the Bafia area are acidic to neutral, with slightly lower pH values during the rainy season. The pH values range from 3.2 to 7.0 in the rainy season and from 3.5 to 7.4 in the dry season, with an annual mean of 5.8. Boreholes, hand-dug wells and surface water have slightly higher pH than springs, which are more acidic. As observed by Appelo and Postma (2005), the consumption of carbonic acid during the dissolution of silicate minerals results in increased alkalinity and pH values. Hence, the low pH (especially in the rainy season) reflects an acidic system which is attributed to the production of $CO_2$ during silicate hydrolysis and the action of biological activities near surface and shallow groundwater (Kuithca et al. 2012; Emvoutou et al. 2018; Kamtchueng et al. 2022; Fongoh et al. 2023). Overall, pH values vary very little throughout the study area. However, groundwater is relatively more acidic than the flowing surface water. Similar pH values have been obtained in other natural crystalline environments in Cameroon where the surface residual aquifer (laterite) with low basic cations is recharged by rainwater (Bon et al. 2021; Fongoh et al. 2023).

Temperatures are within the range of 26.9 °C and 27.6 °C, with an annual average of 27.3°C very close to the ambient temperature in Bafia (26 °C). Similar low temperatures have been observed in shallow groundwater in the Banana Plain (Ako et al. 2011, 2012), Yaounde (Fongoh et al. 2023) and the Douala metropolis (Kamtchueng et al. 2022), and these suggest quick infiltration within a shallow flow path under the influence of atmospheric conditions, with no possible heat source.

Both EC and TDS vary similarly, with higher values in hand-dug wells especially during the rainy season; the EC ranges from 30 µS/cm to 2220 µS/cm, with an annual mean of 307.1 µS/cm; the TDS varies between 10 and 1110 mg/L, with an annual average of 151.9 mg/L. This reflects moderate to high mineralization and also suggests that groundwater chemistry in Bafia is not homogenous given the low mean and median values. As expected, groundwater EC, TDS and other parameters have higher concentrations than surface water sources in both seasons (Table 4.1c). The highest EC and TDS values for groundwater were encountered in samples around low topographic, highly populated areas with poor drainage systems. Amongst the rivers, the Mbam River (BRW 34), which is the main drainage river in the area, has the lowest EC (40 µS/cm and 30 µS/cm) and TDS (20mg/l and 10 mg/l) in the rainy and dry seasons respectively; the Gamba River (BRW 11) has the highest EC (280µS/cm and 360 µS/cm ) and TDS (140mg/l and 180 mg/l) in the rainy season and dry seasons independently. The TDS and EC slightly increase from the high topographic areas towards the low central and southern discharge areas. As indicated by Takounjou et al. (2020) and Ngouokouo et al. (2025), the topography of the area controls the groundwater flow gradient, ion transport and infiltration, with more ions and dissolved solids accumulating in the downward gradient where there is lower flow velocity.

The EC and TDS values in this study are higher than those observed in Yaounde (≤ 950µS/cm) (Bon et al. 2021; Fongoh et al. 2023), the Banana Plain (≤ 530µS/cm) Ako et al. 2012, the Ndop Plain (≤ 44mg/L) (Wirmvem et al. 2013) and other woody areas in the southern parts of Cameroon (≤ 75µS/cm) (Rakotondrabe et al., 2017) where water-rock interaction processes involve mainly silicate minerals with less solubility.

The total hardness (TH) and alkalinity of groundwater are higher than in surface water, with a general increase from the rainy to the dry season in both sources (Fig IV.1a). The TH varies from a 58% soft water in the rainy season to a 27% soft in the dry season and from 9% hard water in the rainy season to 17% very hard water in the dry season, indicating groundwater evolution.

*Table 4.1c: Statistical variation of physico-chemical parameters of different water sources from 2022 to 2023 in Bafia*

| | Groundwater, n = 108 | | | | | | | | | | | | | | | | Surface water, n = 9 | | | |
|---|---|---|---|---|---|---|---|---|---|---|---|---|---|---|---|---|---|---|---|---|
| | Dug wells | | | | Boreholes | | | | Developed wells | | | | Springs | | | | Rivers | | | |
| | Min | Max | Mean | Stdev | Min | Max | Mean | Stdev | Min | Max | Mean | Stdev | Min | Max | Mean | Stdev | Min | Max | Mean | Stdev |
| pH | 5.0 | 7.0 | 5.8 | 0.5 | 5.2 | 7.0 | 5.9 | 0.4 | 4.0 | 7.0 | 5.7 | 0.7 | 3.2 | 6.0 | 4.7 | 1.3 | 3.2 | 7.0 | 6.1 | 1.1 |
| Temp | 25.0 | 31.0 | 27.6 | 1.5 | 25.0 | 30.0 | 27.4 | 1.2 | 26.0 | 30.0 | 27.6 | 1.3 | 24.0 | 28.0 | 25.8 | 1.7 | 24.0 | 28.0 | 25.6 | 1.3 |
| Field EC (µS/cm) | 30.0 | 2220.0 | 357.9 | 411.8 | 70.0 | 1240.0 | 344.3 | 275.7 | 50.0 | 770.0 | 234.7 | 165.8 | 30.0 | 290.0 | 147.5 | 127.6 | 30.0 | 360.0 | 148.2 | 122.5 |
| TDS (mg/L) | 10.0 | 1110.0 | **178.7** | 206.1 | 30.0 | 620.0 | **169.3** | 138.2 | 20.0 | **380.0** | 115.8 | 82.6 | 10.0 | 140.0 | **70.0** | 64.8 | 10.0 | 180.0 | **71.8** | 62.3 |
| Eh (mV) | -597.0 | **261.2** | -127.3 | 169.5 | -355.0 | 218.0 | -94.5 | 152.4 | -296.0 | 211.2 | -43.9 | 139.6 | -126.4 | 16.1 | -47.3 | 70.1 | -126.4 | 16.1 | -44.9 | 42.4 |
| DO | 1.0 | 6.2 | 3.2 | 1.3 | 2.0 | 7.5 | 3.6 | 1.5 | 2.0 | 8.7 | 4.1 | 1.7 | 2.0 | 3.5 | 2.9 | 0.6 | 1.0 | 5.9 | 3.2 | 1.4 |
| TH | 10.0 | 319.0 | 79.5 | 83.0 | 5.7 | 708.0 | 91.5 | 127.1 | 10.3 | 199.0 | 50.0 | 48.0 | 12.3 | 79.0 | 43.2 | 34.0 | 9.8 | 120.0 | 39.2 | 36.4 |
| Salinity | 0.0 | 3.2 | 0.3 | 0.6 | 0.0 | 1.7 | 0.3 | 0.4 | 0.0 | 1.1 | 0.3 | 0.3 | 0.0 | 0.4 | 0.1 | 0.2 | 0.0 | 0.4 | 0.1 | 0.2 |
| Alkalinity(mg/l) | 10.0 | 1314.0 | 126.6 | 204.0 | 4.0 | 1606.0 | 221.5 | 368.2 | 2.0 | 300.0 | 72.6 | 66.8 | 13.0 | 534.0 | 151.5 | 255.3 | 6.0 | 380.0 | 65.5 | 107.9 |
| HCO3 (mg/l) | 10.0 | 439.0 | 95.8 | 95.6 | 4.0 | 305.0 | 109.4 | 81.6 | 14.0 | 220.0 | **65.8** | 52.7 | 13.0 | 98.0 | **42.3** | 39.0 | 10.0 | 214.0 | 50.8 | **59.4** |
| F- (mg/l) | 0.0 | 0.8 | 0.1 | 0.2 | 0.0 | 1.2 | 0.2 | 0.3 | 0.0 | 1.1 | 0.2 | 0.3 | 0.0 | 0.0 | 0.0 | 0.0 | 0.0 | 0.0 | 0.0 | 0.0 |
| Cl-(mg/l) | 1.1 | 244.0 | **27.9** | 47.1 | 1.2 | 72.0 | **11.5** | 14.0 | 1.3 | 36.0 | **8.7** | 8.3 | 1.2 | 19.0 | 9.3 | 8.6 | 1.2 | 30.0 | 8.7 | **8.6** |
| NO3(mg/l) | 0.0 | 230.0 | **27.3** | 53.6 | 0.0 | 176.0 | **12.7** | 34.2 | 0.0 | 82.0 | **19.1** | 25.2 | 0.6 | 29.0 | **12.1** | 13.8 | 0.0 | 2.0 | 2.2 | **5.2** |
| SO4(mg/l) | 0.0 | 69.5 | **7.9** | 14.5 | 0.0 | 497.0 | **31.2** | 95.3 | 0.0 | 109.0 | **7.6** | 24.6 | 0.4 | 8.6 | **4.5** | 3.9 | 0.0 | 27.0 | 5.1 | **7.9** |
| NH4+(mg/l) | 0.0 | 4.9 | 0.3 | 1.1 | 0.0 | 0.1 | 0.0 | 0.0 | 0.0 | 0.0 | 0.0 | 0.0 | 0.0 | 0.0 | 0.0 | 0.0 | 0.0 | 0.1 | 0.0 | 0.0 |
| Na+(mg/l) | 2.1 | 174.5 | **27.6** | 37.3 | 4.0 | 42.0 | **14.9** | 9.0 | 1.3 | 28.3 | **13.0** | 6.9 | 2.5 | 20.0 | **10.0** | 8.6 | 2.0 | 30.0 | **10.2** | **8.8** |
| K+(mg/l) | 1.0 | 64.8 | **8.2** | 12.8 | 0.9 | 7.1 | **3.9** | 1.8 | 1.0 | 17.0 | **5.0** | 4.2 | 1.0 | 12.3 | **6.6** | 5.8 | 1.0 | 17.0 | 5.7 | **5.4** |
| Mg2+(mg/l) | 0.9 | 22.0 | **6.9** | 6.6 | 0.8 | 26.0 | **8.7** | 6.7 | 1.0 | 14.2 | 5.2 | 4.3 | 1.0 | 10.0 | **4.5** | 4.3 | 0.0 | 7.0 | **3.0** | **2.5** |
| Ca2+ (mg/l) | 1.5 | 120.1 | **27.3** | 25.5 | 2.4 | 244.0 | **34.6** | 45.2 | 4.0 | 60.0 | **19.7** | 17.0 | 2.5 | 16.0 | **8.8** | 6.2 | 1.7 | 36.0 | **10.9** | **10.5** |

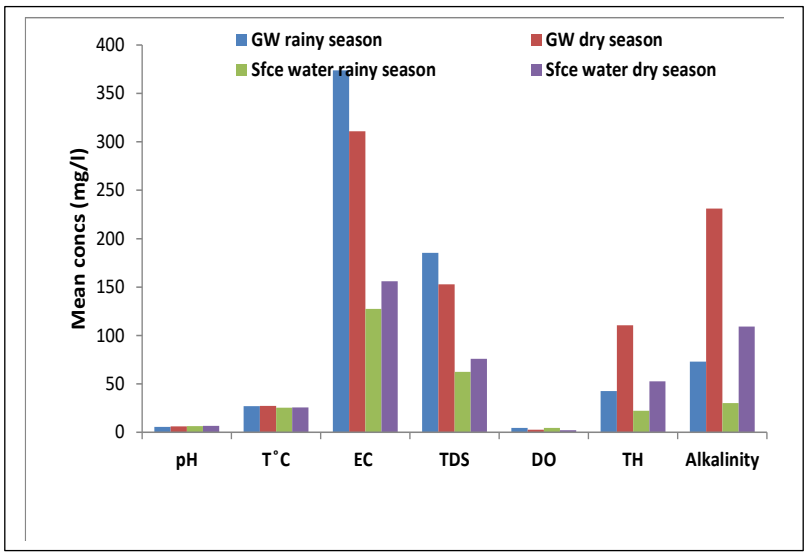


**Figure IV.1a: Seasonal variations of some groundwater and surface water parameters**

Depending on the pH, water hardness >200mg/l often causes scale deposition in distribution networks, pipelines and storage tanks. However, soft water (hardness <100mg/l) with a lower buffering capacity, leads to more corrosive water pipes and is often linked to high blood pressure (excess sodium). Based on the TH, all samples, except BBH 38 in the dry season (TH = 708 mg/l $CaCO_3$), are within the drinking water limits of 500 mg/l established by the WHO. A plot of TH versus TDS shows that more than 90% of the samples are soft-fresh (TDS < 600mg/L), with some hard-brackish types present (Fig. IV.1b).

Redox potentials are higher in shallow hand-dug wells (up to 261.2 mV) due to the presence of dissolved oxygen near surface. These values decrease to about -597 mV in boreholes, reflecting the prevailing reducing conditions with depth. The redox potential and DO are generally higher in the rainy season than in the dry season, possibly due to several factors like water mixing, lower temperatures and increased oxygenated rainfall. Similar scenarios were observed in the Banana Plain (Ako et al. 2011; 2012) reflecting a decrease in oxygen content with well depth. It is observed that in developed wells, most of the studied parameters have values between the dug wells and the boreholes, suggesting a mixture of groundwater between the deep and the shallow aquifers in these wells. All physical parameters are generally within the WHO (2017) drinking water limits, with few exceptions.

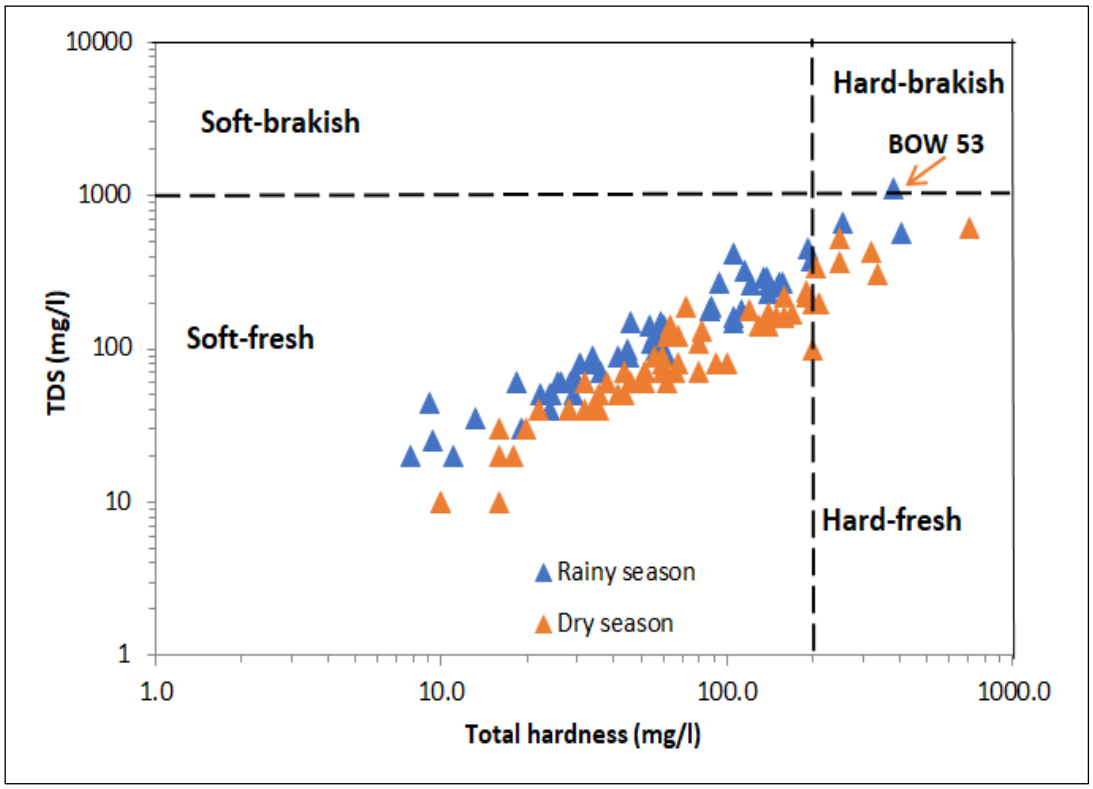


**Figure IV.1: Scatter plot of TDS versus TH showing water quality in the Bafia area**

### IV.1.2. Chemical parameters

#### IV.1.2.1. Cations and water chemistry

Similarly, as observed in Appendix 2 (a,b), the chemical composition of water resources shows slight variability between seasons, with higher concentrations observed in the dry season due to reduced dilution effect. However, the chemical composition is heterogeneous from one place to another, notably for parameters like $NO_3$, $Cl^-$, $K^+$ and even $SO_4^{2-}$. The dominant cation, $Ca^{2+}$, is within the WHO maximum permissible limit of 200 mg/l, and the BIS (2003) desirable limit of 75 mg/l and varies between 1.47 mg/L and 244 mg/L, with an annual mean of 26.2 mg/L. This is closely followed by $Na^+$, with a minimum of 1.28 mg/L, a maximum of 174.5 mg/L and an annual average of 18.8 mg/L. $Mg^{2+}$ concentrations vary from 0.5 mg/L to 26.4 mg/L, with an annual mean of 6.8 mg/L. The low $Mg^{2+}$ concentrations coupled with the moderate $Ca^{2+}$ infers minimal weathering/dissolution of limestone or dolomite but rather points to the weathering of

calc-silicate minerals in amphiboles, pyroxenes, olivine and biotite as main sources of calcium in the area (Tchakounté et al. 2021).

$K^+$ concentrations range between 0.7 mg/L and 64.8 mg/L, with an annual average of 6.0 mg/L while $NH_4^+$ ion was weak in concentration, ranging from below detection limits (BDL) to 4.9 mg/L. Sodium and potassium for all water types/sources are within the WHO (2017) guidelines for drinking water (200mg/l and 12mg/l) respectively, except for some 9% and 4% samples in the rainy and dry seasons which exceeded the limits for potassium. Generally, low potassium is accredited to their resistance to weathering, low geochemical mobility and their fixation on clay minerals (Srinivasamoorthy et al., 2008). Lower potassium levels have been reported in groundwater in the more urbanized city of Yaounde (25.5mg/L). Hence, high concentrations in some samples in Bafia may be attributed to prolonged weathering of potassium feldspars abundant in the syenites and quartz monzonites (abundant in the rocks) and the application of synthetic fertilizers like the N-P-$K_s$ (Singh et al. 2012; Tchakounté et al. 2021; Akenji et al. 2023). Excessive sodium in water might cause hypertension, congenial heart diseases, nervous disorder, and kidney problems.

Similar to physical parameters, groundwater major cations concentrations are higher than those of surface water; with some few exceptions (see Table 4.1c above). For example, groundwater samples like BOW 18, 52, 53, 56, Bdow 49 and Bdsp 08 (rainy season), BOW 53, 56 and 68 (dry season) have exceptionally higher $K^+$, with the peak in BOW 53. Samples BBH 38, BOW 53 (rainy season), BBH 38 and BOW 52 (dry season) have high $Ca^+$ concentrations, with a peak in BBH 38. On the other hand, surface water major cation concentrations ($Ca^{2+}$, $Mg^{2+}$, $Na^+$ and $K^+$) are generally low, increasing from upstream (BRW 23-Mbam River) to downstream (BRW 11-Gamba River). Although within the WHO limits, the Gamba River (BRW 11) in Nyamsong III have the highest concentrations of major cations in both seasons. Just like groundwater, surface water major cations are more concentrated during the dry season than the rainy season, with the exception of $K^+$ in groundwater, which is higher in the rainy season than in the dry season (Fig. IV.2).

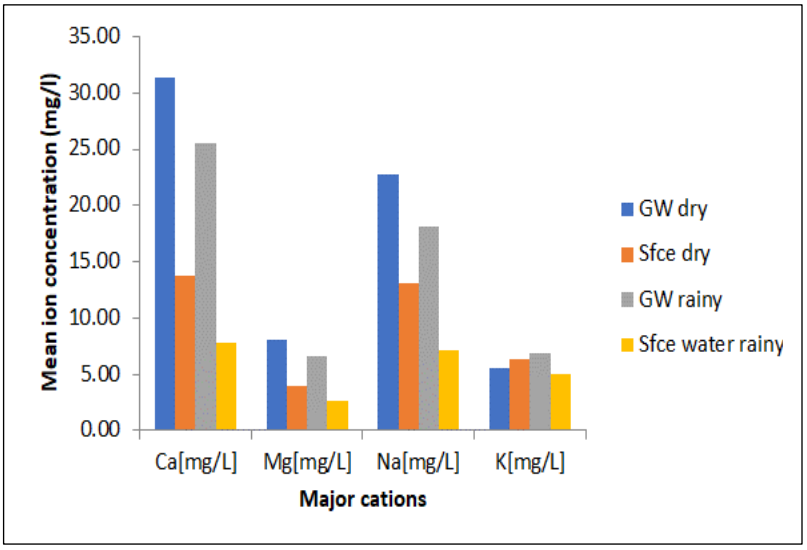


**Figure IV.2: Variation of mean concentrations of cations of groundwater and surface water resources during the rainy and dry season**

### IV.1.2.2. Anions and water chemistry

The dominant anion for both surface and groundwater is $HCO_3^-$, varying from 4 mg/L to 439 mg/l, with an annual mean of 88.9 mg/L. Alkalinity and $HCO_3^-$ evolve in the same direction in space and time for both groundwater and surface water, with higher values in groundwater. They increase slowly from the Mbam River (BRW 34) upstream to the Gamba River River (BRW 11) in Nyamsong III. The soil zone often contains relatively higher $CO_2$ pressure than the atmosphere, produced by organic matter decay and root respiration (Appelo and Postma 1996). Hence, most bicarbonate is derived from this soil zone, coupled with the dissolution of carbonates and silicates by carbonic acid during rainfall. $Cl^-$ ion concentrations range between 1.1 mg/L to 244 mg/L, with an average of 17.0 while $SO_4^{2-}$ concentrations range between 0 mg/L and 496.8 mg/L, with an annual mean of 14.7mg/L. Low chloride contents suggest no salt sources and minimal evaporation before or during groundwater infiltration. Sulfate in water is commonly derived from the oxidative weathering of sulfide minerals, such as pyrite ($FeS_2$); however, gypsum and anhydrite can also be a sulfate source (Han et al. 2014).

Nitrate, which varies from BQL to 229 mg/L, with an annual average of 18.6 mg/L, generally falls within WHO recommended limits for drinking water except for 7% and 12% groundwater samples which have $NO_3$ levels higher than the WHO (2017) nitrogen maximum contaminant

level (MCL) of 10 mg/L, corresponding to 50 mg/L of $NO_3$ in the rainy and dry seasons independently. Nitrate is a known pollutant found in the environment. It can originate from agricultural fertilizers, atmospheric precipitation, human and animal excreta, and the nitrification of $NH_4^+$ and other N-species (Tiwari 2014; Khan et al. 2020). Hence, nitrate in water in Bafia points to anthropogenic impacts especially resulting from agricultural input and poor domestic hygiene conditions. High $NO_3^-$ in drinking water can cause a number of disorders including methemoglobinemia in infants, gastric cancer, goiter, birth malformations, and hypertensions (Appelo and Postma 1996; Wirmverm et al. 2013). Some groundwater samples like BOW 51, 52, 58 and BOW 01, Bdow 16, BOW 52, 56 have $NO_3^-$ concentrations > 50mg/L in the dry and rainy season respectively. Conversely, all surface waters except BRW 26 (dry season), have $NO_3^-$ <1mg/L.

The moderate major ion concentrations in groundwater depict moderate water-rock interactions in the crystalline basement, short residence time, the shallow nature of the aquifer and its acidic nature (Edmunds and Smedley, 1996 The general ionic abundance for groundwater is $Ca^{2+}>Na^+>K^+>Mg^{2+}$ for cations and $HCO_3^- > NO_3^->Cl^->SO_4^{2-}$ for both seasons; and $Ca^{2+}>Na^+>K^+>Mg^{2+}$ (cations) and $HCO_3^->Cl^->NO_3^->SO_4^{2-}$ and $HCO_3^->Cl^->SO_4^{2-}>NO_3^-$ (anions) for surface water during the rainy and dry seasons independently.

Spatial distribution maps for Ca, K and Cl demonstrate a slight increase in ionic concentrations from the rainy to the dry season, from the northern to the central and southern parts of Bafia, but generally within the WHO MCL for drinking water, with few exceptions (Fig. IV.3a).

This tendency suggests the intense dissolution of the 2 mica gneisses, quartz monzonite, syenites and meta-sediments (possibly quartzite) hosted in the Bafia area (Tchakounté et al. 2021; Ganwa et al. 2022), not leaving out ion exchange reactions that occur down south. Furthermore, the $NO_3$ variation/land use map (Fig. IV.3b) shows high nitrate concentrations in the highly populated Bafia center (Kirai, Eldorado, Gondrone, Rigama, hospitals and market areas). This suggests the influence of anthropogenic activities on water quality vis-à-vis the increased population, notably from agriculture, leaky pit latrines and poor waste management/disposal habits.

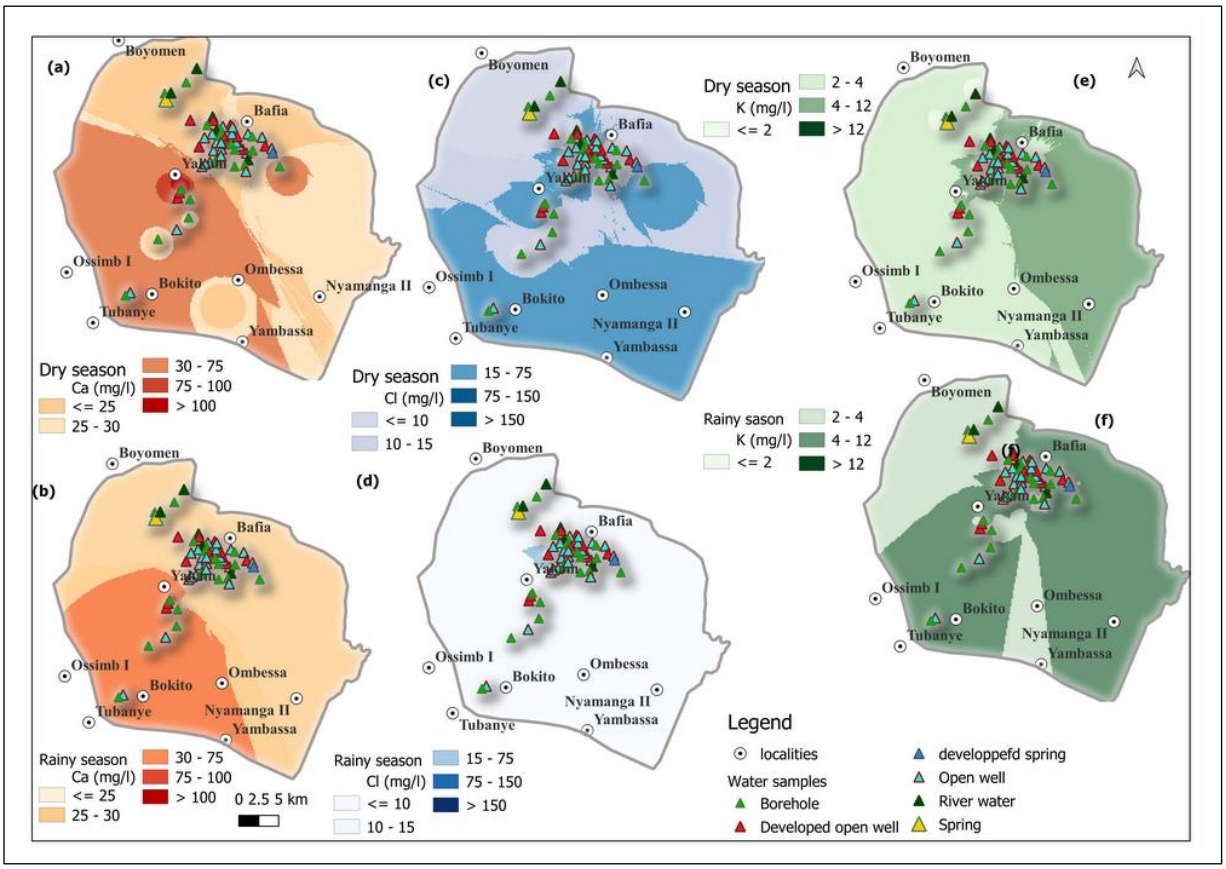


**Figure IV.3a Seasonal spatial distribution maps of some hydrochemical parameters in Bafia**

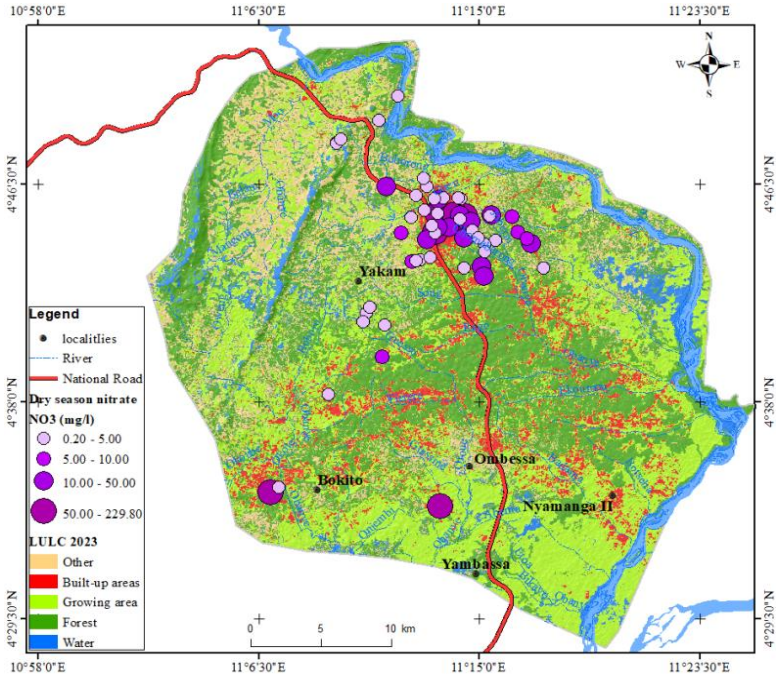


**Fig. IV.3b: Nitrate spatial distribution map based on the Land use of the Bafia area**

## IV.2. Effects of natural processes and human activities on the Natural Background Levels and Threshold Values of major ions

The NBL and TVs were calculated using the cumulative probability method. For major ions, some selected parameters, including $NO_3$, $Cl^-$ and $K^+$ were used to demonstrate anthropogenic input, and while $Ca^{2+}$, $Na^+$ and $HCO_3$ were used to demonstrate the natural system. The calculated NBLs for $NO_3$, $Cl^-$ and $K^+$ are 2.2, 25 and 9.95 mg/L, with TVs of 26.1, 137.5 and 10.98 respectively.

According to Braun et al. (2005), 21% samples with nitrate values corresponding to the geogenic background level for groundwater in tropical forest environments (0.07 – 0.6 mg/L) and 30% which correspond to saprolite weathering milieus (0.07 – 1 mg/L) were used as a reference for the determination of nitrate NBLs. Based on the calculations, 53% and 18% samples exceed the nitrate NBLs and TVs, 15% and 2% exceeded the chloride NBLs and TVs, while 9% samples exceeded the potassium NBLs and TVs respectively. Most of these samples (green points) are shallow wells located around farmlands (BOW 01), market areas (BOW 67), hospitals (Bdow 49) and the city lowlands (BOW 52) (Fig. IV.4 a-c), where there are more intense human influences.

However, the greater majority (>85%) of the samples reflect the natural undisturbed levels, except for nitrate, which have diverse contamination sources. Likewise, about 15% of the samples, exceeded sodium, calcium and bicarbonate NBLs and TVs, reflecting significant inputs from natural weathering and dissolution processes (Fig. IV.4d-e). These are mainly borehole samples (BBH 38, BBH 50) and developed wells (Bdow 36 and Bdow 54) which depict prolonged weathering. Hence, groundwater mineralization in Bafia is predominantly influenced by natural weathering processes, with some anthropogenic activities.

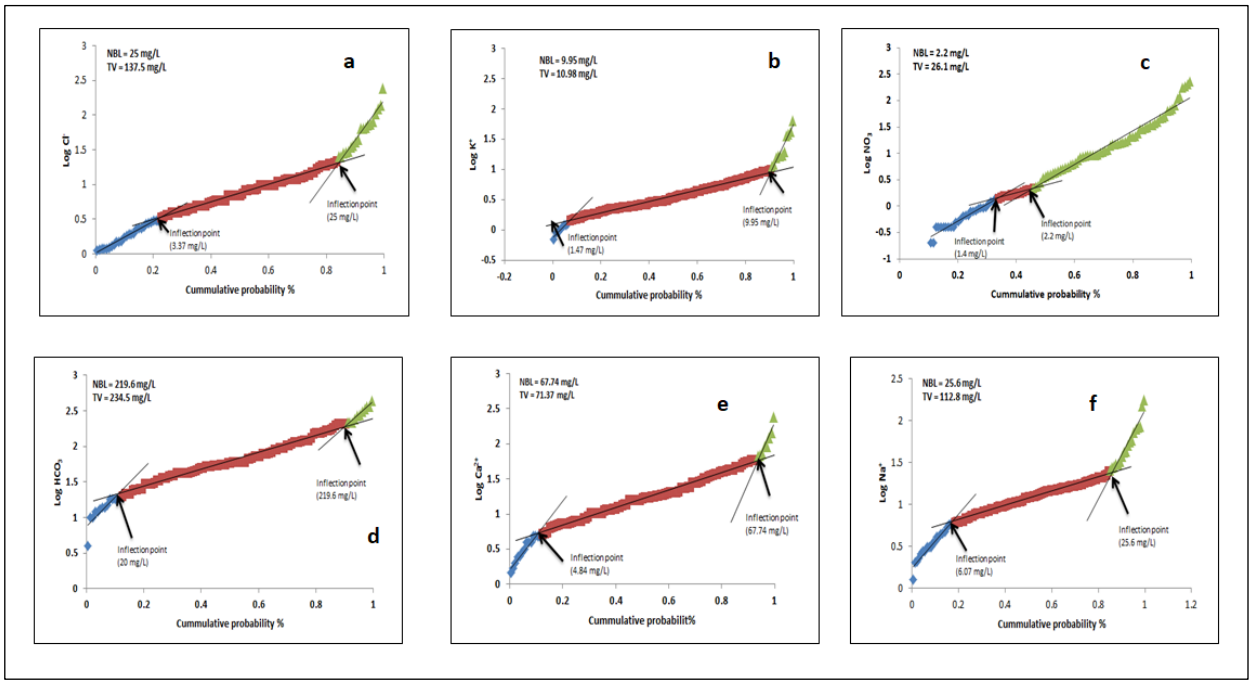


**Figure IV.4: Cumulative probability plots and associated NBLs and TVs of $Cl^-$, $NO_3^-$, $K^+$, $HCO_3^-$, $Ca^{2+}$ and $Na^+$.**

***Different colors represent different groups, separated by upper and lower inflection points representing the background levels.***

## IV.3. Hydrochemical facies and groundwater evolution

The plot of major cations on ternary diagrams show 42.1% and 33.3% plot in $Na^+$+$K^+$ zone; 21.1% and 28.3% samples plot in the $Ca^{2+}$ zone; while 36.8% and 38.3% samples plot in the no dominant type in the rainy and dry season individually (Fig. IV.5a,b). The anion ternary diagrams relating $HCO_3^-$, $Cl^-$ and $SO_4^{2-}$ show that most of the samples (78.9% and 83.3% for rainy and dry season respectively) plot in the $HCO_3^-$domain, with secondary trends towards $Cl^-$ +$NO_3^-$ (17.5% and 11% in the rainy and dry season) and $SO_4^{2-}$ (1.7% in both seasons). (Fig. IV.5c,d).

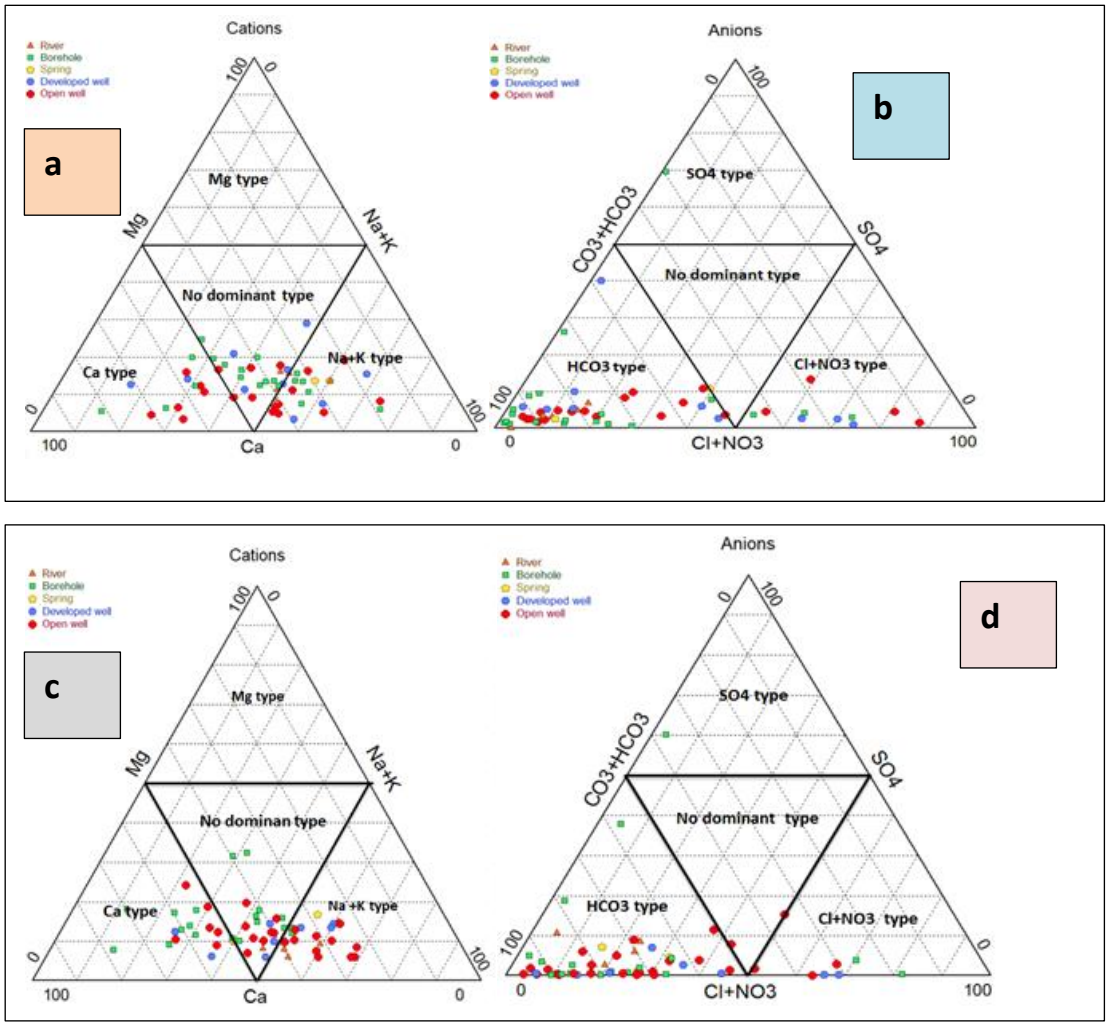


**Figure IV.5: Ternary cation and anion diagrams showing the contribution of individual ions in the rainy (a and b) and dry season (c and d)**

In order to understand the chemical character, groundwater samples were plotted on a Piper trilinear diagram (using Diagramme version 6.77). The Piper diagram (Fig. IV.6 a, b) reveals that the alkaline earth elements ($Ca^{2+}$+$Mg^{2+}$) exceed the alkali metals ($Na^{+}$+$K^{+}$) while the weak acids ($CO_3$+$HCO_3$) dominate the strong acids ($SO_4^{2-}$+$Cl^{-}$). The major water type is the CaMg-$HCO_3$ water type (black rectangle), with about 68% and 85% in the rainy and dry season respectively. In most groundwater chemical evolution models (Adams et al. 2001; Ako et al. 2012), this water type often represents vigorous recharge from fresh water, regarded as early stage circulating water which has undergone limited chemical evolution and/or mixing with other water types. This is recently recharged water with insignificant water-rock interactions, cation exchange and reflects the initial fingerprints of the recharging rain (Adomako et al. 2011; Ako et al. 2012; Tay,

2021). Water samples in this group have low EC/TDS, higher average bicarbonate and the major ions including nitrate (below 10mg/L), potassium, chloride and sulfate.

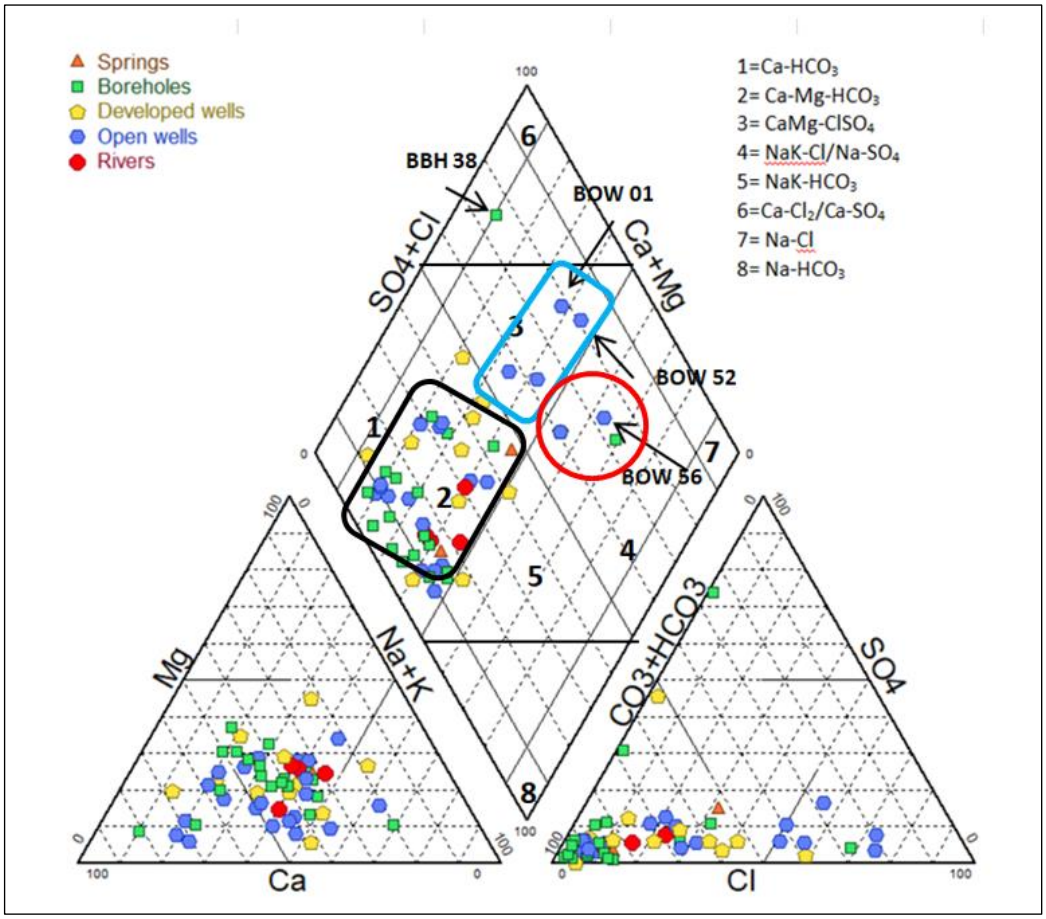


**Figure IV.6a: Piper diagram for the rainy season showing Ca-Mg-HCO3 as the main water type**

The gentle relief of most parts of Bafia gives rise to mixed types like CaMg-$ClSO_4$ (17.5%), NaK-Cl / Na-$SO_4$ (13%) and NaK-$HCO_3$ (5%). These are usually derived from a mixture of water types, including contaminated waters. This mixture is often characteristic of crystalline aquifers like in Bafia, which contribute water through multiple fractures with no defined flow lines. Samples BOW 01 and BOW 52 of group 3 (blue rectangle) have the highest nitrate (204.4 and 188.9mg/l each) concentrations; sample BOW 53 of group 4 (red circle) has the highest chloride (243.9mg/l) and high potassium (64.8mg/l) while BOW 56 has the highest ammonium concentration (4.9mg/l) in addition to high nitrate and potassium.

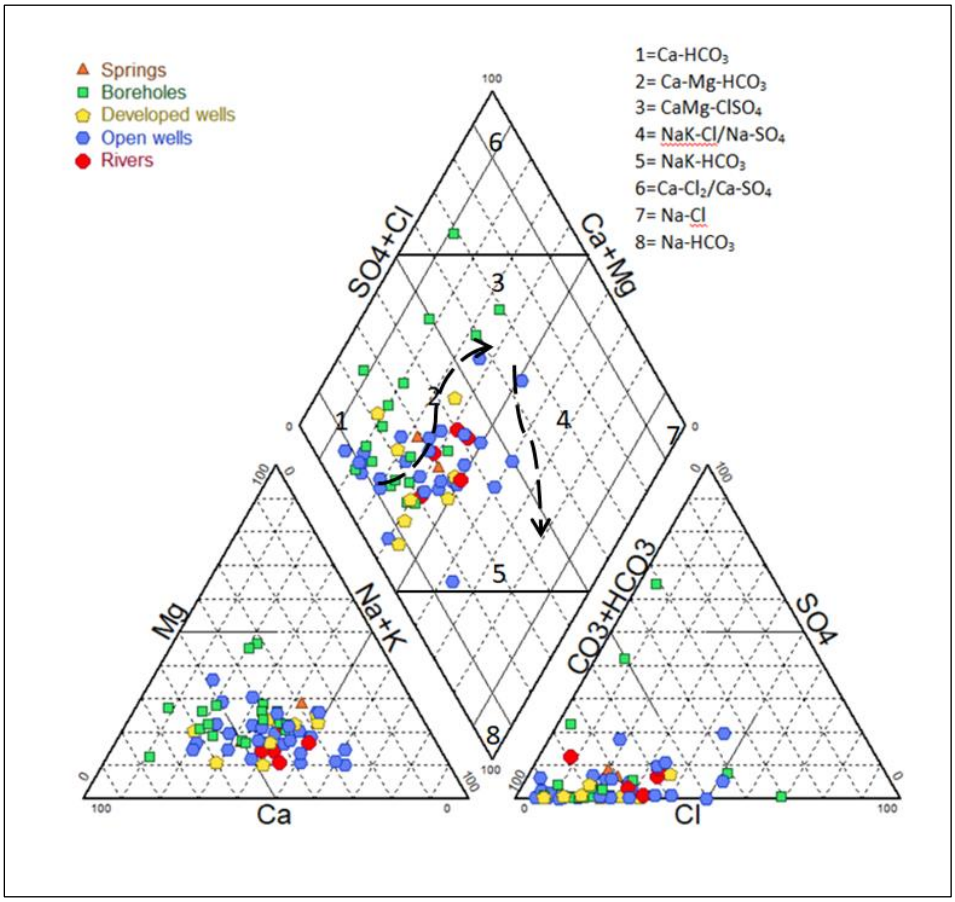


**Figure IV.6b: Dry season Piper diagram showing the evolutionary trend for both surface and groundwater**

As groundwater flows towards the center and south, the incongruent dissolution and possible cation exchange continue, releasing more $Mg^{2+}$ and $Na^{+}$ into the system. The $Na^{+}$ enrichment and slight TDS increase along the flow line testify the groundwater has undergone some slight chemical evolution. Additionally, higher $Mg^{2+}/Ca^{2+}$ ratio (>1) in a few samples in these two groups confirm more water-rock interactions (see next section) enhanced by relatively longer residence times between groundwater and the aquifer media (Adomako et al. 2011; Ako et al. 2012).

No clear pattern is observed in water types between shallow water samples (hand-dug wells) and deep water samples (boreholes) and surface water, suggesting a close hydraulic connection between them. Similar scenarios have been observed in the Ndop Plain (Wirmvem et al. 2013); suggesting mixed groundwater. However, as highlighted in Table 4.1c above, higher mean

concentrations of TDS (178.7 mg/L), $Cl^-$ (27.9 mg/L), $NO_3^-$ (27.3 mg/L), $Na^+$ (27.6 mg/L) and $K^+$ (8.2 mg/L) are observed in shallow wells as opposed to boreholes, developed wells, springs and surface water. Conversely, boreholes have higher $Ca^{2+}$ (34.6 mg/L) and $Mg^{2+}$ (8.7 mg/L) mean concentrations, signifying longer rock-water interactions in deeper wells as opposed to the intense anthropogenic inputs near surface. Similar findings were recorded by Fei et al. (2022), who evaluated the processes controlling the chemical evolution of shallow and deep aquifers in the Hebei Province in China.

### IV.4. Sources of chemical components and hydrogeochemical processes

#### IV.4.1. Ionic correlations

The major ion chemistry of groundwater and surface water and the relationship between ionic species have been used in several studies to reveal the origin of solutes and processes that generate a particular water composition (Adomako et al. 2011; Wirmvem et al. 2013; Kamtchueng et al. 2022). The Spearman correlation matrix (Table 4.2a, b) reveals important details on the processes taking place within the aquifers. Groundwater shows high positive EC correlation ($r > 0.7$) with $Ca^{2+}$, $Mg^{2+}$, $K^+$, $Na^+$, $HCO_3^-$ $Cl^-$; moderate positive correlation with sulfate ($r=0.52$) and weak positive correlation with nitrate ($r=0.38$) and fluoride ($r=0.32$). Similar trends are observed for the TDS, indicating the influence of the unconsolidated sediments and gneissic bedrock material in chemically enriching the water as it percolates through the under-saturated zone (Takounjou et al., 2010). Hence, the weak correlation between EC and sulfate, EC and nitrate, EC and fluoride reflects insinuates that these parameters have different sources which do not coincide with the former. The strong negative correlation between pH and $NO_3^-$ suggests that the presence of nitrate and even ammonium is influenced by some reactions like nitrification which are pH-dependent. The strong positive correlation between major ions is indicative of their common source, which could be from silicate rocks, carbonates or a mixture, as will be discussed in the next sections. The strong relationship between $Na^+$ and $Cl^-$ ($r>0.9$) in both surface and groundwater suggests some halite sources, but given their absence in the study area, they could originate from silicate weathering and anthropogenic processes.

*Table 4.2a: Spearman Correlation matrix for rainy season water samples in the Bafia area*

| **Parameters** | pH | EC | TDS | TH | $HCO_3^-$ | $F^-$ | $Cl^-$ | $NO_3^-$ | $SO_4^{2-}$ | $NH_4^+$ | $Na^+$ | $K^+$ | $Mg^{2+}$ | $Ca^{2+}$ |
|---|---|---|---|---|---|---|---|---|---|---|---|---|---|---|
| pH | 1 | | | | | | | | | | | | | |
| EC (µScm) | 0.43 | 1 | | | | | | | | | | | | |
| TDS | 0.44 | 1.00 | 1 | | | | | | | | | | | |
| TH | 0.44 | **0.96** | **0.96** | 1 | | | | | | | | | | |
| $HCO_3^-$ | 0.54 | **0.82** | **0.83** | 0.85 | 1 | | | | | | | | | |
| $F^-$ | 0.16 | 0.36 | 0.37 | 0.39 | 0.38 | 1 | | | | | | | | |
| $Cl^-$ | 0.13 | 0.61 | **0.61** | 0.49 | 0.24 | -0.02 | 1 | | | | | | | |
| $NO_3^-$ | **-0.14** | 0.07 | 0.07 | 0.00 | -0.35 | -0.31 | **0.55** | 1 | | | | | | |
| $SO_4^{2-}$ | 0.41 | **0.85** | **0.85** | 0.83 | **0.71** | 0.41 | 0.52 | 0.00 | 1 | | | | | |
| $NH_4^+$ | 0.10 | 0.22 | 0.22 | 0.20 | 0.15 | -0.06 | 0.25 | 0.24 | 0.26 | 1 | | | | |
| $Na^+$ | 0.38 | **0.84** | **0.84** | 0.74 | **0.64** | 0.27 | **0.63** | 0.14 | **0.64** | 0.23 | 1 | | | |
| $K^+$ | 0.16 | **0.64** | **0.64** | 0.62 | 0.42 | 0.12 | 0.47 | 0.25 | 0.54 | 0.13 | 0.41 | 1 | | |
| $Mg^{2+}$ | 0.34 | **0.88** | **0.88** | 0.86 | **0.64** | 0.18 | **0.60** | 0.17 | **0.77** | 0.21 | 0.71 | **0.63** | 1 | |
| $Ca^{2+}$ | 0.48 | **0.92** | **0.93** | 0.98 | **0.88** | **0.42** | 0.40 | -0.08 | **0.80** | 0.18 | 0.71 | **0.53** | 0.75 | 1 |

**Correlation is significant at the 0.01 level**

*Table 4.2b: Spearman Correlation matrix for dry season water samples in the Bafia area*

| **Parameters** | pH | EC | TDS | TH | $Ca^{2+}$ | $Mg^{2+}$ | $Na^+$ | $K^+$ | $HCO_3^-$ | $Cl^-$ | $SO_4^{2-}$ | $NO_3^-$ |
|---|---|---|---|---|---|---|---|---|---|---|---|---|
| pH | 1.000 | | | | | | | | | | | |
| ECµScm | 0.32 | 1.0 | | | | | | | | | | |
| TDS | 0.31 | **1.0** | 1.0 | | | | | | | | | |
| TH | 0.38 | **1.0** | **1.0** | 1.0 | | | | | | | | |
| $Ca^{2+}$ | 0.40 | **1.0** | **0.9** | 1.0 | 1.0 | | | | | | | |
| $Mg^{2+}$ | 0.32 | **0.9** | **0.9** | 0.95* | **0.9** | 1.0 | | | | | | |
| Na | 0.23 | **0.9** | **0.9** | 0.8 | **0.8** | **0.7** | 1.0 | | | | | |
| $K^+$ | 0.21 | **0.6** | 0.6 | 0.6 | **0.58** | **0.6** | **0.6** | 1.0 | | | | |
| $HCO_3^-$ | 0.43 | **0.9** | **0.8** | 0.9 | **0.9** | **0.9** | **0.7** | 0.5 | 1.0 | | | |
| $Cl^-$ | 0.21 | **0.7** | **0.7** | 0.7 | **0.7** | **0.7** | **0.7** | **0.5** | 0.5 | 1.0 | | |
| $SO_4^{2-}$ | 0.24 | 0.6 | 0.5 | 0.5 | 0.5 | **0.5** | 0.5 | **0.5** | 0.4 | 0.4 | 1.0 | |
| $NO_3^-$ | 0.28 | 0.1 | 0.1 | 0.0 | 0.0 | 0.1 | 0.2 | 0.2 | -0.2 | 0.2 | -0.1 | 1.0 |

**Correlation is significant at the 0.01 level.**

The strong relationship between $Ca^{2+}$ and $SO_4^{2-}$ (r=0.80) and $Na^+$ and $SO_4^{2-}$ (r > 0.5) suggests the dissolution of some salts like gypsum or glauber's salt. However, being an agricultural area, this high correlation could result from the use of calcium sulfate fertilizers used to improve crop

yields. There is a moderate positive correlation between $F^-$ and $Ca^{2+}$ (r=0.42) relative to $Na^+$ (Table 4.2a). Fluoride in water is usually derived from the weathering of fluoride-bearing minerals such as muscovite, biotite, fluorite, and fluoro-apatite, besides industrial and agricultural sources (Appelo and Postma1996; Edmunds and Smedley, 1996), hence the positive correlation. High F- concentrations (up to 15.2 mg/L) in groundwater have been identified in the Mayo Tsanaga River Basin, North Cameroon, in a granitic alkaline environment from fluorite, amphiboles and micas (Fantong et al., 2009). Lower concentrations (0.39 mg/L) have been identified in more acidic environments in the Ndop Plain, Northwest Region (Wirmvem et al. 2013). Hence the low $F^-$ concentrations in this study (< 1.5 mg/L) may be due to groundwater acidity which renders $F^-$ immobile (Edmunds and Smedley, 1996). High $F^-$ concentration causes dental and skeletal fluorosis such as mottling of teeth, deformation of ligaments, and bending of spinal cord (Maimoona et al. 2016).

### IV.4.2. Natural and anthropogenic factors controlling water chemistry

#### IV.4.2.1. Natural factors controlling water chemistry

Gibbs (Gibbs, 1970) demonstrated that plots of $Na^+/(Na^+ + Ca^{2+})$ and $Cl^-/(Cl^- + HCO_3^-)$ against TDS are effective tools to illustrate relative effects of various natural processes (such as rock weathering, evaporation, precipitation) on groundwater hydrochemistry. Fig. IV.7a illustrates that most of the groundwater samples of the Bafia area are controlled by rock weathering through water-rock interaction processes. Some samples plot towards the precipitation dominance area representing the influence of fresh recharging precipitation water evident by the high bicarbonate.

According to Srinivasamoorthy et al. (2008), the samples that plotted out of the three fields might be under the influence of anthropogenic contaminations which slightly increase the chloride content, especially in the dry season. Thus, surface and groundwater hydrochemistry of the Bafia area is controlled dominantly by rock weathering, with minor contributions from precipitation and anthropic activities.

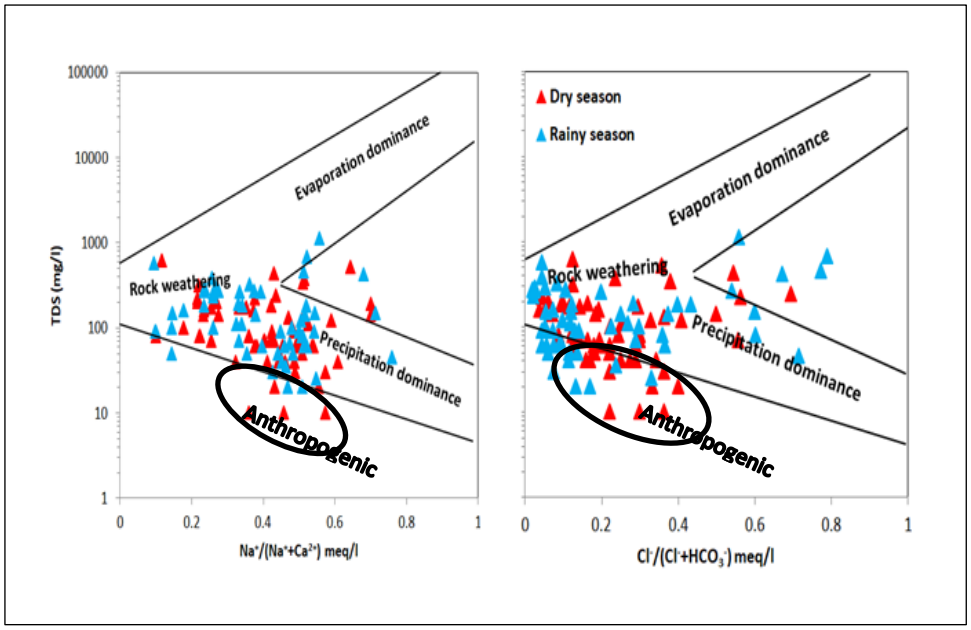


**Figure IV.7a: Gibbs plots showing the mechanisms controlling groundwater chemistry in Bafia.**

### a) Silicate weathering

Different compositional relations among ionic species have been used to reveal the origin of solutes as well as the processes influencing them (Table 4.3). During silicate weathering, $Na^+/Cl^-$ ratio is > 1 implies sodium released through silicate weathering and cation exchange and ratios = 1 implies halite dissolution is the primary process releasing sodium. This work shows that almost all water samples have $Na^+/Cl^-$ molar ratio > 1, with average ratios >3, suggesting the dissolution of sodium feldspars (albite) as the primary source of sodium (Fei et al. 2022). Also, all the samples have Na/Cl values greater than seawater (0.86) values, indicating that seawater has insignificant roles to play vis-à-vis the NaCl content. Additionally, the Na versus chloride bivariate plots for the rainy and dry season show that although some samples plot close to the 1:1 line, majority of them plot away (Fig. IV.7.b and c), excluding halite dissolution and endorsing cation exchange. Hence, the Na originates from weathering/dissolution of the syenites and quartz monzonite (particularly from $NaAlSi_3O_8$) abundant in the area (Jawhar et al. 2024).

*Table 4.3: A statistical summary of ratios between some ionic species in the analysed water*

| | | Groundwater | | | Surface water | | |
|---|---|---|---|---|---|---|---|
| | **Ionic ratios** | **Min** | **Max** | **Mean** | **Min** | **Max** | **Mean** |
| **Rainy season** | $Na^+/Cl^-$ | 1.03 | 19.35 | 4.63 | 1.65 | 5.43 | 3.39 |
| | $Cl^-/HCO_3^-$ | 0.02 | 3.74 | 0.47 | 0.12 | 0.33 | 0.2 |
| | $Ca^{2+}/Mg^{2+}$ | 0.49 | 11.65 | 2.87 | 1.16 | 3.08 | 1.73 |
| | $Ca^{2+} + Mg^{2+}$ | 0.18 | 8.12 | 1.74 | 0.16 | 1.21 | 0.58 |
| | $HCO_3^- + SO_4^{2-}$ | 0.07 | 8.09 | 1.43 | 0.18 | 1.11 | 0.54 |
| | $(Na^+ + K^+ - Cl) / Na^+ + K^+ - Cl^- + Ca^{2+}$ | 0.06 | 0.67 | 0.34 | 0.34 | 0.54 | 0.45 |
| | $Na^+/Ca^{2+}$ | 0.1 | 3.18 | 0.76 | 0.61 | 1.04 | 0.85 |
| | $Ca^{2+} + Mg^{2+}/HCO_3^-$ | 0.54 | 6.91 | 1.69 | 0.95 | 1.47 | 1.15 |
| | CAI – I | -20.17 | -0.11 | -4.7 | -5.71 | -1.47 | -3.46 |
| | CAI – II | -1.38 | -0.07 | -0.38 | -0.67 | -0.42 | -0.53 |
| | $HCO_3^-/TZ^-$ | 0.09 | 0.95 | 0.65 | 0.68 | 0.83 | 0.77 |
| **Dry season** | $Na^+/Cl^-$ | 0.31 | 6.71 | 2.13 | 0.16 | 1.5 | 0.75 |
| | $Cl^-/HCO_3^-$ | 0.04 | 2.25 | 0.38 | 1.09 | 3.6 | 1.74 |
| | $Ca^{2+}/Mg^{2+}$ | 0.67 | 6.1 | 2.28 | 1.73 | 4 | 2.79 |
| | $Ca^{2+} + Mg^{2+}$ | 0.2 | 14.2 | 2.22 | 0.1 | 0.56 | 0.43 |
| | $HCO_3^- + SO_4^{2-}$ | 0.21 | 15.33 | 2.27 | 0.23 | 4.06 | 1.12 |
| | $(Na^+ + K^+ - Cl) / Na^+ + K^+ - Cl^- + Ca^{2+}$ | -0.29 | 0.65 | 0.27 | 0.23 | 0.43 | 0.31 |
| | $Na^+/Ca^{2+}$ | 0.11 | 2.35 | 0.8 | 0.7 | 1.25 | 0.88 |
| | CAI – I | -20.17 | 0.63 | -5.32 | -20.16 | -0.11 | -5.65 |
| | CAI – II | -1.38 | 0.18 | -0.42 | -1.38 | -0.07 | -0.48 |
| | $HCO_3^-/TZ^-$ | 0.15 | 0.94 | 0.64 | 0.58 | 0.79 | 0.66 |
| | $Ca^{2+} + Mg^{2+}/HCO_3^-$ | 0.49 | 4.22 | 1.2 | 0.69 | 1.09 | 0.93 |

Similar trends of $Na^+$ excess were observed in the Ndop Plain, Cameroon (Wirmvem et al. 2013), the Lake Monoun area of Cameroon (Kamtchueng et al. 2016), the Plateaux Region of Togo (Akpataku et al. 2019), the Sor and Gebba watersheds of Ethiopia (Bayou et al. 2024), which were all attributed to silicate weathering, particularly albite.

Based on the highly significant Spearman correlation matrix ($p<0.01$) (Table 4.2b above), the moderate correlation coefficients between K and Ca, Na, Mg for the dry season points to natural silicate weathering (syenites and micas) as the primary K source.

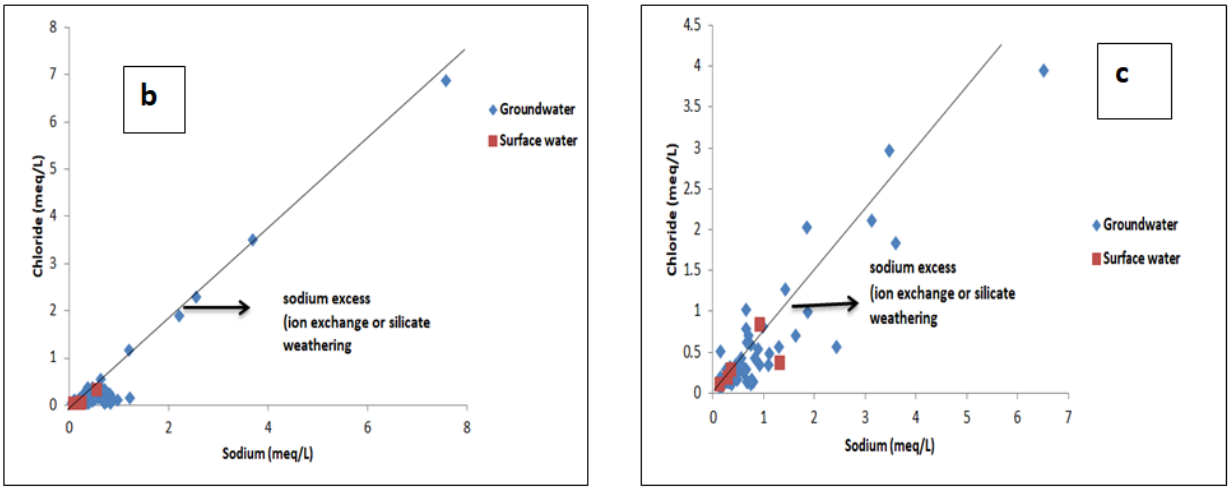


**Figure IV.7: Scattered plots of $Na^+$ and $Cl^-$ during the b) rainy and c) dry season**

In the absence of known halite sources in the area, the strong correlation observed in the Na+K versus Cl plot (Fig. IV.7d) and the high concentration outliers suggests that besides silicate weathering, K and Cl might result from some anthropogenic activities like agricultural runoff (fertilizer and animal waste), septic and domestic wastewater.

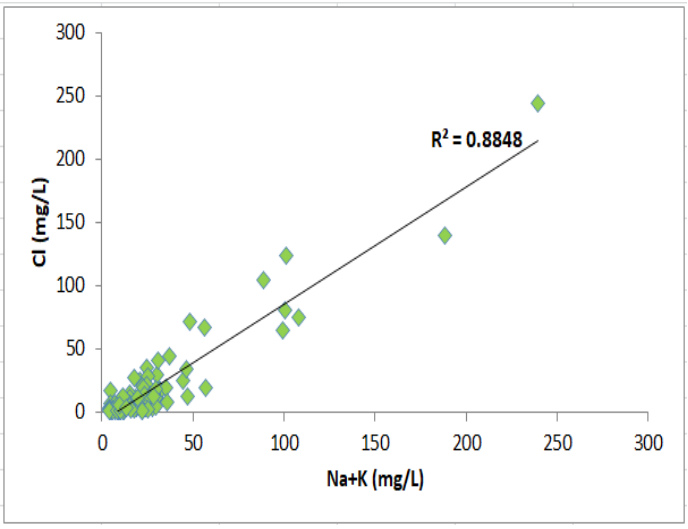


**Figure IV.7d: Na+K versus Cl plot showing silicate weathering and anthropogenic sources of K and Cl**

The molar ratio of $Na^+ + K^+ - Cl^- / Na^+ + K^+ - Cl^- + Ca^{2+}$ was used to determine the dominance of silicate weathering in the entire system. Usually, values > 0.2 and < 0.8 indicate plagioclase

weathering (Hunslow, 1995). In this study, 75% of the samples from both seasons have $Na^+$+$K^+$-$Cl^-$/$Na^+$+$K^+$-$Cl^-$+$Ca^{2+}$ ratio > 0.2 and < 0.8, confirming the dominance of silicate weathering to the evolution of the water chemistry in the area. Furthermore, when of $Na^+$/$Na^+$+$Cl^-$ molar ratio is > 0.5, it signifies feldspar weathering, particularly albite, while ratios = 0.5 imply halite dissolution. This study shows > 90% samples with ratios > 0.5, hence silicate weathering (Saha et al. 2018). Additionally, the high mean $HCO_3^-$/$TZ^-$ and $Ca^{2+}$ + $Mg^{2+}$/$HCO_3^-$ in water suggests silicate and/or carbonate weathering (Hunslow, 1995). However, acid waters (as in the case of Bafia) usually emanates from the dissolution of non-carbonate rocks such as gneisses, syenites and monzonites dominant in the area (Edmunds and Smedley, 1996). Similar observations of silicate dissolution in crystalline formations have been made (Njitchoua and Ngounou-Ngatcha, 1997; Fantong et al., 2009; Fongoh et al. 2023) and based on the geology and correlations between ionic species; the main mineral assemblage in the gneissic basement under dissolution is possibly the plagioclase mineral series, with two end members, Albite ($NaAlSi_3O_8$) and Anorthite ($CaAl_2Si_2O_8$). In the dissolution process, which involves the release of $SiO_2$ and $HCO_3^-$ into solution and the formation of clay minerals (Equation 28), $Ca^{2+}$ is preferentially released into solution more than $Na^+$ (Deutsch, 1997).

$$\text{Rocks} + H_2O + CO_2 = \text{cations} + H_4SiO_4 + HCO_3^- + \text{solids} \quad (28)$$

**b) Carbonate weathering**

To verify the role of carbonate weathering, different bi-plots were made. A plot of $HCO_3^-$ versus $Ca^{2+}$ shows 95% of the samples below the line (Fig. IV.7e). This indicates that carbonate dissolution is not the main factor influencing the bicarbonates but rather the dissolution of atmospheric and plant root $CO_2$. However, a plot of ($Ca^{2+}$+$Mg^{2+}$) versus ($HCO_3^-$ +$SO_4^{2+}$) shows a distribution of samples on both sides of the line, suggesting that besides silicate weathering, some of the $Ca^{2+}$ and $Mg^{2+}$ might result from the dissolution of carbonate minerals (Fig. IV.7f, g). The high concentration of ions in groundwater samples over surface water indicates that some complex geochemical processes like longer water-rock interaction and mixing that occur in groundwater, are absent in surface water. The close clustering of surface water in this plot suggests their uniformity in sources and composition other than the scattered groundwater samples, which are influenced by different interaction processes including ion exchange (Bon et al. 2021) or the dissolution of secondary carbonates (Srinivasamoorthy et al. 2008).

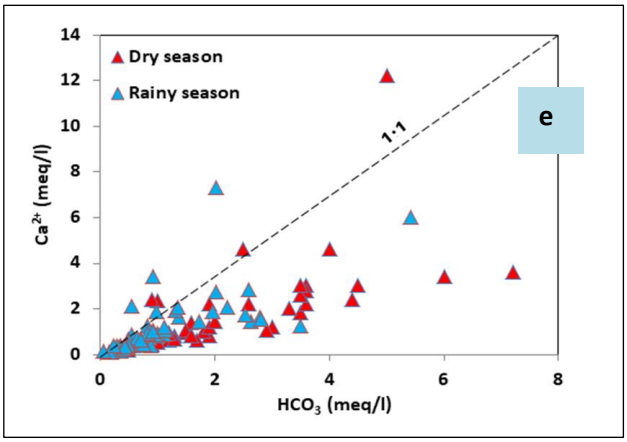


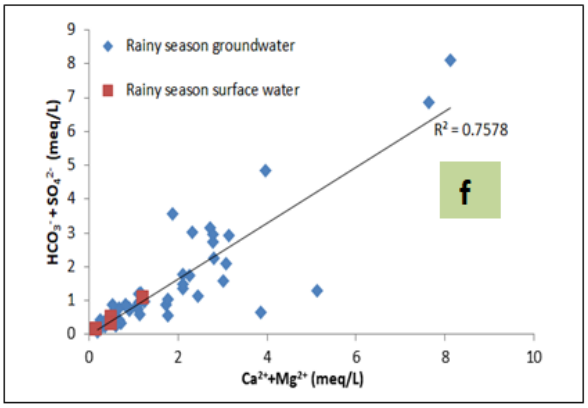


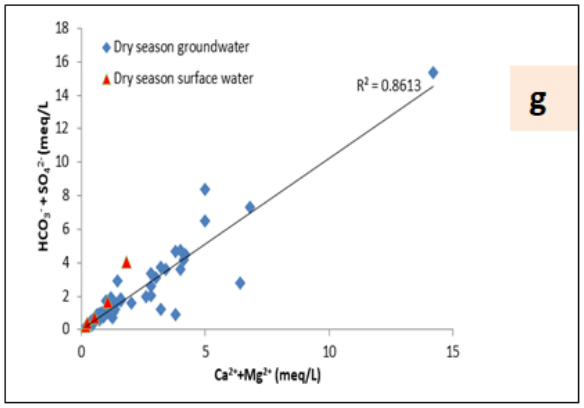


**Figure IV.7: Ionic relationships of (e) $Ca^{2+}$ vs $HCO_3^-$ and (f, g) $Ca^{2+}$ + $Mg^{2+}$ vs $HCO_3^-$ + $SO_4^{2-}$ for the rainy and dry seasons showing**

The $Ca^{2+}/Mg^{2+}$ molar ratio was used as a tool used to differentiate the role of dolomite, calcite and silicate weathering in a system. Generally, for a dolomite dissolution, the molar ratio is ≤1; for a calcite dissolution, the molar ratio is between 1 and 2 while for silicate weathering, the molar ratio is >2 (Han and Liu, 2004). In an annual point of view, this research shows 49.6% samples silicate weathering, 7.7% dolomite and 42.7% calcite, with more calcite dissolution in the rainy season. The high rainfall amounts during the rainy season, accompanied with dissolved carbon dioxide, enhance the dissolution of calcite, which slows down as saturation increases during the dry season. The less soluble silicate minerals on the other hand, increase in solution during the dry rainy season due to increased residence time which allows more interaction between the rocks and the water (Hunslow, 1995).

Finally, gypsum dissolution was evaluated using a plot of $Ca^{2+}$ versus $SO_4^{2-}$ (Fig. IV.7h). More than 97% of the samples plot above the line, indicating that gypsum dissolution is not an effective process in the water chemistry in the Bafia area, and this is confirmed by gypsum under-saturation as seen in section 4.2.3. Conversely, calcium is derived either from silicates or carbonates (Aghazadeh et al. 2016). Also, if $Ca^{2+}$ and $SO_4^{2-}$ originate from gypsum, the ratio is 1:1. However, just about 5% of the samples plot along that line, thus minimizing gypsum/anhydrite or sulfate dissolution processes. Hounslow (1995) proposed some key parameters which have been used to deduce the source rock/events that influence the water chemistry in the Bafia area (Table 4.4).

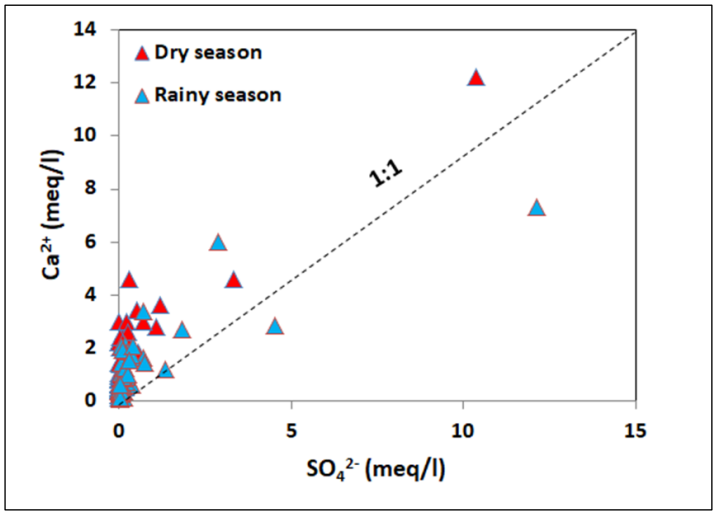


**Figure IV.7h: Bivariate plot of $Ca^{2+}$ versus $SO_4^{2+}$ in water resources reflecting minimal gypsum dissolution**

## C) Cation exchange and Chloro-alkaline indices (CAI)

During geochemical reactions, calcium (magnesium) can be freely exchanged with sodium on clay surfaces, depending on the phases present. This often transforms the freshly recharged Ca-Mg-$HCO_3$ waters into the Na-$HCO_3$ or Na-K-$HCO_3$ types observed in the discharge areas, hence the shift observed on the Piper diagrams. In order to determine the significance of base-exchange in enriching the water chemistry, a plot of $(Ca^{2+} + Mg^{2+}) – (HCO_3^- + SO_4^{2-})$ versus $Na^+ - Cl^-$ was used. If cation exchange is a significant process controlling water chemistry, the relation between these two parameters will be linear with a slope of -1.0 (Adomako et al. 2011).

***Table 4.4 Source rock deduction summary of the water samples in the Bafia area*** (Hounslow 1995)

| Parameters | Critical value | Analysis range | Conclusions |
|---|---|---|---|
| $\frac{Na^+ + K^+ - Cl^-}{Na^+ + K^+ - Cl^- + Ca^{2+}}$ | > 0.2 and <0.8<br>< 0.2 and > 0.8 | 75% >0.2 and < 0.8 in both seasons | Possible plagioclase weathering<br>Plagioclase weathering unlikely |
| $\frac{Na^+}{Na^+ + Cl^-}$ | > 0.5<br><0.5TDS>500mgL<br><0.5TDS<500mgL | 100% > 0.5 (rainy season),<br>91% > 0.5 (dry season) | Sodium sources other than halite (possibly albite)<br>Halite solution<br>Reverse softening |
| $\frac{ca^{2+}}{Ca^{2+} + SO_4}$ | = 0.5<br>< 0.5, pH < 5.5<br>< 0.5 neutral<br>> 0.5 | 100 % > 0.5 in both seasons | Gypsum dissolution<br>pyrite oxidation<br>Ca removal- Fe exchange or calcite precipitation<br>Calcium sources other than gypsum-carbonates or silicates |
| $\frac{Cl^-}{Sum\ of\ anions}$ | >0.8TDS>500<br>>0.8TDS<100<br><0.8 | 100% <0.8 in both seasons | Sea water or brine or evaporates<br>Rainwater<br>Rock weathering |
| TDS | >500<br><500 | 96.5%< 500 in both seasons | Carbonate weathering of brine or sea wate<br>Silicate weathering |

Otherwise, points will cluster towards the origin (Jalali, 2007). In this research, the relationship in the rainy season is far from linear, suggesting that ion exchange is not the major factor influencing the chemistry (Fig. IV.8a). However, during the dry season, some points cluster towards the origin while others plot close to the line, suggesting some exchange (Fig. IV.8b). This somehow contributes to changes in water types from the rainy to the dry season.

Chloro-alkaline indices (CAI – I and CAI – II) were calculated (eq 11, 12) as proposed by Schoeller (1965) to further identify the type of ion exchange taking place in the system. When there is direct ion exchange between $Ca^{2+}$ or $Mg^{2+}$ in the groundwater with $Na^+$ and K+ in the aquifer material, both the above indices are negative, and if there is a reverse ion exchange, then both these indices will be positive (Schoeller 1965, 1967). In this study, both surface and groundwater samples had negative CAI values in the rainy season while in the dry season, all

surface water and 91% groundwater samples had negative CAI values, indicating dominance of direct ion exchange processes over reverse ion exchange (Fig. IV.8 c, d).

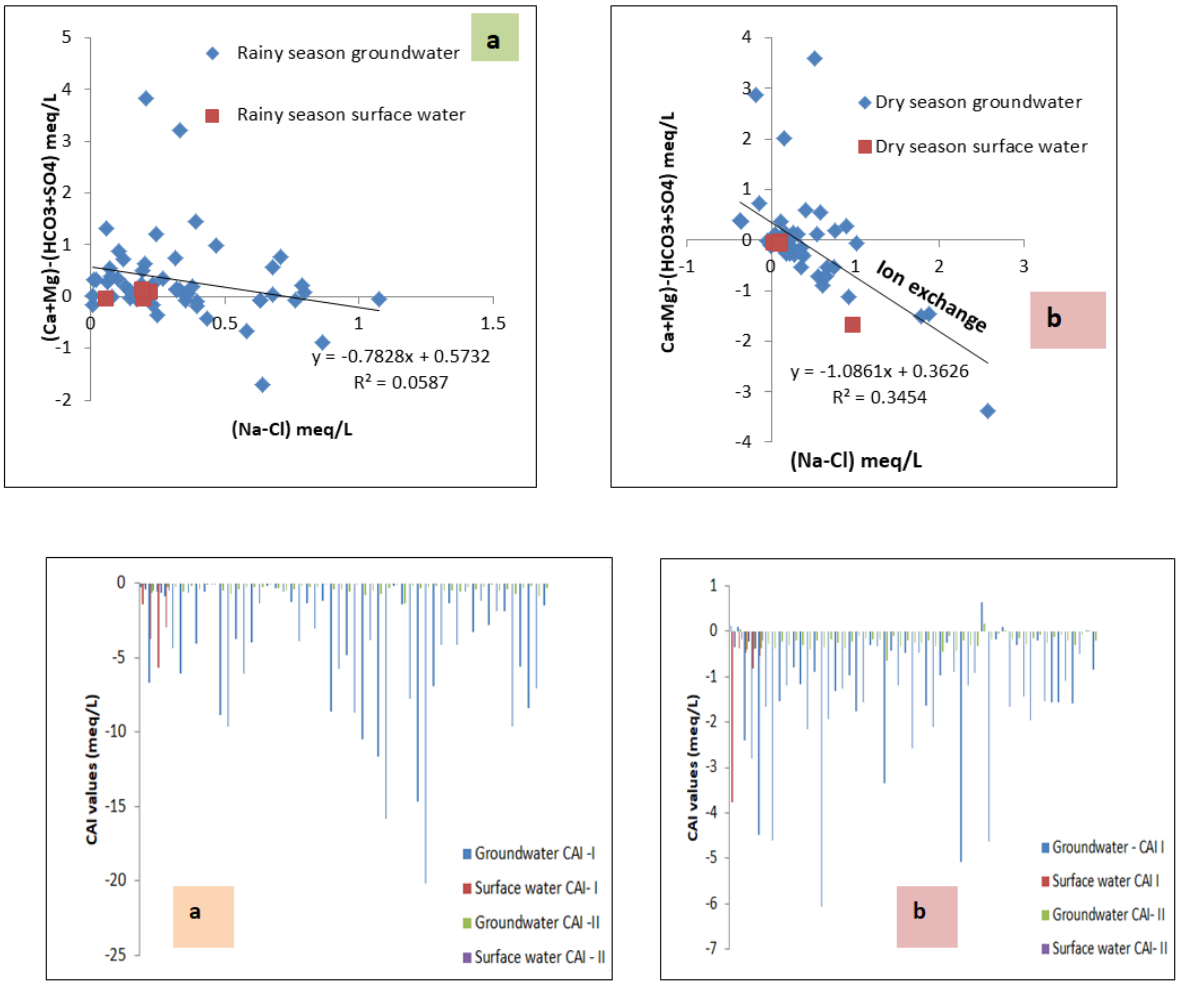


**Figure IV.8: Scatter plots of ($Ca^{2+}$ + $Mg^{2+}$) – ($HCO_3^-$ + $SO_4^{2-}$) versus $Na^+$ - $Cl^-$ (a,b) and CAI-I and II (c,d) of water resources in Bafia**

### d) Mineral dissolution and reverse geochemical modelling

One of the ways to characterize the degree of interaction and dissolution rate is calculating the amount mineral species dissolved in water using PHREEQC geochemical software (Parkhurst and Appelo, 1999). Generally, Saturation indices (SI) <0, it implies under-saturation with no precipitation of mineral phases; while SI >0 indicates super-saturation, with possibility of precipitation.

All the surface and groundwater samples in this study are under-saturated with respect to calcite, aragonite, dolomite, anhydrite, gypsum and halite, indicating their continuous dissolution, without forming precipitates. The samples are weakly under-saturated with respect to the carbonate minerals (calcite and aragonite), moderately under-saturated for sulfate minerals (anhydrite and gypsum) and strongly under-saturated for halite. These results suggest their absence of these mineral phases in the rock formations or limited water-rock interaction time. Hence, the main water type (CaMg-$HCO_3$) reflects continuous interactions between plagioclases, aluminosilicates and groundwater. Given the incongruent dissolution of silicate minerals, these interactions might be accompanied by cation exchange reactions where $Na^+$ or $K^+$ easily replaces $Ca^{2+}$ or $Mg^{2+}$ on clay surfaces (Ako et al. 2011). Despite the presence of some few $SO_4^{2-}$ and $Cl^-$ spikes in the water samples, the under-saturation of gypsum and halite either an absence of host minerals or limited interaction time. Leaky septic tanks, well chlorination, sewage systems and agricultural runoff could be the possible sources of chloride and sulfate in water.

Groundwater and surface water in the Bafia area have higher $CO_2$ partial pressure ($10^{-3.3}$ – $10^{1.6}$ atm) than the atmospheric value of $10^{-3.5}$ atm suggesting that the major source of CO2 governing the above reactions was probably from the oxidation of organic matter in the under saturated zone (Appelo and Postma, 2005). This process reduces the pH (hence the slightly acidic pH) and favors the production of more bicarbonate in solution. High $pCO_2$ facilitates the dissolution of carbonate minerals and silicate minerals, hence release $Ca^{2+}$, $Mg^{2+}$ which positively correlate with $HCO_3$ in the water (Appelo and Postma, 2005). The high PCO2 in groundwater are consistent with findings in the Mt Cameroon area and the Ndop Plain attributed to similar processes (Ako et al., 2012; Wirmvem et al. 2013).

### IV.4.2.2. Anthropogenic factors controlling water chemistry

The recent population increase in the area comes along with increased farming and other small scale and individual industrial activities which degrade water quality in the area. Besides groundwater, some surface water bodies also serve as irrigation water (especially for farms closer to the streams) and disposal of left-over agricultural products. Some like the Mbam River serve as the source for drinking water after treatment. Hence, water resource contamination by irrigation return flow, fertilizer and farm manure application, leaching of soil mineralized nitrogen, domestic sewage, and industrial wastes, constitutes an important issue of groundwater studies in the study area.

Generally, high $Cl^-$, $NO_3^-$ and $SO_4^{2-}$ in groundwater are mainly attributed to human activities and are often used as anthropogenic pollution indicators, especially for aquifers in Sub-Saharan Africa (Han and Liu 2004; Lapworth et al. 2017). The results of this study show that these anions are not only derived from chemical weathering and atmospheric depositions but have some anthropic origins.

Naturally occurring nitrate in groundwater is often in low concentrations but the intervention of diverse human activities like agricultural fertilization and contaminated sewage waters often increase these levels. Usually, a positive linear relationship between potassium and nitrate is expected, if agricultural fertilization plays a key role in groundwater quality deterioration. However, this study shows a non-linear relationship between $NO_3^-$ and $K^+$ (Fig. IV.9a,b), indicating that agricultural practices may not be the sole factors influencing the presence of nitrates in water. Although majority (>85%) of the points plot in the WHO permissible zones, about 15% plot close to the line, suggesting that these samples might be influenced by the application of $KNO_3^-$ fertilizers on farmlands. The presence of some outliers ($NO_3$>50mg/L) indicate excess nitrate from some point sources, especially in low areas. For example, BOW 01, located at 467m a.s.l, is close to a farm while BOW 52 and BOW 53 are located downslope at 491m a.s.l where most of the city's contaminated runoff stagnate and infiltrate the ground. Others like Bdow 67 and BBH 62 are located around market areas. More than 75% samples with high nitrate have low potassium, except BOW 56. This suggests that inorganic NPK fertilizers have little influence on the nitrate load. Additionally, nitrate also had a weak positive correlation with other major ions in groundwater samples, insinuating diversity of sources (Fei et al. 2020).

Despite the generally low chloride concentrations, $NO_3^-$ and $Cl^-$ versus well depth plots show higher $NO_3^-$ and $Cl^-$ within the first few meters of the wells (<20m) as opposed to deeper wells (Fig. IV.9c,d). This is obviously because these shallower wells with no casing are more prone to nitrate contamination from different sources. The high nitrate in shallow wells is an indication of the unconfined, highly vulnerable, aerobic aquifer surface conditions which favor N-fixing while the low nitrate in deeper boreholes is linked to anaerobic conditions which favor denitrification (Chukwura et al. 2015; Akenji et al. 2023).

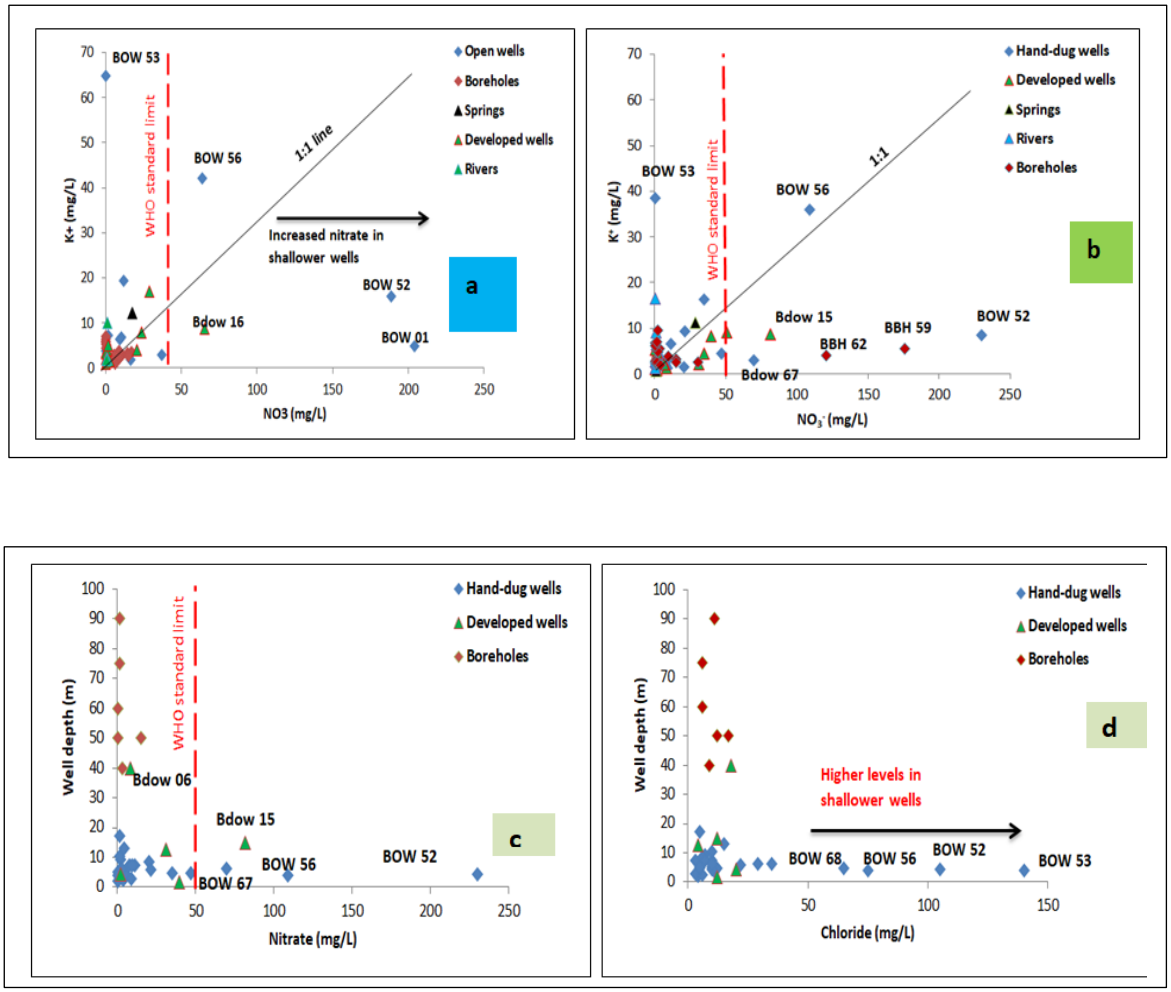


**Figure IV.9: (a,b) Seasonal scatter plots of $NO_3^-$ versus $K^+$; $NO_3^-$ and Cl versus well depth (c,d) demonstrating shallow well vulnerability**

The relationship between $NO_3^-$ and $Cl^-$ in water has been used to track anthropogenic influences (Kamtchueng et al. 2022). In this study, a plot of $Cl^-$ versus $NO_3^-$ (Fig. IV.10a) separates the water resources into three subgroups (A, B and C).

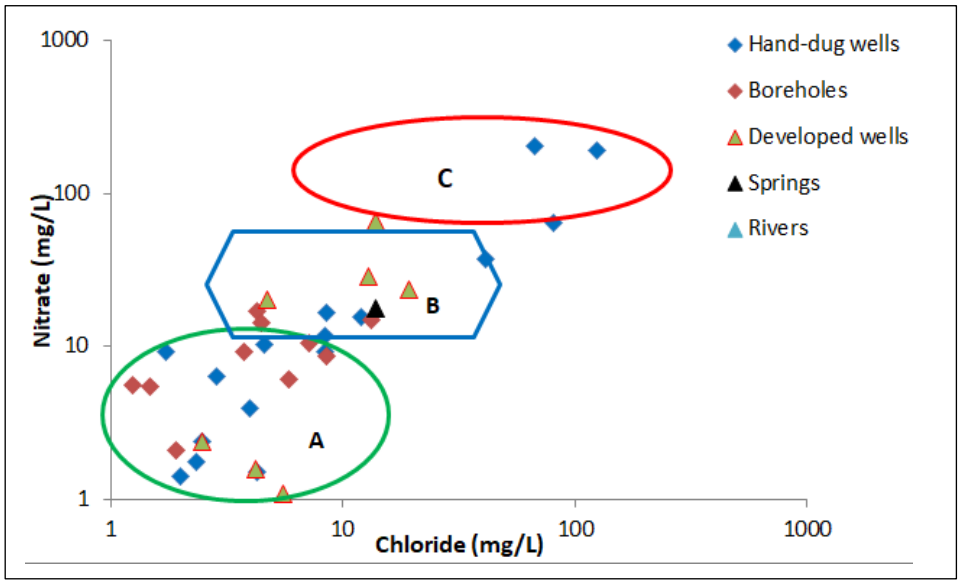


**Figure IV.10a: Relationship between $Cl^-$ and $NO_3^-$ showing three subgroups with different contamination levels (A, B and C)**

Subgroup A, the dominant group, comprises more shallow hand-dug wells influenced by slightly higher chloride than nitrates. Most of these samples are located in the peripheries like Bigna, Donenkeng, Logement Sociaux, and Kon Yambetta, with smaller population and fewer human activities. Subgroup B samples have higher nitrates (10 mg/L>$NO_3^-$< 50 mg/L) than chlorides, indicating more nitrate contamination sources like agriculture and pit toilet leakages. Most of these samples are located in densely populated low areas with shallow, poorly developed wells, some < 3m away from pit latrines (Fig. IV.10b).

Subgroup C shows that as nitrate increases (up to 230 mg/L), chloride also increases (up to 188.9 mg/L), suggesting similar contamination sources (municipal wastes, well chlorination, pit latrines, laundry detergents and fertilizers). The samples are located within farmlands (e.g. BOW 01), market areas (BOW 67) and densely populated valley areas (BOW 52, BOW 56). Some samples like BOW 14, BOW 05 and Bdsp 08, located within cocoa farms, have lower $NO_3$ concentrations (11.3 mg/L, 8.9 mg/L and 28.9 mg/L, respectively) than the market and highly populated areas.


**Figure IV.10b showing open, unprotected shallow wells at close proximity with pit latrines and farmlands**

This suggests that as much as agriculture plays a significant role in nitrate contamination, most of the nitrate in the Bafia area originates from other human-related activities. Unlike the case of the city of Yaounde in the Centre Region, surface waters in the Bafia semi-rural area have lower pollutant loads pollutants, hence could be sustainably managed for drinking water supply in Bafia (Branchet et al. 2018; Fongoh et al. 2024).

A groundwater level variation map (Fig. IV.11) shows a complex subsurface circulation with several flow directions in the Bafia shallow aquifer system. The flow network suggests groundwater mixing but with some localized flow patterns shown by the concentric flow contours. This accounts for the mixture of carbonate and silicate signatures earlier mentioned. Despite the water mixing, $NO_3^-$ still demonstrated a varied distribution across the Bafia groundwater system, with higher levels linked to the land use and the topography of the area.

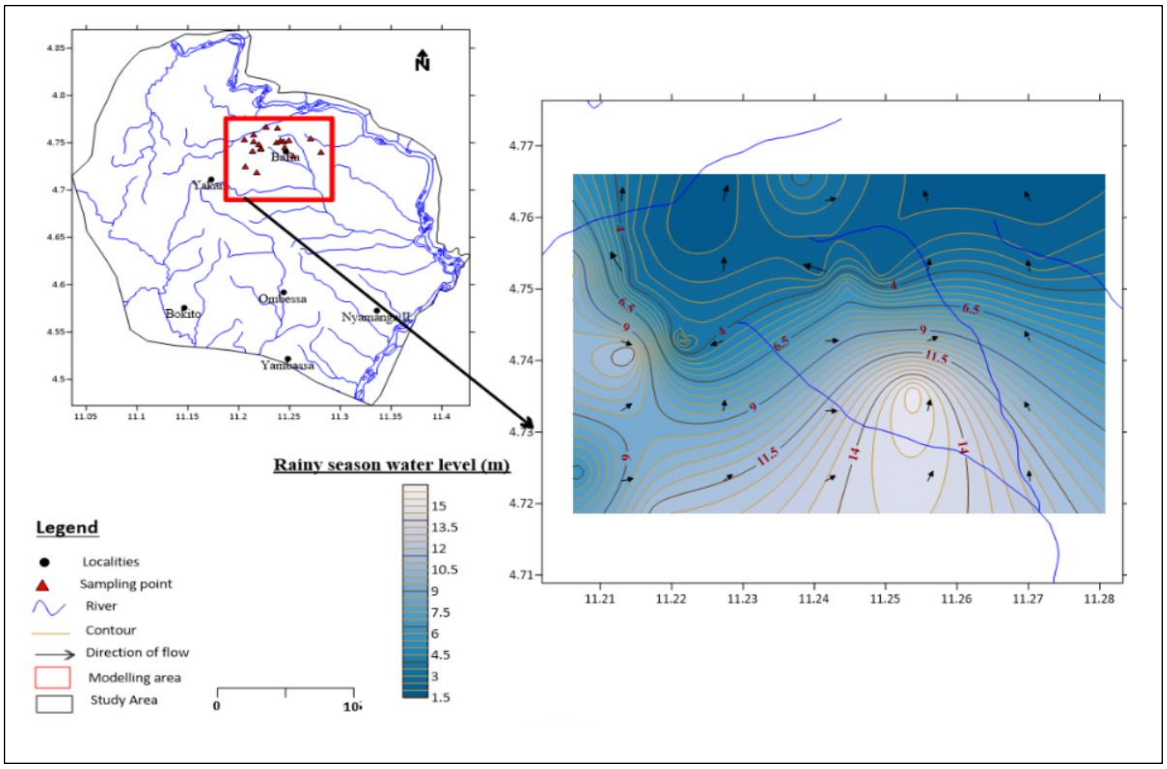


**Figure IV.11: Dry season groundwater level map showing evidence of mixing in groundwater**

### IV.4.3. Hierarchical cluster analysis (HCA) and potential contamination sites

Hierarchical cluster analysis (HCA) was performed using the chemical parameters of the various water sources in the rainy and dry season and in Figure IV.12a and b, we observe two clusters for the rainy season (with two sub-clusters each) and three clusters for the dry season (with two sub-clusters in the 3rd cluster).

Cluster 1 of the rainy season consists of 36 samples (63%), including all four rivers and springs. Group G1 of cluster 1 is made up of 22.8% of the samples, with three rivers and one spring while G2 is made of 40.4% of the samples. G1 samples have the lowest contaminant indicators (nitrate, chloride, potassium, sulfate) and are located at the highest altitudes (mean altitude = 514m) and mostly at the city peripheries. G2 samples are located at slightly lower elevations (mean altitude = 494m) and equally have slightly high concentrations of contaminant indicators and electrical conductivity. According to Fongoh et al. (2023) in their study of shallow groundwater aquifers in Yaoundé, these samples on the lateritic hillsides have lower hydraulic conductivities and thus

present minimal vulnerability to potential aquifer contamination. Additionally, as illustrated by the Piper's diagram, more than 80% of the samples of cluster 1 are of the Ca-Mg-$HCO_3$ water type, indicating they are freshly recharged waters, with little or no contamination (Kamtchueng et al. 2016).

Cluster 2 consists of 20 samples, with subgroup G3 samples (26%) located in the densely populated central parts of Bafia. This group of samples has mean altitude of 492m, with slightly less mean nitrates (7.5 mg/L) as opposed to G2 samples (mean nitrate=11.8 mg/L). G4 samples (9%) are located at lowest altitudes (mean = 491m), hence act like a sink for most of the city's drainage. These samples have the highest mean nitrate (91.4 mg/L), chloride (103.9 mg/L), potassium (26.7 mg/L) and the highest mean bicarbonate (122.8 mg/L). Cluster 2 samples are more mineralized and more contaminated than the cluster one samples, presenting more of Ca-Mg-Cl-$SO_4$ and NaK-$Cl^-$/Na-$SO_4$ types. Cluster 2 is more vulnerable to contamination from anthropogenic sources like agricultural wastes (fertilizers, pesticides, and herbicides), pit toilets and irregular dumping of un-sorted domestic wastes.

The dry season presented three clusters, with similar characteristics as those of the rainy season. Cluster 1 of the dry season is similar to cluster 1 of the rainy season, and they represent the less vulnerable, high topography/city peripheries typical of the recharge areas. Cluster 2 in this case represents samples at the highest altitude (mean = 507m), with high sulfate and EC especially in Muoko-BBH 38, which could be related to the interactions with the host rock. Cluster 3 is similar to cluster 2 of the rainy season, and the samples represent more vulnerable low discharge areas. Similar scenarios have been observed by Fongoh et al. (2023) in Yaoundé and Adomako et al. (2011) in Densu River-Ghana, pointing to cluster 1 as freshly recharging, less contaminated/peripheral hilly areas while clusters 2 and 3 represent the highly contaminated and more populated low land areas.

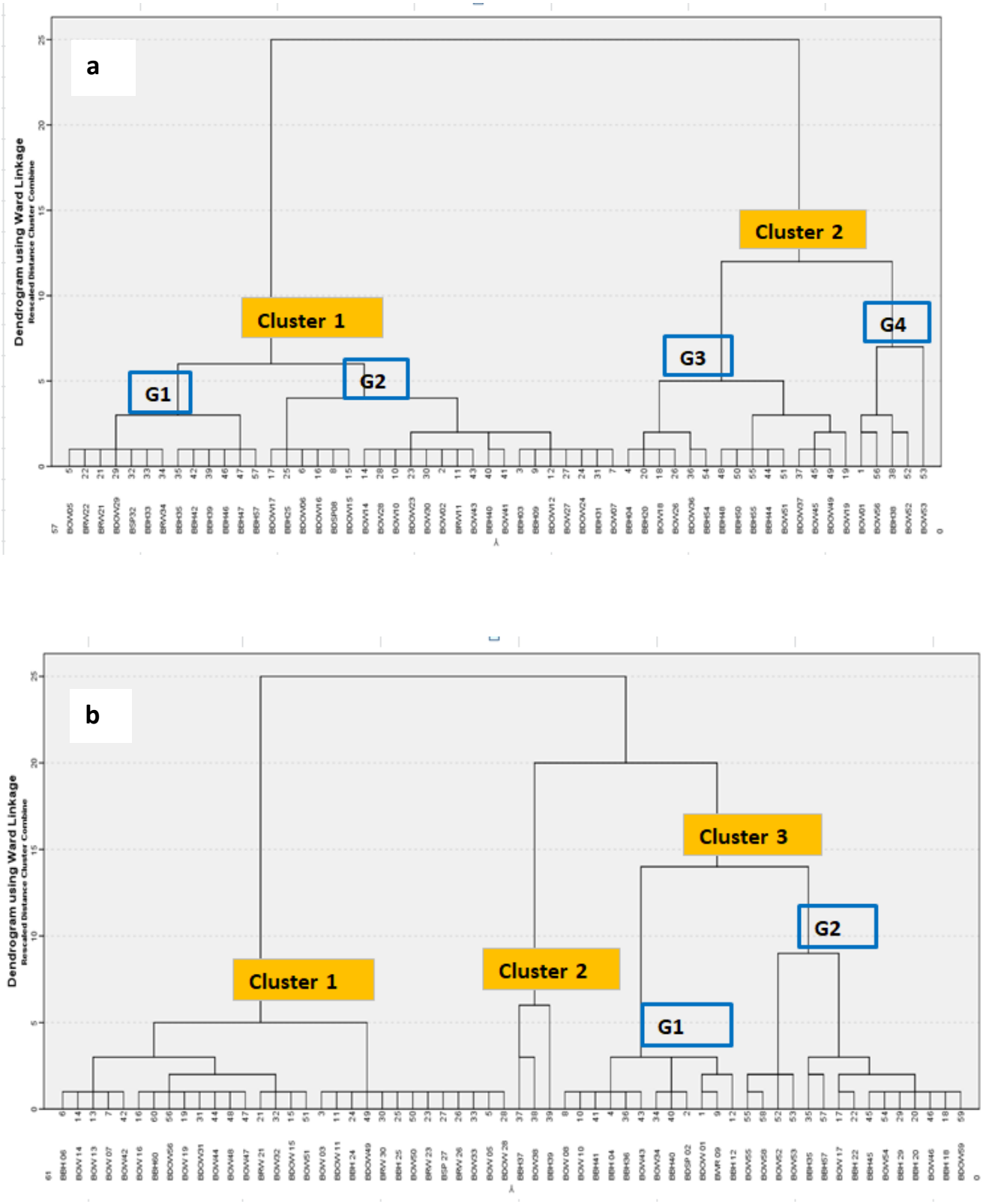


**Figure IV.12 Dendrogram of potential vulnerable areas in Bafia showing cluster 2 of the rainy season (a) and cluster 3 of the dry season (b) as the most vulnerable areas**

## IV.5. Trace element geochemistry

Human mortality related to trace element deficiencies and toxicities affects more than half of the world's population. However, their spatial and temporal distribution in groundwater is controlled by several natural (elevation, rock/soil type, precipitation and dissolution) and anthropogenic (urbanization, industrialization, land use, aerosols created by automobiles through fuel combustion, metal smelting, and excessive dose of pesticides, micronutrient fertilizers and manures) factors (Bing et al. 2019). These elements are generally present in low trace levels (less than 0.1%) in soils, sediments, surface waters and living organisms. Amongst these trace elements is another group of metals known as heavy metals. They have relatively high density (about 5g/cm$^3$) and are toxic to organisms at certain accumulated concentrations. Some like Mn, Fe, Cu, and Zn are essential for the human body in low concentrations but become toxic after bioaccumulation in the system. Other trace elements such as Cd, Pb, Hg and Pb do not have any health benefit (Verma and Dwivedi, 2013). This chapter will evaluate trace element distribution and contamination in water and the associated health risks using different pollution indices. It will also discuss the suitability of different water resources for drinking and irrigation.

### IV.5.1. Petrographical characteristics and trace element distribution in rocks and water

#### IV.5.1.1. Petrographical characteristics

The observed lithologies of the study area consist of 2-mica gneisses, syenites and quartz monzonite (Fig. IV.13a). The gneisses display banding and foliations that trend NE, dipping averagely to the W. The microscopic observation shows that the gneisses are made up of quartz (≈25 %), K-feldspars (≈30 %), plagioclase (≈25 %), biotite (≈15 %), hornblende (≈5 %) and muscovite (≈10 %) (Fig. IV.13c, d). Secondary muscovite derived from alteration occurs within mineral interstices alongside sericite. Syenites were observed in the lowland area along stream beds. They contain a low amount of quartz (<5 %), plagioclase (<15 %) and a high amount of k-feldspars (>70 %) that generally display intense fracturing within grains (Fig. IV.13e). Quartz monzonites outcrop on the hills as large boulders and blocks measuring 2-5 m large. These granites are grey, coarse-grained and weakly deformed (Fig. IV.13b).

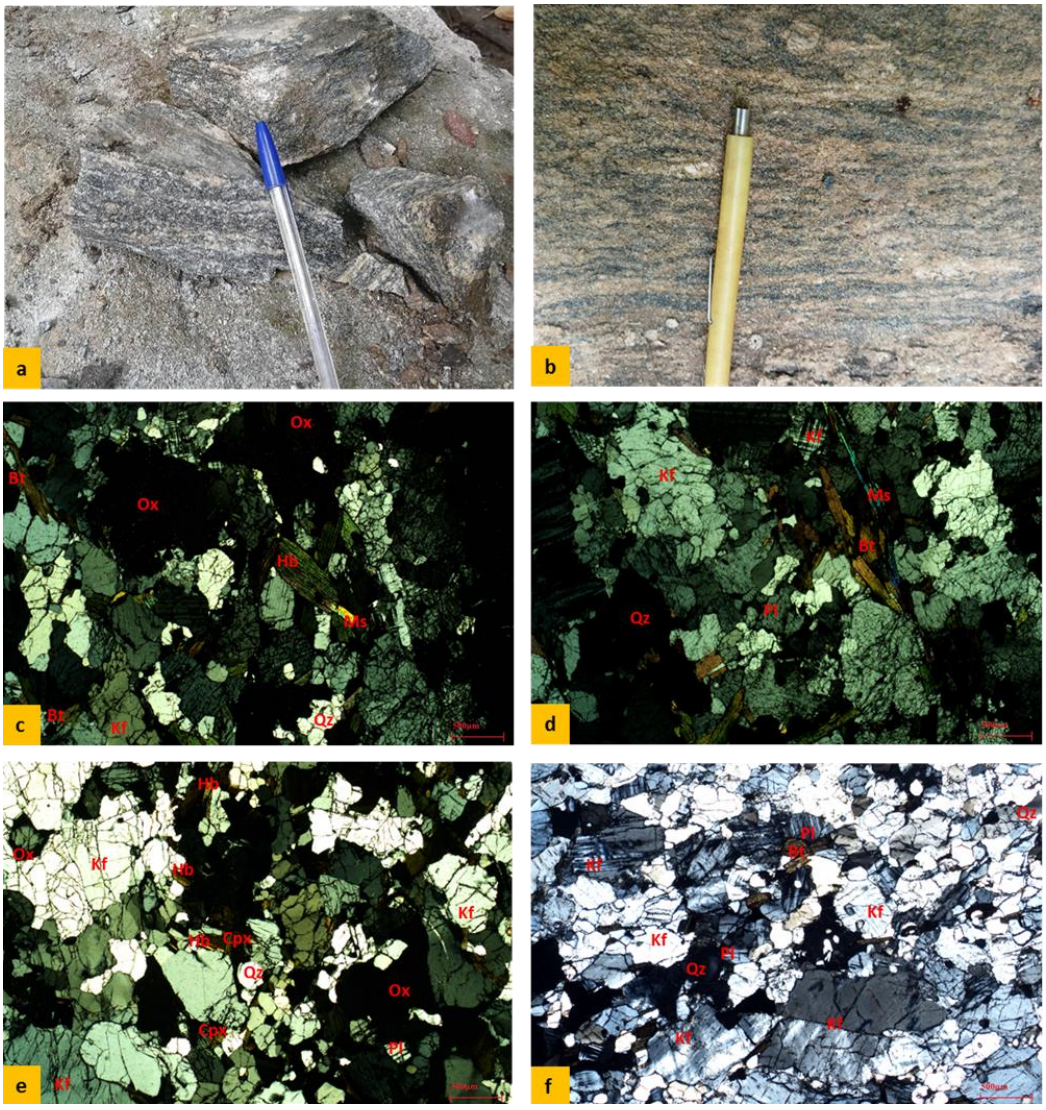


**Figure IV.13: Field and photomicrographs of rocks within the study area:**

**a) rock sample of a 2-mica granite gneiss; b) outcrop of weakly deformed granite with magnetite noddle; c & d) biotite (Bt), muscovite (Ms) and hornblende (Hb) in an inequigranular quartz (Qz), k-feldspar (Kf) and plagioclase (Pl) matrix; e) syenite bearing hornblende, in association with clinopyroxene, oxide seam around feldspar grains and mineral interfaces; f) in-equigranular and subhedral grains, intergrowth between plagioclase and k-feldspar. Note the intensity of broken grains, deformation flame twinning in plagioclase, and iron oxide within grain interstices.**

The mineralogy consists of quartz (≈20 %), plagioclase (≈33 %) and k-feldspars (≈35 %). The mafic phases include biotite (≈10 %), hornblende (≈5 %) and muscovite (≈5 %). Magnetite is the main accessory phase forming flow seams along grain boundaries (Fig. IV.13f). Grains are

generally inequigranular, subhedral to anhedral, and commonly show broken grains. Plagioclase display intense deformation twinning displaying flame-shape, while K-feldspar locally bears exsolution surfaces.

### IV.5.1.2. Trace element distribution in rock and water samples

On the one hand, leached rock samples show low trace element concentrations (<µg/l) except for Fe, Sr and Mn, which display higher concentrations, while boron is BDL in all samples. The rock trace element composition and the statistical summary (Table 4.5a, b) show low mean concentrations (<1µg/l), except for Mn (mean=122.5 µg/l), Sr (mean= 42 µg/l), Fe (mean=9.1 µg/l), Cu (mean=4.3), Al (mean=1.3 µg/l), Zn (mean=1.3 µg/l) and Ni (mean=1.8 µg/l). Mn shows the highest concentration in all four rock samples, with the following relative trace element abundances: Mn>Sr>Fe>Cu>Ni>Al>Zn>As>Co>Sb>Pb>Se>Ti>Cd.

***Table 4.5a: Trace element composition of leached rocks***

| | Rock A | Rock B | Rock C | Rock D |
|---|---|---|---|---|
| **Se** | 0.25 | 0.30 | 0.21 | 0.15 |
| **Ti** | 0.1 | 0.2 | | 0.2 |
| **Sr** | 36 | 41 | 58 | 33 |
| **Sn** | 0.11 | 0.15 | | 0.14 |
| **Sb** | 0.51 | 0.26 | 0.33 | 0.41 |
| **Al** | 1.1 | 1.8 | 0.95 | 0.87 |
| **B** | | | | |
| **Cr** | 0.09 | 2.1 | 0.13 | 0.26 |
| **Cu** | 2.3 | 7.6 | 3.5 | 2.9 |
| **Pb** | 0.15 | 0.36 | 0.14 | 0.11 |
| **Ni** | 1.1 | 3.3 | 1.2 | 2.4 |
| **As** | 0.3 | 0.6 | 0.2 | 0.9 |
| **Cd** | 0.02 | 0.02 | | 0.01 |
| **Zn** | 1.1 | 2.2 | 0.7 | 0.9 |
| **Mn** | 115.0 | 226 | 58 | 91 |

***Table 4.5b: Statistical summary of leached leached rocks***

| | Min | Max | Mean | Std. Dev |
|---|---|---|---|---|
| Fe | 4.00 | 15.00 | 9.10 | 4.55 |
| Co | 0.78 | 1.00 | 0.95 | 0.11 |
| Se | 0.15 | 0.30 | 0.23 | 0.06 |
| Ti | 0.00 | 0.10 | 0.03 | 0.06 |
| Sr | 33.00 | 58.00 | 42.00 | 11.17 |
| Sn | 0.11 | 0.15 | 0.13 | 0.02 |
| Sb | 0.26 | 0.51 | 0.38 | 0.11 |
| Al | 1.00 | 2.00 | 1.25 | 0.50 |
| Cr | 0.09 | 2.10 | 0.65 | 0.97 |
| Cu | 2.30 | 8.00 | 4.33 | 2.55 |
| Pb | 0.11 | 0.36 | 0.19 | 0.11 |
| Ni | 1.00 | 3.00 | 1.78 | 0.93 |
| As | 0.00 | 1.00 | 0.58 | 0.51 |
| Cd | 0.01 | 0.02 | 0.02 | 0.01 |
| Zn | 1.00 | 2.00 | 1.28 | 0.49 |
| Mn | 58.00 | 226.00 | 122.50 | 72.85 |

Water resources (mainly groundwater, Appendix 3) on the other hand, show slightly higher trace elements concentrations than the rocks (Table 4.6a).

***Table 4.6a: Trace element variation between rocks and water samples***

| | Rock trace elements | | | | Water trace elements | | | |
|---|---|---|---|---|---|---|---|---|
| | **Min** | **Max** | **Mean** | **Std. Dev** | **Min** | **Max** | **Mean** | **Stdev** |
| Fe | 4.00 | 15.00 | 9.10 | 4.55 | 0.00 | 1215.91 | 63.67 | 187.44 |
| Co | 0.78 | 1.00 | 0.95 | 0.11 | 0.03 | 4.59 | 0.50 | 0.89 |
| Se | 0.15 | 0.30 | 0.23 | 0.06 | 0.00 | 3.00 | 0.14 | 0.52 |
| Ti | 0.00 | 0.10 | 0.03 | 0.06 | 4.08 | 810.70 | 130.88 | 161.77 |
| Sr | 33.00 | 58.00 | 42.00 | 11.17 | 26.70 | 1650.70 | 327.91 | 373.92 |
| Sn | 0.11 | 0.15 | 0.13 | 0.02 | 0.00 | 0.00 | 0.00 | 0.00 |
| Sb | 0.26 | 0.51 | 0.38 | 0.11 | 0.00 | 2.00 | 0.40 | 0.53 |
| Al | 1.00 | 2.00 | 1.25 | 0.50 | 0.00 | 518.92 | 43.71 | 91.89 |
| B | | | | | 1.00 | 32.00 | 3.19 | 4.41 |
| Cr | 0.09 | 2.10 | 0.65 | 0.97 | 0.00 | 8.00 | 1.98 | 1.64 |
| Cu | 2.30 | 8.00 | 4.33 | 2.55 | 0.00 | 22.00 | 2.09 | 3.62 |
| Pb | 0.11 | 0.36 | 0.19 | 0.11 | 0.00 | 2.00 | 0.07 | 0.32 |
| Ni | 1.00 | 3.00 | 1.78 | 0.93 | 0.00 | 15.00 | 1.68 | 2.23 |
| As | 0.00 | 1.00 | 0.58 | 0.51 | 0.00 | 1.00 | 0.07 | 0.26 |
| Cd | 0.01 | 0.02 | 0.02 | 0.01 | BQL | BQL | BQL | BQL |
| Zn | 1.00 | 2.00 | 1.28 | 0.49 | 0.00 | 159.00 | 10.93 | 27.08 |
| Mn | **58.00** | **226.00** | **122.50** | 72.85 | 0.33 | 712.37 | 125.45 | 196.04 |

However, these elements are found in traces, usually within the WHO allowable limits for drinking water, with the exception of Mn, Fe, Al, Sr and Ti in some cases with concentrations higher than the WHO health guidelines (2017) and the US Environmental Protection Agency (2014) (Table 4.6b). Generally, groundwater, especially boreholes, has the highest concentrations of the analyzed trace elements (borehole>developed well>open well>rivers>springs), with an abundance order of Sr>Fe>Mn>Ti>Zn>B>Cu>Ni>Cr>Co>Se>Sb>Pb>As>Sn>Cd (Table 4.6d).

***Table 4.6b: A statistical summary of trace elements in water resources in the study area***

| Trace elements | Min | Max | Mean | Stdev | WHO (2017) guideline | EPA (2014) MCL |
|---|---|---|---|---|---|---|
| Fe (µg/L) | 0.2 | 1215.9 | 63.7 | 187.4 | 300.0 | 300.0 |
| Co (µg/L) | 0.0 | 4.6 | 0.5 | 0.9 | | |
| Se (µg/L) | BQL | 2.5 | 0.2 | 0.4 | 40.0 | 50.0 |
| Ti (µg/L) | 4.1 | 810.7 | 130.9 | 161.8 | | |
| Sr (µg/L) | 26.7 | 1650.7 | 327.9 | 373.9 | | 1,500 |
| Sn (µg/L) | BQL | 0.1 | 0.0 | 0.0 | | |
| Sb (µg/L) | 0.2 | 2.3 | 0.5 | 0.3 | 20.0 | 6.0 |
| Al (µg/L) | BQL | 518.9 | 43.7 | 91.9 | 100-200 | 10-200 |
| B (µg/L) | 0.5 | 31.8 | 3.2 | 4.4 | 240.0 | |
| Cr (µg/L) | 0.4 | 7.5 | 2.0 | 1.5 | 50.0 | 100.0 |
| Cu (µg/L) | 0.1 | 22.5 | 2.1 | 3.7 | 200.0 | 1300.0 |
| Pb (µg/L) | BQL | 1.6 | 0.2 | 0.3 | 10.0 | 15.0 |
| Ni (µg/L) | BQL | 14.7 | 1.7 | 2.2 | 70.0 | |
| As (µg/L) | 0.0 | 1.3 | 0.1 | 0.2 | 10.0 | 10.0 |
| Cd (µg/L) | BQL | BQL | 0.0 | 0.0 | 3000.0 | 3000.0 |
| Zn (µg/L) | BQL | 158.6 | 10.9 | 27.0 | | 500.0 |
| Mn (µg/L) | 0.3 | 712.4 | 125.4 | 196.0 | 400.0 | 500.0 |

Shallow groundwater (open wells, developed wells and springs) have lower concentrations of trace elements than boreholes except strontium which easily infiltrates shallow wells from agricultural return flow. Similar to major ions, groundwater has slightly higher trace element concentrations than surface water owing to the prolonged water-rock interaction time, longer residence time and anoxic conditions, which promote element solubilty. Conversely, surface water is almost always diluted by rainfall and other tributaries, and given the higher surface oxygen; these elements tend to precipitate, thus reducing surface water concentrations between the former and the aquifer media.

*Table 4.6d: Trace element variation in different water resources in the Bafia area*

| | Dug wells | | | | Boreholes | | | | Dev wells | | | | Springs | | | | Rivers | | | |
|---|---|---|---|---|---|---|---|---|---|---|---|---|---|---|---|---|---|---|---|---|
| | Min | Max | Mean | Std. Dev | Min | Max | Mean | Std. Dev | Min | Max | Mean | Std. Dev | Min | Max | Mean | Std. Dev | Min | Max | Mean | Std. Dev |
| Fe | 3.0 | 58.0 | **14.6** | 13.09 | 0.0 | 1215.9 | **106.9** | 273.59 | 3.0 | 699.0 | **77.4** | 206.62 | 15.0 | 16.0 | **15.5** | 0.71 | 1.0 | 195.0 | **82.8** | 81.99 |
| Co | 0.0 | 3.8 | 0.8 | 1.07 | 0.0 | 1.5 | 0.2 | 0.32 | 0.0 | 4.6 | 0.7 | 1.32 | 0.0 | 0.1 | 0.1 | 0.01 | 0.1 | 0.1 | 0.1 | 0.03 |
| Se | 0.0 | 3.0 | 0.4 | 0.86 | 0.0 | 0.0 | 0.0 | 0.00 | 0.0 | 0.0 | 0.0 | 0.00 | 0.0 | 0.0 | 0.0 | 0.00 | | | | |
| Ti | 4.1 | 690.4 | **138.4** | 160.73 | 23.1 | 810.7 | **170.6** | 205.20 | 22.3 | 397.1 | **103.2** | 110.50 | 8.8 | 48.5 | **28.7** | 28.06 | 8.5 | 81.3 | **34.3** | 32.19 |
| Sr | 26.7 | 1577.4 | **425.3** | 479.20 | 69.2 | 1650.7 | **334.7** | 339.25 | 46.8 | 1293.5 | **269.7** | 348.42 | 79.2 | 252.1 | **165.7** | 122.26 | 29.3 | 202.5 | **115.1** | 71.45 |
| Sn | 0.0 | 0.0 | 0.0 | 0.00 | 0.0 | 0.0 | 0.0 | 0.00 | 0.0 | 0.0 | 0.0 | 0.00 | 0.0 | 0.0 | 0.0 | 0.00 | 0.0 | 0.0 | 0.0 | 0.00 |
| Sb | 0.0 | 1.0 | 0.4 | 0.51 | 0.0 | 1.0 | 0.4 | 0.49 | 0.0 | 1.0 | 0.3 | 0.47 | 0.0 | 1.0 | 0.5 | 0.71 | 0.0 | 2.0 | 0.8 | 0.96 |
| Al | 3.0 | 61.8 | **19.5** | 18.66 | 0.0 | 518.9 | **63.1** | 145.31 | 9.1 | 140.2 | **52.7** | 49.70 | 7.4 | 11.8 | **9.6** | 3.08 | 0.5 | 169.0 | **62.2** | 74.66 |
| B | 1.0 | 32.0 | 5.0 | 7.23 | 1.0 | 5.0 | 1.9 | 1.12 | 1.0 | 5.0 | 2.8 | 1.40 | 1.0 | 2.0 | 1.5 | 0.71 | 1.0 | 10.0 | 3.8 | 4.19 |
| Cr | 0.0 | 8.0 | 1.7 | 1.75 | 0.0 | 6.0 | 2.5 | 1.70 | 0.0 | 4.0 | 1.9 | 1.14 | 1.0 | 2.0 | 1.5 | 0.71 | 0.0 | 3.0 | 0.8 | 1.50 |
| Cu | 0.0 | 7.0 | 1.8 | 1.56 | 0.0 | 22.0 | 3.0 | 5.54 | 0.0 | 10.0 | 1.8 | 2.79 | 0.0 | 1.0 | 0.5 | 0.71 | 1.0 | 1.0 | 1.0 | 0.00 |
| Pb | 0.0 | 0.0 | 0.0 | 0.00 | 0.0 | 2.0 | 0.2 | 0.49 | 0.0 | 1.0 | 0.1 | 0.30 | 0.0 | 0.0 | 0.0 | 0.00 | 0.0 | 0.0 | 0.0 | 0.00 |
| Ni | 0.0 | 15.0 | 2.6 | 3.57 | 0.0 | 4.0 | 1.4 | 1.18 | 0.0 | 2.0 | 1.5 | 0.69 | 0.0 | 1.0 | 0.5 | 0.71 | 0.0 | 1.0 | 0.3 | 0.50 |
| As | 0.0 | 1.0 | 0.2 | 0.38 | 0.0 | 0.0 | 0.0 | 0.00 | 0.0 | 1.0 | 0.1 | 0.30 | 0.0 | 0.0 | 0.0 | 0.00 | 0.0 | 0.0 | 0.0 | 0.00 |
| Zn | 0.0 | 26.0 | 6.6 | 7.02 | 0.0 | 159.0 | 19.2 | 43.75 | 0.0 | 32.0 | 10.5 | 11.28 | 1.0 | 3.0 | 2.0 | 1.41 | | | | |
| Mn | 0.5 | 596.8 | **152.6** | 179.52 | 0.8 | 712.4 | **200.6** | 256.08 | 1.4 | 128.3 | **29.6** | 44.70 | 2.0 | 22.4 | **12.2** | 14.38 | | 1.4 | **0.8** | 0.46 |

### IV.5.2. Natural background levels and threshold values for trace elements

Despite the low trace element concentrations generally observed, some elements exceeded the NBLs and TVs calculated for groundwater in the Bafia area. The NBL for Fe, Cr, Ni, Cu, As and Pb are 58, 3.7, 3.93, 2.11, 0.18 and 0.25 µg/L, with TVs of 179, 26.9, 36.97, 1001, 5.09 and 5.13 µg/L respectively. Over 16% and 9% samples exceeded the NBL and TV for Fe (BBH 04, BBH 46, Bdow 06, BBH 33); 21% and 16% exceed the NBL and TV for Mn (e.g BBH 48, BBH 38, BBH 50, BBH 04), indicating their significance in groundwater toxicity, especially in these deeper wells where reducing conditions favor precipitation and saturation in

solution (Fig IV.14). About 10% samples exceeded the NBL for Cr; 12% for Cu; 9% for Pb; 5% for Ni and 14% for As. These results show that continuous exposure to these elements increases the contamination potentials of these resources and renders the inhabitants of Bafia vulnerable to various diseases, hence the need for regular groundwater monitoring (Ogana et al. 2024).

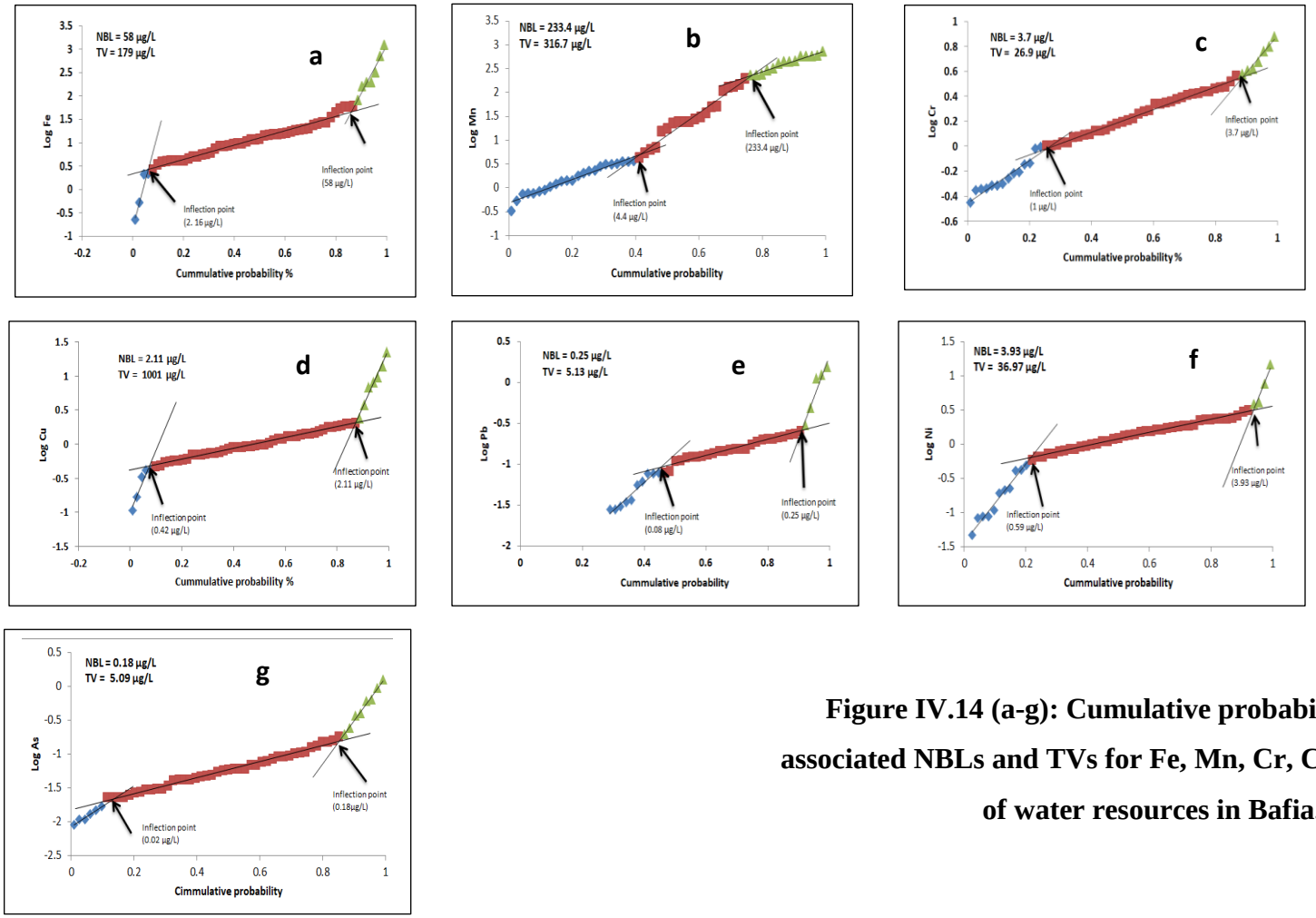


**Figure IV.14 (a-g): Cumulative probability plots and associated NBLs and TVs for Fe, Mn, Cr, Cu, Pb, Ni and As of water resources in Bafia.**

### IV.5.3. Trace element mobility and potential sources

The Ficklin diagram (Ficklin et al. 1992) is a graphical tool used in environmental geochemistry and water quality studies to classify and assess the concentrations of dissolved heavy metals in water. It is obtained by plotting the pH against the sum of metal load per sample, in this case,

$$\text{Metal load (µg/L)} = \sum_{i=1}^{n} \text{Fe} + \text{Ti} + \text{Sr} + \text{Al} + +\text{Cr} + \text{Cu} + \text{Zn} + \text{Mn} \quad (26)$$

The results plotted in Fig IV.15 show that majority of the samples (50% boreholes, 47% open wells, 50% developed wells and 75% rivers) plot in the near neutral-low metal domain. This insinuates that there is a mixture of low metal and high metal loads in the area, and depending on the pH and Eh, these metals have varied mobility. The samples in the near neutral-high metal and acid-high metal fields have the highest Ti, Mn, Fe and Sr.

The low metal concentrations with near-neutral pH for most samples suggest limited anthropogenic influence, reflecting low natural background levels as described above (Boum-Nkot et al. 2023). The figure also refutes the presence of high acid sources like an acid mine drainages, thus a general good water quality with regards to the heavy metals in the Bafia area. For better understanding different pollution indices were used.

The spatial and temporal distribution of trace elements in groundwater is controlled by several natural (elevation, rock/soil type, precipitation, dissolution, mineral solubility, ionic charge/size, pH/redox conditions and the ability to form complexes with organic and inorganic ligands) and anthropogenic (land use, emission sources, distance from mines and cities) factors (Bing et al. 2019).

Besides the potentially toxic trace elements (Pb, As, Zn, Cu, Cd or Hg), high Fe and Mn in groundwater are some of the main reasons behind well abandonment because high Fe leads to the formation of rusty hydroxides while elevated Mn leads to increased intellectual impairment and reduced quotients in children (Bouchard et al. 2011). The major source of Fe and Mn in most groundwater is the interaction between water and minerals like hematite ($Fe_2O_3$), magnetite ($Fe_3O_4$) and manganite (MnO (OH) as shown below:

$$Fe_2O_3 + 3H_2O \longrightarrow 2Fe^{2+} + 3OH^- \quad (29)$$

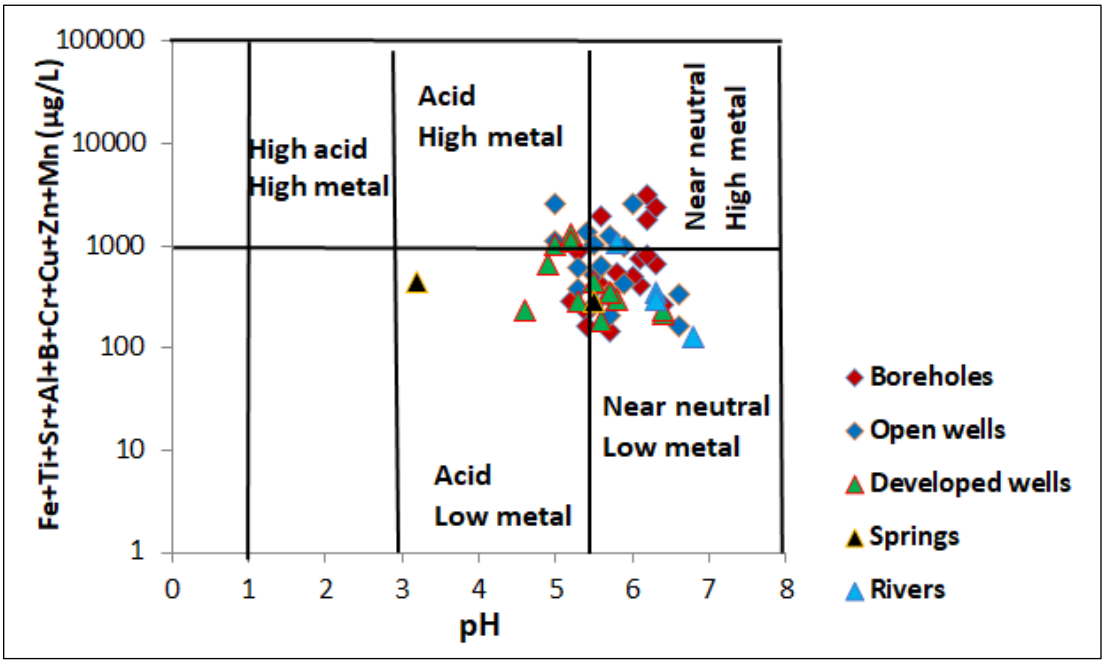


**Figure IV.15: Classification of water samples using the Ficklin diagram**

The relative mobility (RM) of trace elements (Fig. IV.16) was done by normalizing rock and water trace element with Sr, widespread mobile contaminant in surface and subsurface (Davidenko, 1999).

$$RM = [Element/Sr]_{water}/[Element/Sr]_{rock} \quad (30)$$

Sr readily interchanges with cations of similar or higher charges, especially $Ca^{2+}$, but is not influenced by the presence of $Na^{+}$. It is less mobile in clayey silt and more mobile in sandy water-bearing rocks (Keesari et al. 2022). Sr substitutes for Ca through cation exchange in various biological processes; the most important of which is in the bone, affecting skeletal development and leading to osteomalacia and rickets (Malov, 2023). Sr and Ca cation exchange in carbonate environments produces strontianite ($SrCO_3$) or celestine ($SrSO_4$) through in the following equations:

$$Sr^{2+}(aq) + CaCO_3(s) \rightarrow SrCO_3(s) + Ca^{2+}(aq) \quad (31)$$

$$Sr^{2+}(aq) + CaSO_4(s) \rightarrow SrSO_4(s) + Ca^{2+}(aq) \quad (32)$$

For better representation, the RM was calculated for the four rock samples and the five closest water points; the results show an overall high mobility for most elements but for Ti with high immobility rates.

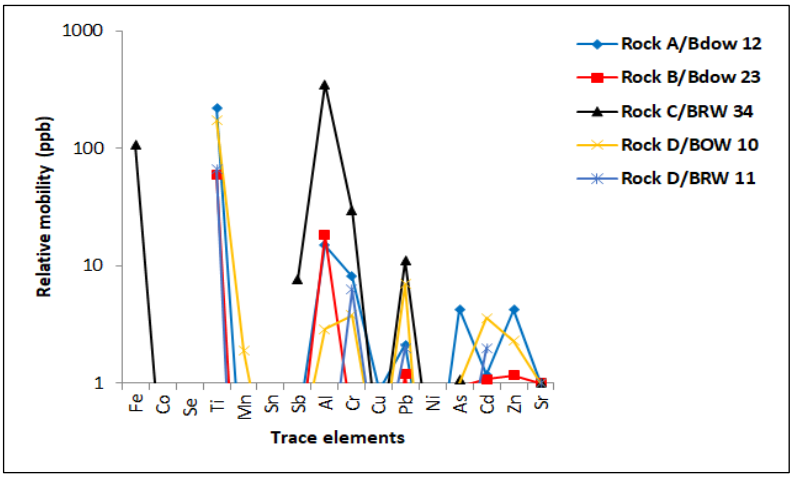


**Figure IV.16: Spider graph showing the relative mobility of trace elements between water and rocks**

Generally, Ti is resistant to weathering regardless of the environmental conditions, hence low mobility. Given that the atmospheric input of Ti is inexistent, its presence in groundwater is tied to the weathering of parent materials like ilmenite and rutile, which are the primary Ti minerals (Xin et al. 2012). These results confirm the existing information of the geology of the area known to have some meta-sediments which host rutile ($TiO_2$) (Tchakounté et al. 2021). The peak in Al in the Mbam River (BRW 34) may be attributed to natural and anthropogenic inputs from different sources along its flow path.

Factor analysis (FA) is an effective statistical tool used in groundwater hydrochemistry to explain the observed relationships as a set of new variables termed factors or components (Yidana et al. 2018) and trace the sources of ions. After performing FA on the centered log-ratio transformed data, three factors were established (Table 4.7), explaining 50.7% of the total variance of the hydrochemical parameters.

***Table 4.7 Factor analysis of water and rock trace elements in the Bafia area***

| Rotated Component Matrix[a] | | | |
|---|---|---|---|
| | Component | | |
| | 1 | 2 | 3 |
| Fe | -0.06 | **-0.50** | 0.42 |
| Co | -0.47 | 0.32 | 0.12 |
| Se | 0.01 | 0.06 | **-0.83** |
| Ti | **0.67** | 0.46 | 0.36 |
| Sr | **0.73** | 0.24 | 0.09 |
| Sn | -0.31 | 0.15 | 0.20 |
| Sb | 0.40 | -0.51 | 0.26 |
| Al | -0.16 | **-0.80** | 0.18 |
| B | 0.62 | -0.28 | 0.09 |
| Cr | 0.38 | 0.29 | 0.20 |
| Cu | -0.02 | **-0.56** | -0.19 |
| Pb | -0.05 | **-0.75** | -0.02 |
| Ni | -0.16 | **0.52** | 0.05 |
| As | -0.71 | 0.12 | -0.04 |
| Zn | -0.71 | 0.12 | -0.04 |
| Mnmgl | -0.22 | 0.61 | 0.36 |
| HCO3 | **0.72** | 0.25 | 0.51 |
| Fmgl | 0.29 | 0.36 | 0.68 |
| Clmgl | 0.34 | 0.10 | **-0.78** |
| NO3mgl | -0.37 | -0.26 | **-0.58** |
| SO42mgl | 0.23 | 0.50 | 0.11 |
| NH4mgl | -0.10 | -0.37 | -0.02 |
| Namgl | **0.75** | 0.13 | -0.19 |
| Kmgl | 0.40 | 0.11 | -0.17 |
| Mg2mgl | **0.61** | 0.46 | 0.00 |
| Ca2mgl | **0.74** | 0.45 | 0.28 |

Extraction Method: Principal Component Analysis.
Rotation Method: Varimax with Kaiser Normalization.

Component 1 accounts for 25.7% of the total variance and has strong positive loadings on Na, Sr, Ca, $HCO_3$, Mg, B and Ti. This component showcases the influence of local geology on groundwater chemistry, notably the dissolution of silicate and carbonate (meta-sediments) rocks in the area. High Na, Sr and Ca loadings equally point to ion exchange processes taking place (Keesari et al. 2022; Fongoh et al. 2023). Despite the relatively high Sr concentration in some water samples, the inverse geochemical model shows that groundwater is under saturated with

respect to Celestite ($SrSO_4$) and Strontianite ($SrCO_3$) (Fig. IV.17). Hence, this component reflects natural processes like rock weathering and cation exchange.

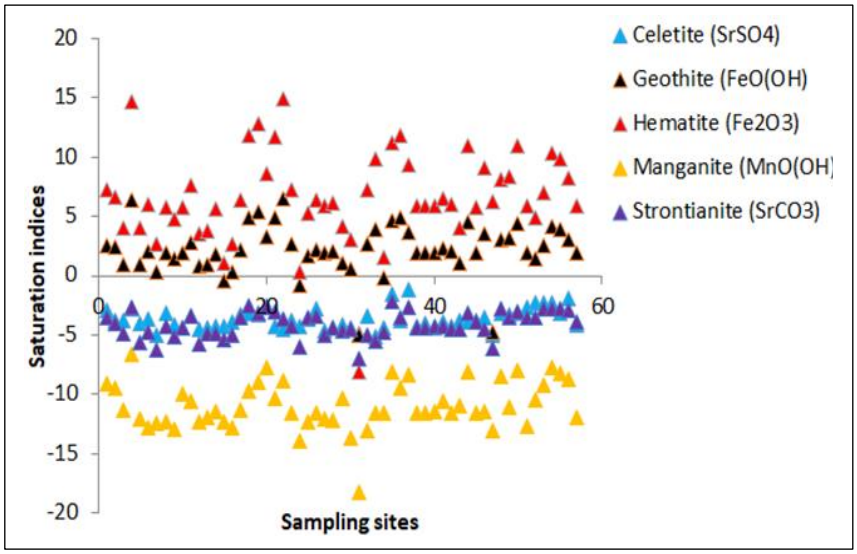


**Figure IV.17: Mineral saturation indices showing Geothite and Hematite super-saturation**

Component 2, which accounts for 14.2% of the total variance, has high negative loadings on Al, Pb, Cu and Fe, which linked to their ability to adsorb unto mineral surfaces, clays, and sediments under acidic conditions (pH between 4 and 6), hence their low concentrations (Marszałek, 2022). Additionally, 96% of groundwater samples are oversaturated with respect to hematite ($Fe_2O_3$) and goethite (FeO(OH). According to Mapoma et al. (2017), mineral precipitation often attenuates their concentration in groundwater. Therefore, the low concentration of Fe in most water samples is attributed to the precipitation of these mineral phases. The hematite and goethite levels align with the geology and stratigraphy of the area known to have iron-rich minerals and a lateritic layer (Enyegue et al. 2014; Tchakounté et al. 2021). The moderate positive loadings of Ni, Mn and $SO_4$, reflects anthropogenic influences, possibly from urban runoff, wastewater and sewage. Manganite (MnO(OH) shows under saturation in all water samples, indicating that it remains in solution; hence some samples have high concentrations. Manganite has a higher solubility product ($K_{SP}$) than hematite, thus it can easily dissolve and stay mobile in solution. Some samples like BBH 38 have high Sr (1650 µg/l), Mn (565.6 µg/l) and high $SO_4$ (291 mg/L), suggesting the presence of evaporite mineral species like $MnSO_4$ and $SrSO_4$ commonly found in the undifferentiated gneisses in Bafia (Ganwa, 2022). Thus, this component represents interplay of natural environmental conditions and human activities.

Component 3 accounts for 10.8% of the total variance. High negative loadings for Se, $NO_3$ and Cl point to high contamination from fertilizers/manure, domestic sewage and agricultural runoff (Kringel et al. 2016). In the absence of halites, bleaching agents (NaClO), leaky pit toilets and well chlorination (using NaCl) are potential chloride sources in the Bafia area (Keesari et al. 2016). Thus, this factor represents the influence of anthropogenic activities. The low Zn concentrations in both water (maximum of 158.6µg/l) and rocks suggest that water-rock interaction controls Zn enrichment rather than human activities.

### IV.5.4. Heavy metal pollution assessment and health risks

#### IV.5.4.1. Heavy Metal Pollution Index (HPI)

The standard (Si) and weightage (Wi) values used for the calculation of the indices are found in Table 4.8. The results of the HPI calculated show a variation from 0.4 to 10.6, with a mean of 2.1. Based on the HPI, all water samples analyzed fall within the excellent range (<25) and below the HPI critical value of 100 (Edet and Offiong, 2003), hence classified as suitable for drinking. However, these low HPI values do not necessarily mean the absence of heavy metal contamination since the latter might have been influenced by dilution or changes in human activities (Boum-Nkot et al. 2023). The spatial distribution of the HPI values in the Bafia area (Fig. IV.18) indicates heterogeneous point sources of groundwater pollution (domestic wastewater and small-scale industries). Sample BOW 07 with the lowest HPI (0.5) and low EC (50µS/cm) is assumed to reflect the geochemical background or "reference concentrations" of trace elements in the Bafia area; hence could be used in monitoring the dynamics of pollutants in this semi-urban ecosystem (Bon et al. 2021).

***Table 4.8: Standard values used for the calculation of metal indices*** (WHO 2017)

| Metals | Si - Standard permissible (µg/L) | Weightage (1/Si) |
|---|---|---|
| Fe | 300 | 0.00333333 |
| Se | 40 | 0.025 |
| Ti | 1500 | 0.00066667 |
| Sr | 4000 | 0.00025 |
| Sn | 2 | 0.5 |
| Sb | 20 | 0.05 |
| Al | 100 | 0.01 |
| B | 2400 | 0.00041667 |
| Cr | 50 | 0.02 |
| Cu | 2000 | 0.0005 |
| Pb | 10 | 0.1 |
| Ni | 70 | 0.01428571 |
| As | 10 | 0.1 |
| Zn | 3000 | 0.0002 |
| Mn | 400 | 0.0025 |

All standards except Ti and Sr, are from the WHO (2017) guideline. Sr (U.S. EPA 2014)

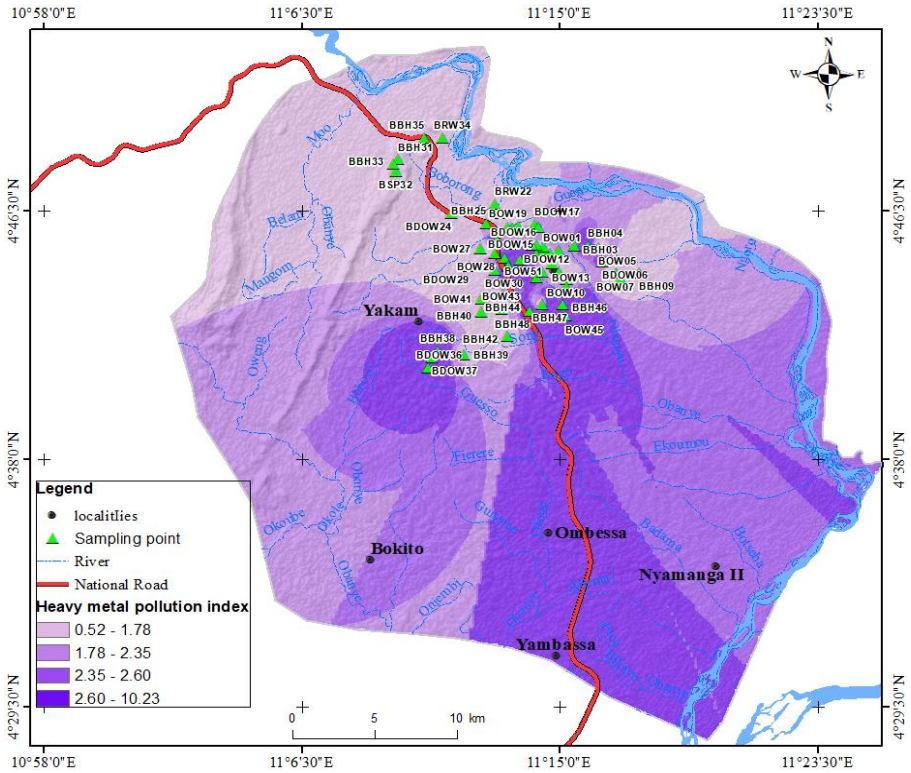


**Figure IV.18 Heavy Metal Pollution index (HPI) distribution map of the Bafia area**

### IV.5.4.2. Heavy metal evaluation index (HEI)

The HEI ranges from 0.2 to 6.1, with a mean of 1.2. Based on the classification scheme (HEI <10= low, HEI = 10 to 20-medium and HEI > 20-high) proposed by Edet and Offiong (2003), all the samples have low contamination index values. These values are slightly higher than those obtained by Boum-Nkot et al. (2023) in Douala (0.09 to 0.9). Just as the case of HPI, the low values do not mean the complete absence of heavy metals in water resources in the Bafia area.

### IV.5.4.3. Contamination degree ($C_d$)

The degree of contamination has the lowest values amongst all computed indices. According to Backman et al. (1998), the degree of contamination for all samples could be classified as low, given that all samples recorded $C_d$ values <1.

Given the low HPI and $C_d$, (Table 4.9), another classification criterion for HEI (HEI <0= low, HEI = 1 to 3-medium and HEI > 3-high) was adopted for this study; and according to this new classification, 61% samples have low HEI, 35% samples have medium HEI and 4% have high HEI values. All surface water samples have low HEI except BRW 34 (Mbam River) with HEI value = 2.5. Being the main and biggest river in the area, the high HEI value could reflect a collection of suspended solids and dissolved solids from smaller tributaries (Embom et al. 2024).

***Table 4.9: Classification of water sources based on pollution indices***

| **HPI** | **Reference ranges** | **Characteristics** | **% samples** |
|---|---|---|---|
| | <25 | Excellent | 100 |
| | 26 to 50 | Good | 0 |
| | 51 to 75 | Poor | 0 |
| | 76 to 100 | Very poor | 0 |
| | >100 | Unsuitable | 0 |
| **HEI** | | **Characteristics** | **% samples** |
| | <1 | Low | 61 |
| | 1 to 3 | Medium | 35 |
| | >3 | High | 4 |
| **$C_d$** | | **Characteristics** | **% samples** |
| | <1 Low | Low | 100 |
| | 1-3 Medium | Medium | 0 |
| | >3 High | High | 0 |

### IV.5.4.4. Assessment of non-carcinogenic and carcinogenic health risks

#### a) Non-carcinogenic health risks

The assessment of human health risks involves estimating and isolating human health impacts to which people could be exposed in an environment that is contaminated by toxic chemicals. This is estimated by comparing the recommended average daily dose with the actual intake dose in water. The ingested computed Average daily dose (ADD), the hazard quotient (HQ) and hazard index (HI) for both adult and child are shown in Table 4.10a. Based on the mean of the ADD, trace element distribution order is Sr>Ti>Fe>Mn>Al>Zn>Cu>Cr>Ni>Pb>As for both adult and child. The estimated ADD values for each heavy metal in drinking water for adults are below the recommended permissible limit for drinking water (WHO 2017). In comparison, children present greater contamination risks with higher average concentrations

***Table 4.10A: Non-carcinogenic human health risks values of Average daily dose (ADD) of the ingestion of heavy metals in water sources in Bafia***

| | Adult ADD (mg/kg/day) | | | Child ADD (mg/kg/day) | | |
|---|---|---|---|---|---|---|
| | Min | Max | Mean | Min | Max | Mean |
| Fe | 7.10E-06 | 0.03821 | 0.002 | 2E-05 | 0.0811 | 0.00418 |
| Ti | 1.20E-04 | 0.02548 | 0.00411 | 0.0003 | 0.054 | 0.00862 |
| Sr | 8.00E-04 | 0.0519 | 0.0103 | 0.0018 | 0.11 | 0.02173 |
| Al | 0 | 0.0163 | 0.0014 | 0 | 0.0346 | 0.00287 |
| Cr | 1.10E-05 | 0.00024 | 6.30E-05 | 2E-05 | 0.0005 | 0.00013 |
| Cu | 3.00E-06 | 0.0007 | 7.00E-05 | 7E-06 | 0.0015 | 0.00014 |
| Pb | 0 | 5.00E-05 | 5.00E-06 | 0 | 0.0001 | 1.1E-05 |
| Ni | 0 | 0.00046 | 5.30E-06 | 0 | 0.001 | 0.00011 |
| As | 2.80E-07 | 3.90E-05 | 4.22E-06 | 6E-07 | 8E-05 | 8.8E-06 |
| Zn | 0 | 0.00498 | 3.43E-04 | 0 | 0.0106 | 0.00073 |
| Mn | 1.03E-05 | 2.24E-02 | 3.94E-03 | 2E-05 | 0.0475 | 0.00822 |

The total HQ for trace element is <1 for all samples irrespective of the geology of the sampling point (Table 4.10b). Therefore, referring to the mean values, the health risk estimation for Fe, Ti, Sr, Al, Cr, Cu, Pb, Ni, As, Zn and Mn shows an acceptable level of the non-carcinogenic health risk for all water samples.

The estimated capability of non-carcinogenic impacts calculated for individual trace elements is summed-up and expressed as the Hazard Index (HI). The HI value, which is the total of the HQs, as shown in Table 4.10b ranges from 0.017 to 0.336, with a mean of 0.094 for adults and 0.037 to 0.709, with a mean of 0.196 for children: all of which are <1. This implies a non-carcinogenic health hazard from ingested heavy metals in the Bafia area. However, similar to the ADD and HQ, children present higher HI values (max=0.7) than adults (max=0.3), signifying increased health risks for children in the Bafia area in the nearest future.

***Table 4.10b: Non-carcinogenic human health risks values of hazard quotient (HQ) and hazard index (HI) due to ingestion of heavy metals in water sources in Bafia***

| | Hazard quotient (HQ)-Adult (mg/kg/day) | | | Hazard quotient (HQ)-Child (mg/kg/day) | | |
|---|---|---|---|---|---|---|
| | Min | Max | Mean | Min | Max | Mean |
| **Fe** | 1.0102E-05 | 0.05459206 | 0.0028616 | 2.1429E-05 | 0.11580133 | 0.00573556 |
| **Ti** | 4.2722E-05 | 0.00849303 | 0.00137114 | 9.0622E-05 | 0.01801551 | 0.00289607 |
| **Sr** | 0.00139773 | 0.08646409 | 0.01717611 | 0.00296489 | 0.18340867 | 0.03603416 |
| **Al** | 0 | 0.00232986 | 0.00019627 | 0 | 0.02134676 | 0.00165449 |
| **Cr** | 0.0036981 | 0.07891714 | 0.02100256 | 0.0000814 | 0.1674 | 0.04401941 |
| **Cu** | 8.4857E-05 | 0.01765971 | 0.00164385 | 0.0000882 | 0.03746 | 0.00306626 |
| **Pb** | 0 | 0.03488571 | 0.00371117 | 0 | 0.0296 | 0.00279422 |
| **Ni** | 0 | 0.02310786 | 0.00266335 | 0 | 0.04901667 | 0.00553844 |
| **As** | 0.00094286 | 0.13126667 | 0.01406383 | 7.3333E-07 | 0.27844444 | 0.02920308 |
| **Zn** | 0 | 0.01661492 | 0.00114307 | 0 | 0.03524378 | 0.00239424 |
| **Mn** | 7.3633E-05 | 0.15992069 | 0.02816202 | 5.5533E-05 | 0.33922571 | 0.05882088 |
| **Hazard index (HI)** | 0.0172323 | 0.33618416 | 0.09399496 | 0.03700105 | 0.70861422 | 0.19632522 |

### b) Carcinogenic health risks

The cumulative effect of certain toxic trace elements in water and the prolonged human exposure to such water sources, that is, the incremental lifetime cancer risk (ILCR), might lead to the breakout of most cancers in the body (Ogana et al. 2024). In this study, Pb, Ni, As, and Cr were used as carcinogens; and the ILCR of the Bafia population was assessed by multiplying the average daily dose (calculated above) by the cancer slope factor (CSF) values. Cancer slope factors (CSF) are often used to estimate the chances of cancer associated with carcinogenic substances within a milieu (Duvva et al. 2022). The acceptable limits of cancer risks are $1.0 \times 10^{-6}$ to $1.0 \times 10^{-4}$, hence ILCR values $>1.0 \times 10^{-4}$ imply carcinogenic risks for humans. The

calculated carcinogenic risk values summarized in Table 4.10c show that the mean values for Cr, Ni, As and Pb are within acceptable limits for adults, thus no carcinogenic risks for adults in the Bafia area. Conversely, the ILCR values of Ni and Cr for children exceed the maximum limit of $10^{-4}$ in open well BOW 02 (0.0168 and 0.0015 respectively), hence Ni and Cr stand out as carcinogenic threats for the children in that area. Additionally, the As concentration in this sample is at the upper limit of the guideline ($4.5 \times 10^{-4}$), thus continuous As inputs in that area exposes children at future arsenic carcinogenic risks (Fig. IV.19 a and b).

***Table 4.10c: Incremental lifetime cancer risk (ILCR) due to the ingestion of heavy metals in the water resources in the Bafia area***

| | ILCR-Adults | | | ILCR-Child | | |
|---|---|---|---|---|---|---|
| | **Min** | **Max** | **Mean** | **Min** | **Max** | **Mean** |
| **Cr** | 5.5471E-06 | 0.00011838 | 3.1504E-05 | 1.1767E-05 | 0.0015 | 9.246E-05 |
| **Pb** | 0 | 4.1514E-07 | 4.4163E-08 | 0 | 0.00002975 | 6.1561E-07 |
| **Ni** | 0 | 0.00038821 | 4.4744E-05 | 0 | 0.0168 | 0.00038735 |
| **As** | 4.2429E-07 | 0.00005907 | 6.3287E-06 | 0.0000009 | 0.00045 | 2.0672E-05 |

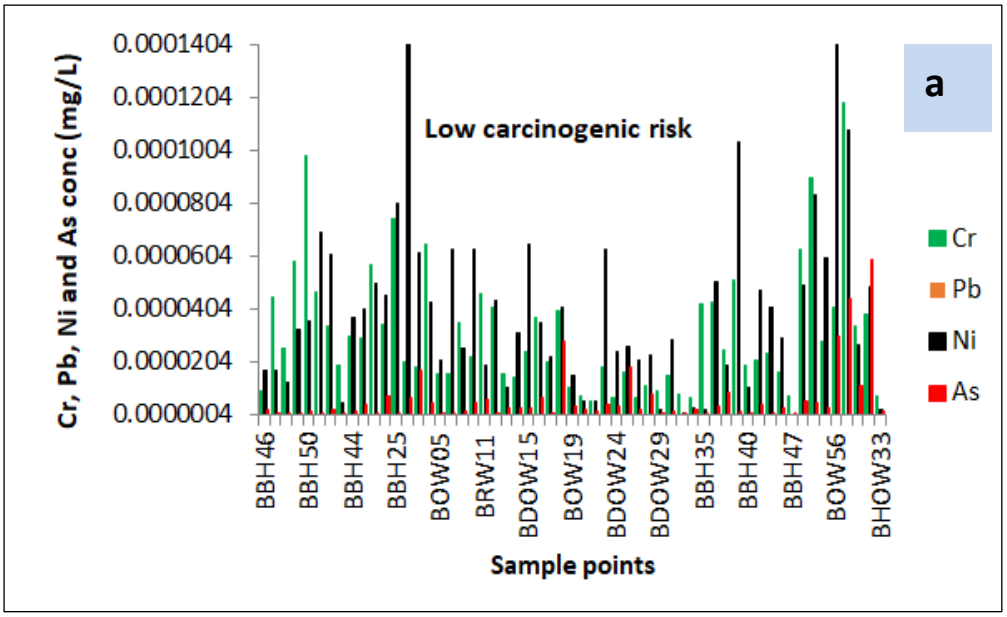

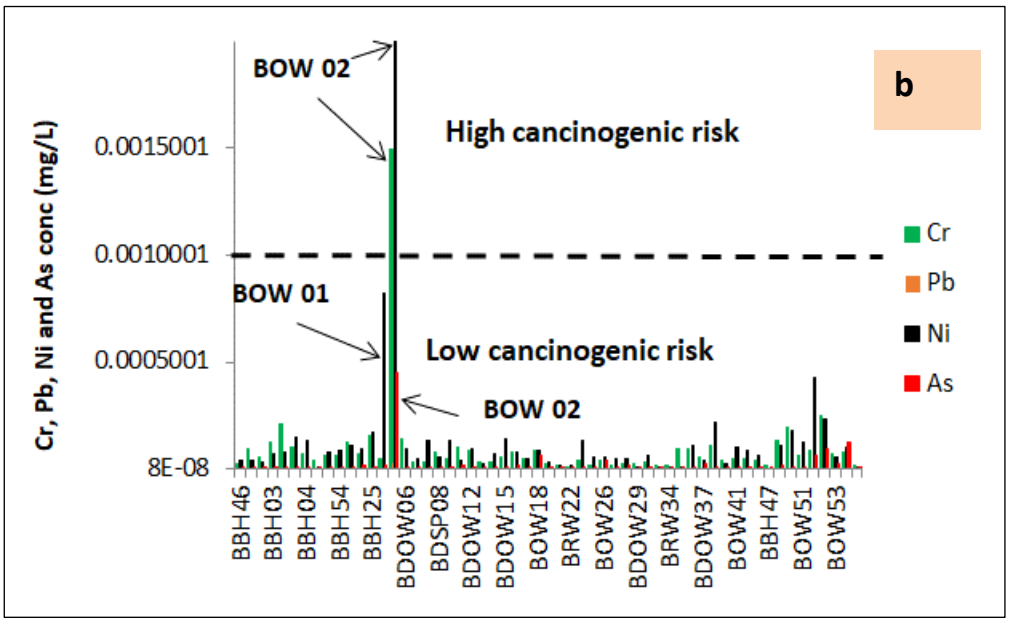


**Figure IV.I9: Potential carcinogenic risks of Cr, Pb, Ni and As showing low risks for (a) adults and higher Cr, Ni risks for (b) children**

### IV.5.5. Local and international comparison of heavy metal concentrations

The results trace elements in groundwater in Bafia were compared to other results in Cameroon and Africa as shown in Table 4.11a It can be observed that the concentration of heavy metals in the Bafia groundwater samples are of a similar magnitude as those of the Ntem watershed in Yaounde (Defo et al. 2016), but lower than those in Kumba and Isangele/Mundemba (Akoachere et al. 2019). Bafia also presents higher values than those reported by Ogana et al. (2024) in South Africa but far lower than those reported by Kana (2022) and Appiah-Opong (2021) in Nigeria and Ghana. However, most these concentrations in Cameroon are below the WHO guideline values except for Fe, Pb and As which exceeded the limits in Isangele/Mundemba (Fe), Ghana (Pb) and Nigeria (Fe, Pb and As).

*Table 4.11a: Comparison of groundwater heavy metal mean concentrations from Bafia and other localities in Cameroon, Africa and the WHO (2017) guidelines*

| | | Fe | Co | Se | Ti | Sr | Sn | Sb | Al | B | Cr | Cu | Pb | Ni | As | Cd | Zn | Mn | Reference |
|---|---|---|---|---|---|---|---|---|---|---|---|---|---|---|---|---|---|---|---|
| **Cameroon** | **Bafia** | 63.74 | 0.51 | 0.18 | 130.88 | 327.91 | 0.02 | 0.50 | 43.71 | 3.16 | 2.00 | 2.09 | 0.16 | 1.69 | 0.13 | BQL | 10.90 | 125.45 | Current study |
| | Yaounde Ntem watershed | / | / | / | / | / | / | / | / | / | 0.92 | / | 0.31 | 0.44 | / | 0.03 | / | / | Defo et al. 2016 |
| | Yaounde Urban | 20.00 | / | / | | / | / | / | 110.00 | / | BDL | 80.00 | 5.72 | 45.00 | / | 2.55 | 10.00 | 88.00 | Bon et al. 2021 |
| | Mount Cameroon | / | / | / | / | / | / | / | / | / | / | / | 0.03 | 0.05 | / | 0.01 | / | / | Neh et al. 2023 |
| | Douala | / | 0.29 | / | / | 33.64 | / | / | / | / | 2.00 | 1.84 | 2.13 | 4.19 | 0.41 | 0.04 | 14.81 | / | Boum-Nkot et al. 2023 |
| | Kumba | 151.71 | 7.47 | / | / | 65.78 | / | / | / | / | 1.53 | 10.12 | 2.31 | 14.50 | 0.12 | 0.16 | 60.29 | 193.11 | Akoachere et al. 2019 |
| | Isangele and Mundemba | 1226.31 | 1.50 | / | / | 88.90 | / | / | / | / | 0.56 | 19.21 | 2.21 | 5.18 | 1.53 | 0.20 | 334.20 | 47.84 | Akoachere et al. 2019 |
| **Africa** | South Africa | 2.10 | 0.20 | 2.50 | 36.40 | 73.30 | / | 0.20 | / | / | 36.00 | 5.40 | 0.03 | 0.09 | 0.20 | 0.00 | 2.70 | 8.00 | Ogana John et al. 2024 |
| | Ghana | / | / | 0.22 | / | / | / | / | / | / | / | 11.50 | 47.67 | / | 3.33 | / | 15.44 | / | Appiah-Opong et al. 2021 |
| | Nigeria | 860.15 | / | / | / | / | / | / | / | / | / | 1.53 | 81.10 | 62.65 | 854.50 | / | 2537.20 | / | Kana, 2022 |
| | WHO guidelines | 300 | 30 | 40 | / | / | 2 | 20 | 200 | 2400 | 50 | 2000 | 10 | 70 | 10 | 3 | 3000 | 400 | WHO 2017 |

Conversely, surface water trace element concentrations in Bafia were compared to some surface water concentrations in Cameroon; Douala (Ndjama et al. 2021), the Western highlands (Tarla et al. 2015) and Betare Oya (Rakontodrabe et al. 2017). There is a close similarity between trace element concentrations in Bafia surface waters and those of the Western highlands, with the exceptions of Sr, Ti and Fe which are slightly higher in Bafia. This similarity is as a result of the presence of the Mbam River (main drainage river in Bafia) which is a collector of other rivers from the West like the noun River. However, trace element concentrations (As, Ni, Pb, Fe, Al, Cr and Cu) of surface waters in Betare Oya (a gold mining sector) and Douala (active industrial zone) are significantly higher than

those in Bafia, a less industrially active area. A comparison of Bafia surface water trace element content with global studies (Zhou et al. 2020) shows lower concentrations in Bafia area (Table 4.11b). The distribution is linked to the geology and land use practices, which in Africa, ranges from rock weathering, to mining, fertilizer and pesticide use (Zhou et al. 2020).

***Table 4.11b: Comparison of surface water heavy metal concentration from Bafia and other localities in Cameroon, Africa, Europe and the WHO (2017) guidelines***

| | | Fe | Co | Se | Ti | Sr | Sn | Sb | Al | B | Cr | Cu | Pb | Ni | As | Cd | Zn | Mn | References |
|---|---|---|---|---|---|---|---|---|---|---|---|---|---|---|---|---|---|---|---|
| **Cameroon** | **Bafia** | 82.76 | 0.07 | 0 | 34.29 | 115.05 | 0.02 | 1.06 | 62.18 | 3.86 | 1.06 | 1.13 | 0.10 | 0.32 | 0.07 | 0 | 0 | 0.84 | Current study |
| | **Western Highlands** | 92.64 | 0.06 | 0 | 12.81 | 53.43 | 0.01 | 0.59 | 64.43 | 1.59 | 0.39 | 1.01 | 0.05 | 0.15 | 0.04 | 0 | 0 | 0.88 | Tarla et al 2015 |
| | **Betare Oya** | 1067.50 | / | / | / | / | / | / | / | / | 60.00 | 275.00 | 100.00 | / | 10.00 | 50.00 | 175.00 | 400.00 | Rakotondrabe et al.2017 |
| | **Douala** | 8151.60 | 37.04 | / | 64.68 | 162.91 | / | / | 237.80 | / | 3089.03 | 40.10 | 18.83 | 4355.84 | 1.02 | 0.12 | 275.90 | 0.42 | Ndjama et al. 2021 |
| **Africa** | **Africa** | 2012.82 | 12.60 | / | / | / | / | / | 945.48 | / | 388.77 | 190.79 | 83.82 | 131.69 | 33.46 | 45.04 | 1169.00 | 483.54 | Zhou et al. 2020 |
| **Europe** | **Europe** | 243.75 | 0.36 | / | / | / | / | / | 569.75 | / | 13.61 | 14.63 | 14.31 | 137.47 | 18.54 | 5.69 | 133.99 | 257.89 | Zhou et al. 2020 |
| | WHO guidelines | 300 | 30 | 40 | / | / | 2 | 20 | 200 | 2400 | 50 | 2000 | 10 | 70 | 10 | 3 | 3000 | 400 | WHO 2017 |

## IV.6. Water resource suitability for drinking and irrigation

### IV.6.1. Water Quality Index (WQI) for drinking water assessment

The WQI varies in this study from 2.1 to 385.3, with a mean of 24.2 and standard deviation of 59.2 in the rainy season and from 1.4 to 219.7, with a mean of 14.7 and standard deviation of 30.4 in the dry season. In both seasons, the majority of samples (89.5%) have WQI values < 50, thus classified as excellent water for drinking purposes (Table 4.12). Just about 5% samples in both seasons are classified in the poor to unsuitable range. The high WQI of the latter group of samples is mostly attributed to high iron, total hardness and nitrate contents. These samples include shallow open wells (e.g Bdow 16, Bdow 06, BOW 67) and one borehole (BBH 04). Based on the WQI distribution map below (Fig. IV.20) and the HPI distribution map (Fig. IV.18 above), Bafia has an overall excellent water

quality, which deteriorates to unsuitable water quality from the NNW to the South eastern parts of Bafia; hence appropriate for drinking and other domestic purposes. These maps represent invaluable tools for decision-makers in the area.

***Table 4.12: Classification of water resources in Bafia based on the WQI***

| Rainy season | | | Dry Season | | |
|---|---|---|---|---|---|
| **WQI range** | % samples | Category | **WQI range** | % samples | Category |
| **< 50** | 89.5 | Excellent | **< 50** | 92 | Excellent |
| **50-100** | 5.2 | Good | **50-100** | 5 | Good |
| **101-200** | 1.8 | Poor | **101-200** | 1.5 | Poor |
| **201-300** | 1.8 | Very poor | **201-300** | 1.5 | Very poor |
| **> 300** | 1.8 | Unsuitable for drinking | **> 300** | 0 | Unsuitable for drinking |

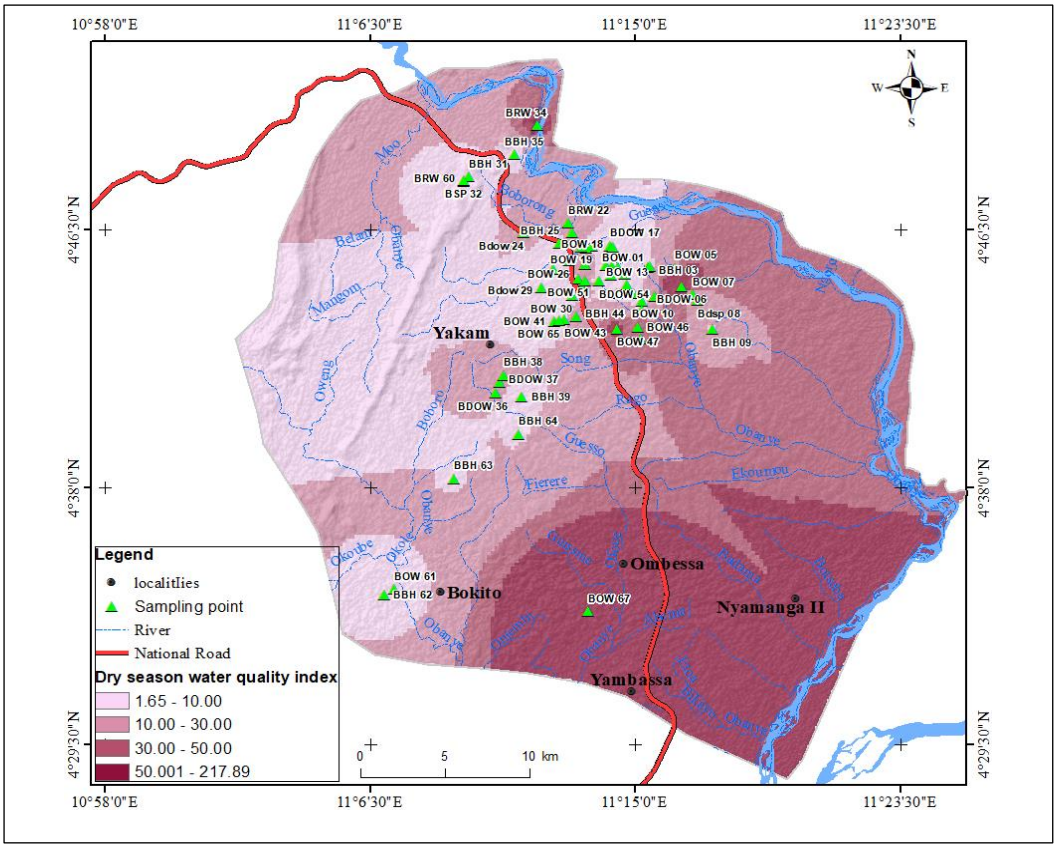


**Figure IV.20 WQI distribution map showing excellent quality for most of the area**

### IV.6.2. Groundwater suitability for irrigation

The suitability of groundwater for irrigation depends on the effects of constituent minerals of water on both the plant and soil. The high concentration of certain dissolved ions affects plant growth and the soil structure, hence reducing productivity (Ravikumar et al. 2011). Generally, the suitability of water for irrigation is evaluated based on the EC, chlorides, percent $Na^+$, Sodium adsorption ratio (SAR), Magnesium hazard, Permeability index (PI) and Residual sodium carbon (RSC) (Table 4.13).

#### IV.6.2.1. Electrical conductivity (EC)

EC is a good factor to measure salinity hazard to crops as it reflects the TDS in groundwater. Generally, high EC causes an increase in soil solution osmotic pressure, which in turn causes drought that lowers plant water availability, even when the soil looks moist. Hence, high EC irrigation waters affect the soil structure and the overall crop productivity. According to the U.S Salinity Laboratory (1954) classification, 56% and 65% of the samples are excellent, 33% and 30% are good while 11% and 5% are permissible for irrigation in the rainy and dry season respectively. This indicates that there are no salts leaching down into the aquifers.

#### IV.6.2.2. Chloride classification

The mobility and inability of chloride ion to be absorbed or adsorbed are unique attributes used to identify chloride pollution. Excess chloride levels beyond plant intake often lead to the appearance of yellow and burning leaf tissues (Nadjai et al. 2024). Groundwater contamination by chloride can occur locally as a result of factors like agricultural fertilizers, dissolving salt deposits, wastewater discharge, and irrigation runoff. The classification of Stuyfzand (1989) in Table 4.13 shows that 59.6%, 31.6%. 7% and 1.8% of the rainy season samples; and 8.3%, 76.7% and 15% of the dry season samples are extremely fresh, very fresh, fresh and fresh brackish. This implies no chloride hazard for plants, thus suitable for irrigation.

#### IV.6.2.3. Percent sodium (%$Na^+$)

High sodium concentration in irrigation water leads to sodium adsorption onto clay particles, displacing $Mg^{2+}$ and $Ca^{2+}$. This exchange process reduces soil permeability, leading to soils with poor internal drainage and low crop yields (Ravikumar et al. 2009).

*Table 4.13: Classification of irrigation water suitability in the Bafia area*

| Parameters | Range | Categories | Rainy season | Dry season |
|---|---|---|---|---|
| | | | % Samples | % Samples |
| **Based on EC (USSL 1954)** | <250 | Excellent | 56 | 65 |
| | 250-750 | Good | 33 | 30 |
| | 750-2250 | Permissible | 11 | 5 |
| | 2250-5000 | Doubtful | 0 | 0 |
| | >5000 | Unsuitable | 0 | 0 |
| **Based on chloride meq/L (Stuyfzand 1989)** | <0.14 | Extremely fresh | 59.6 | 8.3 |
| | 0.14-0.85 | Very fresh | 31.6 | 76.7 |
| | 0.85-4.23 | Fresh | 7 | 15 |
| | 4.23-8.46 | Fresh brackish | 1.8 | 0 |
| | 8.46-28.21 | Brackish | 0 | 0 |
| | 28.21-282.06 | Brackish salt | 0 | 0 |
| | 582.06-564.13 | Salt | 0 | 0 |
| | >564.13 | Hyper saline | 0 | 0 |
| **Percent sodium (%Na)** | <20 | Excellent | 7 | 8.8 |
| | 20-40 | Good | 32 | 56.1 |
| | 41-60 | Permissible | 17 | 38.6 |
| | 61-80 | Doubtful | 1 | 1.8 |
| | >80 | Unsuitable | 0 | 0 |
| **Sodium adsorption ratio (SAR)** | <10 | Excellent | 57 | 100 |
| | 10 to 18 | Good | 0 | 0 |
| | 18 to 26 | Doubtful | 0 | 0 |
| | >26 | Unsuitable | 0 | 0 |
| **Residual sodium carbonate (RSC)** | <1.25 | Good | 57 | 100.0 |
| | 1.25-2.5 | Doubtful | 0 | 0 |
| | >2.5 | Unsuitable | 0 | 0 |
| **Magnesium hazard** | <1.5 | Safe | 55 | 98.3 |
| | 1.5-3 | Doubtful | 2 | 1.7 |
| | >3 | Unsafe | 0 | 0 |
| **Permeability index (PI)** | < 75 | Suitable | 54 | 76.7 |
| | > 75 | Unsuitable | 3 | 23.3 |
| | | | | |

This kind of water saturates the sodium ions in soil and causes deflocculation (dispersion), thus reducing soil infiltration. The $\%Na^+$ was calculated using the following formula:

$$\%Na^{+} = [(Na^{+}+K^{+}) / (Ca^{2+}+Mg^{2+}+Na^{+}+K^{+})]*100 \quad (32)$$

The $\%Na^{+}$ in this study range from 17 to 68, (average of 35.5) and 11 to 63 (average of 35.7) in the rainy and dry season respectively and according to the Wilcox diagram (Wilcox, 1955) (Fig. IV.21a and b), the majority (90%) of the samples are excellent to good for irrigation, especially in fine-textured soils with normal leaching conditions like the sandy-loam and sandy-clay-loam soils of Bafia.

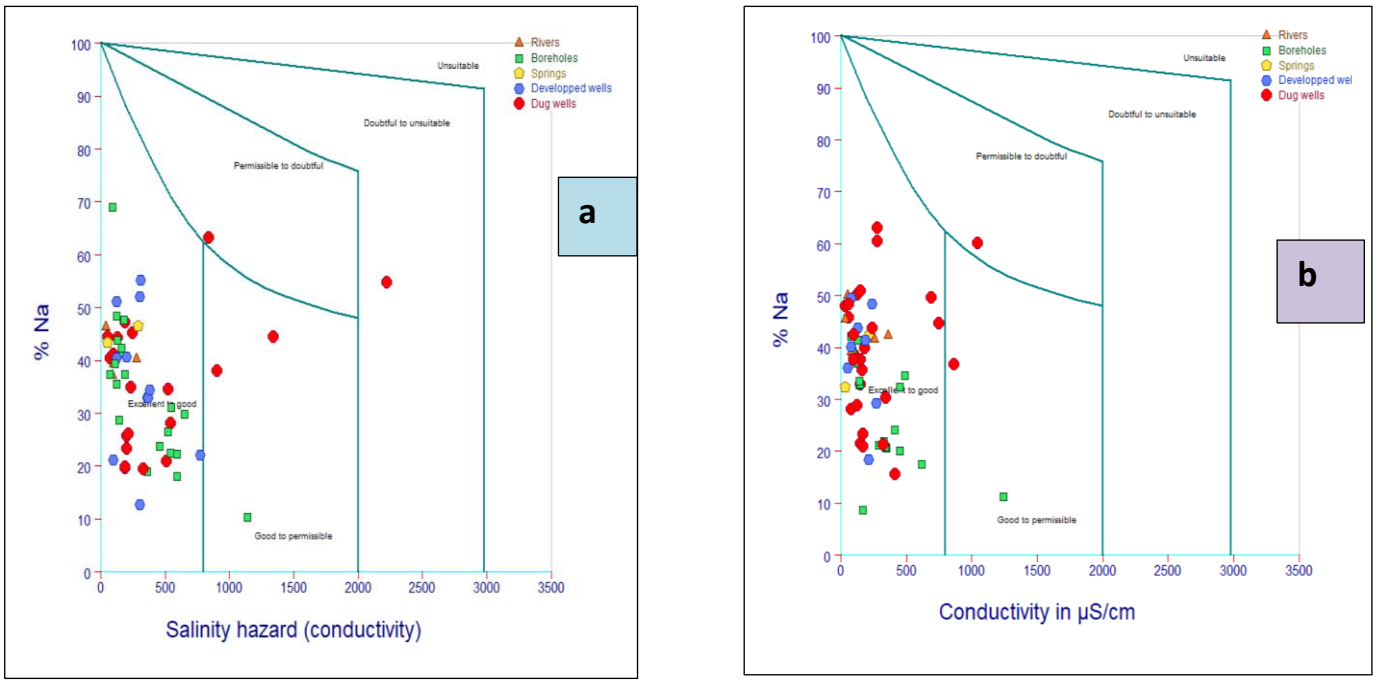


**Figure IV.21: USSL (1954) classification for irrigation waters in the Bafia area during the (a) rainy and (b) dry season**

### IV.6.2.4. Sodium adsorption ratio (SAR)

SAR is the ability of $Na^{+}$ in water to cling onto soil (clay) in exchange for $Ca^{2+}$ and $Mg^{2+}$, thus reducing the permeability capacity of the soil (Nadjai et al. 2024). In fact, it indicates the degree of cation exchange reactions between the irrigation water and the soil. When irrigation water is rich in sodium and poor in calcium, it may damage the soil structure, making it compact and impervious. It is calculated using the following formula:

$$SAR = Na^{+}/[(Ca^{2+}+Mg^{2+})/2]^{0.5} \quad (33)$$

In this study, the SAR values are generally low, ranging from 0.08 to 2.08 and 0.07 to 1.69 in the rainy and dry season respectively. Based on the U.S salinity laboratory diagram (Fig IV.22 a and b), 83% of the samples fall in equal proportions in the C1S1 and C2S1 fields in both seasons, indicating low sodium-low salinity and low sodium- medium salinity, with no anticipated alkali hazard on the crops. Low salinity hazard class (C1) can be good for the irrigation of most crops and on the majority of soils. Nevertheless, some leaching is required, but this occurs under normal irrigation practices except in soils with extremely low permeability. The medium salinity hazard class (C2) is good for moderate amount of leaching. About 17% samples plot in the C3S1 field, indicating low sodium with high salinity (USSL, 1954; Nadjai et al. 2024).

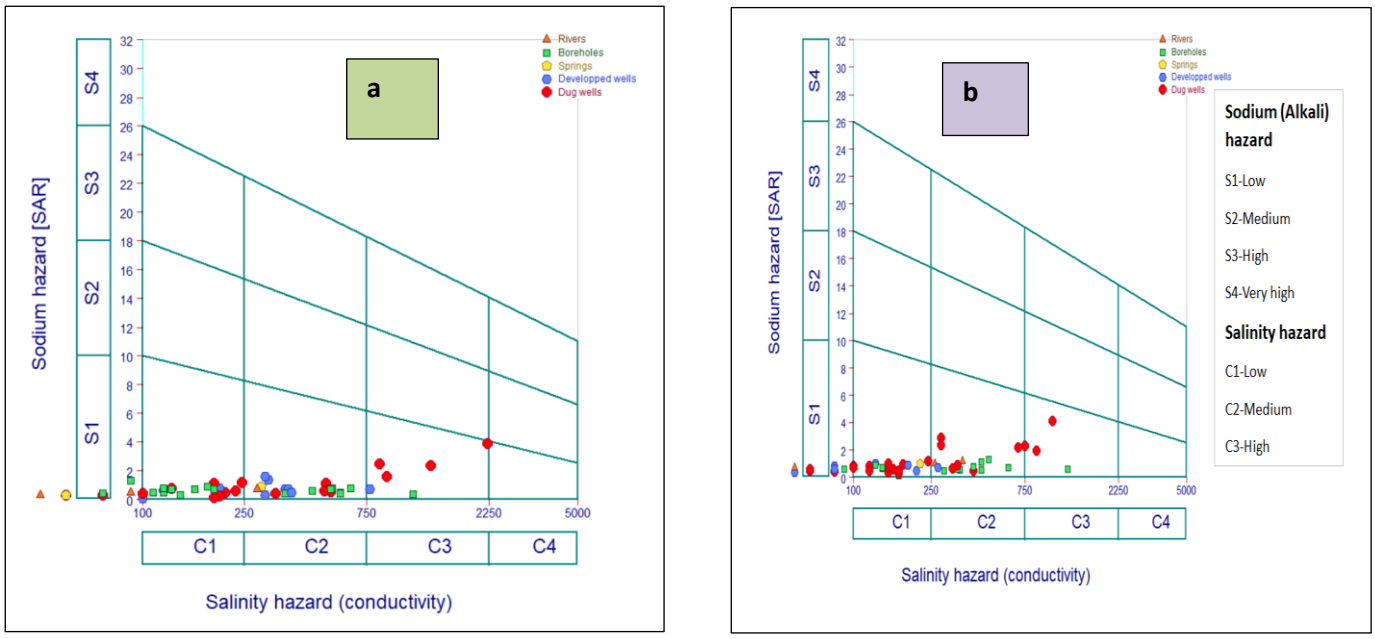


**Figure IV.22: Classification of irrigation waters in the Bafia area during the (a) rainy and (b) dry season. Samples show low to moderate Na with low salinity (Wilcox, 1955)**

High salinity hazard class (C3) is good for plants with moderate salt tolerance, and for soils with moderate permeability. Such water is good because although the salinity is a little high, the soil does not require extra calcium to improve soil flocculation. But however, it is advisable to plant crops that are resistant to high salinity content.

### IV.6.2.5. Magnesium hazard

Despite the equilibrium state that exists between $Ca^{2+}$ and $Mg^{2+}$ in water, both of them behave differently in soil systems. Magnesium ions are about 50% bigger in size than calcium ions, thus slows water infiltration rate. $Mg^{2+}$ does not easily get adsorbed on clay soils like $Ca^{2+}$ will do, thereby contributing to the destruction of the soil structure (Nadjai et al. 2024). Magnesium hazard is the ratio of $Mg^{2+}/Ca^{2+}$ in water and according to the classification, $Mg^{2+}$ hazard values <1.5 is safe for irrigation, between 1.5-3 is doubtful while a value >3 is unsuitable. In this study, the values ranged from 0.1 to 2 and 0.2 to 1.5 in the rainy and dry season respectively, with only 2 samples within the doubtful range.

### IV.6.2.6. Permeability index (PI)

The prolonged use of irrigation water with high salt, calcium, magnesium, and bicarbonate affects soil permeability over time. To determine whether or not soil permeability is suitable for irrigation, Doneen (1964) elaborated the Permeability Index (PI) formula as follows:

$$\text{PI} = \frac{Na^{+} + \sqrt{HCO_3^{-}}}{Ca^{2+} + Mg^{2+} + Na^{+}} \times 100 \qquad (34)$$

According to this classification, PI values < 75 are good for irrigation, with no permeability issues, while PI values > 75 have permeability problems, hence unsuitable for irrigation. In this study, the PI values ranged from 20.1 to 94.6 and from 26.1 to 100.3 in the rainy and dry season individually, with 77% and 95% of the samples in the rainy and dry season good for irrigation.

### IV.6.2.7. Residual sodium carbonate (RSC) index

RSC index for irrigation water indicates the alkalinity hazard which has to do with an excess of carbonate and bicarbonate ions over calcium and magnesium, where the calcium and magnesium precipitate and further disperse the soil. High RSC index favors the formation of alkali soils, which usually form a hard layer of sodium carbonate that causes the soil to swell (Ravikumar et al. 2011). Hence, prolonged irrigation with such water leads to soil infertility. The RSC index can be calculated using the following formula:

$$RSC = (CO_3+HCO_3)-(Ca^{2+}+Mg^{2+}) \quad (35)$$

According to the U.S Department of Agriculture RSC <1.25 is safe for irrigation, values between 1.25 and 2.5 are doubtful and values >2.5 are unsuitable for irrigation. The RSC in this study ranged from -6.1 to 1.6 and from -9.2 to 2.2 in the rainy and dry seasons respectively, thus suitable for irrigation.

## CONCLUSION

Water resources are generally soft-fresh, with hardness increasing slightly from the rainy to the dry season. The pH is slightly acidic to neutral; moderate DO and slightly reducing. TDS and EC increase from the NNW higher topographic recharge areas towards the low center and south discharge areas. Major cations and anions vary slightly from one season to another and are generally within the WHO norms for drinking water, except for some few samples with higher nitrate, sulfate, calcium and potassium concentrations. More than 85% samples have major ions levels within the calculated NBLs and TVs, except for nitrate. The main water type identified is the Ca-Mg-$HCO_3$. There is a slight shift in the Ca-Mg-$HCO_3$ type percentage from the rainy (68%) to the dry season (85%), and the appearance of the Na-K-$HCO_3$ type indicating slight chemical evolution of groundwater. Shallow wells have higher mean TDS, $Cl^-$, $NO_3$, $Na^+$ and K than the boreholes, developed wells, springs and rivers, indicating greater vulnerability to surface contaminants; Boreholes have higher mean $Ca^{2+}$ and $Mg^{2+}$, revealing deeper aquifer interactions, with longer water-rock contact time; while Developed wells had intermediary compositions, suggesting a mixture of both the deep and shallow aquifer sources.

Ionic correlations indicate the release of ions from silicate and weathering sources. Both surface and groundwater have higher $CO_2$ partial pressure than the atmospheric pressure and this facilitates the dissolution of carbonate minerals and silicate minerals, hence release $Ca^{2+}$, $Mg^{2+}$ and $HCO_3$ in water. The Gibbs diagram reveals rock weathering as main source of ions in water. Two chloro-alkaline indices (CAI – I and CAI – II) reveal 100% negative indices for surface and groundwater during the rainy season while 91% groundwater samples had negative CAI values, indicating dominance of direct ion exchange processes with minimal reverse ion exchange.

All the surface and groundwater samples are under-saturated with respect to all target minerals, thus indicating their continuous dissolution, without forming precipitates. The weak positive correlation between potassium and nitrate indicates that inorganic fertilizers (e.g NPKs) are not the only sources of nitrates in water. Additionally, chloride and nitrate exhibit weak relationships, confirming diverse sources, besides their common sewage and fertilizer sources. Most samples located within farmlands (e.g. BOW 01), market areas (BOW 67) and densely populated valley areas (BOW 52, BOW 56) have the highest nitrate and chloride values. However, others like BOW 14, BOW 05 and Bdsp 08 located within cocoa farms had lower nitrate concentrations (11.3 mg/l, 8.9 mg/l and 28.9 mg/l, respectively) than the market and highly populated areas, suggesting that most of the nitrate in the Bafia area originates from other human-related activities like domestic waste production, market, and hospital sewage generation.

Rock leachates reveal relatively lower trace element contents, with a general distribution of Mn>Sr>Fe>Cu>Ni>Al>Zn>As>Co>Sb>Pb>Se>Ti>Cd as opposed to groundwater, with a distribution of Sr>Fe>Mn>Ti>Al>Zn>B>Cu>Ni>Cr>Co>Se>Sb>Pb>As>Sn>Cd. Element mobility shows high immobility for Ti, an element known for its high resistance to both physical and chemical conditions. PCA involving both trace element and major ion data reveals three components representing (1) natural processes like rock weathering and cation exchange, (2) a combination of natural environmental conditions and human practices (3) anthropogenic activities.

Based on the HPI, $C_d$ and HEI, all water samples analyzed fall within the excellent range and below the HPI critical value of 100, hence classified as suitable for drinking. The non-carcinogenic health risks of heavy metals for both adults and children reveals low hazard quotients and hazard indices for adults, with relatively higher risks for children. The incremental lifetime carcinogenic risks of Cr, Pb, Ni and As are low for adults but slightly higher for children (Ni and Cr). Additionally, the As concentration in one sample (BOW 02 in Lable) is at the upper guideline limit ($4.5 \times 10^{-4}$), thus slight additions expose children to future arsenic carcinogenic risks.

Groundwater/surface water quality (WQI) shows an overall excellent water quality in Bafia, which degrades to unsuitable water quality from the NNW to the South eastern parts of Bafia,

depicting the reduction of water quality going from the recharge point to discharge point. All irrigational suitability parameters reveal excellent to good irrigation water in Bafia.

# CHAPTER V: RECHARGE SOURCES, MECHANISMS AND APPARENT GROUNDWATER AGE

## INTRODUCTION

Stable isotopes of oxygen and hydrogen are very useful in water resource studies. Unless in diluted or mixed waters, these isotopes often maintain and reflect the initial isotopic composition of recharging rainwater. This chapter presents and discusses the distribution of stable isotopes, groundwater origin and recharge mechanism. Additionally, isotopic tracers like tritium and dual nitrogen isotopes have been respectfully used to determine groundwater age and apportion nitrate contamination sources.

With rapid growth in population, urbanization, industrialization and competition for economic development, groundwater resource has become vulnerable to depletion and degradation. Thus ground water management on scientific lines is the key for sustainability of this vital resource. Groundwater resources management includes the planning, development, monitoring, protection and sustainable use of groundwater. Being the main drinking water resource in Bafia, it entails an equitable and sustainable use of groundwater, while preventing it from pollution, over-exploitation and degradation.

This chapter also discusses the recharge elevation and salinization by evaporation based on the relationship between $\delta^{18}O$ and Cl, TDS and $NO_3^-$. This chapter gives an overview of the groundwater age with their implications and the potential sources on nitrate in water in the Bafia area as well as the implications for water resources management.

## V.1. Stable isotopic composition of water

### V.1.1. Yaounde rainfall (2020) stable isotope content and groundwater recharge patterns

Given that precipitation is the main source of groundwater recharge in the area, it's important to evaluate its isotopic composition to see how it varies in time and space. In the absence of precipitation data in the Bafia area, we explored data from the nearest IAEA Global network of isotopes in precipitation (GNIP) station, which is in Yaoundé. The data show a complete absence of rains from January to March. However, between April and December, $\delta^{18}O$ values ranged from -6.8 to 0.8‰, with a mean of -3.3‰ and standard deviation of 2.3‰; δD varied between -

44.8 and 17.2‰, with a mean of -14.2‰ and standard deviation of 18.5 ‰; d-excess ranged from 6.9 to 16.4‰, with a mean of 12.1‰ and standard deviation of 2.6‰. The standard deviation of $\delta^{18}O$, $\delta D$ and d-excess present a relatively wide variation linked to different meteorological conditions at moisture source and along its path or during rainfall events (Dansgaard 1964).

The main factor controlling the distribution of the isotopic composition of precipitation in the tropics is the amount effect, which is described as the negative correlation between δ values and precipitation amount at monthly or longer time scales (Dansgaard 1964; Clark and Fritz 1997). As precipitation progresses during the year, the amount of oxygen and hydrogen gradually changes, usually depleting during heavier rains (April- June and September-October) and relatively enriched during lighter or no rains July-August and November-March) (Fig. V. 1).

Generally, the amount effect is more visible in small rains because during low rainfall, re-evaporation of rainwater leads to enrichment, which is absent during heavy rains (Kebede and Travi, 2012).

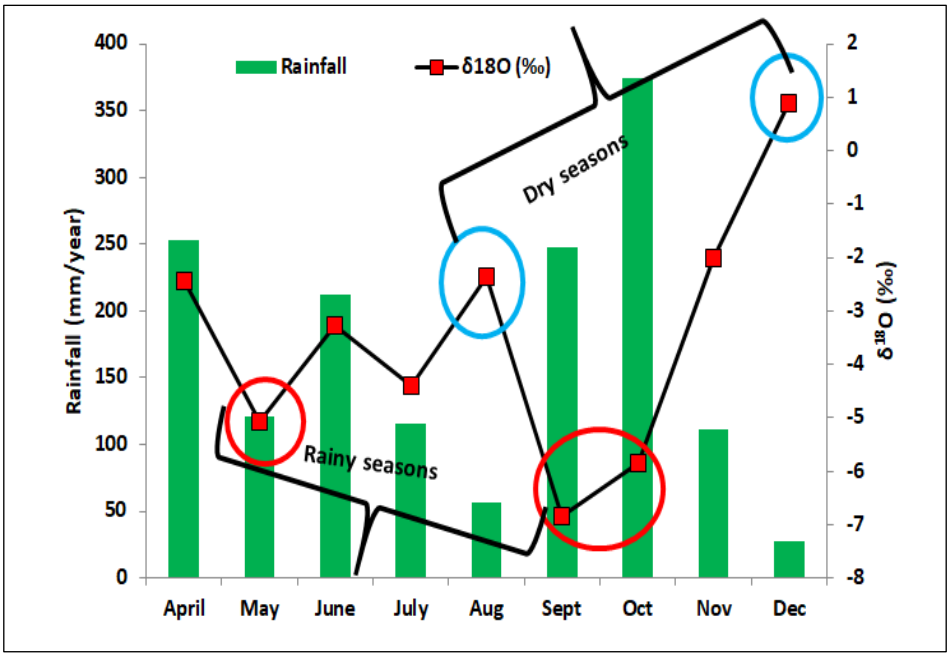


**Figure V.1: Rainfall amount versus $\delta^{18}O$ in Yaounde (2020 data) showing two wet and two dry seasons**

An additional consideration is that evaporation-induced enrichment in water stable isotopes is related to fractionation processes that are affected by altitude and seasonal temperature variations (Adomako et al. 2015; Wirmvem et al. 2015). Hence in Yaounde, isotopic enrichment and depletion are affected by rainfall amounts, moisture conditions, and altitude convective rainfall. This remark aligns with the amount effect in tropical low-latitude precipitations observed in Cameroon (Kamtchueng et al. 2022); West Africa (Akpataku et al. 2019) and East Africa (Kebede and Travi, 2012). Additionally, the four- season characteristic of the Yaoundé area is clearly highlighted by the amount effect, distinguishing two rainy and two dry seasons.

### V.1.2. Spatio-temporal variations in stable isotopes in Bafia

Appendix 4 (a and b) presents the stable isotope content of surface and groundwater in the Bafia area while Table 5.1 presents their statistical summary. On the one hand, groundwater stable isotopes ($\delta^{18}O$ and $\delta$ D) vary between -5.0‰ and -3.0‰, with an annual average of -3.9‰ for $\delta^{18}O$; between -27.0‰ to -9.0‰, with an annual average of -17.9‰ for deuterium ($\delta$ D) and the d-excess ranges from 10‰ to 15‰, with an annual average of 13.4‰. On the other hand, surface water stable isotopes vary from -5.2‰ to -1.0‰, with a mean of -3.5‰ for $\delta^{18}O$; between -28.0‰ and -6.1‰, with a mean of -17.1‰ for $\delta$D and the d-excess varies from 3‰ to 14‰, with a mean of 11.1‰. A plot of the $\delta^{18}O$ and $\delta$D values for surface and groundwater on the classical $\delta^{18}O$ - $\delta$D Craig diagram, together with the Yaounde rainfall data provides information on the origin and recharge processes of groundwater in the Bafia area. Figure V.2 shows that surface, ground and rainwater plot in a narrow range along the Yaounde Local Meteoric Water Line (YLMWL) and above the GMWL, indicating their meteoric origin and insinuating that modern rainfall predominantly influences the isotopic components.

***Table 5.1: Statistical summary of stable isotope data in the Bafia area***

| | Groundwater | | | | Surface water | | | |
|---|---|---|---|---|---|---|---|---|
| | Min | Max | Mean | Stdev | Min | Max | Mean | Stdev |
| $\delta^{18}O$ (‰) | -27.0 | -9.0 | -17.9 | 3.0 | -28.0 | -6.0 | -17.1 | 6.0 |
| $\delta^{18}O$ (‰) | -5.0 | -3.0 | -3.9 | 0.4 | -5.2 | -1.0 | -3.5 | 1.1 |
| d-excess (‰) | 10.0 | 15.0 | 13.4 | 0.9 | 3.0 | 14.0 | 11.1 | 3.4 |

The slope of the YLMWL (8.35) is very close to the slope of the GMWL (8), indicating a meteoric origin. This alignment also suggests that the process of rain formation in the tropical

rainforest region of Cameroon occurred under equilibrium conditions and that evaporation during the intense tropical rainfall is less critical (Gat, 2010). Considering the low mean groundwater temperatures (27°C), the $\delta^{18}O$ and $\delta D$ could be regarded as being conservative in reactions with aquifer materials. More so, the sandy-clay loam soils in the area, with about 71% sand, are porous enough to allow rapid flow with minimal changes.

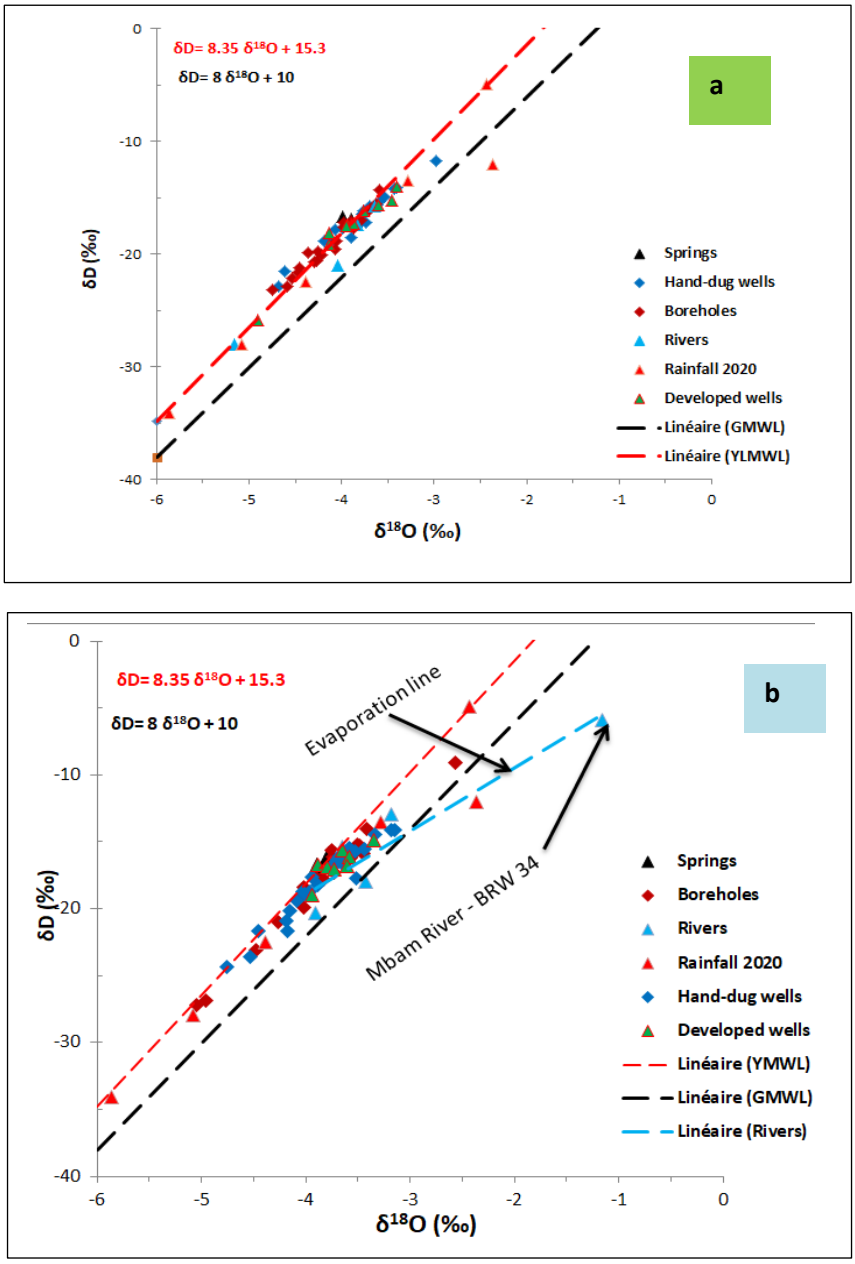


**Figure V.2: Plots of $\delta^{18}O$ versus $\delta D$ for water resources in the Bafia area for the (a) rainy and (b) dry season**

Hence the δ values are a replica of the original rainfall isotopic composition, rapidly infiltrated with minimal changes in isotopic content (Taylor and Howard, 1996; Gat, 2010; Wirmvem et al. 2017). A few rainwater samples (Yaounde samples) show relative enrichment than the groundwater and surface water samples possibly due to factors like (i) re-evaporation of rain droplets prior to infiltration, (ii) recharge of groundwater from higher elevation areas and (iii) the isotopic exchange between groundwater and the host rocks (Clark and Fritz, 1997).

Apart from surface water, most shallow hand dug wells and developed wells plot below the YLMWL, demonstrating relative enrichment over boreholes. This is attributed to their close proximity to surface atmospheric conditions and interfering anthropic activities, which change the isotopic composition slightly before or during infiltration (Fongoh et al. 2024).

However, in a general sense, groundwater isotopes vary insignificantly throughout the year. While some groundwater samples like BOW 01 (Fin goudrong Ndengue), BOW 05 (Nyamsong I), BOW 26 (Polyvalent) and BBH 38 (Lycée Muoko) became more depleted in the dry season, others like Bdow 17 (Lycée classique) BOW 02 (Lable), BOW 07 (Donenkeng hospital), Bdsp 08 (Donenkeng spring), BBH 44 (Rigama transformateur) and many others, showed slight enrichment from the rainy to the dry season. Conversely, all surface water samples show enrichment from the rainy to the dry season, with the Mbam River (BRW 34) being the most enriched sample. These slight changes are equally recognized in the d-excess values; higher d-excess values in the rainy season and lower values in the dry season, with the lowest dry season value (3.38‰) in the Mbam River (BRW 34). This shows that water mixing takes place in the aeration zone or in the aquifer (Clarks and Fritz, 1997) and that could attenuate the influence of the variations of the isotopic composition of the annual rainfall. There is almost no difference between both surface and groundwater δ values and, according to Ako et al. (2012) and Kamtchueng et al (2022), the overlaps and similarities between the δD, $\delta^{18}O$ and d-excess values of rivers and shallow groundwater suggest a good hydrological connection in the Bafia groundwater system. Parallel to Yaounde rainfall data, $\delta^{18}O$ values for surface and groundwater in Bafia are more depleted in the rainy season and slightly enriched in the dry season. Similar trends have been observed in Yaounde (Kuitcha et al. 2012; Wirmvem et al. 2016; Fongoh et al. 2024) and in the Lake Bosumtui area of Ghana (Akosua et al. 2022), which they all attributed it to an "amount effect" and the recharge of groundwater by re-evaporated rain drops.

### V.1.3. Deuterium-excess and moisture origin

In the GMWL, the d-excess has a value of 10‰, representing evaporation at 85% relative humidity. However, this value can be higher if the evaporation at the source takes place at lower RH or lower, if evaporation at source takes place at higher relative humidity (Isao et al. 2022). The annual mean d-excess of water resources in Bafia (13.1‰) is lower than that of Yaounde (14.3‰) but similar to that of Douala (13.2‰) (Wirmvem et al. 2016). These trends could be related to the fact that Bafia is relatively closer to the coast of Douala (≈187km straight line distance) than Yaounde is to Douala (≈202km), and that Bafia is located at a lower altitude than Yaounde. Furthermore, there is a similarity between the mean RH of Bafia (80.2% from 1990 to 2021) and that of Douala (80% between 2013 and 2014), suggesting an influence of moisture from the coast of Douala. These values are lower than that of Yaounde (68% between 2013 and 2014), hence the low d-excess in Bafia. Additionally, the moisture recycled by evapotranspiration contributes vapor into the atmosphere in Bafia, which is almost identical to rainfall vapor and heavier than the residual vapor, thus it is slightly enriched (Gonfiantini et al. 2001). These imply that besides continental and altitudinal effects, atmospheric relative humidity and evaporation play significant roles in modifying the isotopic signature in Yaounde than Bafia.

The d-excess values are close to those observed from air masses originating from the Atlantic Ocean (+10‰) (Craig, 1961), thus confirming that the Gulf of Guinea is the primary moisture source, with little input from continental moisture (Wirmvem et al. 2016). Hence, just like in Douala (Kamtchueng et al. 2022) and the Banana Plain, both groundwater and surface water in the Bafia area is recharged under insignificant evaporation conditions during rapid infiltration. The highest d-excess values were recorded in the rainy season (up to 15.4‰) and according Bony et al. (2008), the monsoon reaches its peak in this period, accompanied with increased convective activities and increased kinetic effects during oceanic evaporation. These convective activities are often associated with less re-evaporation of rain droplets, hence higher d-excess. During the dry season, lower d-excess is caused by lower RH over continents that facilitate sub-cloud raindrop re-evaporation.

### V.1.4. $\delta^{18}O$, chloride and TDS -based salinization

A plot of $\delta^{18}O$ versus $Cl^-$/TDS has been used to evaluate the role of evaporation in the isotopic content of water (Clark and Fritz, 1997; Ako et al. 2012). Usually, the increase in chloride and TDS is a function of the recharge dynamics and the evolution of groundwater from upstream (recharge) to downstream (discharge) (Adomako et al. 2011; Takounjou et al. 2020). However, in this study, chloride values are distributed along the $\delta^{18}O$ axis as $\delta^{18}O$ slightly increases while TDS shifts slightly the right (Fig. V.3). This suggests that changes in $\delta^{18}O$ do not necessarily affect the chloride concentration and salinity levels. It could be assumed that the observed deviation from the YLMWL is a result of enrichments of the stable isotope contents on the surface before groundwater recharge. Thus, groundwater salinization (especially shallow hand-dug wells) in the Bafia area is slightly influenced surface evaporation before recharge.

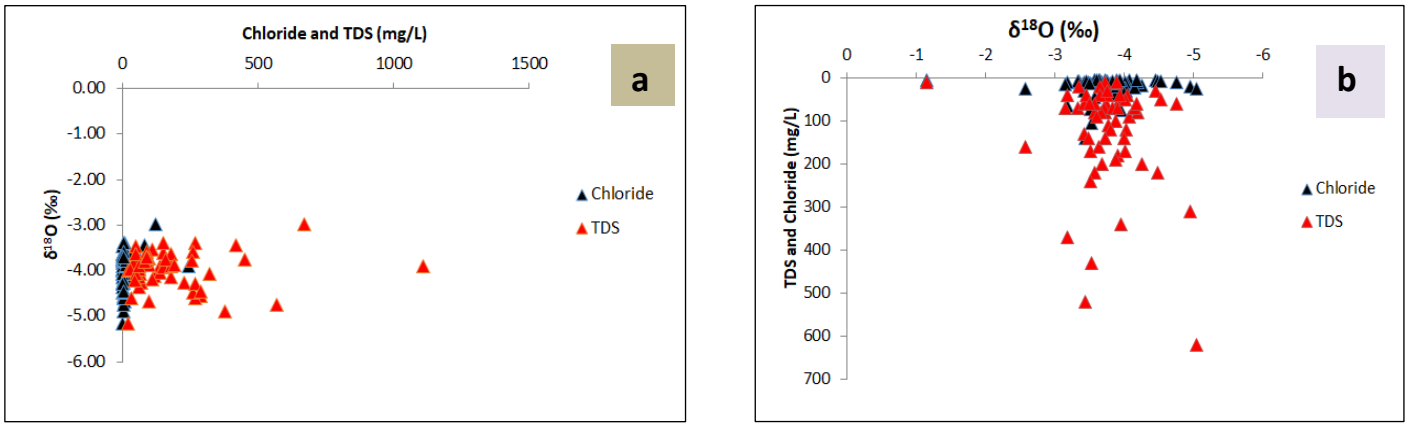


**Figure V.3: Plot of chloride and TDS versus $\delta^{18}O$ for water samples in the (a) rainy and (b) dry season**

### V.1.5. Groundwater recharge elevation and possible recharge areas in the Bafia area

Generally, rain becomes depleted in the heavier isotopes with increasing altitude due to decreasing temperature and rainout of the air mass (Dansgaard, 1964; Clark and Fritz, 1997; Gat, 2010), thus there might exist negative correlations between two regions depending on the altitude difference. Dansgaard (1961) observed that due to altitude effect, $\delta^{18}O$ value of precipitation in temperate regions portrays about 0.2‰ decrease for every 100m increase in elevation and this reflects the temperature dependence of isotopic fractionation during condensation. However, this phenomenon can be hindered or deviated by several aspects, including air humidity, moisture

source, evapotranspiration, rainfall amount, irrigation and surface runoff (Dansgaard, 1964; Gat, 2010). Cloud water interception by vegetation also contributes to groundwater recharge, as the accumulated water droplets later coalesce into heavier rain drops which hit the ground (Scholl et al. 2002).

The Bafia area is mostly made up of lowlands and gentle slopes; hence the altitudinal variations are not so obvious. Groundwater recharge elevation was estimated by plotting $\delta^{18}O$ against elevation (Fig. V.4). The altitudinal gradient of 0.2‰ per 100m (rainy season) and -0.15‰ per 100m (dry season) for $\delta^{18}O$ was established for boreholes; -0.09‰ per 100 m and -0.11‰ per 100m was established for springs in the Bafia area. Group I samples (93% samples) plot at lower altitudes (between 457 m and 510 m a.s.l.), while Group II samples (7% samples) plot at higher elevation. However, the most isotopically depleted samples (<-4‰), especially the boreholes, are found in Group I. The relative penury in $\delta^{18}O$ and $\delta D$ contents for these borehole samples signifies that they were either recharged during much humid climates (more rainfall or low temperatures) or they were recharged at higher altitudes (Gat 2010; Ako et al. 2012). Additionally, some of these boreholes (e.g BBH 04, BBH 20, BBH 44, BBH 50 and BBH 55) also record the lowest tritium activity (< 1 TU) as shown in the next section. This suggests the presence of older groundwater, which most often, is more depleted due to paleoclimatic events and low in tritium.

In like manner, the samples found in group II which plotted at higher elevation (between 570 m to 606 m a.s.l.), have $\delta$ values similar to the shallow hand-dug wells in group I, suggesting that although sampled at higher altitude, they might have been influenced by evaporation prior to recharge or cloud water events which slightly enriched their isotopic contents (Scholl et al. 2002).

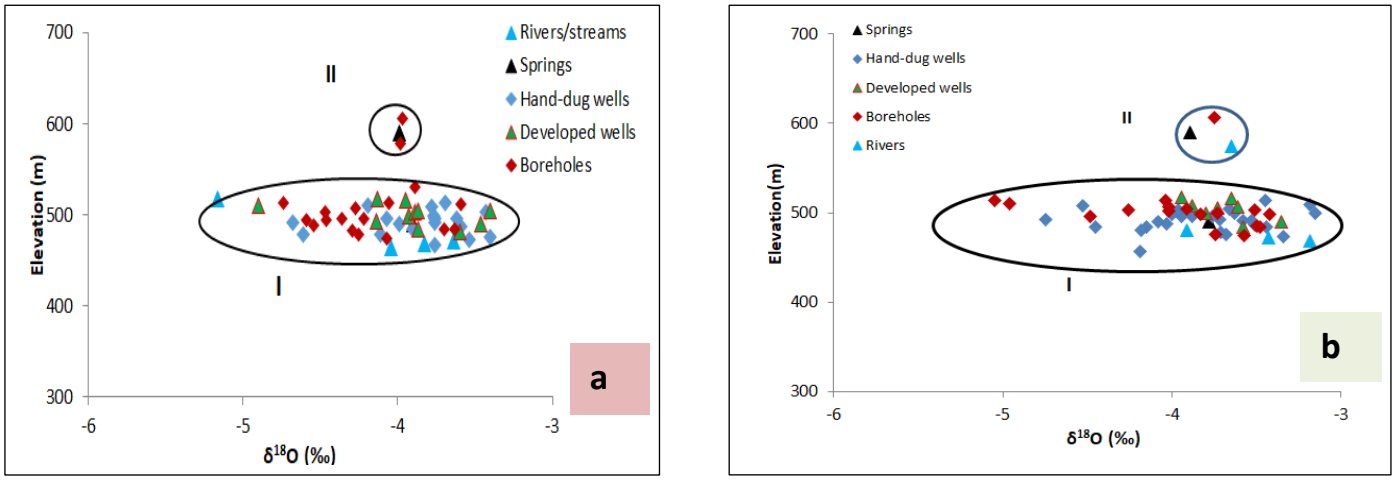


**Figure V.4: Relationship between elevation and oxygen-18 showing a mixture of higher altitude and lower altitude water**

These scenarios also assume the possibility of mixing between groundwater from higher elevation and some pre-existing water which have been enriched by evaporation or longer residence times. According to their δ values, about 79% of open hand-dug wells and boreholes were recharged from local precipitations occurring at lower elevations (457-510 m) within Bafia and immediate surroundings. Conversely, 21% of the samples were recharged by rainfall from higher elevations-notably the Bapé area in the NNW of Bafia. The irregular pattern observed in the $\delta^{18}O$ spatial distribution map for Bafia (Fig. V. 5) confirms a mixture in the hydrological system as earlier mentioned.

## V.2. Tritium content in water

### VI.2.1. Apparent age of groundwater and implications for nitrate contamination

In groundwater studies, tritium data provide information on the approximate time of groundwater recharge within an aquifer. Groundwater with tritium values less than the detection limit of 0.3 TU is considered to be recharged before 1952 (Izbicki, 1996). Additionally, Lindsey et al. (2019), observed that tritium in recent groundwater usually range from about 2–3 nowadays, thus even less in 2023 (the sampling time). This implies that groundwater with tritium contents >1 TU represents young recharge. Dating groundwater with all accuracy is often challenging because groundwater has the tendency to mix along its flow paths (Dafny et al. 2006).

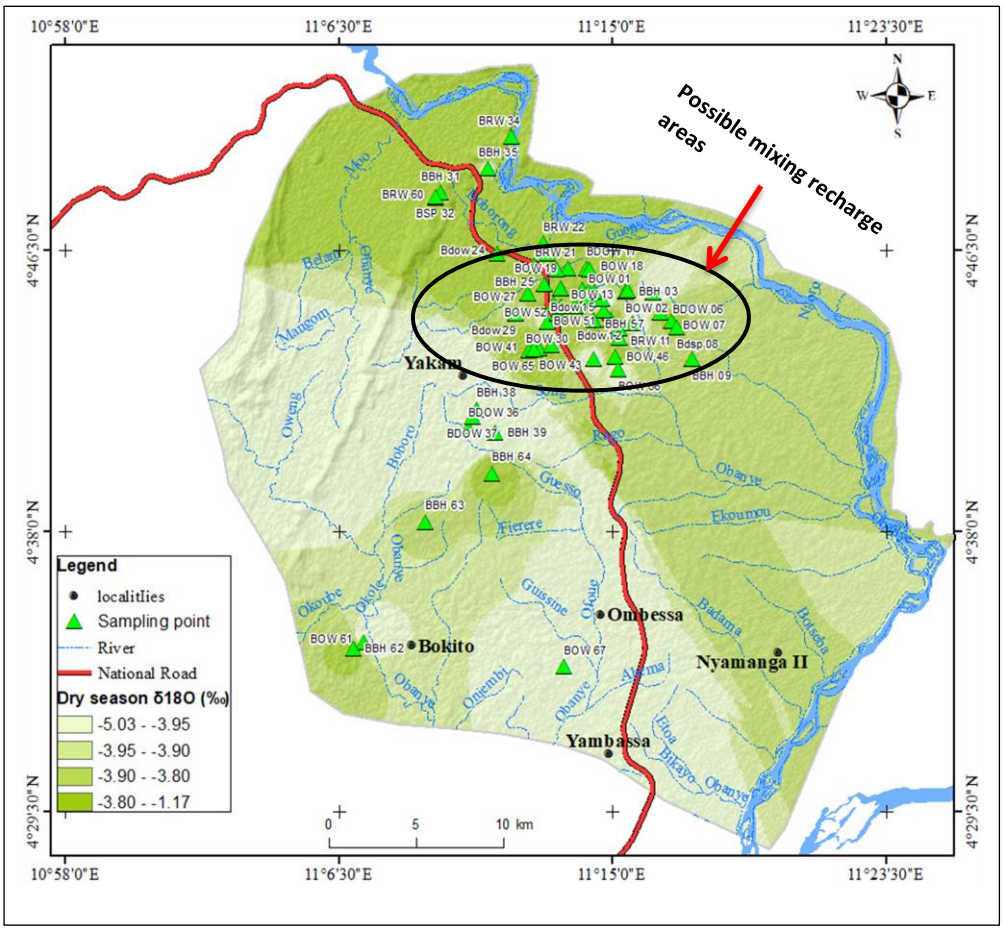


**Figure V.5: Spatial distribution of $\delta^{18}O$ showing possible recharge areas in the Bafia area**

Nonetheless, assuming groundwater flows through an isolated path (piston flow) where there is little or no mixing (Clark and Fritz, 1997), two end-members with different tritium concentrations have proven helpful: (1) one end-member with very low tritium (almost zero content) representing pre-modern recharge with tritium decay enhanced by longer residence and possible isolation from modern recharge and (2) another end-member with higher tritium content very similar to recent rainwater content, corresponding to modern-day recharge (Dafny et al. 2006).

Given that rainfall tritium data is non-existent in Bafia, this study explored tritium data from different IAEA GNIP monitoring stations and other research works closest to the study area. For example, in 1979 Loehnert, 1988 observed tritium levels of 12.3 TU in Southeast Nigeria; in 2004, the tritium concentration was 2.5 TU in Douala (Ketchemen-Tandia et al. 2007); values between 1.2 and 5.1 TU (mean of 3.0 TU) were found in Ghana (Adomako et al. 2011); between

2009/2010, Ako et al. (2012) observed a mean of 0.9 TU in the Banana Plain of Cameroon; a mean of 1.4 TU was obtained between 2014 and 2016 in Douala (Emvoutou et al. 2023); the Douala IAEA GNIP station recorded a mean of 0.13 TU from 2016 to 2019 (IAEA/VMO 2024) and, 1.5 TU at the Libreville (Gabon) GNIP station from 2015 to 2019 (Emvoutou et al. 2023). These low $^{3}H$ values align with the depleted atmospheric concentrations in the northern hemisphere at low latitudes close to the equator (IAEA 2006). For this study, the mean rainwater tritium content from 2016 to 2019 (0.1 TU) of the Douala GNIP station was used as a reference value for Bafia. Besides their proximity to the equator, Bafia is 187 km away from Douala, hence equally influenced by the dilution effect of the Atlantic Ocean vapor.

Table 5.2 shows the tritium content of analyzed boreholes. Groundwater tritium contents in this study vary respectively from 0.01 to 2.94 TU and 0.34 to 2.98 in the rainy and dry seasons, with an annual mean of 1.36 TU, at a detection limit of 0.2 TU. The mean value (1.36 TU) in Bafia is close to the mean rainfall tritium value in Libreville, Gabon (1.5 TU) and lower that that in the Ndop plain of the Northwest Region of Cameroon (2.4 to 3.2 TU) as observed by Wirmvem et al. (2017). However, it is higher than those obtained in Douala GNIP station (mean = 0.13 TU). Given that there is a difference between the tritium contents in continental and coastal regions, Clark and Fritz (1997) established that for continental regions like Bafia, groundwater with tritium levels <0.8 TU is considered sub-modern (recharged before 1952); levels between 0.8 and 4 TU are considered a mixture between sub-modern and recent; a range from 5 to 15 TU is modern (< 5 to 10 years); 15 to 30 TU infers the presence of bomb tritium; > 30 TU implies recharge from 1960 or 1970 while > 50 TU was dominantly recharged in 1960.

*Table 5.2: Borehole tritium content for the rainy and dry seasons in Bafia*

| Wet Season | TU | Dry season | TU |
|---|---|---|---|
| BBH03 | 1.8 | BBH06 | 2.3 |
| BBH04 | 0.3 | BBH12 | 0.3 |
| BBH09 | 1.3 | BBH18 | 2.1 |
| BBH20 | 0.7 | BBH20 | 0.7 |
| BBH25 | 1.1 | BBH22 | 1.4 |
| BSP 32 | 1.4 | BBH24 | 1.2 |
| BBH39 | 1.8 | BBH25 | 1.2 |
| BBH44 | 0.6 | BBH29 | 1.3 |
| BBH46 | 2.9 | BBH35 | 2.6 |
| BBH50 | 0.5 | BBH39 | 1.4 |
| BBH54 | 1.7 | BBH43 | 3.0 |
| BBH55 | 0.0 | | |
| BBH57 | 1.1 | | |

A plot of tritium data obtained from the Douala GNIP station (rainwater) and Bafia (groundwater) is shown in (Fig. VI.6). Based on the above classification, all the samples from Douala, located at the coast and at lower altitude (5m a.s.l) and 29% of the groundwater samples from Bafia are either of the sub-modern (before 1952) recharge age or have undergone decay over time. The majority (71%) of the samples from Bafia show a mixture of sub-modern and recent recharge (possibly the last 30-40 years). Additionally, samples with the lowest tritium content (< 1 TU) have nitrate levels below detection limits (BDL) and vice versa, with few exceptions. Nonetheless, the presence of high nitrate in some shallow well indicates recent contamination from recently recharged water (Castaldo et al. 2021). Also, the dominance of the CaMg-$HCO_3$ water type (that represents water recently recharged water which is at its early stage of evolution), the under-saturation of carbonate, sulfate and halite minerals and the low mean TDS (159mg/L) confirms young groundwater in Bafia.

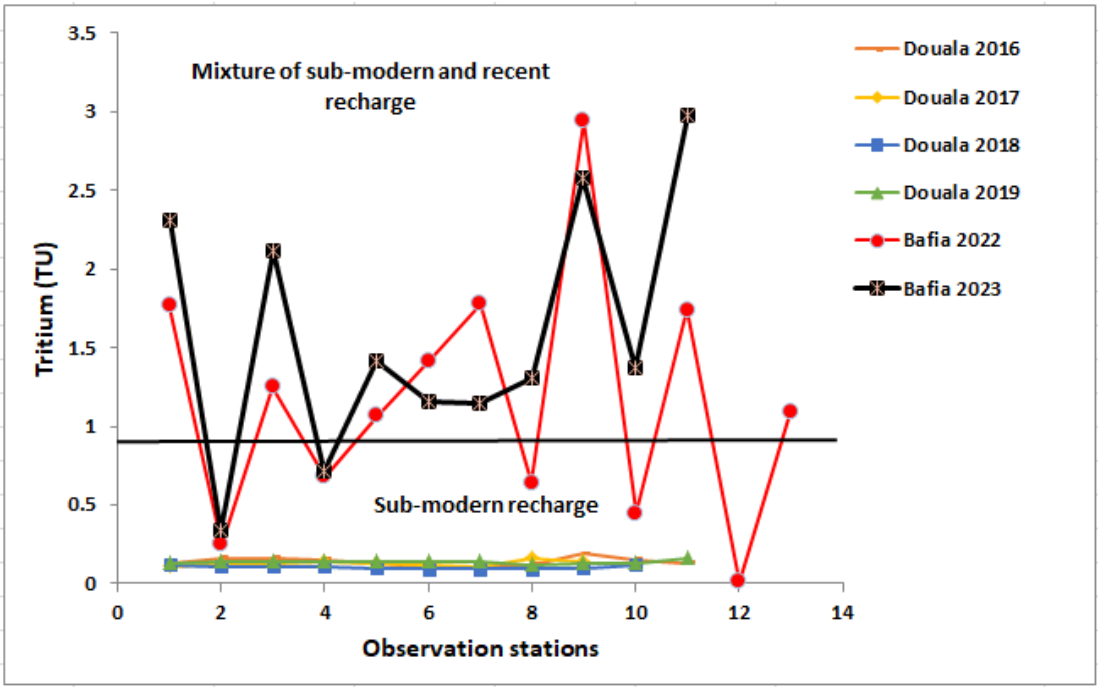


**Figure V.6: Tritium variations over the years in Douala GNIP monitoring station (2016 to 2019) and in Bafia (2022 to 2023)**

### V.2.2. Aquifer vertical structure and groundwater mixing

Stratifying the aquifer into two parts; namely the shallow (< 20 m) and the deep (> 20 m) and comparing the chemical and isotopic signatures provides insight on the vertical structure and homogeneity and/or heterogeneity of the aquifer. As groundwater is being recharged, the younger water in the unsaturated zone pushes the old water in a vertical downward manner, which finally gets to a portion of the aquifer where it becomes isolated from fresh recharge (Clark and Fritz, 1997; Emvoutou et al. 2023). At this point, the tritium levels start decreasing by decay processes, thus referred to as old water.

In the absence of borehole information in most of the studied wells, interpreting this phenomenon is challenging. Usually, tritium levels are lower in deeper wells which have older water. However, a plot of tritium content versus well depths (Fig. V.7) shows an overlap in both seasons.

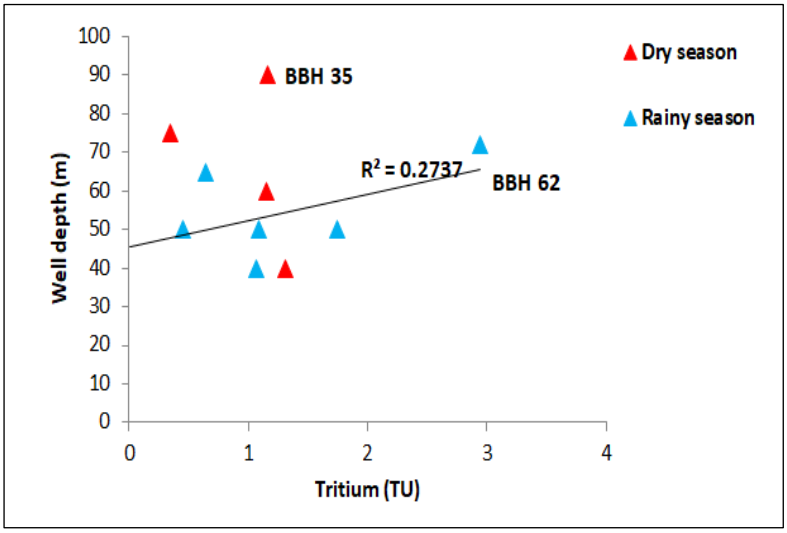


**Figure V.7: Relationship between well depth and tritium content demonstrating possible groundwater mixing**

Some deeper wells like BBH 35 (Carreffour Claude) had noticeable tritium levels at greater depths (90m) in the dry season, indicating the possibility of mixing of older and younger water. The weak correlation suggests that several factors are involved, including vertical aquifer mixing through fractures, which serve as quick conduits for recharge from shallower, younger wells.

The aquifer vulnerability/protection zone maps (Fig. V.8 a, b) for the rainy and dry seasons based on the tritium data distinguishes zones with less vulnerable aquifer areas like in Rigama Transformateur (BBH 44), Rimis (BBH 50), the Catholic Diocese area (BBH 20), Nyamsong I (BBH 04) and parts of Bigna (BBH 55). However, given the localized high nitrate and low TDS, further studies (e.g $^{14}C$ dating and bacteriological analyses) should be carried out in these areas for better conclusions.

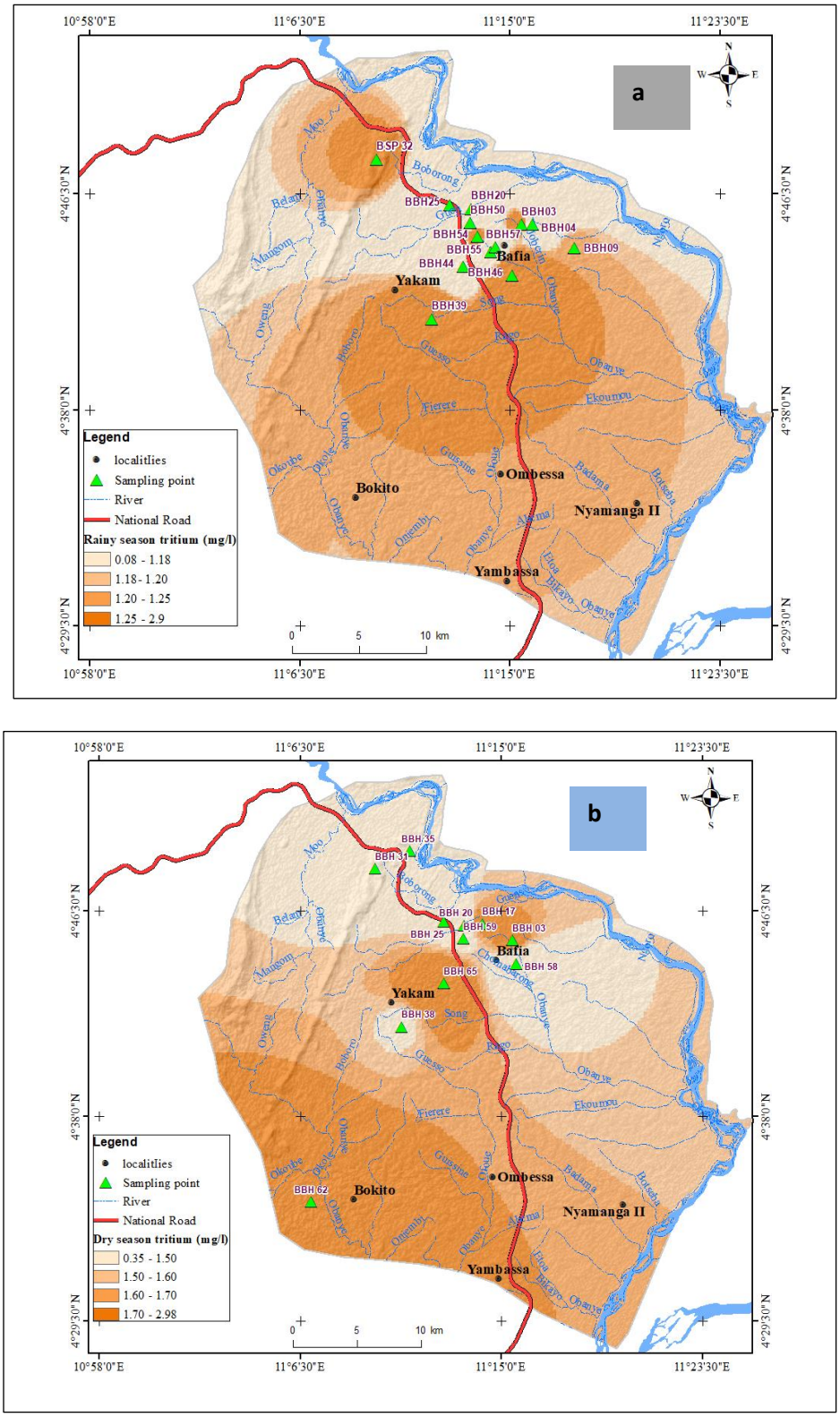


**Figure V.8: Vulnerability/Protection zone map for the (a) rainy and (b) dry seasons based on tritium levels**

## CONCLUSION

This research illustrates faint variability of isotopic composition between Bafia groundwater and surface water, with no clear distinction between both resources. The rainy season samples are relatively more depleted than the dry season samples, with an evaporation trend displayed by the rivers and some shallow hand-dug wells. Majority of the water samples plot close to and below the YLMWL, and above the GMWL, confirming their meteoric origin. The d-excess exemplifies recharge at lower elevations with less significant evaporation effects on the rapidly infiltrated water. $\delta^{18}O$ displays weak positive correlations with Chloride and TDS, reflecting minimal effects of evaporation on groundwater salinization.

Tritium shows slight seasonal variations, with relatively higher values in the dry season. More than 70% samples demonstrate a mixture of sub-modern and recently recharged contaminated water, showcased by the high nitrate in some cases. High tritium encountered in some deeper wells confirms the vertical mixing within the aquifer.

# CHAPTER VI: NITRATE CONTAMINATION, SOURCE IDENTIFICATION AND OVERALL IMPLICATIONS FOR WATER MANAGEMENT

## INTRODUCTION

Nitrate ($NO_3^-$) contamination is one of the rapidly spreading groundwater quality problems recently, often associated to agricultural activities, wastewater infiltration, and natural soil nitrogen. Nitrate is one of the reactive forms of molecular nitrogen ($N_2$), which has both natural and anthropogenic sources. The natural sources of nitrogen in soils and groundwater include weathering, atmospheric deposition, microbial transformation of ammonia in soil and cyanobacteria-plant symbioses. The anthropogenic sources include leaching from inorganic fertilizers, untreated wastewater effluents, leachate from landfills and livestock manure (Pare and Bonzi-Coulibaly, 2013; Ako et al. 2014). Understanding not only the concentrations but also the origins and transformation processes of nitrate is important to effectively manage water resources, proposing suitable groundwater protection and management strategies.

This chapter evaluates the spatial distribution, temporal variation, and isotopic fingerprints of nitrate in the Bafia area, with the goal of identifying the relative contributions of natural and anthropogenic sources. Both chemical indicators ($NO_3^-$ and DO) and isotopic tracers ($\delta^{15}N–NO_3^-$ and $\delta^{18}O–NO_3^-$) are used to identify the dominant nitrate sources and the biogeochemical processes affecting nitrate in groundwater.

### VI.1.1. Spatio-temporal concentrations of nitrate

As mentioned in section IV.1.2.2 above, nitrate, concentrations are higher in the dry season due to limited dilution effects. It has an annual variation from below quantification limit (BQL) to 229 mg/L, for which 7% and 12% groundwater samples exceed the WHO (2022) nitrogen maximum contaminant level (10 mg/L) corresponding to 50 mg/L nitrate. High nitrate levels are associated to most shallow wells around low topography densely populated areas, around market places and a few points around farmlands. However, deeper wells and some shallow wells located in relatively elevated areas record very little nitrate concentrations (< 10mg/l) in both seasons.

### VI.1.2. Biogeochemical processes affecting nitrate

#### VI.1.2.1. Nitrification

The results of the dual nitrogen isotope (Table 6.1) show a variation in $\delta^{15}$N-$NO_3$ from below detection limit to 27.51‰, with a mean of 14.3‰ while $\delta^{18}$O-$NO_3$ varies between below detection limit and 14.65‰, with a mean of 9.48‰.

***Table 6.1: Dual nitrogen isotope and theoretical microbial nitrification in water***

| Sample ID | $\delta^{15}$N $NO_3$ ‰ | $\delta^{18}$O $NO_3$ ‰ | Microbial nitrification $\delta^{18}O_{NO3}$ |
|---|---|---|---|
| Bdow 01 | 12.00 | 8.00 | 5.38 |
| Bdsp 02 | 14.70 | 6.44 | 5.45 |
| BOW 03 | 11.32 | 6.95 | 5.49 |
| BBH 06 | 12.39 | 7.13 | 5.47 |
| BOW 08 | 12.96 | 9.73 | 5.25 |
| BOW 14 | 3.74 | 8.62 | 4.80 |
| Bdow 15 | 19.25 | 9.12 | 5.43 |
| BOW 16 | 10.38 | 11.28 | 5.53 |
| BBH 18 | 10.28 | 10.26 | 6.25 |
| Bdow 28 | 11.05 | 7.16 | 5.53 |
| BRW 30 | BDL | BDL | 5.85 |
| BOW 32 | 17.88 | 10.20 | 5.28 |
| BBH 39 | BDL | BDL | |
| BOW 44 | 13.94 | 11.68 | 5.87 |
| BOW 46 | 23.92 | 14.65 | 5.63 |
| BOW 48 | BDL | BDL | |
| BOW 52 | 27.51 | 12.40 | 5.54 |
| Bdow 59 | 13.24 | 8.54 | 5.48 |

Studies investigating the behavior of $NO_3$-isotope compositions in groundwater, with decreasing $NO_3$ concentrations due to reduction from denitrification, have observed a progressive increase of $\delta^{18}$O-$NO_3$ and $\delta^{15}$N-$NO_3$ values in the remaining $NO_3$ pool. However, this change of $NO_3$-isotope composition may not always be an indication of denitrification because $NO_3$ in the pool can be simultaneously supplied by other $NO_3$ sources as some $NO_3$ is removed via denitrification. Hence, it is important to know the initial $\delta^{18}$O-$NO_3$ and $\delta^{15}$N-$NO_3$ to accurately track the initial nitrate sources. Several approaches have been used to reconstruct the initial $NO_3$-isotope composition, namely: Heaton et al. (1983) model; Böhlke et al. (2002) Model; Theoretical ($\delta^{18}$O-$NO_3$) Model; Bourke et al. (2019) Model and the Rayleigh Model-Based Approach. Amongst all, the Heaton et al. (1983) and Böhlke et al. (2002) models are very limited

since these models reconstruct just the $\delta^{15}N\text{-}NO_3$ without the $\delta^{15}N\text{-}NO_3$. In this study, the Theoretical ($\boldsymbol{\delta^{18}}O\text{-}NO_3$) Model was used, with the Mayer equation (Mayer et al. 2001) as shown below.

During nitrification processes, the nitrifying bacteria in the soil converts $N_2$ to $NO_3$ by using two oxygen atoms from water and one from the atmosphere. Based on the atmospheric oxygen isotope value (23.5‰) and the measured $\delta^{18}O_{NO3}$ values of this study, the bacteria nitrification was calculated using the following equation by Mayer et al. (2001):

$$\delta^{18}O_{NO3} = 2/3\ \delta^{18}O_{H2O} + 1/3\ \delta^{18}O_{O2} \quad (36)$$

The theoretical bacteria nitrification values obtained range from 4.8to 6.3‰, with a mean of 5.3‰, consistent with $NO_3$ derived from leaching of $NO_3$ formed by ammonification and organic decomposition processes in the soil of the recharge area (<10 ‰). The measured $\delta^{18}O_{NO3}$ values (which range from 6.4 to 14.7‰, with a mean of 9.5‰) are higher than the theoretical $\delta^{18}O_{NO3}$ values, representing enrichment in $\delta^{18}O_{NO3}$, possibly due to denitrification occurring in the studied groundwater system (Boumaiza, et al. 2023). However, other case studies where $\delta^{18}O_{NO3}$ (theoretical) values are lower than the measured values have been attributed the decrease to other mechanisms such as evaporation, respiration, and increased precipitation (Mayer et al. 2001). Considering the range of $\delta^{18}O_{NO3}$ values measured in this study, more than 60% of the samples have $\delta^{18}O_{NO3}$ values <10 ‰, and they fall in the range of $\delta^{18}O_{NO3}$ derived from nitrification of ammonium fertilizers and soil N. Hence, most of the nitrate is primarily generated by nitrification (e.g $NH_4^+$ in fertilizers). Given that nitrification occurs almost immediately, the concentration of $NH_4^+$ in all water samples was generally low, ranging from BDL (91% samples) to 4.9mg/L. These low ammonium concentrations are evidences of continuous nitrification taking place in groundwater and surface water resources in Bafia (Fei et al. 2020).

### VI.1.2.2. Denitrification

Conversely, denitrification processes occur when phytoplankton and microbes consume lighter isotopes ($^{14}N$ and $^{16}O$), thus enriching the residual water with $^{15}N$ and $^{18}O$. Hence, there is a linear increase in $\delta^{15}N\text{-}NO_3$ and $\delta^{18}O\text{-}NO_3$ as the nitrate concentration decreases (McCallum et al. 2008; Anormu et al. 2017). The plot showing the relationship between $\delta^{15}N\text{-}NO_3$ and $\delta^{18}O$-

$NO_3$ (Fig VI.1a) shows a moderate positive relationship ($R^2$ = 0.335), suggesting that each sampling site has specific denitrification conditions, depending on local hydrogeochemical conditions and mixing processes (McCallum et al., 2008; Boumaiza et al. 2024). Usually, denitrification processes are favored by anaerobic conditions, which often occur at greater well depths, where DO concentration is limited to < 2mg/L (Kendall, 1998). However, the DO concentrations in this study are not too high, ranging between 1.3 and 3.4mg/L, with a mean of 2.4mg/L in the dry season. Additionally, as observed in figure IV.9c above, shallow wells (< 50m) have higher nitrate concentrations than the deeper wells, confirming denitrification at greater depths.

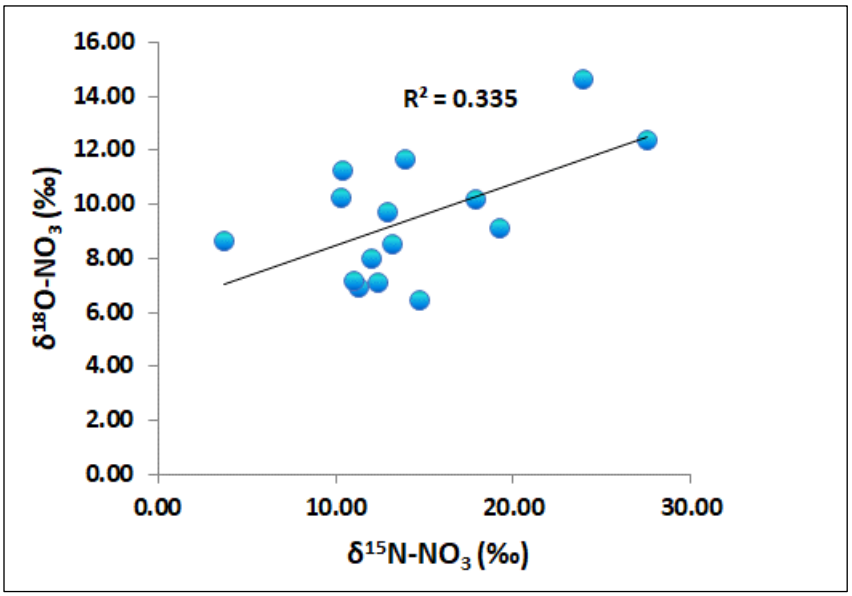


**Figure VI.1a: Relationship between $\delta^{15}$N-$NO_3$ and $\delta^{18}$O-$NO_3$ showing less denitrification processes**

According to Mariotti et al. (1988), a linear relationship between $^{15}N$ and $^{18}O$ of $NO_3^-$ is consistent with groundwater denitrification, which is not exactly the case in this study. Furthermore, there is a moderate positive correlation ($R^2$ = 0.51) between $NO_3^-$ concentration and $\delta^{15}$N-$NO_3$ (Fig. VI.1b). This implies that several factors operate within the groundwater system, including denitrification and mixing from multiple sources (fertilizers, manure, septic systems, or natural soil nitrogen) (McCallum et al. 2008). More than 88% samples have high $\delta^{15}$N-$NO_3$ values (> 10‰), revealing nitrate contributions from human and animal. 17% samples have $\delta^{15}$N values below detection limit and these have low nitrate concentrations (BRW 34, $NO_3$=0.2mg/l; BBH 38, $NO_3$=0.4mg/l and BOW 47, $NO_3$=04.7mg/l). Additionally, the plot of

$\delta^{15}N$ versus the inverse of $NO_3$ ($1/NO_3$) shows no significant relation between the two ($R^2$ = 0.0169,) suggesting that denitrification occurs weakly within the water sources, except in deeper wells (Fig. VI.1c).

It is worth noting that 4 out of 5 surface waters sampled for this work have the lowest (<2mg/L) nitrate content. This observation in this Semi-Urban area is different from that of the more urbanized cities in Cameroon like Yaounde (Takounjou et al. 2013; Fongoh et al. 2023) and Douala (Wirmverm et al. 2017), where higher nitrate in surface water has been attributed to increased urbanization activities.

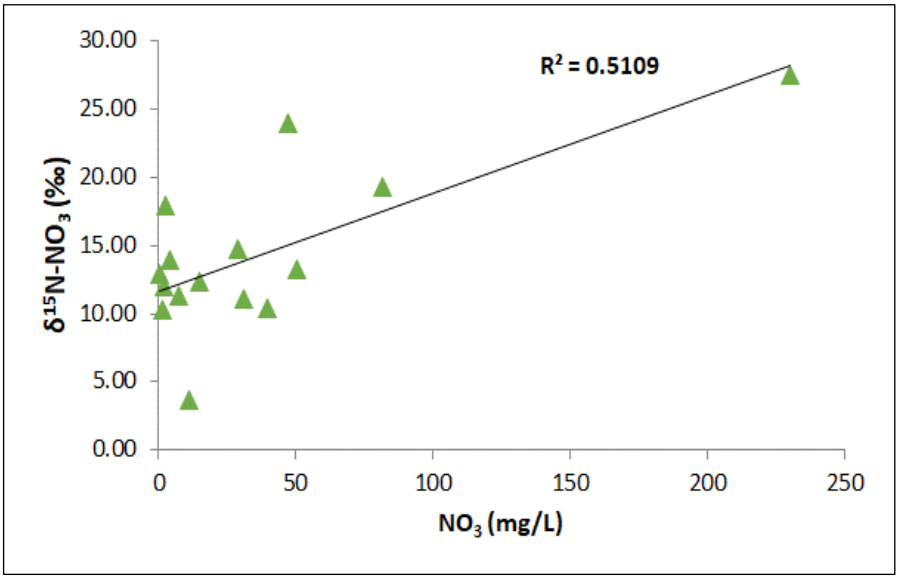


**Figure VI.1b: Correlation between $\delta^{15}N$ and groundwater nitrate concentrations. Trend line is consistent with an overall increase of nitrogen-15 isotope composition**

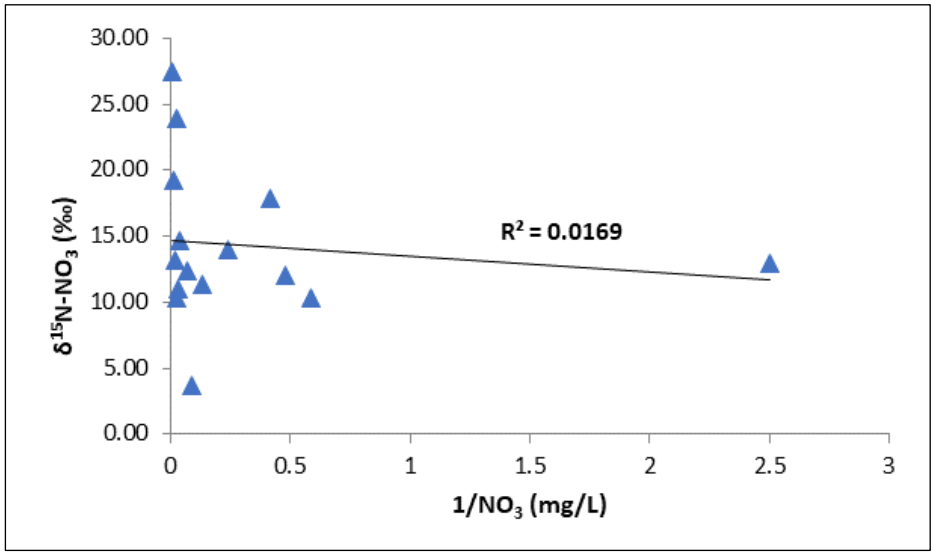


**Figure VI.1c: Trend of inverse nitrate concentration ($1/NO_3$) versus $\delta^{15}N$ of nitrate. Simple mixing or dilution of a single source would be indicated by a linear correlation.**

## VI.2. Nitrate source identification and mixing processes

### VI.2.1. Nitrate source identification using hydrochemistry

The conservative nature of chloride ($Cl^-$) in natural waters can be exploited to provide useful information for tracking groundwater contamination sources (Yue et al., 2013). Generally, $Cl^-$ and $Na^+$ in groundwater systems originate from mineral dissolution (from geology), road salt, household, and industrial effluents. The chloride value in BOW 53 (rainy season) showed a relatively higher concentration compared to other samples. Furthermore, a positive correlation with $p < 0.01$ was observed in Table 4.2a above between chloride and nitrate. The study area, located far away from the coast, is underlain by crystalline rocks with no halite deposits and no leaching road salts.

Generally, $NO_3^-$ emanating from different sources has been shown to have different $NO_3^-/Cl^-$ ratios. For example, chemical fertilizers have high $NO_3^-/Cl^-$ ratios with small $Cl^-$ concentrations while untreated effluent from manure/sewage is characterized by low $NO_3^-/Cl^-$ ratios and high Cl- values (Fig. VI.2a) (Xia et al., 2017). Hence, $NO_3^-/Cl^-$ ratios in meq/L have been used as a pointer for nitrate sources, assuming the absence of halite deposits (McCallum et al. 2008). In this study, the ratios vary widely in all water types: In open wells, ratios vary between 0 and 3.1,

with a mean of 0.8; borehole ratios vary between 0 and 2.6, with a mean of 0.7; developed well ratios vary between 0 and 2.7, with a mean of 0.8; river ratios range between 0.03 and 0.4, with a mean of 0.2 while springs have ratios between 0.3 and 0.7, with a mean of 0.5. The wide variation of $NO_3^-/Cl^-$ ratios also signifies a mixture of multiple sources. The possible sources of the observed chloride in the groundwater could be due to anthropogenic sources, notably sewage/manure, industrial/ domestic waste.

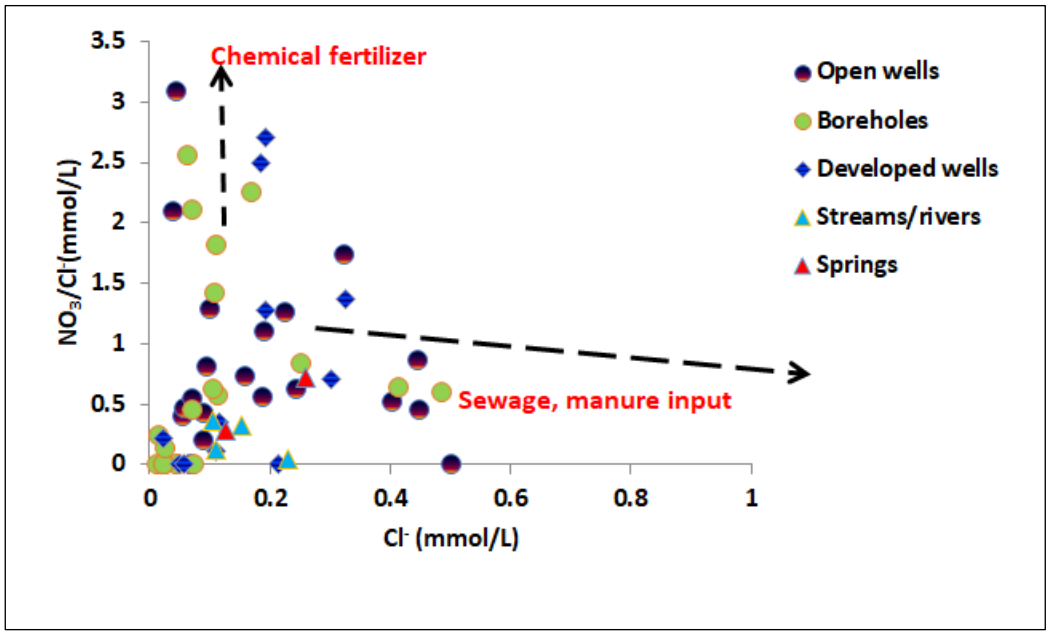


**Figure VI.2a $NO_3^-/Cl^-$ versus $Cl^-$ variation showing mixing, with higher $NO_3^-$ input from sewage/manure sources**

### VI.2.2. Nitrate source identification using $^{15}N\text{-}NO_3$ and $^{18}O\text{-}NO_3$

In addition to hydrochemistry, stable isotopes, tritium and dual nitrogen isotopes were also used to identify the main nitrate sources. The irregular pattern and overlapping $\delta^{18}O$ values observed in the spatial distribution map (Fig. V. 5 above) confirms a mixture in the Bafia hydrological system. Additionally, the low tritium levels encountered in some deeper wells indicate that deeper water entered the groundwater prior to atomic testing. However, a plot of tritium versus well depths shows an overlap in both seasons, confirming mixing possibilities (Fig. V.7 above).

Nitrate is the most mobile form of N fertilizer and easily infiltrates groundwater through soil profile. However, the mobility of the ammonium and urea form of N fertilizer is slowed down due to the process of microbiological conversion to nitrate. This implies that, if $NO_3$ originates

from the leaching of chemical fertilizers, the $\delta^{18}O\text{-}NO_3$ would be > 8 and plot preferentially in the region of $NO_3$ fertilizer. Based on the minimum and maximum theoretical nitrification values of $\delta^{18}O\text{-}NO_3$ (4.8 and 6.3‰) and $\delta^{15}N\text{-}NO_3$ values, about 29% of the nitrate in groundwater originates from anthropogenic sources such as manure and sewage (Fig. VI.2b).The results show that preferential leaching of nitrate fertilizer to the groundwater did not occur, suggesting that fertilizer nitrate is not leached past crop – rooting zone (Gibrilla et al. 2020). The study area is predominantly semi-rural with animal breeding (cattle, sheeps, goats, etc.) and agricultural activities. Furthermore, with the exception of a few households with pit latrines, most households resort to open defecation especially in the peripheries; thus, manure is the most likely source of $NO_3^-$. Majority of the samples have higher $\delta^{18}O\text{-}NO_3$ and $\delta^{15}N\text{-}NO_3$, hence plot outside these boxes. These samples reveal a combination of denitrification processes and mixing from diverse sources. The low, insignificant input from fertilizers aligns with the low sulfate and potassium contents, given that they are common components of fertilizers like the NPKs.

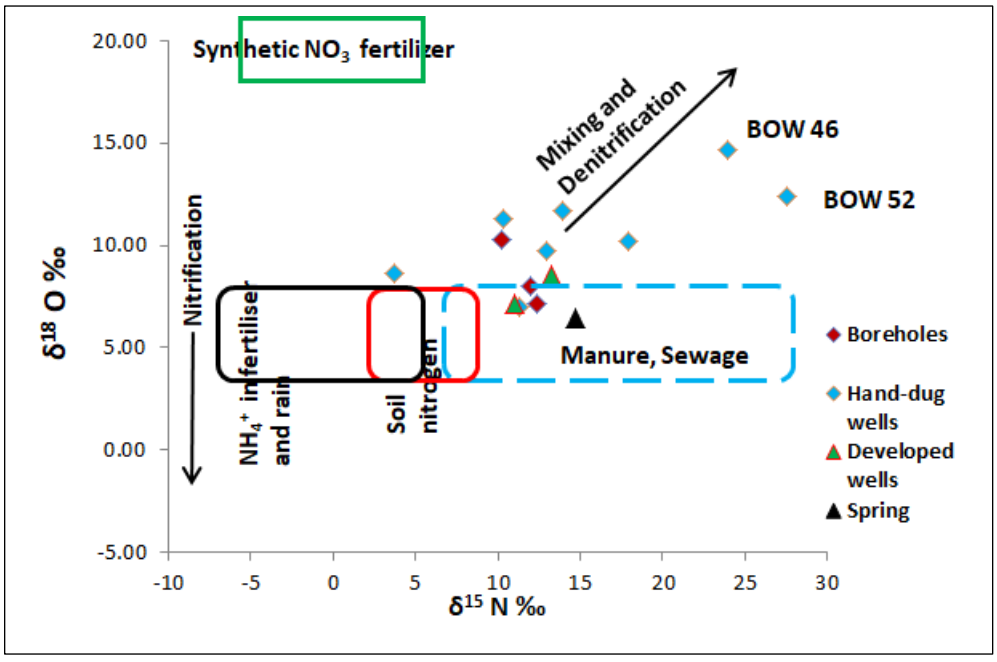


**Figure VI.2b: Cross plot of $\delta^{15}N\text{-}NO_3$ versus $\delta^{18}O\text{-}NO_3$ in some selected wells showing manure and sewage as major sources of nitrate in Bafia**

Studies by Appelo and Postma (2007) showed that nitrate in groundwater originating from the soil due to organic matter decay usually ranges from 0.062 to 12.4 mg/L. In our study, more than 30% of the samples have $NO_3^-$ concentrations > 10 mg/L in both seasons, establishing manure/septic as the dominant nitrate source. Further analysis of the potential sources of nitrate depends on the presence/absence of denitrification, a process which causes the reduction of $NO_3^-$ concentration. Denitrification in the aquifer is usually indicated by decreasing (dilution-corrected) $NO_3$/Cl ratios (Fig. VI.2c), often associated with decreasing DO concentrations below 2 mg/L and increasing $\delta\ ^{15}N\text{-}NO_3$ and $\delta\ ^{18}O\text{-}NO_3$ (Fig. VI.2b above). According to Figure VI.2c, there is a mixture between the upwelling deeper wells and the shallow more aerated wells, hence a mixture of signatures as earlier mentioned.

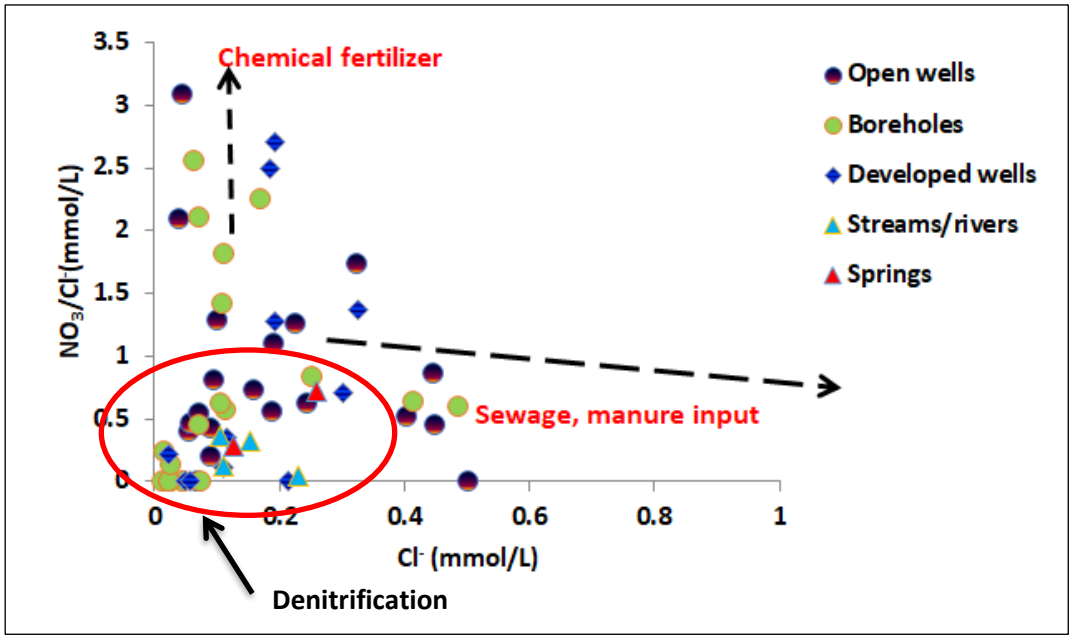


**Figure VI.2c $NO_3^-/Cl^-$ versus $Cl^-$ variation showing denitrification**

### VI.2.3. Nitrate reduction by iron

Low nitrate concentrations in groundwater could be attributed to attenuation by the presence of super-saturation of hematite ($Fe_2O_3$) and goethite (FeO(OH) and well depth in deeper wells. Several studies (Van Hecke et al. 1990; Cheng et al. 1997) have investigated the chemical reduction of nitrate using ferrous iron as bulk reducing agent. These studies showed that at lower pH (2-4), nitrate is inactive; no biochemical conversion to nitrite. But as pH increases due to the

oxidation of $Fe^0$ to $Fe^{2+}$, the nitrate is converted to nitrite, through the following equations:

$$2H_3O^+ + Fe^0 = H_{2(g)} + Fe^{2+}\ 2H_2O \quad (37)$$

$$NO_3^- + Fe^0 + 2H_3O = Fe^{2+} + NO_2^- + 3H_2O \quad (38)$$

In this study, the trace element saturation indices demonstrated over-saturation of hematite ($Fe_2O_3$) and goethite (FeO(OH) in more than 95% of the water samples. In shallow and surface waters, high DO levels in water indicate aerobic conditions which favor nitrate accumulation. Therefore, DO levels < 2mg/L in shallow domestic wells depict wells that are devoid of oxygen. Only about 7% and 11% of water samples have nitrate >50mg/l, illustrating aerobic conditions in the rainy and dry season individually. As demonstrated on Figure VI.3, this over-saturated iron explains the low nitrate concentration in some samples, given that nitrate is reduced to $N_2$, $N_2O$, $NH_4^+$ etc. after receiving electrons from Fe especially under acidic pH like in most Bafia water samples The presence of hematite enhances nitrate reduction by fostering biofilm formation, altering microbial community structure, and augmenting nitrate reductase activity (Wang et al. 2025).

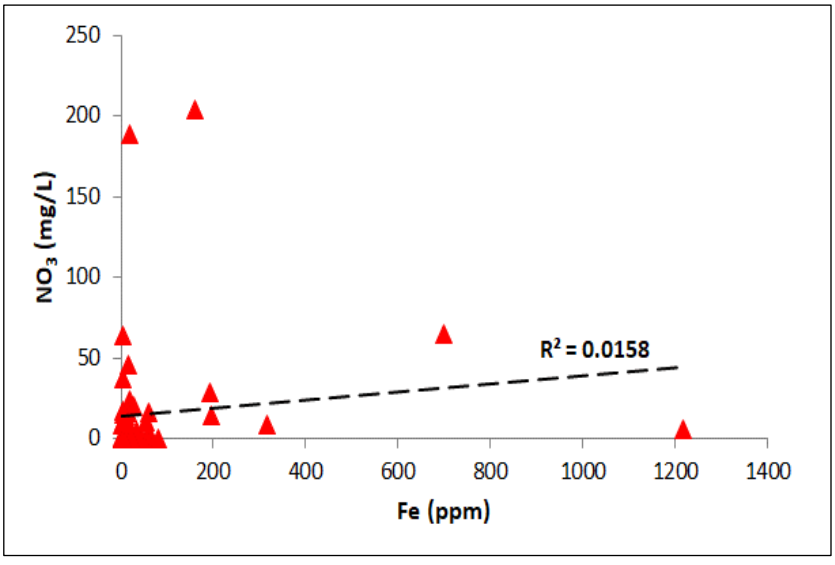


**Figure VI.3: Plot of $NO_3$ versus Fe in water**

## VI.3. Implications for water resources management

### VI.3.1. Key challenges in water resource uses in the Bafia area

Groundwater in the Bafia area is mostly hosted by fractured crystalline aquifers, which are very complex in nature, with low porosity and limited storage capacity. However, there are limited hydrogeochemical data on these aquifers within the area (Enyegue et al. 2014, 2020; Ngouokouo et al. 2025). Hence most boreholes have been drilled in the wrong locations (away from the main fractures), leading to low recharge, borehole failures and consequently, inadequate supplies. In addition, the sandy-loam and sandy-clay-loam soils in Bafia are unstable in some areas, leading to the collapse of some hand-dug wells, especially in the over-exploited sources.

Rainfall is the main source of recharge in Bafia; thus shallow wells are mainly affected by seasonal variations in water levels. During the field campaigns, there were several rainy season sampling points which were dry during the dry season, including some streams. This leads to long periods of water scarcity, thus redirecting the population to alternative, unsecured sources. Bafia is also plagued with water quality issues, especially from the presence of some natural (like Mn and Fe) and human contaminants (from leaky pit latrines, agricultural runoff, open defecation, well chlorination and poor waste dumping habits). This renders some water points useless and equally increases human health risks in Bafia. Besides the local geology, some areas like Fin Goudrong Ndengue (BOW 01), Eldorado (BOW 56), Kirai (BOW 52, 53) revealed a mixture of different contamination sources. BOW 01, 52 and 53 are exceptionally located in low areas with poor drainage systems, whereby surface runoff from most parts of the town accumulate and infiltrate.

### VI.3.2. Identifying and protecting groundwater recharge zones

The chemistry of every water resource is often a reflection of its point of recharge and the hydrogeological processes which modify them along their flow path. Interpreting groundwater $\delta^{18}O$ values vis-à-vis the elevation reveal that > 70% of groundwater in Bafia is recharged by local precipitations within Bafia (low elevations), with minor contributions from higher topography peripheries (Bapé area). In compliance with the stable isotopes, there is a gradual increase in TDS and EC from the high topographic areas towards low central parts, reflecting an evolution from recharge points.

Furthermore, tritium data shows that > 71% groundwater is recently recharged (within the last 40 years), with high amounts of nitrate (up to 229mg/L). Most of these high nitrate points, as indicated by the dual nitrogen isotopes, are close to market areas, farmlands, dumpsites and pit latrines. Nonetheless, about 29% of boreholes in Rigama Transformateur (BBH 44), Rimis (BBH 50), the Catholic Diocese area (BBH 20), Nyamsong I (BBH 04) and parts of Bigna (BBH 55) have tritium < 1TU and nitrate < 1mg/L, suggesting the possibility of older, non-renewable water which might have been isolated from recent atmospheric conditions, hence considered as protected zones.

Hence, there should be a restriction concerning the use of certain fertilizers around these neighborhoods. Also, the sanitation standards in such areas must be revisited, including the construction of good pit latrines and septic systems at safe distances from these wells. Additionally, nitrate levels should be regularly monitored to track and identify new trends. Given the role of the forest milieu on groundwater infiltration and contamination, reforestation practices are encouraged to protect these potential recharge/old groundwater zones.

### VI.3.3. Capacity building and socio-hydrology

In spite of all groundwater characterization and management studies carried out around the world, Africa and Cameroon, most community dwellers in Bafia are still ignorant of the basic aspects. In socio-hydrology, both the hydrologists and the community have their roles to play: the hydrologists/hydrologists get information on the recharge source, water budget, water quality and every other hydrodynamics and inform the community on what is at stake and how to manage it. To sustainably manage groundwater, especially in less-developed areas like Bafia with low educational abilities and poor hygiene conditions, it is pivotal to get the people involved. Furthermore, capacity building programs gearing towards catchment maintenance, Community Led Total Sanitation (CLTS), local water treatment techniques and the right land use practices equips the community, allowing them to set up local monitoring and maintenance systems. Additionally, a well-informed population facilitates the tasks of policy makers, speeds up implementation stages and waste fewer funds on remediation projects.

### VI.3.4 Policy and water management

Besides the scientific aspects involved, water resources management plans are liable to fail when some managerial aspects are deficient, like the lack of trained personnel, deficient institutional arrangements, and poor or nonexistent resource management rules, regulations, programs, and software. There exists some National Water Policies in Cameroon like that between the Ministry of Water Resources and Energy (MINEE) and UNICEF (2025), which highlights current issues such as water pollution, increasing pressure due to demographics and urbanization, and the consequences of climate change. The policy proposed solutions like: implementing Integrated Water Resources Management (IWRM), improving access to drinking water and sanitation, strengthening institutional and regulatory capacities, investing in water infrastructure, promoting public-private partnerships, and decentralization to ensure equitable and sustainable management. Additionally, in Cameroon, there are laws which guide the distribution and appropriate use of agrochemicals, especially synthetic pesticides. These laws are in line with certain international conventions like Stockholm Convention that aims to eliminate or restrict the production and use of persistent organic pollutants.

However, most inhabitants in semi-rural areas like Bafia, with marginal knowledge on these aspects fail in the implementation of these policies. Hence, the vulgarization of existing laws and data from passed water-related projects enhance sustainable water management and the protection of these resources.

## CONCLUSION

This research also reveals that as much as agriculture plays a significant role in the supply of nitrate into groundwater, other anthropogenic activities equally contribute high quantities of nitrate. More than 29% of the nitrate in the system is linked to manure and sewage sources, with very insignificant inputs from inorganic fertilizers and atmospheric depositions. The wide variation of $NO_3^-/Cl^-$ ratios also signifies a mixture of multiple sources, with manure/sewage as main sources. There are equally denitrification and mixing processes as exhibited by the low $\delta^{18}O\text{-}NO_3$ and the high $\delta^{15}N\text{-}NO_3$, thus lowering the nitrate concentration. Additionally, the hematite and goethite super-saturation in the samples also attenuate nitrate levels in water; hence

the low concentrations observed in some areas (BDL) despite the agricultural and urban activities.

The combination of different techniques to evaluate water resources in Bafia serves as a basis for their sustainable management. Amongst many, the identification of key challenges affecting Bafia water resources, the protection of recharge areas, policy enforcements, capacity building and community involvement are critical for ensuring the long-term sustainability of groundwater resources in the Bafia area.

# GENERAL CONCLUSION AND PERSPECTIVES

The study area (1200 $km^2$) is located in Bafia, head quarter of the Mbam and Inoubou Division of the Centre Region of Cameroon. It has an equatorial and tropical transitional climate, with two alternating rainy and dry seasons. Besides small scale businesses, animal farms and fishing, agriculture is the main income-generation activity for the population of Bafia. The geomorphology is made up of high rectilinear reliefs, medium hills and plains. The Mbam River is the biggest river draining the area. The geology is made up of undifferentiated gneisses and meta-sediments which give rise to ferralitic soils (mainly of the sandy loam and the sandy-clay-loam groups). Two aquifer types have been identified in these formations: the deep fractured aquifer which taps from the basement and the shallow unconfined aquifer which taps from weathered alterites.

The main goal of this Ph.D research was to characterize groundwater and surface water resources in the Bafia area in order to fully understand the origin, recharge, hydrogeochemical processes/evolution and contamination sources. This was done by evaluating the hydrochemical/hydrogeochemical characteristics, isotopic properties, apparent age, nitrate contamination sources, and the suitability of water resources for sustainable management purposes. To achieve this, 57 water samples were analyzed during the rainy season and 60 during the dry season and the results/data obtained were treated using different software packages like SPSS, Excel (for descriptive and multivariate statistics), ARC-GIS 9.3, Q-GIS, Diagramme and Phreeqc-USGS.

Groundwater is more mineralized than surface water, with higher concentrations observed in the dry season. On a physico-chemical point of view, water resources in the Bafia area are acidic to neutral (pH between 3.2 and 7.4), moderately to highly mineralized (30 µS/cm ≤ EC ≤ 2220 µS/cm) and generally soft-fresh in nature. Calcium is the dominant cation, ranging between 1.47 mg/L and 244 mg/L, closely followed by $Na^+$ (1.28 mg/L ≤ $Na^+$ ≤ 174.5 mg/L), Potassium (0.7 mg/L ≤ $K^+$ 64.8 mg/L) and magnesium (0.5 mg/L ≤ $Mg^{2+}$ ≤ 26.4 mg/L). Similarly, bicarbonate is the dominant anion (ranging from 4 mg/L to 439 mg/L), closely followed by Chloride (1.1 mg/L Cl ≤ 244 mg/L) and sulfate (0 mg/l ≤ $SO_4^{2-}$). More than 85% samples have major ions levels within the calculated NBLs and TVs, except for nitrate, reflecting the influence of natural weathering processes. The presence of the Ca-Mg-$HCO_3$ water type insinuates active and rapid recharge of fresh water, which slightly evolves to the NA-K-$HCO_3$ type that is chemically more

evolved. The main processes modifying the ionic content of groundwater in Bafia are rock/mineral weathering/dissolution through water-rock interaction, ion exchange and anthropoenic activities.

Factor analysis reveals a mixture of natural and anthropogenic factors influencing water quality in Bafia. Relatively higher mean TDS, $Cl^-$, $NO_3$, $Na^+$ and $K^+$ in shallow wells around more populated/market/low topographic areas point to greater vulnerability to surface contaminants especially nitrate from agriculture and pit latrines, and chloride from well treatment. Conversely, higher mean Ca, Mg and $HCO_3$ in boreholes insinuate longer water-rock interaction time in deeper wells as opposed to shallow wells, with reduced surface contamination effects. Trace element contentrations are generally low, except for Fe, Mn and Ti, indicating natural influences from rock weathering. Despite the low trace element levels, low HPI, $C_d$ and HEI, there are high incremental lifetime cancer risks (ILCR) of Cr and Ni for children in the Ndengue Fin goudrong neighborhood (BOW 02). More than 90% of samples have WQI < 25, implying excellent quality. Based on the different parameters used to classify irrigation water, Bafia water resources are excellent for irrigation, requiring little or no extra treatment before use.

Groundwater in the Bafia area has a meteoric origin, with > 70% recharge originating from rainfall at lower elevations (within Bafia). The low TDS and chloride variability with respects to the $\delta^{18}O$ demonstrates low evaporation impacts on groundwater salinization processes in Bafia. The overlapping of $\delta^{18}O$ and $\delta D$ values in both seasons indicates the possibility of mixing between groundwater recharged at higher (Bapé area) and lower (Bafia town) elevations.

The tritium content shows that > 70% of analyzed groundwater in the Bafia area is a mixture of modern and pre-modern recharge (between 1960 and present), hence considered as young water, which is open to nitrate and other surface contaminations. High tritium levels encountered in some deep boreholes (BBH 35) confirms the vertical mixture of groundwater earlier revealed by stable isotopes. Some samples like BBH 44, BBH 50, BBH 20, BBH 04 and BBH 55 located in Rigama Transformateur, Rimis, the Catholic Diocese, Nyamsong I and parts of Bigna neighborhoods with low tritium (< 0.8 TU) and lowest nitrate (BDL) point to insignificant influences from recent recharge; hence have been identified as protected areas for safe quality drinking water in Bafia.

The dual nitrogen isotope points sewage and maure as main nitrate sources in Bafia. However, the nitrate level is almost immediately reduced by denitrification processes; hence the low nitrate in most samples. High $NO_3$/Cl ratios and $\delta^{15}N\text{-}NO_3$ (>10%) represent a mixture of urban (sewage, septic tanks, leaky pit latrines) and agricultural (manure, organic wastes) contamination sources as main nitrate producers in Bafia groundwater resources. The risk of nitrate contamination in groundwater resources in Bafia, especially in shallow wells is already significant and requires extra preventive measures.

This study has successfully used a robust approach, combining different techniques, including hydrochemical, isotopic and statistical techniques, to evaluate the sources, evolution, age, contamination risks and the implications for water management. From the aforementioned techniques, it is concluded that groundwater in the fractured crystalline aquifers of Bafia, Cameroon, is significantly influenced by natural geochemical processes and human activities like agriculture and poor sanitation, which pose serious threats to water quality. The findings of this thesis contribute to the identification of groundwater origin, quality evolution and shallow groundwater vulnerability to nitrate contamination and also serve as a reference for groundwater studies in similar crystalline aquifer systems in a local and regional scale. However, as perspectives,

- We plan to investigate the pesticide and bacteriological content of water resources in Bafia, to link them to our current findings.
- To better comprehend the isotope hydrology in the area, we envisage doing a continous monitoring of the stable isotope content of water in order to establish the Bafia Local Meteoric Water Line (BLMWL).
- Given the presence of low tritium with corresponding low nitrate levels in some samples, it is recommended to carryout extensive groundwater studies using carbon-14 and strontium isotope to isolate protected areas.

In the part of socio-hydrology,

We recommend

- ✓ An improvement in the general sanitation (latrine construction, proper sewage treatment and waste disposal systems) of the Bafia population to minimize contamination risks.
- ✓ We recommend constant checks on the types and dosage of fertilizers, manure and other agrochemicals used.
- ✓ Finally, there should be community sensitization on groundwater protection strategies for a sustainable management.

# REFERENCES

**Abascal, E., Gómez-Coma, L., Ortiz, I, A. Ortiz (2022).** Global diagnosis of nitrate pollution in groundwater and review of removal technologies, *Science of The Total Environment*, **810**, https://doi.org/10.1016/j.scitotenv.2021.152233

**Action Contre la Faim, (2008).** Eau-Assainissement-Hygiène pour les populations à risque. Ed. Hermann, Paris. 785p.

**Adams, S., Titus, R., Pietersen, K., Tredoux, G., Harris, C. (2001**). Hydrochemical characteristics of aquifers near Sutherland in the western karoo, South Africa. *Journal of Hydrology***. 241,** 91–103.

**Adebowale, T., Surapaneni, A., Faulkner, D., McCance, W., Wang, S., Currell, M. (2019).** Delineation of contaminant sources and denitrifcation using isotopes of nitrate near a wastewater treatment plant in peri-urban settings. *Science of the Total Environment,* **651,** 2701–2711. https://doi.org/10.1016/j.scitotenv.2018.10.146

**Adomako D., Osae S., Akiti T. T., Faye S., Maloszewski P. (2011).** Geochemical and isotopic studies of groundwater conditions in the Densu River Basin of Ghana. *Environmental Earth Science*, **62:**1071–1084, DOI 10.1007/s12665-010-0595-2

**Adomako, D., Gibrilla, A., Maloszewski, P., Ganyaglo, S., Rai, S. P. (2015).** Tracing stable isotopes (δ D and $\delta^{18}$ O) from meteoric water to groundwater in the Densu River basin of Ghana. *Environmental Monitoring and Assessment*, **187.** 4498, DOI: 10.1007/s10661-015-4498-2

**Agbeve, S.K., Osei-Fosu, P., Carboo, D. (2014).** Levels of organochlorine pesticide residues in Mondia whitei, a medicinal plant used in traditional medicine for erectile dysfunction in Ghana. *International journal of advance agricultural research* **1**:9–16.

**Aggarwal, P.K., Romatschke, U., Araguas, L., Belachew, D., Longstaffe, F.J., Berg, P., Schumacher, C., Funk, A. (2011).** Proportions of convective and stratiform precipitation revealed in water isotope ratios. *Nature Geoscience.* **9**, 624–629.

**Aghazadeh, N., Chitsazan, M., Golestan, Y. (2016).** Hydrochemistry and quality assessment of groundwater in the Ardabil area, Iran, **Applied Water Science**, doi 10.1007/s13201-016-0498-9

**Aitchison, J. and Greenacre, M. (2002).** Biplots of compositional data, Journal of the Royal Statistical Society, *Series C (Applied Statistics)* **51** (4), 375–392.

**Akenji, V. N., Ayonghe, S. N.i, Naminjo, S., Tarkang, C. E., Lumnwi, M., Bijingsi, M., Amungwa, I T. and Azise, H. A. (2023).** Pollution of Water Resources by Agrochemicals in the

Agroindustrial Areas at the South Western Flank of Mount Cameroon. JOURNAL OF THE *Cameroon Academy of Sciences*, **19** (2), DOI: https://dx.doi.org/10.4314/jcas.v19i3.4

**Akiti, T.T. (1980).** Geochemical and isotopic studies of groundwater in Upper West Region of Ghana. Unpublished PhD Thesis, Universitie´ de Paris Sud.

**Ako, A. A., Gloria, E. T. E., Jun, S., Katsuaki, K., Takahiro, H., Kimpe,i I., Akoachere, R., Beatrice, K.-T., George, E.N., Ntankouo, N. R. (2014).** Nitrate contamination of groundwater in two areas of the Cameroon Volcanic Line (Banana Plain and Mount Cameroon area). *Applied Water Science* **4,** 99–113, DOI 10.1007/s13201-013-0134-x

**Ako, A.A., Jun, S., Takahiro, H., Kimpei, I., George, E. N., Gloria, E. T. E., Ntankouo, N, R. (2012).** Hydrogeochemical and isotopic characteristics of groundwater in Mbanga, Njombe and Penja (Banana Plain) – Cameroon, *Journal of African Earth Sciences* **75**, 25–36, http://dx.doi.org/10.1016/j.jafrearsci.2012.06.003.

**Ako, A.A., Shimada, J., Hosono, T., Ichiyanagi, K., Nkeng, G.E., Fantong, W.Y., Eyong, G.E., Roger, N.N. (2011).** Evaluation of groundwater quality and its suitability for drinking, domestic, and agricultural uses in the Banana Plain (Mbanga, Njombe, Penja) of the Cameroon Volcanic Line. *Environmental Geochemistry and Health*. **(6):**559-75. doi: 10.1007/s10653-010-9371-1

**Akoachere, R. A.II, Takahiro, H., Thomson, A. E., Marcelle-Carole, P. N., Tom, T. O. (2019).** Assessing the Trace Metal Content of Groundwater in the Bakassi Peninsular, Onshore Rio Del Rey, Akwa-Mundemba, Cameroon. *Journal of Geoscience and Environment Protection*, **7**, DOI: 10,4236/gep.2019.710003

**Akosua Loh, Y.S., Fynn, O.F., Manu, E., Afrifa, G.Y., Addai, M.O., Akurugu, B.A., Yidana, S.M. (2022).** Groundwater-Surface Water Interactions: Application of Hydrochemical and Stable Isotope Tracers to the Lake Bosumtwi Area in Ghana. *Environmental Earth Sciences*, doi.org/10.1007/s12665-022-10644-x

**Akpataku, K. V., Shive, P. R., Masamaéya, D.-T. G., Lallébila, T., Limam, M. B., Gbandi, D.-B., Serigne, F. (2019).** Hydrochemical and isotopic characterization of groundwater in the Southeastern part of the Plateaux Region, Togo, *Hydrological Sciences Journal*, https://doi.org/10.1080/02626667.2019.1615067

**Altabet, M.A., Wassenaar, L.I., Douence, C., Roy, R. A. (2019).** Ti(III) reduction method for one-step conversion of seawater and freshwater nitrate into $N_2O$ for stable isotopic analysis

of $^{15}N/^{14}N$, $^{18}O/^{16}O$ and $^{17}O/^{16}O$. *Rapid Commun Mass Spectrom*, **15;**33(15):1227-1239. doi: 10.1002/rcm.8454. PMID: 30980427.

**Anaba, O. A.B., Ndam Ngoupayou, J.R., Mvondo, O. J. (2017).** Analysis of Crystalline Bedrock Aquifer Productivity: Case of Central Region in Cameroon. *Groundwater for Sustainable Development*, **5**, 66-74, doi.org/10.1016/j.gsd.2017.05.003

**Andersen, H.E., Blicher-Mathiesen, G., Bechmann, M., Povilaitis, A., Iital, A., Lagzdins, A., Kyllmar, K. (2014).** Reprint of "Mitigating diffuse nitrogen losses in the Nordic-Baltic countries". *Agriculture, Ecosystems and Environment* **198**, 127–134. https://doi.org/ 10.1016/j.agee.2014.05.009.

**Anornu, G., Gibrilla, A., Adomako, D. (2017**). Tracking nitrate sources in groundwater and associated health risk for rural communities in the white Volta River basin of Ghana using isotopic approach (δ15N, δ18O NO3 and 3H). *Science of the Total Environment* https://doi.org/ 10.1016/j.scitotenv.2017.01.219

**Appelo, C. A. J., & Postma, D. (2004).** Geochemistry, groundwater and pollution. *CRC press*.

**Appelo, C.A.J. and Postma, D. (2005).** Geochemistry, groundwater, and pollution (2nd ed.). Balkema, Amsterdam, 635.

**Appelo, C.A.J., Postma, D., (2007).** Geochemistry, Groundwater and Pollution, 2nd ed. Balkema, Rotterdam.

**Appiah-Opong, R.., Amoako, O., Mark, O., Ebenezer, O.-A., Francis, K. E. N., Isaac, T., Christopher, G., Daniel, K. A., Alexander, K. N., Benedicta, Y. F.-M. (2021).** Heavy metals concentration and pollution index (HPI) in drinking water along the southwest coast of Ghana, *Applied Water Science*, **11**:57 https://doi.org/10.1007/s13201-021-01386-5

**Araguás-Araguás, L., Froehlich, K., Rozanski, K., (2000).** Deuterium and oxygen-18 isotope composition of precipitation and atmospheric moisture. *Hydrological Processes* **14**, 1341–1355. https://doi.org/10.1002/1099-1085(20000615)14:8<1341::AID-HYP983>3.3.CO;2-Q

**Backman, B., Bodiš, D., Lahermo, P. (1998).** Application of a groundwater contamination index in Finland and Slovakia. *Environmental Geology* **36** (1–2): 55–64.

**Baldini, L.M., McDermott, F., Foley, A.M., Baldini, J.U.L. (2008).** Spatial variability in the European winter precipitation δ18O-NAO relationship: Implications for reconstructing NAO-mode climate

variability in the Holocene. *Geophysical Reseatch Letters* **35**. https://doi.org/10.1029/2007GL032027

**Bayou, W. T., Mebruk, M., Tenalem, A., Tesfay, K. M., Stefan, W.(2024).** Hydrochemistry and isotope hydrology of groundwater and surface water in the Sor and Gebba watershed, southwestern Ethiopia, *Environmental Earth Sciences*, **83**:316 https://doi.org/10.1007/s12665-024-11620-3

**Bello, M., Ketchemen-Tandia, B., Nlend, B., Huneau, F., Fouepe, A. T., Fantong, W., Boum-Nkot, S., Garel, E., Celle, H. (2019).** Shallow groundwater quality evolution after 20 years of exploitation in the southern Lake Chad: hydrochemistry and stable isotopes survey in the far north of Cameroon. *Environmental Earth Sciences*, **78**. 10.1007/s12665-019-8494-7

**Bijay-Singh and Eric Craswell (2021).** Fertilizers and nitrate pollution of surface and groundwater: an increasingly pervasive global problem Review, *SN Applied Sciences (2021)* **3**:518 | https://doi.org/10.1007/s42452-021-04521-8

**Bing H., Wu Y., Zhou J., Sun H., Wang X., Zhu H. (2019).** Spatial variation of heavy metal contamination in the Riparian sediments after two-year flow regulation in the Three Gorges Reservoir, China. *Science of the Total Environment*, ***649,*** 1004-1016.

**Boateng, T. K., Opoku, F., Opok, F., Akot, O. (2019).** Heavy metal contamination assessment of groundwater quality: a case study of Oti landfill site, Kumasi. *Applied Water Science*, **9**(2), 1–15. https://doi.org/10.1007/S13201-019-0915-Y

**Böhlke, J. K., Wanty, R., Tuttle, M., Delin, G., Landon, M. (2002).** Denitrification in the Recharge Area and Discharge Area of a Transient Agricultural Nitrate Plume in a Glacial Outwash Sand Aquifer, Minnesota. *Water Resources Research* 2002, ***38*** (7), 10-1.

**Bon, A. F., Ndam Ngoupayou, J. R., Guillaume, E. M., Georges, E. E. (2016).** Hydrogeological characterization of weathered and fssured basement aquifers of the Olezoa watershed in Yaoundé, Cameroon. *Revue des Sciences de l'Eau* **29**(2) (2016) 149-166.

**Bon, A.F., Therese, A. M., Guillaume, E. M., Lucian, A. B., Ndam Ngoupayou, J. R., Georges, E. E. (2021).** Groundwater flow patterns, hydrogeochemistry and metals background levels of shallow hard rock aquifer in a humid tropical urban area in sub-Saharan Africa- A case study from Ol´ezoa watershed (Yaound´e-Cameroon). *Journal of Hydrology: Regional Studies* **37** (2021) 100904, https://doi.org/10.1016/j.ejrh.2021.100904

**Bony, S., Risi, C., Vimeux, F. (2008).** Influence of convective processes on the isotopic composition (d18O and dD) of precipitation and water vapor in the tropics: 1. Model description, vertical profiles and isotopic composition of precipitation. *Journal of Geophysical Resources* **113**:D19305.

**Boretti, A. and Rosa, L. (2019).** Reassessing the projections of the world water development report. *Clean Water* **2**:15.

**Bouchard, M. F., Sauvé, S., Barbeau, B., Legrand, M., Brodeur, M.E., Boufard, T. et al (2011).** Intellectual impairment in school-age children exposed to manganese rom drinking water. *Environment health perspectives*, **119** (1), 138-143.

**Boumaiza, L., Randy, L. S., Bernhard, M., Ioannis, M., Elisa, S., Neus, O., Karen, H. J., Frédéric, H., Romain, C., Mónica, L., Viviana Re, Kay, K. (2024).** How the $\boldsymbol{\delta^{18}}ONO_3$ versus $\boldsymbol{\delta^{15}}NNO_3$ Plot Can Be Used to Identify a Typical Expected Isotopic Range of Denitrifcation for $NO_3$-Impacted Groundwaters, *ACS EST Water* https://doi.org/10.1021/acsestwater.4c00796

**Boum-Nkot, N. S., Nlend, B., Komba, D., Nkoue, N. G.R., Bello M., Fongoh, E.J., Ntamak-Nida, M.-J., Etame, J. (2023).** Hydrochemistry and assessment of heavy metals groundwater contamination in an industrialized city of sub-Saharan Africa (Douala, Cameroon). Implication on human health. *Hydro Research* **6** (2023) 52–64, https://doi.org/10.1016/j.hydres.2023.01.003

**Boutin Anne and Tally Guy (2012).** IRCOD Évaluation externe finale du projet « Gouvernance de l'Eau dans le Mbam et Inoubou » (GEMI) au Cameroun (Décembre 2007 – Décembre 2011) SYNTHÈSE

**Bowen, G.J., Putman, A., Brooks, J.R., Bowling, D.R., Oerter, E.J., Good, S.P. (2018).** Inferring the source of evaporated waters using stable H and O isotopes. *Oecologia* **187,** 1025–1039. https://doi.org/10.1007/s00442-018-4192-5

**Branchet, P., Emmanuelle, C., Hélène, F., David, S., Benjamin, N. N., Valérie, B.-E., Ndam Ngoupayou, J. R., Ives, K., Jean-Jacques, B., Catherine, G. (2018).** Polar pesticide contamination of an urban and peri-urban tropical watershed affected by agricultural activities (Yaounde, Center Region, Cameroon) *Environmental Science and Pollution Research* doi.org/10.1007/s11356-018-1798-4

**Braun, J.-J., Ndam Ngoupayou, J., Viers, J., Dupre, B., Bedimo Bedimo, J.-P., Boeglin, J.-L., Robain, H., Nyeck, B., Freydier, R., Nkamdjou, L.S., Rouiller, J., Muller, J.-P. (2005).**

Present weathering rates in a humid tropical watershed: nsimi, South Cameroon. *Geochimica and Cosmochimica Acta* **69** (2), 357–387. https://doi.org/10.1016/j.gca.2004.06.022

**Brown, R.M., McCleiland, N.J., Deininger, R.A., O'Connor, M.F. (1972).** A Water Quality Index—Crossing the Psychological Barrier. Proceedings of the International Conference on Water Pollution Research, *Jerusalem*, 18-24 June 1972, 787-797.

**BUCREP (2010).** Recensements de la population camerounaise. *Presses du BUCREP*, Yaounde.

**Bureau of Indian Standards (BIS) (2003)** Drinking Water Specifications, IS: 10500.

**Castaldo, G., Visser, A., Fogg, G. E., Harter, T., (2021).** Effect of groundwater age and recharge source on nitrate concentrations in domestic wells in the San Joaquin Valley. *Environmental science & technology*, ***55***(4), 2265-227.

**Cheng, I. F., Muftikian, R. and Fernando, Q. (1997).** Reduction of Nitrate to Ammonia by Zero-Valent Iron. Extended Abstract, presented at Division of Environmental Chemistry, American Chemical Society, San Francisco, CA, April 13–17.

**Chérif, R. and Gargouri-Ellouze, E. (2023).** Flow signatures and catchment's attributes for HCA clustering in a hydrologic similarity assessment (Tunisian case). *Scientific Reports* **13**, 12144 (2023). https://doi.org/10.1038/s41598-023-38608-6

**Chinye-Ikejiunor, N., Iloegbunam, G.O., Chukwuka, A., Ogbeide, O., (2021).** Groundwater contamination and health risk assessment across an urban gradient: Case study of Onitcha metropolis, south-eastern Nigeria. *Groundwater for Sustainable Development* **14,** 100642. https://doi.org/10.1016/j.gsd.2021.100642

**Christofi, C., Adriana, B., Christoph, K., Costas, C. (2020).** Isotope hydrology and hydrogeochemical modeling of Troodos Fractured Aquifer, Cyprus: The development of hydrogeological descriptions of observed water types, *Applied Geochemistry*, **123,** https://doi.org/10.1016/j.apgeochem.2020.104780

**Chukwura U. O., Udom G. J., Cuthbert S. J., Hursthouse A. S. (2015).** Evaluation of hydrochemical characteristics and flow directions of groundwater quality in Udi Local Government Area Enugu State, Nigeria. *Environmental Earth Sciences*, ***73***, 4541-4555

**Clark, I. and Fritz, P., (1997).** Environmental isotopes in hydrogeology. Boca Raton, New York: *CRC press*

**Clément, R., Luc, A., Olivier, B., Jean-Christophe, M., Benoît, D., Hélène, P., Thierry, L., Virginie, V.-A., Rebecca, H. (2014).** Groundwater sources and geochemical processes in a crystalline fault aquifer, *Journal of Hydrology*, **519**, Part D, 3110-3128, https://doi.org/10.1016/j.jhydrol.2014.10.052

**Coetsiers, M., Blaser, P., Martens, K., Walraevens, K. (2009).** Natural background levels and threshold values for groundwater in fluvial Pleistocene and Tertiary marineaquifers in Flanders, Belgium. *Environmental Geology* **57**, 1155–1168. https://doi.org/ 10.1007/s00254-008-1412-z

**Comas-Bru, L., McDermott, F., Werner, M. (2016).** The effect of the East Atlantic pattern on the precipitation δ18ONAO relationship in Europe. *Climate Dynamics* **47**, 2059–2069. https://doi.org/10.1007/s00382-015-2950-1

**Craig H. and Gordon L. (1965).** Deuterium and oxygen-18 variations in the ocean and marine atmosphere, in: Tongiorgi, E. (Ed.), Proceedings of a Conference on Stable Isotopes in Oceanographic Studies and Paleotemperatures. *Spoleto*, Italy, 9–130

**Craig H., (1961).** Isotopic variation in meteoric waters. *Science* **133**, 1702–1703.

**Custodio, E. (2002).** Aquifer overexploitation: What does it mean?. *Hydrogeology Journal*, **10**(2), 254–277.

**Dafny, E., Burg, A., Gvirtzman, H. (2006).** Deduction of groundwater flow regime in a basaltic aquifer using geochemical and isotopic data: The Golan Heights, Israel case study. *Journal of Hydrology*, doi:10.1016/j.jhydrol.2006.04.002

**Dansgaard, W. (1961).** The Isotopic Composition of natural waters. *Meddr Groenland* **165**, 1-20.

**Dansgaard, W. (1964).** Stable isotopes in precipitation. *Tellus* **16**(4):1386–1398.

**Davis, S.N. and Turk, L.J. (1964).** Optimum Depth of Wells in Crystalline Rocks. *Groundwater*, **2,** 6-11. https://doi.org/10.1111/j.1745m 6584.1964.tb01750.x

**Defo, C., Yerima, B. K. R., Bemmo, N. (2016).** Heavy metal pollution of groundwaters of the Ntem watershed in Yaoundé-Cameroon (West Africa)

**Deutsch, W.J. (1997).** Groundwater geochemistry: Fundamentals and applications to contamination. *CRC Press, Florida* p. 221

**Dieng, N.M., Orban, P., Otten, J., Stumpp, C., Faye, S., Dassargues, A. (2016).** Effects of seasonal and climate changes on groundwater quality in the Saloum coastal aquifer (Senegal*). Journal of Hydrology Regional Studies*, **9**, 163–182.

**Djoufounna, J., Bamou, R., Mayi, M., Paul A., Kala-Chouakeu, N. A., Tabue, R. Awono-Ambene, P., Achu-Fosah, D., Antonio-Nkondjio, C., Tchuinkam, T. (2022**). Population knowledge, attitudes and practices towards malaria prevention in the locality of Makenene, Centre-Cameroon. *Malaria Journal***. 21.** 10.1186/s12936-022-04253-z. https://doi.org/10.1016/j. ejrh.2016.12.082

**Doneen, L.D. (1964).** Notes on water quality in agriculture published as a water science and engineering paper 4001, department of water science and engineering, university of California, Davis

**Drever, J. I. (1982).** The geochemistry of natural waters. Prentice-Hall, Inc., *Englewood Cliffs, N.J***. 388** 31.95.

**Drew, L. J., Schuenemeyer, J. H., Armstrong, T. R., Sutphin, D. M. (2001).** Initial Yield to Depth Relation for Water Wells Drilled into Crystalline Bedrock - Pinardville Quadrangle, New Hampshire. *Ground Water* **39**(5): 676-684.

**Dumort, J.F. (1968).** Notice explicative sur les feuilles de Douala Est et Douala Ouest ; carte géologique de reconnaissance au 1/500 000. *Direction des mines et de la géologie du Cameroun.*

**Duvva L.K., Panga K.K., Dhakate R. et al (2022)**. Health risk assessment of nitrate and fluoride toxicity in groundwater contamination in the semi-arid area of Medchal, South India. *Applied Water Science* **12**, 11 (2022). https://doi.org/10.1007/s13201-021-01557-4

**Edet, A.E. and Offiong, O.E. (2003).** Evaluation of water quality pollution indices for heavy metal contamination monitoring. A study case from Akpabuyo-Odukpani area, Lower Cross River Basin (southeastern Nigeria), *Geo Journal* **57**:295–304.

**Edmunds, W.M. and Smedley, P.L. (1996).** Groundwater geochemistry and health: An overview. In: Appleton JD, Fuge R, McCall GJH (eds.) Environmental geochemistry and health with special reference to developing countries. *Geological Society Special Publication* No.113, pp. 91-105

**Edmunds, W.M., Shand, P., Hart, P., Ward, R.S. (2003).** The natural (baseline) quality of groundwater: a UK pilot study. *Science of the Total Environment*, **310**, 25–35.

**Elumalai, V., Nethononda, V. G., Manivannan, V., Rajmohan, N., Li, P., Elango, L. (2020).** Groundwater quality assessment and application of multivariate statistical analysis in Luvuvhu catchment, Limpopo, South Africa. *Journal of African Earth Sciences*, **171**, 103967.

**Embom, C. E., Jean, A. M., Vincent, L. O., Paul-Désiré, N. (2024).** Provenance and depositional environment of the Mbam River overbank clay deposits, Central Africa: evidence from mineralogical and geochemical variations, *Arabian Journal of Geosciences*,**17**:265 https://doi.org/10.1007/s12517-024-12068-2

**Emvoutou, H/ C., Estelle, N. E.P., Djim, M.L., Ndam Ngoupayou, J. R., Christine, S., Béatrice, K.-T., Georges, E. E., Yves, T., Serigne, F. (2024).** Hydrochemical and isotopic studies providing a new functional model for the coastal aquifers in Douala Coastal Sedimentary Basin (DCSB)/Cameroon, *Science of the Total Environment* **912** , doi.org/10.1016/j.scitotenv.2023.169412

**Enyegue, A.N.F., Eyike, A., Tchikangoua, A.N., Bounoung, C.P., Nouayou, R. (2020).** Assessment and characterization of groundwater quality under domestic distribution using hydrochemical and multivariate statistical methods in Bafia, Cameroon. *Groundwater for Sustainable Development.* 10. 100347. 10.1016/j.gsd.2020.100347

**Enyegue, A.N.F.M., Ndougsa, M.T., Njandjock, N.P., Assembe, S. and Manguelle, D.E. (2014).** Groundwater Exploration Using Geoelectrical Investigation in Bafia Area, Cameroon. *Journal of Earth Sciences and Geotechnical Engineering*, **4,** 61-75.

**Ewodo, M. G., Ombolo, A., Fouepe, T. A., Bon, A. F., Bineli, A. E., Bello, M., Ekodeck, G. E., (2012).** Etude des paramètres hydrauliques des aquifères de sub-surface du bassin versant de la Mingosso, région de Yaoundé. *Revue CAMES-Série A*, **13** (1), 123-127.

**Fantong, W. Y., Satake, H., Ayonghe, S. N., Aka, F. T., & Asai, K. (2009).** Hydrogeochemical controls and usability of groundwater in the semi-arid Mayo Tsanaga River Basin: Far North Province, Cameroon. *Environmental Geology*, **58**, 1281– 1293. doi:10.1007/s00254-008-1629-x.

**FAO-UNEP (1999).** The Future of Our Land: Facing the Challenge. Guidelines for Integrated Planning for Sustainable Management of Land Resources. FAO/AGLS, Rome, 71 [The third publication in a series of three explains how to operate participative land use planning].

**Fei, L., Jiawen, Z., Jingran, L., Jingkun, Z/, Pinna, Z. (2022).** Factors controlling groundwater chemical evolution with the impact of reduced exploitation. *Catena* **214**, 106261, https://doi.org/10.1016/j.catena.2022.106261

**Fei, L., Wang, S., Yeh, T.-CJ, Zhen, P., Wang, L., Shi, L. (2020).** Using multivariate statistical techniques and geochemical modelling to identify factors controlling the evolution of groundwater chemistry in a typical transitional area between Taihang Mountains and North China Plain. *Hydrological Processes*. 2020; **34**: 1888–1905. https://doi.org/10.1002/hyp.13701

**Ficklin, W. H., Plumlee, G. S., Smith, K. S., McHugh, J. B. (1992).** Geochemical classification of mine drainages and natural drainages in mineralized areas. In International symposium on water-rock interaction 381-384.

**Fonge, B.A., Egbe, E.A., Fongod, A.N., Tening, A.S., Achu, R.M., Yinda, G.S., Mvondo, Z.E.A. (2012).** Effects of land use on macrophyte communities and water quality in the Ndop wetland plain, Cameroon. *Journal of Agricullture and Social Sciences* **12:** 41-49.

**Fongoh, E. J., Helene, C., Bertil, N., Frederic, H., Boum-Nkot, N. S., Gloria, E. T., Mapoma, Y.F., Akoanung, A. A., Ntamak-Nida M. J. (2024).** Groundwater quality constrains and new opportunities for water supply from hard rock aquifers in a fast-expanding city of Sub-Saharan Africa, Yaound'e-Cameroon. *Journal of African Earth Sciences* **212**, 105207, doi.org/10.1016/j.jafrearsci.2024.105207

**Fongoh, E. J., Helene, C., Nlend, B., Boum-Nkot, S. N., Ako, A. A., Huneau, F., Caillon, N., Ntamak-Nida, M. J. (2023).** Multitracer approach towards an improved understanding of shallow hard rock aquifers and a more sustainable groundwater management, case of Yaounde, Cameroon, *Environmental Earth Sciences* **82**:106 https://doi.org/10.1007/s12665-023-10783-9

**Fontes, J.C. (1980).** Environmental isotopes in groundwater hydrology. In: P. Fritz and J.C. Fontes (Eds.) Handbook of Environmental isotope geochemistry, 1. *The terrestrial environment*, 75-134.

**Foster, S.S.D. and Chilton, P.J. (2003).** Groundwater: The Processes and Global Significance of Aquifer Degradation. *Philosophical Transactions of the Royal Society B*, **358**, 1957-1972. https://doi.org/10.1098/rstb.2003.1380

**Fosu-Mensah, B.Y., Okoffo, E. D., Godfred, D., Christopher, G. (2016).** Organophosphorus pesticide residues in soils and drinking water sources from cocoa producing areas in Ghana. *Environmental Systems Research*, DOI 10.1186/s40068-016-0063-4

**Galliari, J., Santucci, L., Misseri, L., Carol, E., & del Pilar Alvarez, M. (2021).** Processes controlling groundwater salinity in coastal wetlands of the southern edge of South America. *Science of the Total Environment*, **754**, 141951.

**Ganwa, A. A., Urs, K., Tchakounté, J.N., Eva, K. A. E., Bernard, D. (2022).** Structural and Chemical Characteristic of Tourmaline, and Mineralogy of Associated Micas from Tourmaline Bearing Quartzite of Kombé II (Bafia Group, Central Africa Fold Belt); Implication on the Metamorphic Conditions. *International Journal of Geosciences* **13,** 882-904. doi.org/10.4236/ijg.2022.1310044

**Ganwa, A. A., Wolfgang, F., W. S., Cosmas, K. S., Joseph, M. O., Muharrem, S., Tchakounté, J. N. (2008).** Zircon 207Pb/206Pb Evaporation Ages of Panafrican Metasedimentary Rocks in the Kombé-II Area (Bafia Group, Cameroon): Constraints on Protolith Age and Provenance. *Journal of African Earth Sciences,* **51**, 77-88. doi.org/10.1016/j.jafrearsci.2007.12.003

**Gat, J. R. (1981).** Isotopic fractionation. In: Stable isotope hydrology, deuterium and oxygen-18 in water cycle, *Technical Reports Series* **210**, IAEA, Vienna, 21–3.

**Gat, J. R. (1996).** Oxygen and hydrogen isotopes in the hydrologic cycle. *Annual Review Of Earth And Planetary Sciences***, 24**, 1996, 225-262, https://doi.org/10.1146/annurev.earth.24.1.225.

**Gat, J. R. (2010).** Isotope Hydrology: A Study of the Water Cycle. *Series on Environmental Science and Management* **6**. Imperial College Press, London.

**Gat, J.R. and Gonfiantini, R., Eds. (1981).** Stable Isotope Hydrology: Deuterium and Oxygen-18 in the Water Cycle. *IAEA Technical Report Series* #210, Vienna, 337.

**Gentry, F. C., Nkoumbou, C., Tchakounte Numbem, J., Kundu Okia Mukete, Tchouankoue, J.P. (2021).** Petrology, geochemistry, Ar\\Ar isotopes of an arc related calk-alkaline pluton from Mamb (Pan-African Yaounde group, Cameroon): A testimony to the subduction of a hot oceanic crust. *Lithos* 384–385, doi.org/10.1016/j.lithos.2021.105973

**Gibbs, R. J. (1970).** Mechanisms controlling world water chemistry. *Science,* **17**, 1088–1090.

**Gibrilla ,A., Joseph, R. F., Samuel, G., Dickson, A., Geophrey, A., Nafisatu, Z. (2020).** Nitrate contamination and source apportionment in surface and groundwater in Ghana using dual isotopes (15N and 18O-NO3) and a Bayesian isotope mixing model, **Journal of Contaminant Hydrology,** 233, https://doi.org/10.1016/j.jconhyd.2020.103658

**Gonfiantini R., Roche M.-A., Olivry J.-C., Fontes J.-C., Zuppi G.M. (2001).** The altitude effect on the isotopic composition of tropical rains. *Chemical Geology* **181**, 147–167. https://doi.org/10.1016/S0009-2541(01)00279-0

**Goufo, P. (2008).** Rice production in Cameroon: a review. *Research Journal of Agriculture and Biological Sciences*, **4**(6), 745-756. http://www.aensionline.com/rjabs/rjabs/2008/745-756.pd

**Han, D. M., Song, X. F., Currell, M. J., Yang, J. L., Xiao, G. Q. (2014).** Chemical and isotopic constraints on evolution of groundwater salinization in the coastal plain aquifer of Laizhou Bay, China. *Journal of Hydrology*, **508**, 12-27

**Han, G., Liu, C-Q (2004).** Water geochemistry controlled by carbonate dissolution: a study of the river waters draining karst-dominated terrain, Guizhou Province, China. *Chemical Geology* **204**:1–21

**Heaton, T. H. E.; Talma, A. S.; Vogel, J. C. (1983).** Origin and History of Nitrate in Confined Groundwater in the Western Kalahari. *Journal of Hydrology.* 1983**, *62*,** 243-262

**Hem, J. D. (1989).** Study and Interpretation of Chemical Characteristics of Natural Waters. *3rd Edition, US Geological Survey Water Supply Paper* 2254

**Hinton, R. G., Macleod, C. J., Troldborg, M., Kanjaye, M. B., & Kalin, R. M. (2023).** The status of sanitation in Malawi: is SDG6. 2 achievable?. *International Journal of Environmental Research and Public Health*, **20**(15), 6528.

**Hounslow, A.W. (1995).** Water quality data: analysis and interpretation. Lewis Publishers, Boca Raton

**IAEA (2006).** Use of chlorofluorocarbons in hydrology: A guide book. International Atomic Energy Agency, (2006) STI/PUB/1238, Vienna.

**IAEA/WMO (2024).** Global Network of Isotopes in Precipitation. The GNIP Database Accessible at: https://nucleus.iaea.org/wiser.

**Isao, M., Masahiko, O, Takafumi, K., Yasuhide, M. (2022).** Applicability of d-excess and $^{17}$O-excess as groundwater tracers for determination of recharge area. *Hydrogeology Journal* (2022) **30**:2027–2041, https://doi.org/10.1007/s10040-022-02526-0

**Izbicki, J.A., (1996).** Use of 818O and 6D to define seawater intrusion, in Bathala, C.T., ed., North American Water and Environmental Congress: *American Society of Civil Engineers, IR Div/ ASCE.*

**Jalali, M. (2007).** Hydrochemical identification of groundwater resources and their changes under the impact of human activity in the Chah Basin in Western Iran. *Environmental Monitoring and Assessment*, **130**, 347-364.

**Jawhar, M.-S. T., Erkan, D., Masoud, H. H. (2024).** Hydrogeochemical evolution processes, groundwater quality, and non-carcinogenic risk assessment of nitrate-enriched groundwater to human health in diferent seasons in the Hawler (Erbil) and Bnaslawa Urbans, Iraq.

*Environmental Science and Pollution Research*, **31**:26182 26203 https://doi.org/10.1007/s11356-024-32715-1

**Jiofack, T., Guedje, N. M., Tchoundjeu, Z., Fokunang, C., Lejoly, J., Kemeuze, V. (2013).** Agroforestry typology of some cocoa based agroforests in the Mbam and Inoubou division: The importance for local population livelihoods, *Journal of Ecology and the Natural Environment*, **5**(12), 378-386. doi.org/10.5897/JENE12.085

**Jokam Nenkam, T. L., Kringel, R., Fantong, W. Y., Nbendah, P., Fouépé Takoundjou, A., Elisabeth, Z., & Kamtchueng, B. T. (2022).** Hydrochemistry of nutrients in groundwater under farmland in the Benue River Basin, North-Cameroon. *Environmental Earth Sciences*, ***81***(7), 209.

**Jung, H., Koh, D. C., Kim, Y. S., Jeen, S. W., Lee, J. (2020).** Stable isotopes of water and nitrate for the identification of groundwater flowpaths: A review. *Water*, ***12*(**1), 138.

**Kaiser, H. F. (1960).** The Application of Electronic Computers to Factor Analysis. *Educational and Psychological Measurement*, **20**, 141-151. http://dx.doi.org/10.1177/001316446002000116

**Kamga, G.R., Dissak-Delon, F.N., Nana-Djeunga, H.C., Biholong, B.D., Mbigha-Ghogomu, S., Souopgui, J., Zoure, H.G., Boussinesq, M., Kamgno, J., Robert, A. (2016).** Still mesoendemic onchocerciasis in two Cameroonian community-directed treatment with ivermectin projects despite more than 15 years of mass treatment. 2016 Nov 14;9(1):581. doi.org/ 10.1186/s13071-016-1868-8.PMID: 27842567; PMCID: PMC5109673

**Kamtchueng, B. T., Foupouagnigni, A., Mero, Y., Josephine, N., Mumbfu, E. M., Mengnjo, J. W., Muga, Y., Gloria, E. T., Andrew, A. A., Yetoh, F. W., Emmanuel, N., Takeshi, O. (2022).** Major ions, trace elements and stable isotope characteristics of shallow groundwater in the Bonaberi district, Douala, Cameroon, *Sustainable Water Resources Management*, **8:**162 doi.org/10.1007/s40899-022-00737-7

**Kamtchueng, B.T., Fantong, W.Y., Wirmvem, M.J., Tiodjio, R.E., Takounjou, A.F., Ndam Ngoupayou, J.R., Kusakabe, M., Zhang, J., Ohba, T., Tanyileke, G., Hell, J.V. and Ueda, A. (2016).** Hydrogeochemistry and Quality of Surface Water and Groundwater in the Vicinity of Lake Monoun, West Cameroon: Approach from Multivariate Statistical Analysis and Stable Isotopic Characterization. *Environmental Monitoring and Assessment*, **188,** 524. https://doi.org/10.1007/s10661-016-5514-x

**Kana, A. A. (2022).** Heavy metal assessment of groundwater quality in part of Karu, Central Nigeria. *Water Practice & Technology* **17** No 9, 1802, doi: 10.2166/wpt.2022.102

**Karklins, S. (1996).** Groundwater sampling desk reference. *Wisconsin Department of Natural Resources Bureau of Drinking Water and Groundwater*, (1996) PUBL-DG-037 96.

**Kebede, S. and Travi, Y. (2012).** Origin of the d18O and d2H composition of meteoric waters in Ethiopia. *Quartenary International* **257**:4–12

**Keesari, T., Ramakumar, K.L., Chidambaram, S., Pethperumal, S., Thilagavathi, R. (2016).** Understanding the hydrochemical behavior of groundwater and its suitability for drinking and agricultural purposes in Pondicherry area, South India–a step towards sustainable development. *Groundwater for Sustainable Development* (2016) **2**: 143–153.

**Kendall, C. (1998).** Tracing Nitrogen Sources and Cycling in Catchments, In: M. J. Kendall, Ed., Isotope Tracers in Catchment Hydrology, *Elsevier Science B.V.,* 1998, pp. 519-576. doi:10.1016/B978-0-444-81546-0.50023-9

**Kendall, C., Elliott, E. M., Wankel, S. D. (2007).** Tracing anthropogenic inputs of nitrogen to ecosystems in stable isotopes in ecology and environmental science, 10.1002/9780470691854.ch12

**Ketchemen-Tandia, B., Ntamak-Nida, M.J., Boum-Nkot, S., Wonkam, C., Emvoutou, H., Ebonji Seth, C., Aranyossy, J.E. (2007).** First results of the isotopic study ($^{18}O$, $^{2}H$, $^{3}H$) of the Douala Quatenary aquifer (Cameroon). In IAEA (Ed), Advances in isotope hydrology and its role in sustainable water resources management (IAEA-CN 151/37). Vienna: IAEA.

**Ketchiemo, T., F., Fotso, B., Djabou, A. S., Eyamo, J., Essambita, J., Tang, F., Niemenak, N. (2024).** Soil Physico-Chemical Properties and Different Altitudes Affect Arbuscular Mycorrhizal Fungi Abundance and Colonization in Cacao Plantations of Cameroon. *American Journal of Plant Sciences*. **15.** 57-82. 10.4236/ajps.2024.152005

**Khan, F., Krishnaraj, S., Raja P., Selvaraj G., Cheelil R. (2020).** Impact of hydrogeochemical processes and its evolution in controlling groundwater chemistry along the east coast of Tamil Nadu and Puducherry, India. *Environmental Science and Pollution Research*, **28** (15), 18567–18588, doi.org/10.1007/s11356-020-10912y

**Khan, M., Xiao, Y., Yang, H., Zhang, Y., Wang, L., Wang, J., Hu, W., Chen, F., & Shrestha, R. (2024).** Geochemical characteristics, mechanisms, and suitability of groundwater resource for sustainable water supply in Quetta valley. *Water Supply*. **24.** 10.2166/ws.2024.108.

**Kuitcha, D., Fouépé Takounjou, A.L., Ndjama, J., Takem, E. G., Tita, A. M., Kamgang, K. B., Ekodeck, G.E. (2012).** Chemical and Isotopic Signal of Precipitation in Yaounde-Cameroon, *Scholars Research Library, Archives of Applied Science Research* (2012) **4** (6), 2591-2597.

**Lachassagne, P. and Wyns, R. (2005).** Aquifère du socle: Nouveaux concepts. Application à la prospection et la gestion de la ressource en eau. *Géosciences***, 2**, 32-37.

**Lachassagne, P., Dewandel, B., Wyns, R. (2021).** Hydrogeology of weathered crystalline/hard-rock aquifers-guidelines for the operational survey and management of their groundwater resources [Review]. *Hydrogeology Journal*, [Early access], **34**, ISSN 1431-2174.

**Lachassagne, P., Robert, W., Dewandel, B. (2011).** The fracture permeability of Hard Rock Aquifers is due neither to tectonics, nor to unloading, but to weathering processes. *Terra Nova*, doi: 10.1111/j.1365-3121.2011.00998.x

**Lapworth, D.J., Nkhuwa, D.C., Okotto-Okotto, J., Pedley S., Stuart, M.E., Tijani, M.N., Wright, J. (2017).** Urban groundwater quality in SubSaharan Africa: current status and implications for water security and public health. *Hydrogeology Journal***, 25,** 1093–1116.

**Leumbe, O., Ouafo, M., Ndjigui P.-D. (2022).** Mapping Agronomic Suitability of Soils in Forest Savannah Transition Zone in Cameroon: A Case Study from Bokito District of the Central Region. *Environmental Sciences Proceedings*, **16**. 38. 10.3390/environsciproc2022016038

**Lindsey, B.D.; Jurgens, B.C.; Belitz, K. (2019).** Tritium as an Indicator of Modern, Mixed, and Premodern Groundwater Age; US Geological Survey: Reston, VA, USA.

**Lloyd, W. and Heathcote, A. (1985).** Natural Inorganic Hydrochemistry in Relation to Groundwater, an Introduction. Oxford: Clarendon Press.

**Loanathan, K. and Ahamed, A. J. (2017).** Multivariate Stiatistical Techniques for the Evaluation of Groundwater Quality of Amaravathi River Basin, Sounth India. *Applied Water Sciences*, **7**, 4633-4649, https://doi.org/10.1007/s13201-017-0627-0

**Loehnert, E.P. (1988).** Major chemical and isotope variations in surface and subsurface waters of West Africa. *Journal of African Earth Science* **7**:579–588

**Maimoona, R., Abida, F., Nabeel, K. N., Arslan, A. (2016).** Geochemical control on spatial variability of fluoride concentrations in groundwater from rural areas of Gujrat in Punjab, Pakistan. *Environmental Earth Science* (2016) **75**:1364, DOI 10.1007/s12665-016-6155-7

**Malov, A.I. (2023).** Features of the Formation of Strontium Pollution of Drinking Groundwater and Associated Health Risks in the North-West of Russia. *Water*, **15,** 3846. https://doi.org/10.3390/ w15213846

**Mapoma, H. W. T., Xianjun, X., Mathews, T. N., Liping, Z., Chikumbusko, C. K., Rex, M. (2017).** Trace elements geochemistry of fractured basement aquifer in southern Malawi: A case of Blantyre rural, *Journal of African Earth Sciences*, http://dx.doi.org/10.1016/j.jafrearsci.2017.04.011

**Mariotti, A., Landreau, A., Simon, B. (1988).** 15N isotope biogeochemistry and natural denitrification process in groundwater: application to the chalk aquifer of northern France. *Geochimica Cosmochimica Acta* **52**, 1869–1878.

**Marszałek Anna (2022).** Adsorption of copper and lead from rainwater using adsorbents based on diatomite and calcium alginate, *Desalination and Water Treatment*, 275, 81-91, https://doi.org/10.5004/dwt.2022.28763

**Masiol, M., Zannoni, D., Stenni, B., Dreossi, G., Zini, L., Calligaris, C., Karlicek, D., Michelini, M., Flora, O., Cucchi, F., Treu, F. (2021).** Spatial distribution and interannual trends of δ18O, δ2H, and deuterium excess in precipitation across North-Eastern Italy. *Journal of Hydrology***, 598**, 125749. https://doi.org/10.1016/j.jhydrol.2020.125749

**Mayer, B., Sandra, M. B., Tim, M., Birgit, H., Jan, V. (2001).** The oxygen isotope composition of nitrate generated by nitrification in acid forest floors, *Geochimica et Cosmochimica Acta*, **65,** Issue 16, 2743-2756, https://doi.org/10.1016/S0016-7037(01)00612-3

**McCallum, J. E., Ryan, M. C., Mayer, B., Rodvang, S. J. (2008).** Mixing-induced groundwater denitrification beneath a manure field in southern Alberta, Canada. *Applied Geochemistry*, **23** (8) 2146-2155, https:/doi.org/10.1016/j.apgeochem.2008.03.018

**Menti, A. N., Egome, R. W., Agyingi, C., Menjo, J. W., Nfor, J. N. (2023).** Hydrogeochemical characterization of ground and surface water in the eastern part of the Adamawa-Yade domain, Bertoua-Cameroon. *Discover Water*, **3**:10, | https://doi.org/10.1007/s43832-023-00034-0

**Mfonka, Z., Amidou, K., Ngouh, A. N., Mouncherou, O,, Nsangou, D., Rakotondrabe, F., Fouepe Alain, T., Zammouri, M., Ndam Ngoupayou, J., Ndjigui, P.-D. (2021).** Water Quality Assessment in the Bamoun Plateau, Western-Cameroon: Hydrogeochemical Modelling and Multivariate Statistical Analysis Approach. *Journal of Water Resource and Protection*, **13**, 112-138, 10.4236/jwarp.2021.132007

**Mink, P. J., Dominik, D. A., Leila, M. B., Michael, A. K., Joyce, S. T. (2008).** Low-level arsenic exposure in drinking water and bladder cancer: A review and meta-analysis, *Regulatory Toxicology and Pharmacology*, **52**, Issue 3, 299-310, https://doi.org/10.1016/j.yrtph.2008.08.010.Jobby et al. 2018

**Morales, J. C. (2017).** Groundwater/Surface Water Interface and Radioactive Contaminant Ecological Risk Assessment Using EPA Method at the F-Area Seepage Basins-Savannah River Site (SRS) Aiken, SC (Doctoral dissertation, Florida International University).

**Moshood, N. T., Saheed, A. O., Akinyemi, T. O. (2014).** Hydrogeochemical characterization of a shallow groundwater system in the weathered basement aquifer of Ilesha area, southwestern Nigeria. Evolving Water Resources Systems: Understanding, Predicting and Managing Water–Society Interactions Proceedings of ICWRS2014, Bologna, Italy, June 2014 (*IAHS Publ*. **364**, 2014), doi:10.5194/piahs-364-475-2014.

**Muller, D., Blu, A., Hooke, J., Kunke, R., Scheidlede, A., Tomli, C., Wendlan, F. (2006).** Final proposal of a methodology to set up groundwater threshold values in Europe. Specifc targeted EU research project BRIDGE (contract No SSPI-2004- 006538)- report D18. *Environmental Forensics* **18**, 62–73. https://doi.org/10.1080/ 15275922.2016.1263904 wfd-bridge.net ain

**Mutin, G., (2000).** De l'eau pour tous. Documentation photographique, Bimestriel N° 8014 64 p.

**Mvongo, V. D., Celestin, D., Paul Fabrice, N., Boniface, E., Mbey, J. G. O.(2024).** Analysis of water losses in seven small and medium-sized water distribution networks in the south region of Cameroon (Central Africa). *Water Practice and Technology* 1 December 2024; **19** (12): 4682–4698. doi: https://doi.org/10.2166/wpt.2024.248

**Nadjai, S., Hichem, K., Bouchema, N., Nabed, N., Bouderbala, A., Benaabidate, L. (2024).** Groundwater availability for irrigation purposes: Case of Middle Cheliff aquifer Algeria. *Journal of Agriculture and Applied Biology*. **6**. 13-37. 10.11594/jaab.06.01.02

**Ndjama, J., Gustave, R. N., Eyong, G., Biram À Ngon, E. B., Takounjou, A., Mafany, G.T., Mewouo, C. (2021).** Assessment of Sediment Contamination by Heavy Metals in the Water of

Mgoua Catchment in the Industrial Zone of Douala (Cameroon). *Science Journal of Analytical Chemistry*. **9**. 58. 10.11648/j.sjac.20210903.11

**Ngouokouo, T., A., Enyegue A Nyam, F.M., Kouamou, N,, S.R. et al. (2025)**. Bivariate statistical and neural network models to map groundwater potential zones in Bafia area (Central Cameroon). *Modeling Earth Systems and Environment*, **11**, 44 (2025), https://doi.org/10.1007/s40808-024-02206-w

**Ngoupayou Ndam, J.R., Dzana, J.G., Kpoumie ,A., Tanwi, G. R., Fouepe Takounjou, A., Braun, J.J., Ekodeck, G.E. (2016).** Present-day sediment dynamics of the Sanaga catchment (Cameroon): from the total suspended sediment (TSS) to erosion balance. *Hydrological Science Journal* **61**(6):1080–1093. https://doi.org/10.1080/02626667.2014. 968572

**Ngoupayou, J. R. N., Bon, A. F., Guillaume, E. M., Nasser, N. A. and Ekodeck, G. E. (2019).** Hydrogeological Characteristics of Shallow Hard Rock Aquifers in Yaounde (Cameroon, Central Africa) *Groundwater Hydrology*, DOI: http://dx.doi.org/10.5772/intechopen.84631

**Nlend, B., Huneau, F., Boum-Nkot, N. S., Song, F., Komba, D., Gwodog, B., Meyoupe, P., Djieugoue, B., Fongoh, E. (2023).** Review of isotope hydrology investigations on aquifers of Cameroon (central Africa): what information for the sustainable management of groundwater resources? *Water* **15**, 4056. https://doi. org/10.3390/w15234056

**Noizet G. (1982).** "Disposition Géologique des Régions de Yaounde et Bafia," Annales de la Faculté des Sciences Yaounde

**Nyilitya, B., Stephen, M., Marijn, B., Pascal, B. (2021).** Nitrate source apportionment in the complex Nyando tropical river basin in Kenya. *Journal of Hydrology* **594** (2021) 125926 https://doi.org/10.1016/j.jhydrol.2020.125926

**Ogana, S. J., Friday, O., Kupi, T., Mathuthu, M. (2024).** Health risk assessment of heavy metals and physicochemical parameters in natural mineral bottled drinking water using ICP-MS in South Africa. *Applied Water Science*. **14**. 17. 10.1007/s13201-024-02267-3

**Olivry, J.C., (1986).** Fleuves et rivières de Cameroun. Monographie hydrologiques. MESRES/ORSTOM ,733.

**Ondoa Mvondo J. (2009).** Caractérisation des évènements tectoniques dans le domaine Sud de la chaine Panafricaine au Cameroun: Styles tectoniques et géochronologiques des séries de Yaoundé et Bafia. Unpublished Ph.D Thesis, University of Yaoundé I.

**Panno, S.V., Kelly, W.R., Martinsek, A.T., Hackley, K.C. (2006).** Estimating background and threshold nitrate concentrations using probability graphs. *Ground Water* **44**, 697–709.

**Pare, Samuel and Bonzi-Coulibaly L. Y. (2013).** Water quality issues in West and Central Africa: present status and future challenges, *Proceedings of H04*, IAHS-IAPSO-IASPEI (IAHS Publ. 361).

**Parhurs, D. L., and Appelo, C. A. J. (1999).** PHREEQC for Windows version 1.4.07.A Hydrogeochemical transport model. US Geological Survey software

**Piper, A. M. (1944).** A graphic procedure in the geochemical interpretation of water analyses. *American Geophysical Union Transcript*, **25**, 914–923.

**Powlson, D., Addiscott, T., Benjamin, N., Cassman, K., de Kok Theo, Grinsven, H., L'Hirondel J.-L., Avery, A., Kessel, C. (2008).** When Does Nitrate Become a Risk for Humans? *Journal of Environmental Quality*, **37**, 291-5. 10.2134/jeq2007.0177

**Rakotondrabe, F., Ndam Ngoupayou, J., Zakari, M., Rasolomanana, E., Abolo, A., Asone, B., Ako, A., Rakotondrabe, M (2017).** Assessment of Surface Water Quality of Bétaré-Oya Gold Mining Area (East-Cameroon). *Journal of Water Resource and Protection.* **09**. 960-984. 10.4236/jwarp.2017.98064

**Ravikumar, P. and Somashekar, R.K. (2017).** Principal component analysis and hydrochemical facies characterization to evaluate groundwater quality in Varahi river basin, Karnataka state, India. *Applied Water Science*, **7**, 745–755 https://doi.org/10.1007/s13201-015-0287-x

**Ravikumar, P., Somashekar, R.K., Angami, M. (2011).** Hydrochemistry and evaluation of groundwater suitability for irrigation and drinking purposes in the Markandeya River basin, Belgaum District, Karnataka State, India. *Environmental Monitoring and Assessment*. **173**. 459-487. 10.1007/s10661-010-1399-2

**Ravikumar, P., Venkatesharaju, K., Somashekar, R.K. (2009).** Major ion chemistry and hydrochemical studies of groundwater of Bangalore South Taluk, India. *Environmental Monitoring and Assessment* **163**:643–653.

**Re, V., Sacchi, E., Kammoun, S., Tringali, C., Trabelsi, R., Zouari, K., Daniele, S. (2017).** Integrated socio-hydrogeological approach to tackle nitrate contamination in groundwater resources. The case of Grombalia Basin (Tunisia). *Science of the Total Environment*, ***593,*** 664-676.

**Rencher, A. C. (2002).** Methods of multivariate analysis (2nd ed.p.732). Inc: John Wiley & Sons

**Risi, C., Bony, S., Vimeux, F., Descroix, L., Ibrahim, B., Lebreton, E., Mamadou, I., Sultan, B. (2008).** What controls the isotopic composition of the African monsoon precipitation? Insights from event-based precipitation collected during the 2006 AMMA field campaign. *Geophysical Research Letters* **35**:L24808.

**Rodier, J., (2009).** Analyse de l'eau. Dunod, 9ème Ed. Paris, 1579.

**Rooyen, V. J. D., Palcsu, L., Visser, A., Vennemann, T.W., Miller, J.A. (2021).** Spatial and temporal variability of tritium in precipitation within South Africa and it's bearing on hydrological studies, *Journal of Environmental Radioactivity*, **226**, https://doi.org/10.1016/j.jenvrad.2020.106354

**Schoeller, 1962.** Les eaux souterraines. Ed. Masson et Cie. Paris.Sci. *Geol.Bull*., **39**, 3-77.

**Schoeller, H. (1965).** Qualitative Evaluation of Groundwater Resources. In: Methods and Techniques of Groundwater Investigations and Development, UNESCO, Paris, 54-83.

**Schoeller, H. (1967).** Qualitative Evaluation of Groundwater Resources. In Methods and Technics of Groundwater Investigation and Development, 44-52. *Water Resource Series* No. **33**, Paris: UNESCO.

**Scholl, M. A., Gingerich, S. B., Tribble, G. W. (2002).** The influence ofmicroclimates and fog on stable isotope signatures used in interpretationof regional hydrology: East Maui, Hawaii, *Journal of Hydrology*, **264**, 170 – 184,doi:10.1016/S0022-1694(02)00073-2

**Segalen, P. (1967).** Les Sols et la Geomorphologie du Cameroun. *Cahier ORSTOM Series Pédologique*, **2,**137-187.Hoffmann et al. 2012.

**Sellerino, M. (2014).** Methods of determination ofnatural background levels in groundwater: a review. The defnition of natural background levels (NBLs) in groundwater and soils – case studies in Italy and Portugal. In: Implementation of Eco-Compatible Protocols for Agricultural Soil Remediation in Litorale DomizioAgro Aversano NIPS. Naples, 26th February, 2014.

**Silva, T. R., Teresa, E. L., Mariucha, M.C. L., Tiago, N. M., Manuel, M. O., Mateus, S.C., Waldir, D. C. (2021).** Hydrogeochemistry and isotope compositions of multi-layered aquifer systems in the Recife Metropolitan Region, Pernambuco (NE Brazil): An integrated approach using multivariate statistical analyses, *Journal of South American Earth Sciences*, **109**, https://doi.org/10.1016/j.jsames.2021.103323

**Singh, A.K., Mondal, G.C., Singh, T,B,, Singh, S., Tewary, B.K., Sinha, A. (2012).** Hydrogeochemical processes and quality assessment of groundwater in Dumka and Jamtara districts, Jharkhand, India. *Environmental Earth Science*, **67:**2175–2191.

**Singh, G. and Rakesh K.K. (2016).** Heavy Metal Contamination and Its Indexing Approach for Groundwater of Goa Mining Region, India. *Applied Water Sciences*, **7,** 1479-1485. https://doi.org/10.1007/s13201-016-0430-3

**Spearman, C. (1904).** The Proof and Measurement of Association between Two Things. *America Journal of Psychology*, **15,** 72-101.

**Srinivasamoorthy, K., Chidambaram, S., Prasanna, M. V., Vasanthavihar, M., John, peter A., Anandhan, P. (2008).** Identification of major sources controlling groundwater chemistry from a hard rock terrain – A case study from Mettur taluk, Salem District, Tamil Nadu, India: *Journal of Earth System Science* **117**(1) 49–58.

**Stuyfzand, P. J. (1989).** Nonpoint sources of trace elements in potable groundwaters in the Netherlands. Proceedings 18th TWSA water workings, Testing and Research Institute (IWSA), Copenhagen.

**Subba, R. N., Prakasa, R. J., John, D. D., Srinivasa, R. K. V., Krishna, C., Nagamalleswara, R. B. (2002).** Hydrogeochemistry and Groundwater Quality in a Developing Urban Environment of a Semi-Arid Region, Guntur, Andhra Pradesh, India. *Journal of the Geological Society of India*, **59,** 159-166.

**Tabué, Y. J. G., (2013).** Vulnérabilité de la nappe superficielle en zone de socle cristallin urbanisé : cas du bassin versant de la Mingoa à Yaoundé au Cameroun. *Revue de l'Université de Moncton*, **40** (2), 71-96.

**Tabué, Y. J. G., Ntep, F., Feumba, R., Ngamy, A., Madi, B., Ngos II Simon, Ngounou, N. (2021).** Influence of Local Structural Factors on the Hydraulic Productivity of Bores in the Fractured Cristalline Zone: Case of the Mbam and Lékié Region – Cameroon, *International Journal of Innovative Science, Engineering and Technology* **8** (7).

**Tabué, Y. J. G., Roger, F., Valérie, T. N., Ghislain de Marsily, Georges, E. E. (2009).** Pollution de l'eau souterraine et risques sanitaires à Yaoundé au Cameroun, *Comptes Rendus Biologies*, **336**, Issues 5–6, 310-316, https://doi.org/10.1016/j.crvi.2013.04.013

**Takounjou, F. A., Ndam Ngoupayou, J.R., Riotte, J., Takem, G.E. (2010).** Estimation of groundwater recharge of shallow aquifer on humid environment in Yaounde, Cameroon using hybrid water-fuctuation and hydrochemistry methods. *Environmental Earth Sciences* **64**:107–118.

**Takounjou, F. A., Takem, E. G., Kuitcha, D., Kringel, R., Fantong, Y. W., Ndjama, J., Tejiobou, A. (2020).** Hydrogeochemistry and groundwater fow mechanisms in shallow aquifer in Yaounde, Cameroon. *Water Supply* **20**:1334–1348.

**Takounjou, F. A.., Kuitcha, D., Fantong, W.Y., Ewodo, M.G., Khan, H. H., I., Takeshi, O. (2013).** Assessing groundwater nitrate pollution in Yaounde, Cameroon: Modelling Approach. World *Applied Science Journal*, **23** (3): 333-344.

**Takounjou, F.A., Gurunadha V.V.S., Ndam, N.J., Sigha-Nkamdjou, L., Ekodeck, G. (2009).** Groundwater flow modelling in the upper Anga'a River watershed, Yaounde, Cameroon. African *Journal of Environmental Science and Technology.* **3.** 341-352.

**Tamehe, L. S., Chongtao, W., Ganno, S., Simon, S. J., Nono, G. D. K., Nzenti, J. P., ... & Lin, N. H. (2019).** Geology of the Gouap iron deposit, Congo craton, southern Cameroon: Implications for iron ore exploration. *Ore Geology Reviews*, **107**, 1097-1128.

**Tarla, D.Bantar, V., Mfopou, M., Fotio, D., Fontem, D. (2015).** Determination of Heavy Metal Concentration in Surface Waters of the Western Highlands of Cameroon. *Journal of Geography, Environment and Earth Science International.* **2**. 46-53. 10.9734/JGEESI/2015/15726

**Tay, C. K. (2021).** Hydrogeochemical framework of groundwater within the Asutif-North District of the Brong-Ahafo Region, Ghana, *Applied Water Science* **11**:72, doi.org/10.1007/s13201-021-01398-1

**Taylor, R.G. and Howard, K.W.F. (1996).** Groundwater recharge in the Victoria Nile basin of East Africa: support for the soil moisture balance method using stable isotope and fow modelling studies. *Journal of Hydrology* **180**:31–53

**Tchakounté, J. N., Fuh, C. G., Aurélie, N. K., Metang, V., Joseph, M. O., Nkoumbou, C. (2021**). Petrology and geochemistry of the Pan-African high-K calc-alkaline to shoshonitic–adakitic Bapé plutonic suites (Adamawa-Yade block, Cameroon): evidence of a hot oceanic crust subduction. *International Journal of Earth Sciences*. **110,** 2067–2090 doi.org/10.1007/s00531-021-02060-6

**Tchakounté, J. N., Toteu, S.F., William, R. V., Joseph, P., Etienne, D., Mvondo, O., Merlain, B. H., Ganwa, A., William, M. W. (2007).** Evidence of ca 1.6-Ga detrital zircon in the Bafia Group

(Cameroon): Implication for the chronostratigraphy of the Pan-African Belt north of the Congo craton. Comptes Rendus. *Géoscience*, **339** (2007) no. 2, 132-142.

**Tchakounté, J., Eglinger, A., Toteu, S.F., Zeh, A., Nkoumbou, C., Mvondo-Ondoa, J., Penaye, J., de Wit M., Barbey, P. (2017).** The Adamawa-Yadé Domain, a Piece of Archaean Crust in the Neoproterozoic Central African Orogenic Belt (Bafia Area, Cameroon). *Precambrian Research*, **299,** 210-229. doi.org/10.1016/j.precamres.2017.07.001

**Temkin, A., Evans, S., Manidis ,T., Campbell, C., Naidenko, O. V. (2019).** Exposure-based assessment and economic valuation of adverse birth outcomes and cancer risk due to nitrate in United States drinking water. *Environmental research*, **176**, 108442

**Thatcher, L.L., Janzer, V.J., Edwards, R.W. (1977).** Methods for determination of radioactive substances in water and fluvial sediments. Techniques of water resources investigations of US Geological survey, Washington: US Government printing office (1977) 79-81.

**Tiwari, A.K. and Singh A.K. (2014).** Hydrogeochemical investigation of groundwater quality assessment of Pratapgarh district, Uttar Pradesh. *Journal of Geological Science India* **83**, 329–343.

**Toteu, S.F., Penaye, J., Poudjom, D. Y. (2004).** Geodynamic evolution of the Pan African belt in central Africa with special reference to Cameroon, *Canadian Journal of Earth Sciences* **41** 73–85.

**U.S. Salinity Laboratory. (1954).** Diagnosis and improvement of saline and alkali soils (p. 160) (Agriculture Handbook NO. 60). USDA.

**United Nations (2016)** The sustainable development goals report.

**United Nations Development Programme (2023)** UNDP at the UN Water Conference: Robust actions needed to manage, conserve, protect water and improve live.

**United States Environmental Protection Agency (1989).** Risk Assessment Guidance for Superfund. Volume I. Human Health Evaluation Manual (Part A). https://rais.ornl.gov/documents/HHEMA.pdf.

**United States Environmental Protection Agency (USEPA) (1995).** Final water quality guidance for the Great Lakes system; fnal rule: Washington, DC. Federal Register. 1995;**60**(56):15365-15425.

**Vallerie, M. (1973).** Contribution à l'étude des sols du centre sud Cameroun types de différenciation morphologique et pédogénétique sous climat subéquatorial. O.R.S.T.O.M.

**Van Hecke, K., Van Cleemput, O., Baert, L. (1990).** Chemo-denitrification of nitrate-polluted water. *Environmental Pollution*. **63,** 261–274

**Vengosh, A., Gill, J., Davisson, M.L., Hudson, G.B. (2002).** A multi-isotope (B, Sr, O, H, and C) and age dating ($^{3}H$ – $^{3}He$ and $^{14}C$) study of groundwater from Salinas Valley, California: hydrochemistry, dynamics, and contamination processes. *Water Resources* **38.** No 1 1008.0043-1397/02/2001WR000517.

**Verma, R., and Dwivedi, P. (2013).** Heavy metal water pollution-A case study. *Recent research in Science and Technology*, **5**(5).

**Viennois, G., Bétard, F., Freycon, V., Barbier, N., Couteron, P. (2022).** Automated landform classification and mapping using a combined textural-morphometric approach: The Congo basin and surroundings. *Journal of Geomorphology*, **1** (1): 79-102. https://doi.org/10.1127/jgeomorphology/2022/0752

**Vijay, S. and Tripathi (1979).** Factor analysis in geochemical exploration, *Journal of Geochemical Exploration,* 11, 263-275, https://doi.org/10.1016/0375-6742(79)90004-9

**Wang, Z., Wan, Y., Ma, Z., Xu L., Zhai, Y., Su X. (2025).** Impact of Iron Minerals on Nitrate Reduction in the Lake–Groundwater Interaction Zone of High-Salinity Environment. *Water*. **17.** 1241. 10.3390/w17091241.

**Ward. J.H. (1963).** "Hierarchical Grouping to Optimize an Objective Function*", Journal of the American Statistical Association,* **58**, 236–244.

**WHO and UNICEF (2013).** Progress on Sanitation and Drinking Water, update. *Rapport technique*, 40p

**Wilcox, L. V. (1955).** Classification and use of irrigation water. *US Geological Department Agri. Circ.* 969: 19

**Wirmvem, M. J., Mumbfu, E. M., Brice, T.K., Engome, R. W., Tasin, G. B., Asobo, N. E. A., Yetoh, F., Samuel, N. A., Takeshi, O. (2017).** Shallow Groundwater Recharge mechanism and apparent age in the Ndop plain, northwest Cameroon, *Applied Water Science* **7,** 89–502. https://doi.org/10.1007/s13201-015-0268-0

**Wirmvem, M. J., Takeshi, O., Brice, T.K., Eldred, T. T., Yetoh, F., Ako, A. A., (2016).** Variation in stable isotope ratios of monthly rainfall in the Douala and Yaounde cities, Cameroon: local meteoric lines and relationship to regional precipitation cycle, *Applied Water Science* doi.org/ 10.1007/s13201-016-0413-4

**Wirmvem, M. J., Takeshi, O., Yetoh, F., Ayonghe, S. N., Justice, Y. S., Asobo, N. E. A., Gregory, T., and Joseph V. H. (2013).** Hydrochemistry of shallow groundwater and surface water in the Ndop plain, North West Cameroon. *African Journal of Environmental Science and Technology*, **7(**6), 518-530, June 2013 DOI: 10.5897/AJEST2013.1456

**Wirmvem, M.J., Mimba, M.E., Kamtchueng, B.T., Wotany, E.R., Bafon, T.G., Asaah, A.N.E., Fantong, W.Y., Ayonghe, S.N., Ohba, T. (2015).** Shallow groundwater recharge mechanism and apparent age in the Ndop plain, northwest Cameroon. *Applied Water Science*, doi:10.1007/s13201-015-0268-0

**Wongsasuluk, P., Chotpantarat, S., Siriwong, W., Robson, M. (2014).** Heavy Metal Contamination and Human Health Risk Assessment in Drinking Water from Shallow Groundwater Wells in an Agricultural Area in Ubon Ratchathani Province, Thailand. *Environmental Geochemistry and Health,* **36**, 169-182.

**World Health Organization (2017).** Guidelines for Drinking-Water Quality: *Fourth Edition Incorporating the First Addendum. WHO, Geneva.*

**World Health Organization (2022).** Guidelines for drinking-water quality: *fourth edition incorporating the first and second addenda.*

**Xia, Y.Q., Li, Y.F., Zhang, X.Y., Yan, X.Y., (2017).** Nitrate source apportionment using a combined dual isotope, chemical and bacterial property, and Bayesian model approach in river systems. *Journal of Geophysical Research: Biogeoscience* **122** (1), 2–14. https://doi.org/ 10.1002/2016JG003447

**Xiantao, F., Stephen, J. H., Sonja, M. ., Klaus, B.-B., Rafaela, F. C., Lutz, M., Michael, D., Antony, O., Shuwei, L., Jianwen, Z., Johan, S., Matti, B. (2024).** Mechanisms behind high N2O emissions from livestock enclosures in Kenya revealed by dual-isotope and functional gene analyses, *Soil Biology and Biochemistry*, **196,** https://doi.org/10.1016/j.soilbio.2024.109505

**Xin, D., Andrew, W. Rate, M.A. Mary, G. (2012).** Redistribution and mobilization of titanium, zirconium and thorium in an intensely weathered lateritic profile in Western Australia, *Chemical Geology* (2012) 330–331, 101-115, https://doi.org/10.1016/j.chemgeo.2012.08.030

**Yidana, S. M., Banoeng-Yakub, B., Sakyi, P. A. (2012).** Identifying key processes in the hydrochemistry of a basin through the combined use of factor and regression models. *Journal of Earth System Science*, **121(**2), 491–507.

**Yidana, S. M.,, Patrick, B., Patrick, S., Obed, F. F. (2018).** Evolutionary analysis of groundwater flow: Application of multivariate statistical analysis to hydrochemical data in the Densu Basin, Ghana, *Journal of African Earth Sciences*, **138**, 167-176, https://doi.org/10.1016/j.jafrearsci.2017.10.026

**Yue, F.J., Li, S.L., Liu, C.Q., Zhao, Z.Q., Hu, J. (2013).** Using dual isotopes to evaluate sources and transformation of nitrogen in the Liao River, Northeast China. *Applied. Geochemistry*. **36**, 1–9.

**Zhang, Y., Chen, Z., Sun, J., Wang, J. (2017).** Natural Background Levels of Chemical Components in Groundwater of Hutuo River Catchment Area. North China Pl.; Rahman, A., Tiwari, K.K., Mondal, N.C., 2020. Assessment of hydrochemical backgrounds and threshold values of groundwater in a part of desert area, Rajasthan, India. *Environmental Pollution* https://doi.org/10.1016/j.envpol.2020.115150

**Zhou, J., Du, B., Liu, H., Cui, H., Zhang, W., Fan, X., et al. (2020).** The bioavailability and contribution of the newly deposited heavy metals (copper and lead) from atmosphere to rice (Oryza sativa L.). *Journal of hazardous materials*, **384**, 121285.

## SCIENTIFIC CONTRIBUTIONS

**Tarkang Carine Enow-Ayor,** Dmitri Rouwet, Mero Yannah, Akenji Victorine Neh, Zobo Mbele Henri, Jules Rémy Ndam Ngoupayou, Franco Tassi, Ako Andrew Ako, Takounjou Alain Fouépé, Fantong Wilson Yetoh, Suzanne Ngo Boum-Nkot and Ndjama Joséphine. Hydrogeochemical and isotopic characterization of water resources in crystalline aquifers of Bafia, Cameroon, Scientific African (3rd revision **Under Review**).

## CONFERENCE PROCEEDINGS

IAH World Groundwater Congress, 8th-13th September 2024, Davos Switzerland: Evaluation of the geochemical processes, heavy metal contamination and nitrate pollution of water resources in the Bafia area, Centre Region Cameroon: An Isotopic approach.

## GRANTS

Tarkang Carine Enow-Ayor received a 15 months Fellowship grant from the International Atomic Energy Agency (IAEA) between 2022 and 2025 for a PhD Sandwich programme in the Istituto Nazionale di Geofisica e Vulcanologi, Bologna, Italy, with fellowship code EVT2106130-0001-CMR.

# LIST OF APPENDICES

*Appendix 1a Physical parameters of water resources in Bafia during the rainy season (September, 2022)*

| Code | Location | Lat | Long | Type | CH | WD | WL | Alt | pH | Temp | EC | TDS | Eh | DO | TH | Salinity | Alkalinity |
|---|---|---|---|---|---|---|---|---|---|---|---|---|---|---|---|---|---|
| **BOW01** | Ndengue | 4.752 | 11.241 | OW | 49 | 4.17 | 2.28 | 467 | 5.9 | 26 | 900 | 450 | -38.8 | 5.64 | 72.71 | 1.4 | 34 |
| **BOW02** | Lable 1 | 4.752 | 11.249 | OW | 38 | 3.93 | 2.03 | 479 | 5.7 | 28 | 245 | 120 | -55.2 | 3.12 | 14.01 | 0.4 | 68 |
| **BBH03** | Lable | 4.755 | 11.258 | BH | | | | 486 | 5.4 | 28 | 160 | 80 | -4.1 | 5.31 | 21.07 | 0.2 | 22 |
| **BBH04** | Nyamsong I | 4.755 | 11.265 | BH | | | | 489 | 6.4 | 28 | 590 | 290 | -80 | 7.51 | 61.58 | 0.7 | 170 |
| **BOW05** | Nyamsong I | 4.754 | 11.271 | OW | 26 | 3.38 | 2.53 | 478 | 5 | 27 | 70 | 35 | -78 | 3.21 | 13.05 | 0.1 | 22 |
| **BDOW06** | Donenkeng II | 4.746 | 11.273 | DW | | | | 493 | 5 | 26 | 360 | 180 | 22.5 | 4.56 | 46.85 | 0.6 | 50 |
| **BOW07** | Donenkeng II | 4.739 | 11.281 | OW | 70.9 | 8.22 | 6.58 | 490 | 5 | 28 | 50 | 25 | 39 | 3.45 | 13.27 | 0.1 | 10 |
| **BDSP08** | Donenkeng hospital | 4.736 | 11.283 | DSP | | | | 490 | 5.5 | 26 | 290 | 140 | 16.1 | 3.22 | 65.48 | 0.4 | 40 |
| **BBH09** | Egona | 4.739 | 11.294 | BH | | | | 479 | 5.3 | 27 | 140 | 70 | -27 | 4.56 | 24.88 | 0.3 | 18 |
| **BOW10** | Nyamsong III | 4.736 | 11.254 | OW | 70 | 17.11 | 15.86 | 496 | 5.7 | 26 | 190 | 90 | -15 | 4.86 | 35.08 | 0.3 | 57 |
| **BRW11** | Gamba River | 4.731 | 11.254 | RW | | | | 464 | 6.3 | 24 | 280 | 140 | -33.9 | 5.89 | 49.84 | 0.4 | 61 |
| **BDOW12** | Nyamsong III | 4.74 | 11.249 | DW | | | | 490 | 5.2 | 27 | 100 | 50 | 19.6 | 8.65 | 23.91 | 0.2 | 14 |
| **BOW13** | Bigna Savana | 4.744 | 11.245 | OW | 68 | 10.1 | 8.4 | 496 | 5.3 | 26 | 130 | 65 | | 5.68 | 11.02 | 0.2 | 39 |
| **BOW14** | Lable | 4.751 | 11.244 | OW | 32 | 7.2 | 6.01 | 492 | 5.4 | 26 | 200 | 100 | 14.9 | 6.01 | 22.55 | 0.3 | 34 |
| **BDOW15** | Lable | 4.754 | 11.241 | DW | | 15 | | 499 | 4.9 | 27 | 310 | 150 | 82.8 | 6.22 | 49.75 | 0.5 | 22 |
| **BDOW16** | Biabezock | 4.755 | 11.237 | DW | | | | 503 | 5.2 | 27 | 370 | 180 | 56.5 | 4.35 | 71.25 | 0.6 | 31 |
| **BDOW17** | Lycee Classique | 4.767 | 11.236 | DW | | | | 482 | 5.8 | 28 | 300 | 150 | 21.3 | 4.86 | 18.48 | 0.5 | 84 |
| **BOW18** | Biabezock (behind lycee) | 4.766 | 11.238 | OW | 90 | 6.3 | 4.38 | 476 | 6.6 | 27 | 540 | 270 | -34.8 | 3.98 | 117.17 | 0.8 | 120 |
| **BOW19** | R.A.C | 4.766 | 11.227 | OW | 0 | 4.28 | 1.55 | 473 | 6.6 | 27 | 210 | 110 | -589.5 | 3.12 | 19.35 | 0.3 | 40 |
| **BBH20** | Catholic Diocesse | 4.765 | 11.224 | BH | | | | 474 | 6.3 | 28 | 650 | 320 | -32.7 | 4.12 | 52.49 | 1 | 161 |
| **BRW21** | Nguen river | 4.766 | 11.221 | RW | | | | 472 | 6.3 | 27 | 100 | 50 | -58.4 | 3.01 | 14.99 | 0.2 | 30 |
| **BRW22** | Bohboro river | 4.779 | 11.214 | RW | | | | 469 | 6.8 | 25 | 90 | 40 | -71 | 5.62 | 14.77 | 0.2 | 20 |
| **BDOW23** | Biamo | 4.773 | 11.216 | DW | | 11 | | 484 | 5.6 | 27 | 200 | 100 | -34.2 | 4.75 | 23.53 | 0.3 | 44 |
| **BDOW24** | Sanaam | 4.773 | 11.19 | DW | | 12.5 | | 516 | 4.6 | 28 | 120 | 60 | 11 | 4.85 | 19.63 | 0.2 | 14 |
| **BBH25** | péage | 4.768 | 11.209 | BH | | 40 | | 484 | 5.6 | 27 | 360 | 180 | 6.9 | 5.21 | 41.29 | 0.6 | 105 |
| **BOW26** | Polyvalent | 4.758 | 11.215 | OW | 55 | 3.6 | 2.7 | 488 | 5.7 | 27 | 520 | 260 | -1.1 | 6.02 | 28.77 | 0.8 | 60 |
| **BOW27** | Logement Sociaux | 4.753 | 11.206 | OW | 56 | 11 | 10.2 | 496 | 5.5 | 28 | 100 | 50 | 7.2 | 3.21 | 19.72 | 0.2 | 30 |
| **BOW28** | Logement Sociaux | 4.751 | 11.214 | OW | 59 | 4.58 | 3.75 | 509 | 5.6 | 27 | 190 | 90 | 36.8 | 4.32 | 10.25 | 0.3 | 53 |
| **BDOW29** | Don Ribouem school | 4.743 | 11.2 | DW | | | 3 | 517 | 5.5 | 27 | 120 | 60 | -50.5 | 4.23 | 13.45 | 0.2 | 54 |

| | | | | | | | | | | | | | | | | | |
|---|---|---|---|---|---|---|---|---|---|---|---|---|---|---|---|---|---|
| **BOW30** | Biabetom | 4.741 | 11.214 | OW | 44 | 13.75 | 12.16 | 510 | 5.5 | 26 | 230 | 110 | -4.9 | 2.86 | 36.63 | 0.4 | 59 |
| **BBH31** | Lalle | 4.804 | 11.161 | BH | | 60 | | 606 | 5.2 | 25 | 120 | 60 | 21.7 | 3.78 | 15.96 | 0.2 | 45 |
| **BSP32** | Mbong | 4.797 | 11.16 | SP | | | | 590 | 3.2 | 25 | 50 | 20 | -126.4 | 3.45 | 12.26 | 0.1 | 13 |
| **BBH33** | Kon Yambetta square | 4.802 | 11.159 | BH | | | | 579 | 5.3 | 25 | 70 | 30 | -117.1 | 5.65 | 11.63 | 0.1 | 25 |
| **BRW34** | Mbam river | 4.816 | 11.186 | RW | | | | 518 | 5.8 | 26 | 40 | 20 | -92.6 | 3.21 | 9.79 | 0.1 | 10 |
| **BBH35** | Carrefour Claude | 4.816 | 11.175 | BH | | 90 | 8.7 | 514 | 5.4 | 30 | 110 | 50 | -209.4 | 4.56 | 15.16 | 0.2 | 25 |
| **BDOW36** | Kiki Health centre | 4.685 | 11.178 | DW | | | | 510 | 6.4 | 30 | 770 | 380 | 261.2 | 5.89 | 55.27 | 1.1 | 158 |
| **BDOW37** | Kiki highway | 4.691 | 11.18 | DW | 65 | | 1.59 | 504 | 6.4 | 27 | 300 | 150 | -217.5 | 5.67 | 10.37 | 0.5 | 69 |
| **BBH38** | Entrée lycee Mouko | 4.695 | 11.183 | BH | | | | 514 | 6.1 | 28 | 1140 | 570 | -183.9 | 4.65 | 48.67 | 1.7 | 124 |
| **BBH39** | Mouko upslope | 4.693 | 11.197 | BH | | | | 530 | 5.7 | 28 | 120 | 60 | -249 | 4.85 | 16.14 | 0.2 | 26 |
| **BBH40** | Nyouka II | 4.717 | 11.207 | BH | | | | 512 | 5.5 | 29 | 180 | 90 | 118.9 | 3.45 | 21.27 | 0.3 | 47 |
| **BOW41** | Nouka II Chefferie | 4.724 | 11.207 | OW | 75 | 7.81 | 6.14 | 514 | 5.7 | 28 | 200 | 100 | 210.5 | 4.2 | 29.23 | 0.3 | 53 |
| **BBH42** | Behind Nyouka Mosque | 4.703 | 11.221 | BH | | | | 496 | 5.6 | 27 | 130 | 60 | -191.4 | 7.45 | 18.93 | 0.2 | 26 |
| **BOW43** | Rionong | 4.719 | 11.218 | OW | 40 | 12.25 | 11.96 | 513 | 5.3 | 26 | 190 | 90 | -101.2 | 2.56 | 42.69 | 0.3 | 50 |
| **BBH44** | Rigama transformateur | 4.727 | 11.219 | BH | | 65 | | 507 | 6.2 | 27 | 460 | 230 | -146.2 | 3.54 | 45.63 | 0.7 | 135 |
| **BOW45** | Bigna | 4.715 | 11.253 | OW | | 6.8 | 2.9 | 492 | 5.7 | 27 | 330 | 160 | -257.7 | 2.87 | 21.61 | 0.5 | 80 |
| **BOW 46** | Bigna chefferie | 4.721 | 11.252 | BH | | 6.3 | 2.6 | 486 | 5.7 | 27 | 160 | 80 | -218.3 | 3.12 | 18.18 | 0.3 | 15 |
| **BBH47** | Bigna Ebeghe | 4.721 | 11.24 | BH | 68 | 4.25 | 2.9 | 496 | 5.2 | 26 | 90 | 45 | -173.8 | 3.45 | 5.73 | 0.1 | 4 |
| **BBH48** | Bigna primary school | 4.718 | 11.233 | BH | | | | 494 | 6 | 26 | 550 | 270 | -260.5 | 2.98 | 38.05 | 1 | 213 |
| **BDOW49** | Bafia district hospital | 4.755 | 11.235 | DW | | | | 505 | 6.1 | 27 | 380 | 190 | -254.8 | 5.69 | 93.87 | 0.6 | 56 |
| **BBH50** | Rimis | 4.756 | 11.223 | BH | | 50 | | 503 | 6.2 | 26 | 520 | 260 | -263.7 | 3.87 | 54 | 0.8 | 155 |
| **BOW51** | Gondone Ginaroo | 4.748 | 11.22 | OW | 50 | 5.5 | 3.47 | 499 | 5.5 | 27 | 510 | 255 | -270.9 | 4.56 | 39.45 | 0.8 | 83 |
| **BOW52** | Kirai behind congelcam | 4.744 | 11.222 | OW | 87 | 5.07 | 3.9 | 491 | 5.5 | 27 | 1340 | 670 | -237.5 | 2.45 | 117.34 | 2 | 57 |
| **BOW53** | Kirai behind congelcam | 4.743 | 11.222 | OW | 66 | 3.7 | 1.39 | 484 | 6 | 26 | 2220 | 1110 | -252.5 | 3.12 | 315.38 | 3.2 | 331 |
| **BBH54** | Rigama | 4.747 | 11.228 | BH | | 50 | 8.9 | 483 | 6.3 | 27 | 540 | 270 | 200 | 3.45 | 25.32 | 0.9 | 123 |
| **BBH55** | Bigna Lycee technique | 4.737 | 11.237 | BH | | | | 494 | 6.2 | 27 | 590 | 290 | -310.7 | 4.56 | 58.9 | 0.9 | 172 |
| **BOW56** | Ndjama's | 4.75 | 11.237 | OW | 68 | 4 | 3.57 | 503 | 5.9 | 27 | 840 | 420 | -325.9 | 6.23 | 200.71 | 1.3 | 68 |
| **BBH57** | Goufan II | 4.74 | 11.24 | BH | | 50 | | 485 | 5.8 | 29 | 190 | 90 | -322.1 | 5.96 | 19.29 | 0.3 | 43 |

*Appendix 1b Physical parameters of water resources in Bafia during the dry season (March, 2023)*

| Code | LAT | LONG | Location | Type | CH | WD | WL | Altitude | DO | pH | T˚C | EC | TDS | Eh | TH | Salinity | Alkalinity |
|---|---|---|---|---|---|---|---|---|---|---|---|---|---|---|---|---|---|
| BOW 01 | 4.752 | 11.238 | Fin Goudrong Ndegue | OW | 49 | 2.16 | 1.66 | 490 | 1.8 | 6 | 27 | 180 | 90 | 15.3 | 59.72 | 0.09 | 352 |
| BOW 02 | 4.754 | 11.257 | Lable | OW | 38 | 3.7 | 1.9 | 478 | 2.3 | 5.9 | 28 | 150 | 70 | 28.4 | 59.72 | 0.07 | 219 |
| BBH 03 | 4.755 | 11.258 | Lable | BH | | | | 476 | 2.5 | 5.4 | 27 | 120 | 60 | 18.6 | 37.79 | 0.06 | 150 |
| BOW 05 | 4.754 | 11.271 | Nyamsong I | OW | 26 | 2.85 | 2.5 | 484 | 2.2 | 5.1 | 26 | 60 | 30 | -86 | 15.92 | 0.03 | 58 |
| BDOW 06 | 4.744 | 11.275 | Donenkeng Iwa | DW | | 40 | | 499 | 3 | 6.1 | 27 | 170 | 80 | -105 | 99.57 | 0.08 | 290 |
| BOW 07 | 4.739 | 11.281 | Donenkeng | OW | 70.9 | 7.45 | 6.3 | 492 | 2.7 | 5 | 28 | 30 | 10 | -56 | 9.94 | 0.02 | 93 |
| Bdsp 08 | 4.736 | 11.283 | Donenkeng | DSP | | | | 505 | 2.5 | 5.8 | 28 | 220 | 110 | -86 | 79.48 | 0.11 | 534 |
| BBH 09 | 4.720 | 11.291 | Egona | BH | | | | 508 | 2.4 | 6.2 | 27 | 210 | 100 | -78 | 199.24 | 0.1 | 300 |
| BOW 10 | 4.736 | 11.254 | Nyamsong III | OW | 70 | 17 | 16.7 | 491 | 2.8 | 5.8 | 27 | 170 | 80 | -11 | 67.71 | 0.08 | 320 |
| BRW 11 | 4.731 | 11.254 | Gamba River | RW | | | | 481 | 2 | 6.7 | 25 | 360 | 180 | -17 | 119.54 | 0.17 | 380 |
| Bdow 12 | 4.740 | 11.249 | Nyamsong III | DW | | | | 490 | 2.6 | 5.6 | 27 | 50 | 20 | -39 | 15.92 | 0.03 | 119 |
| BOW 13 | 4.744 | 11.245 | Bigna Savanah | OW | 68 | 9.38 | 8.34 | 496 | 2.7 | 5.6 | 26 | 100 | 50 | 14.5 | 35.85 | 0.05 | 182 |
| BOW 14 | 4.751 | 11.244 | Lable,  Touristique hotel | OW | 32 | 7.2 | 6.2 | 492 | 2.7 | 5.5 | 26 | 120 | 60 | 15.1 | 31.84 | 0.06 | 141 |
| Bdow 15 | 4.754 | 11.241 | Lable | DW | | 15 | | 499 | 2.8 | 5.3 | 27 | 240 | 120 | 75.5 | 61.61 | 0.12 | 107 |
| BOW 16 | 4.755 | 11.238 | Biabezock | OW | | 1.65 | 0.15 | 504 | 2.2 | 5.5 | 27 | 160 | 80 | 49.7 | 426.15 | 0.8 | 103 |
| BDOW 17 | 4.766 | 11.237 | Lycee classique | DW | | | | 482 | 2.3 | 6.4 | 28 | 330 | 160 | -42 | 148.88 | 0.16 | 79 |
| BOW 18 | 4.766 | 11.238 | Behind Lycée Classique | OW | 90 | 5.06 | 4.56 | 476 | 2.2 | 6.1 | 27 | 410 | 200 | 20.4 | 208.80 | 0.2 | 56 |
| BOW 19 | 4.766 | 11.227 | Renascent school | OW | 0 | 2.6 | 4.4 | 473 | 1.3 | 6.8 | 26 | 150 | 70 | -230 | 79.59 | 0.07 | 71 |
| BBH 20 | 4.765 | 11.224 | Catholic Diocese | BH | | | | 474 | 3.3 | 6.1 | 29 | 350 | 170 | -42 | 138.99 | 0.17 | 62 |
| BRW 21 | 4.766 | 11.221 | Nuen River | RW | | | | 472 | 1.3 | 6.5 | 27 | 260 | 130 | -65 | 81.59 | 0.13 | 102 |
| BRW 22 | 4.779 | 11.214 | Bororo | RW | | | | 469 | 1.9 | 6.7 | 25 | 80 | 40 | -5.4 | 33.88 | 0.04 | 33 |
| Bdow 23 | 4.773 | 11.216 | Biamo | DW | | | | 484 | 2.4 | 6.4 | 26 | 130 | 60 | 19.7 | 49.73 | 0.06 | 61 |
| Bdow 24 | 4.773 | 11.190 | Sa'nam | DW | | 12.5 | | 516 | 2.8 | 4.3 | 27 | 80 | 40 | 31.8 | 21.87 | 0.04 | 2 |
| BBH 25 | 4.768 | 11.209 | Péage | BH | | 40 | | 484 | 2.4 | 5.9 | 26 | 290 | 140 | -65 | 139.41 | 0.14 | 136 |
| BOW 26 | 4.758 | 11.215 | Polyvalent | OW | 55 | 6.02 | 5.01 | 488 | 2.6 | 5.8 | 27 | 240 | 120 | -136 | 67.71 | 0.11 | 55 |
| BOW 27 | 4.753 | 11.206 | Logement Sociaux uphill | OW | 56 | 10.3 | 9.93 | 496 | 2.8 | 6.3 | 25 | 60 | 30 | -161 | 19.87 | 0.03 | 32 |
| Bdow 29 | 4.743 | 11.200 | Don Ribouem skool | DW | | | | 517 | 3.4 | 6.6 | 30 | 80 | 40 | - | 27.88 | 0.04 | 33 |

| | | | | | | | | | | | | | | | | | | |
|---|---|---|---|---|---|---|---|---|---|---|---|---|---|---|---|---|---|---|
| | | | | | | | | | | | | | | | 265 | | | |
| BOW 30 | 4.739 | 11.216 | Biabetom | OW | 44 | 8.6 | 8.3 | 508 | 2.1 | 6 | 31 | 100 | 50 | -271 | 43.76 | 0.05 | 31 |
| BBH 31 | 4.804 | 11.161 | Lalle | BH | | 60 | | 606 | 2.5 | 5.6 | 26 | 90 | 40 | 6 | 31.84 | 0.03 | 41 |
| BSP 32 | 4.802 | 11.159 | Mbong/ Kon Yambetta | SP | | | | 579 | 1.9 | 3.5 | 24 | 30 | 10 | 7 | 15.94 | 0.02 | 19 |
| BRW 34 | 4.832 | 11.198 | Mbam river | RW | | | | 518 | 2.5 | 7.4 | 28 | 30 | 10 | -35 | 9.97 | 0.01 | 6 |
| BBH 35 | 4.816 | 11.186 | Carrefour Claude | BH | | 90 | | 514 | 2.5 | 6 | 27 | 80 | 40 | 9 | 27.86 | 0.04 | 41 |
| BDOW 36 | 4.685 | 11.175 | Kiki Health centre | DW | | | | 510 | 2.6 | 6.3 | 27 | 620 | 310 | -232 | 338.44 | 0.23 | 1568 |
| BDOW 37 | 4.691 | 11.178 | Kiki high way | DW | 65 | 4.49 | 3.15 | 496 | 2.3 | 6 | 26 | 280 | 190 | -198 | 71.70 | 0.07 | 1314 |
| BBH 38 | 4.695 | 11.180 | Lycee Mouko entrance | BH | | | | 514 | 2.6 | 5.9 | 27 | ### | 620 | -268 | 708.10 | 0.55 | 1606 |
| BBH 39 | 4.683 | 11.189 | Lycee Mouko uphill | BH | | | | 504 | 2.7 | 5.7 | 27 | 150 | 70 | 98.6 | 65.65 | 0.07 | 600 |
| BOW 41 | 4.724 | 11.207 | Chefferie Nyouka II | OW | 75 | 7.21 | 6.48 | 514 | 3 | 5.3 | 28 | 80 | 40 | -288 | 35.85 | 0.04 | 247 |
| BOW 43 | 4.726 | 11.212 | Rionong | OW | 40 | 13.2 | 12.6 | 500 | 2.8 | 5.8 | 27 | 150 | 70 | -166 | 51.83 | 0.08 | 47 |
| BBH 44 | 4.727 | 11.219 | Rigama Transformateur | BH | | | | 507 | 1.9 | 6.4 | 28 | 340 | 170 | -241 | 169.17 | 0.16 | 33 |
| BOW 46 | 4.721 | 11.252 | Bigna chefferie | OW | | | | 486 | 2.8 | 6.7 | 30 | 340 | 170 | -207 | 139.52 | 0.18 | 68 |
| BOW 47 | 4.720 | 11.240 | Bigna Ebeghe | OW | 68 | 4.7 | 4.5 | 480 | 1.4 | 6.4 | 31 | 120 | 60 | -254 | 45.74 | 0.04 | 57 |
| Bdow 49 | 4.755 | 11.235 | Bafia district hospital | DW | | | | 505 | 2.4 | 6.2 | 30 | 270 | 140 | -156 | 129.63 | 0.13 | 74 |
| BBH 50 | 4.756 | 11.223 | Maison Blanche | BH | | 50 | | 503 | 3.2 | 7 | 30 | 490 | 240 | -355 | 189.04 | 0.08 | 10 |
| BOW 51 | 4.748 | 11.220 | Gondrone | OW | 50 | 4.95 | 3.15 | 499 | 2.4 | 6.5 | 29 | 320 | 160 | 167 | 159.49 | 0.15 | 94 |
| BOW 52 | 4.744 | 11.222 | Kiria/behind Congelcam | OW | 87 | 4.15 | 3.85 | 491 | 2.8 | 5.6 | 31 | 860 | 430 | -246 | 318.67 | 0.47 | 76 |
| BOW 53 | 4.743 | 11.222 | Kiria/behind Congelcam | OW | 66 | 3.75 | 3.7 | 484 | 2.3 | 6.5 | 30 | ### | 520 | -290 | 248.97 | 0.44 | 33 |
| BDOW 54 | 4.747 | 11.231 | Mr Ibrahim | DW | | | | 507 | | 6.3 | 27 | 180 | 90 | -296 | 55.86 | 0.25 | 57 |
| BOW 56 | 4.750 | 11.237 | Eldorado/Mme Ndjama | OW | 68 | 4 | 3.6 | 503 | 2.4 | 6 | 29 | 690 | 340 | -249 | 205.17 | 0.21 | 145 |
| BBH 57 | 4.740 | 11.240 | Goufan II | BH | | 50 | | 485 | 2 | 6 | 30 | 140 | 60 | 45 | 61.76 | 0.07 | 117 |
| BBH 58 | 4.739 | 11.261 | Bigna Barn | BH | | 75 | | 496 | 2.4 | 6 | 27 | 450 | 220 | 20.1 | 189.25 | 0.22 | 704 |

| | | | | | | | | | | | | | | | | |
|---|---|---|---|---|---|---|---|---|---|---|---|---|---|---|---|---|
| BBH 59 | 4.756 | 11.223 | Rimis | BH | | | 503 | 2.3 | 6.6 | 28 | 410 | 200 | -76 | 199.24 | 0.2 | 157 |
| BRW 60 | 4.802 | 11.159 | Ronfi | RW | | | 574 | 2.9 | 6.2 | 24 | 50 | 20 | -5.9 | 17.92 | 0.02 | 25 |
| BOW 61 | 4.577 | 11.121 | Bokito entrance | OW | 4.34 | 3.04 | 457 | 1.9 | 6.6 | 25 | 170 | 80 | -100 | 91.68 | 0.08 | 582 |
| BBH 62 | 4.574 | 11.116 | Bokito market square | BH | | | 475 | 2.2 | 5.5 | 27 | 450 | 220 | -216 | 159.37 | 0.22 | 302 |
| BBH 63 | 4.638 | 11.153 | Asala 1 | BH | | | 498 | 3 | 5.7 | 27 | 140 | 70 | 130 | 51.71 | 0.07 | 486 |
| BBH 64 | 4.663 | 11.188 | Chefferie Gah Dang | BH | | | 498 | 2.5 | 5.5 | 28 | 130 | 60 | 92.2 | 51.73 | 0.07 | 309 |
| BOW 65 | 4.725 | 11.210 | Tomachock | OW | 6.2 | 5.4 | 502 | 2.7 | 5.3 | 28 | 100 | 50 | -118 | 41.78 | 0.05 | 395 |
| BOW 66 | 4.715 | 11.253 | Mangon | OW | 5.8 | 5.4 | 484 | 2.2 | 6.2 | 29 | 150 | 70 | -180 | 43.84 | 0.08 | 24 |
| BOW 67 | 4.565 | 11.225 | Rigama/behind market | OW | 6.32 | 6.26 | | 2.7 | 5.5 | 30 | 280 | 140 | -260 | 63.67 | 0.14 | 26 |
| BOW 68 | 4.747 | 11.223 | Gondrone Vallée | OW | 4.86 | 3.66 | 509 | 2.8 | 6.3 | 30 | 750 | 370 | -285 | 248.86 | 0.38 | 160 |

**Note:** OW=Open hand-dug well, BH=Borehole, DW=Developed well, RW=River water, SP=Spring water, Dsp=Developed spring, CH=Colar height, WL=Water level, WD=Well depth, DO=Dissolved oxygen, TH=Total hardness

*Appendix 2a Rainy season chemical parameters*

| | | | | | RAINY SEASON | | | | | | | | | |
|---|---|---|---|---|---|---|---|---|---|---|---|---|---|---|
| Code Echantillon | Location | Lat | Long | Type | HCO3- | F- | $Cl^-$ | $NO_3$ | $SO_4^{2-}$ | NH4+ | $Na^+$ | $K^+$ | $Mg^{2+}$ | $Ca^{2+}$ |
| BOW01 | Ndengue Fin goudrong | 4.752 | 11.241 | OW | 34 | <LD | 67.12 | 204.38 | 4.46 | <LD | 51.13 | 4.93 | 20.99 | 42.1 |
| BOW02 | Lable 1 (Mireille) | 4.752 | 11.249 | OW | 68 | 0.24 | 4.26 | 1.51 | 3.3 | <LD | 20.32 | 1.54 | 3.07 | 17.29 |
| BBH03 | Lable | 4.755 | 11.258 | BH | 22 | <LD | 7.17 | 10.56 | 3.35 | <LD | 8.97 | 2.94 | 3.59 | 7.46 |
| BBH04 | Nyamsong I | 4.755 | 11.265 | BH | 170 | 0.39 | 5.62 | 0 | 16.82 | <LD | 13.62 | 7.12 | 12.92 | 32.75 |
| BOW05 | Nyamsong I | 4.754 | 11.271 | OW | 22 | <LD | 3.98 | 3.93 | 3.2 | 0.08 | 2.77 | 2.26 | 1.5 | 2.78 |
| BDOW06 | Donenkeng II | 4.746 | 11.273 | DW | 50 | <LD | 19.28 | 23.76 | 2.54 | <LD | 14.85 | 7.78 | 5.93 | 24.89 |
| BOW07 | Donenkeng II | 4.739 | 11.281 | OW | 10 | <LD | 2.86 | 6.31 | 0.7 | <LD | 2.05 | 2.38 | 1.39 | 1.47 |
| BDSP08 | Donenkeng hospital | 4.736 | 11.283 | DSP | 40 | <LD | 13.92 | 17.68 | 8.62 | <LD | 14.28 | 12.25 | 6.02 | 11.61 |
| BBH09 | Egona | 4.739 | 11.294 | BH | 18 | <LD | 4.28 | 16.92 | 1.46 | <LD | 4.48 | 3.64 | 3.96 | 7.84 |
| BOW10 | Nyamsong III | 4.736 | 11.254 | OW | 57 | <LD | 2 | 1.42 | 1.49 | <LD | 2.73 | 7.21 | 2.16 | 21.21 |
| BRW11 | Gamba River | 4.731 | 11.254 | RW | 61 | <LD | 11.89 | 0.83 | 5.36 | <LD | 12.76 | 9.95 | 3.55 | 18.22 |
| BDOW12 | Nyamsong III | 4.740 | 11.249 | DW | 14 | <LD | 1.3 | 0.79 | 1.76 | <LD | 1.28 | 3.92 | 3.11 | 6.54 |
| BOW13 | Bigna Savana | 4.744 | 11.245 | OW | 39 | <LD | 2.35 | 1.74 | 1.03 | <LD | 9.68 | 1.79 | 1.46 | 9.33 |
| BOW14 | Lable | 4.751 | 11.244 | OW | 34 | <LD | 8.39 | 9.15 | 1.74 | <LD | 7.03 | 3.48 | 3.29 | 17.4 |
| BDOW15 | Lable | 4.754 | 11.241 | DW | 22 | <LD | 19.15 | 45.88 | 0.89 | <LD | 21.35 | 8.03 | 6.68 | 7.46 |
| BDOW16 | Biabezock | 4.755 | 11.237 | DW | 31 | <LD | 13.83 | 65.58 | 2.81 | <LD | 14.55 | 8.71 | 14.17 | 11.67 |
| BDOW17 | Lycee Classique | 4.767 | 11.236 | DW | 84 | 0.27 | 2.81 | 0 | 5.33 | <LD | 6.44 | 0.99 | 5.77 | 32.59 |
| BOW18 | Biabezock (behind lycee) | 4.766 | 11.238 | OW | 120 | <LD | 8.37 | 11.84 | 6.42 | <LD | 16.16 | 19.43 | 14.88 | 36.91 |
| BOW19 | Renascent Academic Complex | 4.766 | 11.227 | OW | 40 | <LD | 8.52 | 16.49 | 4.87 | <LD | 7.78 | 1.83 | 4.73 | 14.08 |
| BBH20 | Catholic Diocesse | 4.765 | 11.224 | BH | 161 | 0.75 | 8.62 | 0 | 17.58 | <LD | 18.91 | 6.3 | 10.63 | 28.85 |
| BRW21 | Nguen river (Biamo) | 4.766 | 11.221 | RW | 30 | <LD | 2.32 | 0.51 | 1.12 | 0.06 | 5.91 | 2.13 | 2.49 | 5.5 |
| BRW22 | Biamo/Bohboro river | 4.779 | 11.214 | RW | 20 | <LD | 1.49 | 0.95 | 0.7 | <LD | 5.25 | 2.1 | 2.45 | 5.53 |
| BDOW23 | Biamo | 4.773 | 11.216 | DW | 44 | <LD | 7.49 | 0 | 2.85 | <LD | 12.23 | 3.32 | 3.95 | 11.5 |
| BDOW24 | Sanaam | 4.773 | 11.190 | DW | 14 | <LD | 4.69 | 20.42 | 1.12 | <LD | 6.44 | 4.01 | 1.25 | 5.26 |
| BBH25 | péage | 4.768 | 11.209 | BH | 105 | 0.21 | 8.55 | 8.62 | 1.67 | <LD | 9.94 | 3.78 | 10.3 | 28.12 |
| BOW26 | Polyvalent | 4.758 | 11.215 | OW | 60 | <LD | 40.97 | 37.19 | 6.47 | <LD | 27.85 | 2.82 | 6.87 | 37.33 |
| BOW27 | Logement Sociaux | 4.753 | 11.206 | OW | 30 | <LD | 1.13 | 0.93 | 0.82 | 0.09 | 4.71 | 4.23 | 0.92 | 7.44 |

| | | | | | | | | | | | | | | |
|---|---|---|---|---|---|---|---|---|---|---|---|---|---|---|
| **BOW28** | Logement Sociaux | 4.751 | 11.214 | OW | 53 | <LD | 2.47 | 2.36 | 1 | <LD | 16.09 | 1.55 | 1.55 | 13.99 |
| **BDOW29** | Don Ribouem school | 4.743 | 11.200 | DW | 54 | <LD | 1.9 | 0 | 0 | <LD | 6.94 | 2.03 | 2.04 | 7.09 |
| **BOW30** | Biabetom | 4.741 | 11.214 | OW | 59 | <LD | 4.61 | 10.39 | 2.37 | <LD | 10.28 | 6.78 | 3.49 | 17.29 |
| **BBH31** | Lalle | 4.804 | 11.161 | BH | 45 | <LD | 1.2 | 0 | 0.53 | <LD | 6.07 | 2.45 | 2.35 | 8.01 |
| **BSP32** | Mbong Kon Yambetta | 4.797 | 11.160 | SP | 13 | <LD | 1.17 | 0.57 | 0.37 | <LD | 2.54 | 2.28 | 1.15 | 2.51 |
| **BBH33** | Kon Yambetta square | 4.802 | 11.159 | BH | 25 | <LD | 1.18 | 0.93 | 0.45 | <LD | 4.14 | 1.8 | 1.69 | 4.84 |
| **BRW34** | Mbam river | 4.816 | 11.186 | RW | 10 | <LD | 1.2 | 0.67 | 0.59 | 0.1 | 2.01 | 1.85 | 0.87 | 1.68 |
| **BBH35** | Ngongol carrefour Claude | 4.816 | 11.175 | BH | 25 | <LD | 1.92 | 2.09 | 0.65 | 0.14 | 5.82 | 2.45 | 2.03 | 6.4 |
| **BDOW36** | Kiki Health centre | 4.685 | 11.178 | DW | 158 | 1.11 | 4.21 | 1.57 | 108.96 | <LD | 22.55 | 5.12 | 13.69 | 56.57 |
| **BDOW37** | Kiki highway, Mouko lycee | 4.691 | 11.180 | DW | 69 | 0.44 | 5.55 | 1.08 | 4.11 | <LD | 28.28 | 1.47 | 1.73 | 20.54 |
| **BBH38** | Entrée lycee Mouko | 4.695 | 11.183 | BH | 124 | 1.16 | 3.37 | 0 | 291.3 | <LD | 17.77 | 5.95 | 9.68 | 146.26 |
| **BBH39** | Mouko upslope | 4.693 | 11.197 | BH | 26 | <LD | 1.48 | 5.45 | 1.33 | <LD | 9.28 | 2.95 | 1.6 | 7.63 |
| **BBH40** | Nyouka II | 4.717 | 11.207 | BH | 47 | <LD | 4.46 | 14.19 | 0.5 | <LD | 12.02 | 3.43 | 2.86 | 8.79 |
| **BOW41** | Nouka II Chefferie | 4.724 | 11.207 | OW | 53 | <LD | 1.72 | 9.28 | 3.04 | <LD | 4.07 | 6.45 | 1.07 | 20.78 |
| **BBH42** | Behind Nyouka Mosque | 4.703 | 11.221 | BH | 26 | <LD | 1.24 | 5.54 | 0.62 | <LD | 8.46 | 2.91 | 2.78 | 6.74 |
| **BOW43** | Rionong | 4.719 | 11.218 | OW | 50 | <LD | 1.38 | 5.05 | 2.81 | <LD | 2.27 | 7.96 | 3.97 | 17.89 |
| **BBH44** | Rigama transformateur | 4.727 | 11.219 | BH | 135 | 0.49 | 1.84 | 0 | 1.92 | <LD | 16.75 | 5.66 | 8.94 | 41.45 |
| **BOW45** | Bigna | 4.715 | 11.253 | OW | 80 | 0.79 | 3.65 | 0 | 2.75 | <LD | 9.56 | 3.81 | 2.37 | 38.28 |
| **BOW 46** | Bigna chefferie | 4.721 | 11.252 | BH | 15 | <LD | 13.16 | 14.87 | 1.86 | <LD | 8.81 | 2.62 | 2.96 | 7.41 |
| **BBH47** | Bigna Ebeghe | 4.721 | 11.240 | BH | 4 | <LD | 5.86 | 6.14 | 0.49 | <LD | 8.81 | 0.93 | 0.76 | 2.41 |
| **BBH48** | Bigna primary school | 4.718 | 11.233 | BH | 213 | 0.32 | 3.45 | 0 | 4.24 | <LD | 16.95 | 4.45 | 7.9 | 24.59 |
| **BDOW49** | Bafia district hospital | 4.755 | 11.235 | DW | 56 | 0.3 | 12.88 | 28.85 | 6.11 | <LD | 11.12 | 17.04 | 9.49 | 19.55 |
| **BBH50** | Rimis | 4.756 | 11.223 | BH | 155 | 0.36 | 2.25 | 0 | 8.59 | <LD | 19.76 | 5.26 | 12.95 | 34.25 |
| **BOW51** | Gondone Ginaroo | 4.748 | 11.220 | OW | 83 | <LD | 12.04 | 15.56 | 10.09 | 0.87 | 16.76 | 2.65 | 11.43 | 41.23 |
| **BOW52** | Kirai behind congelcam | 4.744 | 11.222 | OW | 57 | <LD | 123.87 | 188.91 | 17.32 | <LD | 85.05 | 15.79 | 20.95 | 67.74 |
| **BOW53** | Kirai behind congelcam | 4.743 | 11.222 | OW | 331 | <LD | 243.99 | 0 | 69.47 | <LD | 174.53 | 64.78 | 19.47 | 120.11 |
| **BBH54** | Rigama | 4.747 | 11.228 | BH | 123 | 0.72 | 1.52 | 0.64 | 44.26 | <LD | 19.09 | 3.02 | 5.16 | 54.25 |
| **BBH55** | Bigna behind Lycee technique | 4.737 | 11.237 | BH | 172 | 0.18 | 2.69 | 0.67 | 6.86 | <LD | 10.87 | 5.14 | 15.11 | 30.44 |
| **BOW56** | Ndjama's | 4.750 | 11.237 | BH | 68 | <LD | 81.12 | 63.78 | 32.13 | 4.94 | 58.75 | 42.04 | 11.05 | 24.01 |
| **BBH57** | Goufan II | 4.740 | 11.240 | BH | 43 | <LD | 3.74 | 9.27 | 0.63 | <LD | 11.07 | 2.32 | 3.9 | 11.85 |

*Appendix 2b Dry season chemical parameters*

| | | | | DRY SEASON | | | | | | | | |
|---|---|---|---|---|---|---|---|---|---|---|---|---|
| **Code** | **LAT** | **LONG** | **Location** | **Type** | **HCO3** | **Cl** | **NO3** | **SO4** | **Na** | **K** | **Mg** | **Ca** |
| BOW 01 | 4.752 | 11.238 | Fin Goudrong Ndegue | OW | 115.9 | 4 | 0.4 | 0.4 | 17.4 | 1.6 | 4.8 | 16 |
| BOW 02 | 4.754 | 11.257 | Lable | OW | 79.3 | 11 | 5 | 2.7 | 12.5 | 1.7 | 4.8 | 16 |
| BBH 03 | 4.755 | 11.258 | Lable | BH | 42.7 | 6 | 15 | 0.2 | 8.4 | 3.1 | 3.84 | 8.8 |
| BOW 05 | 4.754 | 11.271 | Nyamsong I | OW | 18.3 | 3 | 8.9 | 1.2 | 4.4 | 3 | 1.44 | 4 |
| BDOW 06 | 4.744 | 11.275 | Donenkeng Iwa | DW | 97.6 | 18 | 8.5 | 1.3 | 3.6 | 1.2 | 7.2 | 28 |
| BOW 07 | 4.739 | 11.281 | Donenkeng | OW | 12.2 | 3 | 7.5 | 0.3 | 3.1 | 1.9 | 1.2 | 2 |
| Bdsp 08 | 4.736 | 11.283 | Donenkeng | DSP | 97.6 | 19 | 28.9 | 6.9 | 20.4 | 11.2 | 9.6 | 16 |
| BBH 09 | 4.720 | 11.291 | Egona | BH | 219.6 | 36.1 | 2.1 | 0.4 | 15 | 9.6 | 12 | 60 |
| BOW 10 | 4.736 | 11.254 | Nyamsong III | OW | 91.5 | 5 | 1.2 | 0.3 | 6.3 | 5.4 | 4.8 | 19.2 |
| BRW 11 | 4.731 | 11.254 | Gamba River | RW | 213.5 | 13 | 0.4 | 27 | 30.4 | 16.6 | 7.2 | 36 |
| Bdow 12 | 4.740 | 11.249 | Nyamsong III | DW | 18.3 | 7 | 0.4 | 1.9 | 3.5 | 1.1 | 1.44 | 4 |
| BOW 13 | 4.744 | 11.245 | Bigna Savanah | OW | 54.9 | 7 | 1.8 | 4 | 9.6 | 1.5 | 2.4 | 10.4 |
| BOW 14 | 4.751 | 11.244 | Lable,  Touristique hotel | OW | 42.7 | 10 | 11.3 | 2.4 | 10.8 | 6.6 | 2.88 | 8 |
| Bdow 15 | 4.754 | 11.241 | Lable | DW | 42.7 | 12 | 81.5 | 0.1 | 21.3 | 8.7 | 7.2 | 12.8 |
| BOW 16 | 4.755 | 11.238 | Biabezock | OW | 48.8 | 12 | 39.5 | 1.7 | 10.4 | 8.2 | 4.8 | 16 |
| BDOW 17 | 4.766 | 11.237 | Lycee classique | DW | 183 | 25 | 1.7 | 5.5 | 16.4 | 4.7 | 21.6 | 24 |
| BOW 18 | 4.766 | 11.238 | Behind Lycée Classique | OW | 268.4 | 10 | 2.2 | 5.5 | 15.2 | 4.7 | 21.6 | 48 |
| BOW 19 | 4.766 | 11.227 | Renascent school | OW | 109.8 | 6 | 3.7 | 1.7 | 7.9 | 3.6 | 7.2 | 20 |
| BBH 20 | 4.765 | 11.224 | Catholic Diocese | BH | 115.9 | 28 | 30.3 | 7.7 | 15 | 2.5 | 19.2 | 24 |
| BRW 21 | 4.766 | 11.221 | Nuen River | RW | 91.5 | 30 | 0.8 | 7.9 | 21.3 | 9.2 | 7.2 | 20.8 |
| BRW 22 | 4.779 | 11.214 | Bororo | RW | 42.7 | 10 | 0.4 | 1.5 | 8.4 | 2.7 | 1.92 | 10.4 |
| Bdow 23 | 4.773 | 11.216 | Biamo | DW | 103.7 | 5 | 1.7 | 0.4 | 16 | 3 | 4.8 | 12 |
| Bdow 24 | 4.773 | 11.190 | Sa'nam | DW | 18.3 | 4 | 31.2 | 0.1 | 8.6 | 2.1 | 2.4 | 4.8 |
| BBH 25 | 4.768 | 11.209 | péage | BH | 201.3 | 9 | 3.4 | 1.5 | 14 | 5.5 | 9.6 | 40 |
| BOW 26 | 4.758 | 11.215 | Polyvalent | OW | 73.2 | 29 | 2.4 | 1 | 22.8 | 2.5 | 4.8 | 19.2 |
| BOW 27 | 4.753 | 11.206 | Logement Sociaux uphill | OW | 30.5 | 10 | 1.6 | 0.3 | 6.2 | 4 | 2.4 | 4 |
| Bdow 29 | 4.743 | 11.200 | Don Ribouem skool | DW | 42.7 | 5 | 6.6 | 0.4 | 7.3 | 2.2 | 1.92 | 8 |

| | | | | | | | | | | | | |
|---|---|---|---|---|---|---|---|---|---|---|---|---|
| BOW 30 | 4.739 | 11.216 | Biabetom | OW | 36.6 | 6 | 20.4 | 8.1 | 11.2 | 1.6 | 4.32 | 10.4 |
| BBH 31 | 4.804 | 11.161 | Lalle | BH | 54.9 | 6 | 0.2 | 0.3 | 7.9 | 2.7 | 2.88 | 8 |
| BSP 32 | 4.802 | 11.159 | Mbong/ Kon Yambetta | SP | 18.3 | 3 | 0.9 | 1.7 | 3.1 | 0.7 | 0.96 | 4.8 |
| BRW 34 | 4.832 | 11.198 | Mbam river | RW | 12.2 | 4 | 0.2 | 1.5 | 3.1 | 1.2 | 0.48 | 3.2 |
| BBH 35 | 4.816 | 11.186 | Carrefour Claude | BH | 36.6 | 11 | 1.2 | 0.4 | 7.9 | 2.4 | 2.4 | 7.2 |
| BDOW 36 | 4.685 | 11.175 | Kiki Health centre | DW | 244 | 20 | 0.4 | 160 | 30 | 5.4 | 26.4 | 92 |
| BDOW 37 | 4.691 | 11.178 | Kiki high way | DW | 176.9 | 20 | 1.9 | 0.4 | 56 | 0.9 | 4.8 | 20.8 |
| BBH 38 | 4.695 | 11.180 | Lycee Mouko entrance | BH | 305 | 25 | 0.4 | 497 | 37.5 | 6.7 | 24 | 244 |
| BBH 39 | 4.683 | 11.189 | Lycee Mouko uphill | BH | 97.6 | 11 | 1.6 | 0.3 | 13.4 | 2.5 | 6.24 | 16 |
| BOW 41 | 4.724 | 11.207 | Chefferie Nyouka II | OW | 36.6 | 7 | 9.2 | 0.1 | 5.7 | 1.3 | 2.4 | 10.4 |
| BOW 43 | 4.726 | 11.212 | Rionong | OW | 61 | 15 | 4.2 | 0.3 | 13 | 2.4 | 2.4 | 16.8 |
| BBH 44 | 4.727 | 11.219 | Rigama Transformateur | BH | 219.6 | 21 | 2 | 0.4 | 17.4 | 4.9 | 14.4 | 44 |
| BOW 46 | 4.721 | 11.252 | Bigna chefferie | OW | 158.6 | 12 | 46.9 | 0.2 | 25.2 | 4.4 | 7.2 | 44 |
| BOW 47 | 4.720 | 11.240 | Bigna Ebeghe | OW | 61 | 5 | 4.7 | 0.3 | 7.4 | 1.9 | 4.8 | 10.4 |
| Bdow 49 | 4.755 | 11.235 | Bafia district hospital | DW | 115.9 | 15 | 50.6 | 5.1 | 19.2 | 9.2 | 4.8 | 44 |
| BBH 50 | 4.756 | 11.223 | Maison Blanche | BH | 54.9 | 72 | 176 | 1 | 42.5 | 5.6 | 16.8 | 48 |
| BOW 51 | 4.748 | 11.220 | Gondrone | OW | 213.5 | 5 | 0.4 | 11.7 | 18.4 | 2.3 | 7.2 | 52 |
| BOW 52 | 4.744 | 11.222 | Kiria/behind Congelcam | OW | 152.5 | 105 | 229.8 | 14.3 | 80 | 8.5 | 21.6 | 92 |
| BOW 53 | 4.743 | 11.222 | Kiria/behind Congelcam | OW | 439.2 | 140 | 0.5 | 56.6 | 150 | 38.5 | 16.8 | 72 |
| BDOW 54 | 4.747 | 11.231 | Mr Ibrahim | DW | 366 | 65 | 34.7 | 24.5 | 15.6 | 4.4 | 2.4 | 18.4 |
| BOW 56 | 4.750 | 11.237 | Eldorado/Mme Ndjama | OW | 213.5 | 75 | 108.8 | 33.2 | 72 | 36 | 13.44 | 60 |
| BBH 57 | 4.740 | 11.240 | Goufan II | BH | 73.2 | 12 | 15.3 | 2.1 | 12.8 | 2.6 | 3.84 | 18.4 |
| BBH 58 | 4.739 | 11.261 | Bigna Barn | BH | 219.6 | 6 | 1.4 | 52.4 | 17.8 | 7 | 12 | 56 |
| BBH 59 | 4.756 | 11.223 | Rimis | BH | 274.5 | 17 | 0.4 | 10.2 | 25.6 | 6.2 | 12 | 60 |
| BRW 60 | 4.802 | 11.159 | Ronfi | RW | 24.4 | 7 | 1.8 | 0.3 | 6.9 | 2.3 | 1.44 | 4.8 |
| BOW 61 | 4.577 | 11.121 | Bokito entrance | OW | 122 | 10 | 4.4 | 0.3 | 9.6 | 2.7 | 4.8 | 28.8 |
| BBH 62 | 4.574 | 11.116 | Bokito market square | BH | 61 | 45 | 120.8 | 9.1 | 32.8 | 4 | 10.08 | 47.2 |
| BBH 63 | 4.638 | 11.153 | Asala 1 | BH | 73.2 | 7 | 4 | 0.4 | 10.4 | 1.9 | 5.28 | 12 |
| BBH 64 | 4.663 | 11.188 | Chefferie Gah Dang | BH | 79.3 | 10 | 9.4 | 0.2 | 14.6 | 3.8 | 4.8 | 12.8 |
| BOW 65 | 4.725 | 11.210 | Tomachock | OW | 61 | 10 | 2.8 | 0.3 | 12.4 | 3.1 | 3.84 | 10.4 |
| BOW 66 | 4.715 | 11.253 | Mangon | OW | 30.5 | 22 | 21.5 | 13.2 | 15.4 | 9.4 | 2.4 | 13.6 |

| | | | | | | | | | | | | |
|---|---|---|---|---|---|---|---|---|---|---|---|---|
| BOW 67 | 4.565 | 11.225 | Rigama/behind market | OW | 61 | 35 | 69.8 | 0.1 | 43.2 | 3 | 5.76 | 16 |
| BOW 68 | 4.747 | 11.223 | Gondrone Vallée | OW | 366 | 65 | 34.7 | 24.5 | 83 | 16.4 | 19.2 | 68 |

***Appendix 3*** *Trace element results (ppb) of groundwater (n=53) and surface water (n=4) in the Bafia shallow aquifer*

| Code | Fe | Co | Se | Ti | Sr | Sn | Sb | Al | B | Cr | Cu | Pb | Ni | As | Cd | Zn | Mn |
|---|---|---|---|---|---|---|---|---|---|---|---|---|---|---|---|---|---|
| **BOW01** | 5.67 | 1.35 | 0.58 | 198.00 | 883.41 | 0.07 | 0.27 | 5.53 | 2.13 | 1.32 | 2.40 | 0.00 | 14.71 | 0.15 | 0.00 | 12.37 | 233.05 |
| **BOW02** | 14.66 | 3.78 | 0.00 | 67.59 | 158.88 | 0.10 | 0.40 | 4.35 | 2.16 | 1.17 | 0.62 | 0.00 | 2.34 | 0.37 | 0.00 | 3.80 | 396.99 |
| **BBH03** | 3.82 | 1.46 | 0.35 | 28.47 | 131.91 | 0.04 | 0.27 | 27.35 | 0.87 | 3.75 | 1.07 | 0.00 | 1.24 | 0.02 | 0.00 | 13.58 | 48.74 |
| **BBH04** | 1215.91 | 0.46 | 0.00 | 319.61 | 394.88 | 0.07 | 0.40 | 6.00 | 2.10 | 2.16 | 0.58 | 0.00 | 2.31 | 0.05 | 0.00 | 6.75 | 575.61 |
| **BOW05** | 58.04 | 1.36 | 0.00 | 9.39 | 63.26 | 0.06 | 0.35 | 18.06 | 1.06 | 1.01 | 0.61 | 0.08 | 0.81 | 0.03 | 0.00 | 12.85 | 133.23 |
| **BDOW06** | 698.95 | 0.44 | 0.42 | 107.30 | 239.48 | 0.05 | 0.30 | 9.30 | 2.53 | 4.16 | 0.95 | 0.00 | 1.64 | 0.11 | 0.00 | 31.60 | 27.74 |
| **BOW07** | 11.45 | 3.16 | 0.00 | 4.08 | 26.68 | 0.05 | 0.25 | 55.14 | 0.58 | 1.01 | 0.96 | 0.03 | 2.39 | 0.01 | 0.00 | 11.74 | 51.50 |
| **BDSP08** | 15.65 | 0.05 | 0.49 | 48.51 | 252.06 | 0.03 | 0.25 | 7.40 | 1.86 | 2.26 | 1.00 | 0.08 | 0.97 | 0.04 | 0.00 | 1.04 | 2.02 |
| **BBH09** | 19.16 | 0.06 | 0.00 | 36.32 | 103.64 | 0.08 | 0.21 | 27.43 | 1.16 | 3.64 | 22.48 | 1.55 | 1.90 | 0.03 | 0.00 | 130.21 | 2.28 |
| **BOW10** | 4.09 | 1.16 | 0.00 | 92.39 | 87.77 | 0.05 | 0.25 | 6.69 | 2.62 | 1.44 | 2.05 | 0.06 | 2.39 | 0.11 | 0.00 | 5.51 | 453.92 |
| **BRW11** | 0.52 | 0.12 | 0.00 | 81.29 | 202.49 | 0.01 | 2.29 | 0.47 | 9.99 | 2.93 | 1.34 | 0.00 | 0.73 | 0.14 | 0.00 | 0.00 | 0.33 |
| **BDOW12** | 8.49 | 0.67 | 0.00 | 28.59 | 46.77 | 0.02 | 0.29 | 21.44 | 0.95 | 2.63 | 0.41 | 0.13 | 1.67 | 0.02 | 0.00 | 6.06 | 15.43 |
| **BOW13** | 6.01 | 0.31 | 0.00 | 39.73 | 104.30 | 0.08 | 0.32 | 4.57 | 1.24 | 1.01 | 0.59 | 0.04 | 0.42 | 0.06 | 0.00 | 5.32 | 24.13 |
| **BOW14** | 27.04 | 0.37 | 0.00 | 73.89 | 92.65 | 0.03 | 0.31 | 4.78 | 1.81 | 0.95 | 0.82 | 0.00 | 1.19 | 0.07 | 0.00 | 2.61 | 30.34 |
| **BDOW15** | 4.09 | 4.59 | 0.00 | 30.82 | 149.07 | 0.02 | 0.35 | 58.15 | 0.86 | 1.55 | 1.34 | 0.08 | 2.47 | 0.06 | 0.00 | 31.49 | 128.28 |
| **BDOW16** | 3.39 | 0.57 | 0.33 | 52.50 | 119.21 | 0.02 | 0.37 | 11.82 | 2.08 | 2.36 | 9.66 | 1.24 | 1.33 | 0.15 | 0.00 | 1.82 | 5.42 |
| **BDOW17** | 4.54 | 0.10 | 0.00 | 147.57 | 339.17 | 0.04 | 0.31 | 9.84 | 4.04 | 1.32 | 0.91 | 0.08 | 0.85 | 0.03 | 0.00 | 2.40 | 2.80 |
| **BOW18** | 10.66 | 0.24 | 0.00 | 174.84 | 407.77 | 0.04 | 0.49 | 32.59 | 8.57 | 2.54 | 1.41 | 0.19 | 1.56 | 0.60 | 0.00 | 0.00 | 0.54 |
| **BOW19** | 27.11 | 0.12 | 0.00 | 67.48 | 281.99 | 0.03 | 0.31 | 61.75 | 5.55 | 0.71 | 1.66 | 0.16 | 0.59 | 0.08 | 0.00 | 1.32 | 2.22 |
| **BBH20** | 2.16 | 0.16 | 0.00 | 340.40 | 509.80 | 0.04 | 0.32 | 4.26 | 3.10 | 2.21 | 1.23 | 0.00 | 1.73 | 0.16 | 0.00 | 0.53 | 434.68 |
| **BRW21** | 53.12 | 0.06 | 0.00 | 25.92 | 126.69 | 0.02 | 0.41 | 55.42 | 2.09 | 0.48 | 0.92 | 0.24 | 0.21 | 0.06 | 0.00 | 0.00 | 0.73 |
| **BRW22** | 82.01 | 0.06 | 0.00 | 21.47 | 101.73 | 0.04 | 0.24 | 23.87 | 1.41 | 0.35 | 1.48 | 0.03 | 0.22 | 0.04 | 0.00 | 0.00 | 0.89 |
| **BDOW23** | 44.48 | 0.09 | 0.00 | 50.62 | 174.47 | 0.02 | 0.24 | 140.17 | 4.04 | 1.18 | 1.82 | 0.12 | 2.39 | 0.10 | 0.00 | 10.92 | 6.90 |
| **BDOW24** | 14.04 | 1.04 | 0.30 | 22.33 | 100.63 | 0.02 | 0.24 | 99.06 | 2.78 | 0.44 | 1.89 | 0.49 | 0.93 | 0.09 | 0.00 | 14.45 | 24.41 |
| **BBH25** | 5.02 | 0.06 | 0.25 | 126.03 | 450.72 | 0.04 | 0.32 | 8.74 | 1.11 | 4.74 | 0.96 | 0.12 | 3.04 | 0.03 | 0.00 | 0.00 | 1.19 |
| **BOW26** | 8.67 | 0.11 | 0.49 | 164.90 | 864.83 | 0.02 | 0.34 | 20.57 | 4.98 | 1.06 | 1.45 | 0.15 | 1.00 | 0.40 | 0.00 | 0.00 | 3.59 |

| | | | | | | | | | | | | | | | | | |
|---|---|---|---|---|---|---|---|---|---|---|---|---|---|---|---|---|---|
| **BOW27** | 16.09 | 0.08 | 0.00 | 33.58 | 65.27 | 0.02 | 0.64 | 25.52 | 1.70 | 0.46 | 1.94 | 0.14 | 0.80 | 0.06 | 0.00 | 14.10 | 4.27 |
| **BOW28** | 12.06 | 0.05 | 0.00 | 59.05 | 111.83 | 0.00 | 0.70 | 29.68 | 2.04 | 0.73 | 0.75 | 0.31 | 0.87 | 0.18 | 0.00 | 0.00 | 1.75 |
| **BDOW29** | 11.54 | 0.03 | 0.00 | 29.04 | 167.51 | 0.00 | 0.48 | 20.63 | 1.11 | 0.60 | 0.42 | 0.06 | 0.09 | 0.02 | 0.00 | 5.38 | 1.37 |
| **BOW30** | 2.65 | 1.36 | 0.00 | 78.89 | 75.82 | 0.00 | 0.67 | 2.99 | 2.30 | 0.99 | 0.50 | 0.00 | 1.11 | 0.05 | 0.00 | 0.00 | 239.62 |
| **BBH31** | 5.48 | 0.03 | 0.00 | 35.14 | 215.98 | 0.03 | 0.22 | 6.24 | 3.28 | 1.22 | 1.32 | 0.11 | 0.19 | 0.01 | 0.00 | 15.67 | 0.83 |
| **BSP32** | 14.95 | 0.06 | 0.00 | 8.83 | 79.19 | 0.00 | 0.80 | 11.75 | 1.18 | 0.55 | 0.17 | 0.00 | 0.05 | 0.01 | 0.00 | 3.33 | 22.36 |
| **BBH33** | 317.45 | 0.10 | 0.00 | 23.07 | 125.27 | 0.00 | 0.56 | 78.16 | 0.84 | 0.48 | 0.91 | 0.21 | 0.09 | 0.04 | 0.00 | 0.00 | 1.39 |
| **BRW34** | 195.39 | 0.06 | 0.00 | 8.48 | 29.28 | 0.00 | 1.28 | 168.95 | 1.96 | 0.45 | 0.78 | 0.12 | 0.11 | 0.05 | 0.00 | 0.00 | 1.43 |
| **BBH35** | 0.23 | 0.06 | 0.00 | 25.26 | 142.73 | 0.00 | 0.49 | 0.17 | 1.04 | 2.71 | 0.11 | 0.00 | 0.09 | 0.01 | 0.00 | 158.60 | 24.27 |
| **BDOW36** | 23.32 | 0.21 | 0.00 | 397.06 | 1293.55 | 0.01 | 0.64 | 76.35 | 4.21 | 2.73 | 1.23 | 0.26 | 1.93 | 0.08 | 0.00 | 1.58 | 107.13 |
| **BDOW37** | 34.64 | 0.08 | 0.00 | 92.19 | 120.70 | 0.00 | 0.69 | 123.54 | 4.52 | 1.60 | 1.15 | 0.18 | 0.74 | 0.20 | 0.00 | 0.00 | 3.48 |
| **BBH38** | 25.21 | 0.55 | 0.00 | 810.70 | 1650.68 | 0.03 | 0.52 | 11.57 | 4.60 | 3.28 | 0.76 | 0.00 | 3.93 | 0.04 | 0.00 | 13.14 | 565.59 |
| **BBH39** | 4.07 | 0.06 | 0.00 | 27.98 | 173.84 | 0.02 | 0.24 | 6.12 | 1.41 | 1.65 | 0.72 | 0.21 | 0.50 | 0.02 | 0.00 | 3.47 | 3.10 |
| **BBH40** | 16.96 | 0.05 | 0.00 | 41.59 | 227.16 | 0.00 | 0.66 | 33.67 | 1.19 | 1.24 | 1.56 | 0.21 | 0.42 | 0.03 | 0.00 | 3.32 | 17.18 |
| **BOW41** | 9.48 | 0.38 | 0.00 | 100.48 | 134.43 | 0.00 | 0.79 | 23.01 | 3.93 | 1.35 | 0.72 | 0.15 | 1.80 | 0.09 | 0.00 | 0.81 | 36.96 |
| **BBH42** | 9.43 | 0.09 | 0.00 | 31.02 | 185.33 | 0.00 | 0.55 | 19.91 | 0.54 | 1.50 | 8.07 | 0.16 | 1.57 | 0.02 | 0.00 | 28.74 | 6.26 |
| **BOW43** | 8.28 | 0.12 | 0.00 | 80.11 | 166.32 | 0.00 | 0.67 | 5.34 | 2.43 | 1.07 | 0.55 | 0.00 | 1.11 | 0.06 | 0.00 | 11.68 | 233.37 |
| **BBH44** | 60.25 | 0.22 | 0.00 | 211.43 | 265.99 | 0.02 | 0.30 | 4.71 | 1.77 | 1.92 | 0.71 | 0.00 | 1.42 | 0.05 | 0.00 | 0.00 | 315.32 |
| **BDOW45** | 4.16 | 0.11 | 0.00 | 177.13 | 215.78 | 0.00 | 0.94 | 9.13 | 2.91 | 2.44 | 1.46 | 0.23 | 1.86 | 1.25 | 0.00 | 10.50 | 3.07 |
| **BBH46** | 160.77 | 0.09 | 0.29 | 48.52 | 237.65 | 0.08 | 0.38 | 518.92 | 4.35 | 0.62 | 14.16 | 1.12 | 0.66 | 0.06 | 0.00 | 5.06 | 3.50 |
| **BBH47** | 192.04 | 0.07 | 0.00 | 23.65 | 69.22 | 0.00 | 0.62 | 448.28 | 1.22 | 0.50 | 0.49 | 0.13 | 0.00 | 0.03 | 0.00 | 0.00 | 3.23 |
| **BBH48** | 9.24 | 0.23 | 0.00 | 476.42 | 549.43 | 0.00 | 0.66 | 19.13 | 2.29 | 4.00 | 0.87 | 0.15 | 1.88 | 0.13 | 0.00 | 0.00 | 712.37 |
| **BBH49** | 5.01 | 0.06 | 0.38 | 97.79 | 257.92 | 0.00 | 0.58 | 9.60 | 1.68 | 5.76 | 1.83 | 0.03 | 3.17 | 0.10 | 0.00 | 2.73 | 0.76 |
| **BBH50** | 59.17 | 0.35 | 0.00 | 214.25 | 278.06 | 0.02 | 0.21 | 0.00 | 1.88 | 6.27 | 0.59 | 0.00 | 1.36 | 0.03 | 0.00 | 0.00 | 569.39 |
| **BOW51** | 20.44 | 0.11 | 0.76 | 195.54 | 785.10 | 0.00 | 1.02 | 10.59 | 1.71 | 1.80 | 2.01 | 0.20 | 2.27 | 0.07 | 0.00 | 25.60 | 1.04 |
| **BOW52** | 7.37 | 0.50 | 2.51 | 690.41 | 1378.12 | 0.00 | 0.84 | 9.81 | 31.80 | 7.53 | 6.86 | 0.11 | 4.10 | 0.94 | 0.00 | 4.31 | 194.10 |
| **BOW53** | 4.00 | 0.38 | 0.84 | 122.02 | 523.36 | 0.00 | 0.71 | 6.33 | 7.86 | 2.17 | 2.11 | 0.03 | 1.03 | 0.25 | 0.00 | 0.00 | 146.96 |
| **BBH54** | 14.83 | 0.22 | 0.00 | 271.61 | 499.02 | 0.03 | 0.27 | 19.35 | 1.95 | 1.87 | 1.02 | 0.08 | 1.54 | 0.09 | 0.00 | 0.00 | 441.60 |
| **BBH55** | 18.19 | 0.15 | 0.00 | 305.63 | 385.10 | 0.07 | 0.28 | 19.19 | 1.54 | 2.98 | 0.74 | 0.15 | 2.62 | 0.03 | 0.00 | 1.18 | 284.38 |
| **BOW56** | 19.40 | 0.64 | 1.86 | 339.39 | 1577.38 | 0.02 | 0.57 | 46.03 | 8.17 | 2.62 | 3.82 | 0.22 | 7.63 | 0.64 | 0.00 | 6.40 | 596.79 |
| **BBH57** | 2.08 | 0.03 | 0.00 | 44.01 | 289.50 | 0.03 | 0.31 | 2.27 | 0.96 | 2.86 | 0.34 | 0.00 | 0.67 | 0.02 | 0.00 | 0.00 | 0.77 |

*Appendix 4a Rainy season stable isotope composition of water resources in Bafia*

| Sample code | Lat | Long | δD ‰ | δ18O ‰ | d-excess ‰ |
|---|---|---|---|---|---|
| BOW01 | 4.752083333 | 11.2409167 | -16.14 | -3.76 | 13.94 |
| BOW02 | 4.75225 | 11.2491667 | -18.88 | -4.11 | 14 |
| BBH03 | 4.7545 | 11.2577222 | -17.63 | 0.00 | -17.63 |
| BBH04 | 4.754916667 | 11.2653611 | -22.13 | -4.54 | 14.19 |
| BOW05 | 4.753861111 | 11.2713889 | -21.48 | -4.61 | 15.4 |
| BDOW06 | 4.745861111 | 11.2730278 | -18.14 | -4.14 | 14.98 |
| BOW07 | 4.73925 | 11.28075 | -17.68 | -3.99 | 14.24 |
| BDSP08 | 4.736027778 | 11.2834167 | -16.87 | -3.90 | 14.33 |
| BBH09 | 4.739305556 | 11.2936667 | -19.76 | -4.25 | 14.24 |
| BOW10 | 4.735861111 | 11.2538333 | -16.42 | -3.76 | 13.66 |
| BRW11 | 4.731194444 | 11.2537222 | -21.03 | -4.04 | 11.29 |
| BDOW12 | 4.740055556 | 11.2493333 | -15.19 | -3.46 | 12.49 |
| BOW13 | 4.744416667 | 11.2454167 | -17.77 | -4.07 | 14.79 |
| BOW14 | 4.750638889 | 11.2443611 | -22.83 | -4.68 | 14.61 |
| BDOW15 | 4.754472222 | 11.2408611 | -17.40 | -3.93 | 14.04 |
| BDOW16 | 4.755194444 | 11.2369722 | -17.36 | -3.89 | 13.76 |
| BDOW17 | 4.766833333 | 11.2363056 | -15.70 | -3.60 | 13.1 |
| BOW18 | 4.765611111 | 11.2380278 | -14.10 | -3.40 | 13.1 |
| BOW19 | 4.766083333 | 11.2270833 | -14.94 | -3.54 | 13.38 |
| BBH20 | 4.765083333 | 11.2236389 | -19.56 | -4.07 | 13 |
| BRW21 | 4.765555556 | 11.2210833 | -15.73 | -3.64 | 13.39 |
| BRW22 | 4.778638889 | 11.2143333 | -17.44 | -3.83 | 13.2 |
| BDOW23 | 4.773166667 | 11.2161667 | -17.26 | -3.87 | 13.7 |
| BDOW24 | 4.773361111 | 11.1901389 | -17.49 | -3.95 | 14.11 |
| BBH25 | 4.767611111 | 11.2093056 | -15.52 | -3.63 | 13.52 |
| BOW26 | 4.758194444 | 11.2151389 | -15.33 | -3.59 | 13.39 |
| BOW27 | 4.753277778 | 11.2061389 | -15.65 | -3.62 | 13.31 |

| | | | | | |
|---|---|---|---|---|---|
| BOW28 | 4.750666667 | 11.2143889 | -16.48 | -3.78 | 13.76 |
| BDOW29 | 4.743138889 | 11.2000028 | -19.13 | -4.13 | 13.91 |
| BOW30 | 4.741166667 | 11.2143056 | -18.82 | -4.19 | 14.7 |
| BBH31 | 4.803944444 | 11.16125 | -17.23 | -3.97 | 14.53 |
| BSP32 | 4.797444444 | 11.1598333 | -16.63 | -3.99 | 15.29 |
| BBH33 | 4.80175 | 11.1586111 | -17.60 | -3.98 | 14.24 |
| BRW34 | 4.816444444 | 11.1856111 | -28.02 | -5.16 | 13.26 |
| BBH35 | 4.816444444 | 11.1754444 | -18.81 | -4.06 | 13.67 |
| BDOW36 | 4.685 | 11.1775833 | -25.90 | -4.90 | 13.3 |
| BDOW37 | 4.690972222 | 11.1797222 | -14.02 | -3.40 | 13.18 |
| BBH38 | 4.694888889 | 11.1829722 | -23.19 | -4.74 | 14.73 |
| BBH39 | 4.692805556 | 11.1973333 | -17.14 | -3.89 | 13.98 |
| BBH40 | 4.716777778 | 11.2069722 | -14.30 | -3.59 | 14.42 |
| BOW41 | 4.724388889 | 11.2069722 | -17.21 | -3.73 | 12.63 |
| BBH42 | 4.703416667 | 11.2212222 | -19.84 | -4.36 | 15.04 |
| BOW43 | 4.718638889 | 11.2179444 | -15.72 | -3.69 | 13.8 |
| BBH44 | 4.727083333 | 11.2186389 | -20.55 | -4.27 | 13.61 |
| BOW45 | 4.714666667 | 11.2528889 | -16.20 | -3.76 | 13.88 |
| BBH46 | 4.721416667 | 11.2515278 | -16.99 | -3.79 | 13.33 |
| BBH47 | 4.721388889 | 11.2400833 | -20.08 | -4.22 | 13.68 |
| BBH48 | 4.717555556 | 11.2334722 | -22.89 | -4.59 | 13.83 |
| BDOW49 | 4.755027778 | 11.2346667 | -17.72 | -3.87 | 13.24 |
| BBH50 | 4.755833333 | 11.2234167 | -21.59 | -4.47 | 14.17 |
| BOW51 | 4.747888889 | 11.21975 | -17.14 | -3.77 | 13.02 |
| BOW52 | 4.743527778 | 11.2219444 | -11.75 | -2.98 | 12.09 |
| BOW53 | 4.743277778 | 11.2217778 | -18.57 | -3.90 | 12.63 |
| BBH54 | 4.746527778 | 11.228 | -20.66 | -4.29 | 13.66 |
| BBH55 | 4.736583333 | 11.2371944 | -21.21 | -4.46 | 14.47 |
| BOW56 | 4.750027778 | 11.2369167 | -14.25 | -3.43 | 13.19 |
| BBH57 | 4.739638889 | 11.2403611 | -16.06 | -3.70 | 13.54 |

*Appendix 4b Dry season stable isotope composition of water resources in Bafia*

| Sample code | Location | Lat | Long | Altitude (m) | δD‰ | $\delta^{18}O$‰ | d-excess ‰ |
|---|---|---|---|---|---|---|---|
| BOW01 | Fin Goudrong Ndegue | 4.752 | 11.238 | 490 | -19.4 | -4.1 | 13.3 |
| BOW02 | Lable | 4.754 | 11.257 | 478 | -16.3 | -3.7 | 13.4 |
| BBH03 | Lable | 4.755 | 11.258 | 476 | -16.2 | -3.7 | 13.8 |
| BOW05 | Nyamsong I | 4.754 | 11.271 | 484 | -21.7 | -4.5 | 13.9 |
| BDOW 06 | Donenkeng Iwa | 4.744 | 11.275 | 499 | -17.3 | -3.7 | 12.6 |
| BOW07 | Donenkeng | 4.739 | 11.281 | 492 | -16.5 | -3.7 | 13.2 |
| BDSP08 | Donenkeng | 4.736 | 11.283 | 505 | -16.0 | -3.8 | 14.2 |
| BDOW09 | Egona | 4.720 | 11.291 | 508 | -16.8 | -3.9 | 14.3 |
| BOW10 | Nyamsong III | 4.736 | 11.254 | 491 | -15.5 | -3.6 | 13.2 |
| BRW11 | Gamba River | 4.731 | 11.254 | 481 | -20.3 | -3.9 | 11.0 |
| BDOW12 | Nyamsong III | 4.740 | 11.249 | 490 | -14.9 | -3.4 | 11.9 |
| BOW13 | Bigna Savanah | 4.744 | 11.245 | 496 | -17.7 | -3.9 | 13.9 |
| BOW14 | LableTouristique hotel | 4.751 | 11.244 | 492 | -24.3 | -4.8 | 13.7 |
| BDOW15 | Lable | 4.754 | 11.241 | 499 | -16.9 | -3.8 | 13.5 |
| BBH17 | Lycee classique | 4.766 | 11.237 | 482 | -9.1 | -2.6 | 11.4 |
| BOW18 | Behind Lycée Classique | 4.766 | 11.238 | 476 | -16.5 | -3.7 | 13.0 |
| BOW19 | Renascent school | 4.766 | 11.227 | 473 | -14.5 | -3.3 | 12.3 |
| BBH 20 | Catholic Diocese | 4.765 | 11.224 | 474 | | | |
| BRW21 | Nuen River | 4.766 | 11.221 | 472 | -18.0 | -3.4 | 9.5 |
| BRW22 | Bororo | 4.779 | 11.214 | 469 | -12.9 | -3.2 | 12.5 |
| BDOW23 | Biamo | 4.773 | 11.216 | 484 | -16.1 | -3.6 | 12.5 |
| BDOW24 | Sa'nam | 4.773 | 11.190 | 516 | -15.7 | -3.7 | 13.5 |
| BBH25 | péage | 4.768 | 11.209 | 484 | -15.3 | -3.5 | 12.5 |

| | | | | | | | |
|---|---|---|---|---|---|---|---|
| BOW26 | Polyvalent | 4.758 | 11.215 | 488 | -18.7 | -4.0 | 13.5 |
| BOW27 | Logement Sociaux uphill | 4.753 | 11.206 | 496 | -17.0 | -3.8 | 13.1 |
| BDOW29 | Don Ribouem skool | 4.743 | 11.200 | 517 | -19.0 | -3.9 | 12.5 |
| BOW30 | Biabetom | 4.739 | 11.216 | 508 | -23.6 | -4.5 | 12.6 |
| BBH31 | Lalle | 4.804 | 11.161 | 606 | -15.6 | -3.8 | 14.4 |
| BSP32 | Bong/ Kon Yambetta | 4.802 | 11.159 | 579 | -16.9 | -3.9 | 14.2 |
| BRW34 | Mbam river | 4.832 | 11.198 | 518 | -5.9 | -1.2 | 3.4 |
| BBH35 | Ngongol carrefour Claude | 4.816 | 11.186 | 514 | -19.0 | -4.0 | 13.3 |
| BBH36 | Kiki Health centre | 4.685 | 11.175 | 510 | -26.8 | -5.0 | 12.8 |
| BOW37 | Kiki high way | 4.691 | 11.178 | 496 | -18.2 | -3.9 | 12.8 |
| BBH38 | Lycee Mouko entrance | 4.695 | 11.180 | 514 | -27.2 | -5.1 | 13.2 |
| BBH39 | Lycee Mouko uphill | 4.683 | 11.189 | 504 | -17.7 | -3.9 | 13.6 |
| BOW 41 | Chefferie Nyouka II | 4.724 | 11.207 | 514 | -15.9 | -3.5 | 11.7 |
| BOW42 | Rionong | 4.726 | 11.212 | 500 | -14.1 | -3.2 | 11.1 |
| BBH43 | Rigama Transformateur | 4.727 | 11.219 | 507 | -19.9 | -4.0 | 12.3 |
| BOW46 | Bigna chefferie | 4.721 | 11.252 | 486 | -17.7 | -3.5 | 10.4 |
| BOW47 | Bigna Ebeghe | 4.720 | 11.240 | 480 | -21.7 | -4.2 | 11.7 |
| BDOW49 | Bafia district hospital | 4.755 | 11.235 | 505 | -17.0 | -3.7 | 12.8 |
| BBH50 | Rimis | 4.756 | 11.22342 | 503 | -21.02 | -4.26 | 13.06 |
| BOW51 | Gondrone | 4.748 | 11.220 | 499 | -16.2 | -3.6 | 12.9 |
| BOW52 | Kiria/behind Congelcam | 4.744 | 11.222 | 491 | -15.7 | -3.5 | 12.5 |
| BOW53 | Kiria/behind Congelcam | 4.743 | 11.222 | 484 | -15.6 | -3.4 | 12.0 |
| BDOW54 | Tchokichado/Mr Ibrahim | 4.747 | 11.231 | 507 | -16.8 | -3.6 | 12.1 |
| BOW56 | Eldorado | 4.750 | 11.237 | 503 | -18.8 | -4.0 | 12.9 |
| BBH57 | Goufan II | 4.740 | 11.240 | 485 | -15.2 | -3.5 | 12.8 |
| BBH58 | Bigna Barn | 4.739 | 11.261 | 496 | -23.1 | -4.5 | 12.7 |

| | | | | | | | |
|---|---|---|---|---|---|---|---|
| BBH59 | Maison Blanche | 4.756 | 11.225 | 503 | -15.8 | -3.5 | 12.3 |
| BRW60 | Ronfi | 4.802 | 11.159 | 574 | -15.4 | -3.7 | 13.8 |
| BOW61 | Bokito entrance | 4.577 | 11.121 | 457 | -20.9 | -4.2 | 12.6 |
| BBH32 | Bokito market square | 4.574 | 11.116 | 475 | -16.3 | -3.6 | 12.3 |
| BBH63 | Asala 1 | 4.638 | 11.153 | 498 | -17.9 | -3.8 | 12.8 |
| BBH64 | Chefferie Gah Dang | 4.663 | 11.188 | 498 | -14.0 | -3.4 | 13.3 |
| BBH65 | Tomachock | 4.725 | 11.210 | 502 | -18.4 | -4.0 | 13.7 |
| BOW66 | Mangon | 4.715 | 11.253 | 484 | -20.1 | -4.2 | 13.1 |
| BOW67 | Rigama/behind the market | 4.565 | 11.225 | 498 | -19.0 | -4.0 | 13.0 |
| BOW68 | Gondrone Vallée | 4.747 | 11.223 | 509 | -14.1 | -3.2 | 11.3 |